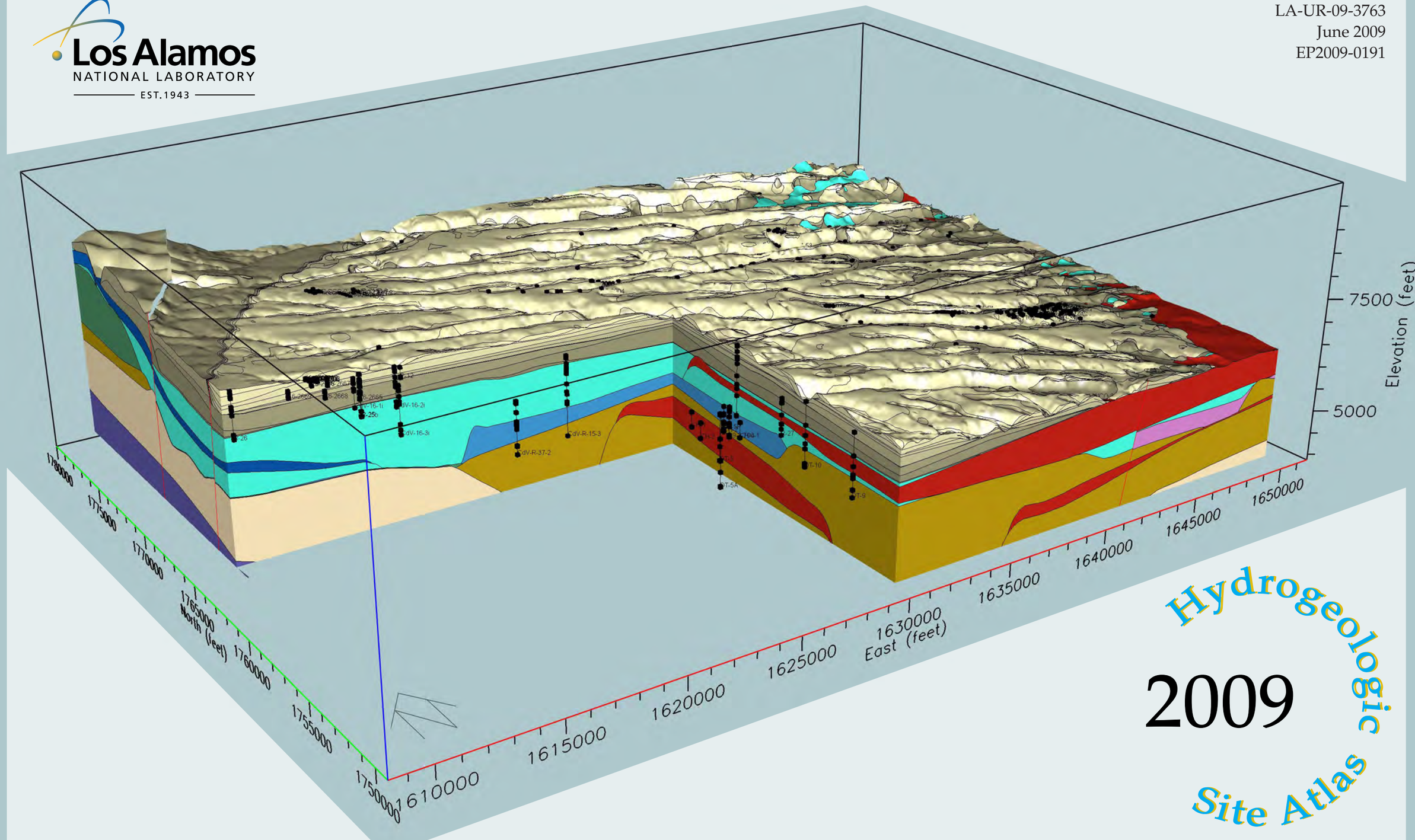
Los Alamos
NATIONAL LABORATORY
EST. 1943

LA-UR-09-3763
June 2009
EP2009-0191



Hydrogeologic Site Atlas

2009

The cover shows a three-dimensional geologic framework model of the region near Technical Area 03, depicting the geology down to a depth of 4000 feet above sea level. The stratigraphic units in the area wells are also shown. For illustrative purposes, a modified color palette was used for this model that differs from that used for illustrations in the rest of the atlas to highlight the large-scale character of the Quaternary tuffs (tan colors), older flows (blues), and the basalt flows (red).

Prepared by the Environmental Programs Directorate–LANL Water Stewardship Project

The primary author of the 2009 Hydrogeologic Site Atlas text and creator of the map plates was Greg Cole. David Broxton and Dan Koning provided figures and text describing the geologic units in Section 2, and Velimir (Monty) Vesselinov provided the text, tables, and water-table data for the plates of Section 3. David Coblentz used Earth Vision software to create the cross-section, three-dimensional views of the geologic framework model, and the atlas cover. Susan Rhyne provided editing support. Pamela Maestas provided graphics and editing support and created the cover using images generated by David Coblentz.

Greg Cole led the development of the 2009 geologic framework model. Other contributors included David Coblentz and Elaine Jacobs, who assisted in the model development; and Dan Koning, David Broxton, David Vaniman, and Fraser Goff, who provided structure contours and/or cross-sections for many of the model units.

Los Alamos National Laboratory, operated by Los Alamos National Security, LLC, for the U.S. Department of Energy under Contract No. DE-AC52-06NA25396, has prepared this document pursuant to the Compliance Order on Consent, signed March 1, 2005. The Compliance Order on Consent contains requirements for the investigation and cleanup, including corrective action, of contamination at Los Alamos National Laboratory. The U.S. government has rights to use, reproduce, and distribute this document. The public may copy and use this document without charge, provided that this notice and any statement of authorship are reproduced on all copies.

LA-UR-09-3763
EP2009-0191

2009 Hydrogeologic Site Atlas

June 2009

Responsible project leader:

Printed Name	Signature	Title	Organization	Date
Ardyth M. Simmons	Ardyth M. Simmons	Program Manager	Environmental Programs	6-29-09

Responsible LANS representative:

Printed Name	Signature	Title	Organization	Date
Michael J. Graham	B. G. Schappell for MJG	Associate Director	Environmental Programs	6-29-09

Responsible DOE representative:

Printed Name	Signature	Title	Organization	Date
David R. Gregory	David R. Gregory	Project Director	DOE-LASO	6/30/09

CONTENTS

ABSTRACT **1**

1.0 INTRODUCTION **1**
1.1 Background 1
1.2 Scope 2
1.3 Data Sets 3

2.0 THE 2009 GFM **3**
2.1 Geologic Overview 4
2.2 Stratigraphic/Geologic Units 6
2.2.1 Tshirege Member, Bandelier Tuff (Qbt) 6
2.2.2 Cerro Toledo Interval (Qct) 7
2.2.3 Otowi Member (Qbo) 7
2.2.4 Puye Formation 7
2.2.5 Tschicoma Formation 7
2.2.6 Cerros del Rio Basalt (Tb4) 7
2.2.7 Ancha Formation 8
2.2.8 Totavi Lentil (Tpt) 8
2.2.9 Bearhead Rhyolite and Fanglomerates (Tjfp) 8
2.2.10 Keres Group Volcanics (Tvk) 8
2.2.11 Chamita Formation 8
2.2.12 8.4–9.3 Ma Basalts (Tb2) 9
2.2.13 11.6–13.1 Ma Basalts (Tb1) 9
2.2.14 Tesuque Formation 9
2.2.15 Bedrock (Bedr) 9

3.0 MAPPING OF THE REGIONAL WATER-TABLE ELEVATION **9**

4.0 MAP SPECIFICATIONS **13**
4.1 Base Map 13
4.2 Geology 13
4.2.1 Surface Geology 13
4.2.2 Geologic Unit Morphology 13
4.3 Cross-Sections 13
4.4 3-D Views of the GFM 13
4.5 Water-Table Elevation and Geology 14

5.0 REFERENCES **14**

Figures

Figure 1-1a. Example of a geologic unit surface (Qbt1g) from the 1995 site geologic model 1
Figure 1-1b. Visualization at TA-21, utilizing the 1995 site geologic model 2
Figure 1-2. Location of the SITE, SEB, and EB models of the 2009 GFM 3
Figure 1-3. Map of geologic unit polygons obtained from the surface geologic maps of the SEB region 4
Figure 2-1. The Laboratory setting along the eastern flank of the Valles Caldera 5
Figure 2-2. Schematic cross-section across the EB 5
Figure 2-3. Units of the northern portion of the SEB model 5
Figure 2-4. Units of the southern portion of the SEB model 6
Figure 2-5. Codes and colors used for the GFM units 6

Tables

Table 1-1. Quantities of Contact Points Available for Past and Present GFMs 2
Table 3-1. Summary of Well-Screen Positions, Water-Level Observations, and Differences between Observed and Contoured Water Levels 11

Plates

Plate 1-1. Base map showing land ownership, water supply and characterization wells, and other wells or boreholes important in constraining the 3-D geologic model 17
Plate 1-2. Locations of all wells contributing data to the 3-D geologic model 18
Plate 1-3. Identification of all wells contributing data to the 3-D geologic model 19
Plate 2-1. Mapped surface geology 20
Plate 2-2. Modeled surface geology 21
Plate 2-3. Fault trace data for the atlas area 22
Plate 2-4. Structure contours of the top of the Tshirege Member (Qbt) 23
Plate 2-5. Thickness of the Tshirege Member of the Bandelier Tuff (Qbt) 24
Plate 2-6. Structure contours of the bottom of the Tshirege Member (Qbt) 25
Plate 2-7. Structure contours of the top of the Tshirege Member, unit 4 (Qbt4) 26
Plate 2-8. Thickness of the Tshirege Member, unit 4 (Qbt4) 27
Plate 2-9. Structure contours of the top of the Tshirege Member, unit 3, transition zone (Qbt3t) 28
Plate 2-10. Thickness of the Tshirege Member, unit 3, transition zone (Qbt3t) 29
Plate 2-11. Structure contours of the top of the Tshirege Member, unit 3 (Qbt3) 30
Plate 2-12. Thickness of the Tshirege Member, unit 3 (Qbt3) 31
Plate 2-13. Structure contours of the top of the Tshirege Member, unit 2 (Qbt2) 32
Plate 2-14. Thickness of the Tshirege Member, unit 2 (Qbt2) 33
Plate 2-15. Structure contours of the top of the Tshirege Member, unit 1, upper vapor-phase portion (Qbt1vu) 34
Plate 2-16. Thickness of the Tshirege Member, unit 1, upper vapor-phase portion (Qbt1vu) 35
Plate 2-17. Structure contours of the top of the Tshirege Member, unit 1, colonnade vapor-phase portion (Qbt1vc) 36

Plate 2-18. Thickness of the Tshirege Member, unit 1, colonnade vapor-phase portion (Qbt1vc) 37
Plate 2-19. Structure contours of the top of the Tshirege Member, unit 1, glassy portion (Qbt1g) 38
Plate 2-20. Thickness of the Tshirege Member, unit 1, glassy portion (Qbt1g) 39
Plate 2-21. Structure contours of the top of the Tsankawi Pumice Bed (Qbtt) 40
Plate 2-22. Thickness of the Tsankawi Pumice Bed (Qbtt) 41
Plate 2-23. Structure contours of the top of the Cerro Toledo interval (Qct) 42
Plate 2-24. Thickness of the Cerro Toledo interval (Qct) 43
Plate 2-25. Structure contours of the bottom of the Cerro Toledo interval (Qct) 44
Plate 2-26. Structure contours of the top of the Otowi Member of the Bandelier Tuff (Qbof) 45
Plate 2-27. Thickness of the Otowi Member of the Bandelier Tuff (Qbof) 46
Plate 2-28. Structure contours of the bottom of the Otowi Member of the Bandelier Tuff (Qbof) 47
Plate 2-29. Structure contours of the top of the Guaje Pumice Bed of the Bandelier Tuff (Qbog) 48
Plate 2-30. Thickness of the Guaje Pumice Bed of the Bandelier Tuff (Qbog) 49
Plate 2-31. Structure contours of the bottom of the Guaje Pumice Bed of the Bandelier Tuff (Qbog) 50
Plate 2-32. Structure contours of the top of the Puye Formation, fanglomerate (Tpf) 51
Plate 2-33A. Thickness of the Puye Formation, fanglomerate (Tpf), including interior flow units 52
Plate 2-33B. Thickness of the Puye Formation, fanglomerate (Tpf), excluding interior flow units 53
Plate 2-34. Structure contours of the bottom of the Puye Formation, fanglomerate (Tpf) 54
Plate 2-35. Structure contours of the top of the Cerros del Rio Basalt (Tb4) 55
Plate 2-36. Thickness of the Cerros del Rio Basalt (Tb4) 56
Plate 2-37. Structure contours of the bottom of the Cerros del Rio Basalt (Tb4) 57
Plate 2-38. Structure contours of the top of the Ancha Formation (Qta) 58
Plate 2-39. Thickness of the Ancha Formation (Qta) 59
Plate 2-40. Structure contours of the bottom of the Ancha Formation (Qta) 60
Plate 2-41. Structure contours of the top of the Tschicoma Formation, Pajarito Mountain, Cerro Grande, and Caballo Mountain lobes (Tvt2) 61
Plate 2-42. Thickness of the Tschicoma Formation, Pajarito Mountain, Cerro Grande, and Caballo Mountain lobes (Tvt2) 62
Plate 2-43. Structure contours of the bottom of the Tschicoma Formation, Pajarito Mountain, Cerro Grande, and Caballo Mountain lobes (Tvt2) 63
Plate 2-44. Structure contours of the top of the Tschicoma Formation, Rendija Canyon lobe (Tvt1) 64
Plate 2-45. Thickness of the Tschicoma Formation, Rendija Canyon lobe (Tvt1) 65
Plate 2-46. Structure contours of the bottom of the Tschicoma Formation, Rendija Canyon lobe (Tvt1) 66
Plate 2-47. Structure contours of the top of the Totavi Lentil (Tpt) 67
Plate 2-48. Thickness of the Totavi Lentil (Tpt) 68
Plate 2-49. Structure contours of the bottom of the Totavi Lentil (Tpt) 69
Plate 2-50. Structure contours of the top of the Bearhead Rhyolite and Fanglomerates (Tjfp) 70
Plate 2-51. Thickness of the Bearhead Rhyolite and Fanglomerates (Tjfp) 71
Plate 2-52. Structure contours of the bottom of the Bearhead Rhyolite and Fanglomerates (Tjfp) 72
Plate 2-53. Structure contours of the top of the Keres Group volcanics (Tvk) 73
Plate 2-54. Thickness of the Keres Group volcanics (Tvk) 74
Plate 2-55. Structure contours of the bottom of the Keres Group volcanics (Tvk) 75
Plate 2-56. Structure contours of the top of the Chamita Formation, lithosome A (Tcac) 76
Plate 2-57. Thickness of the Chamita Formation, lithosome A (Tcac) 77
Plate 2-58. Structure contours of the bottom of the Chamita Formation, lithosome A (Tcac) 78
Plate 2-59. Structure contours of the top of the Tesuque Formation, Chamita lithosome B (Ttca) 79
Plate 2-60. Thickness of the Tesuque Formation, Chamita lithosome B (Ttca) 80
Plate 2-61. Structure contours of the bottom of the Tesuque Formation, Chamita lithosome B (Ttca) 81
Plate 2-62. Structure contours of the top of the Chamita transitional zone: lithosome B, axial river gravels (Tcara) 82
Plate 2-63. Thickness of the Chamita transitional zone: lithosome B, axial river gravels (Tcara) 83
Plate 2-64. Structure contours of the bottom of the Chamita transitional zone: lithosome B, axial river gravels (Tcara) 84
Plate 2-65. Structure contours of the top of the 8.2–9.3 Ma Basalts (Tb2) 85
Plate 2-66. Thickness of the 8.2–9.3 Ma Basalts (Tb2) 86
Plate 2-67. Structure contours of the bottom of the 8.2–9.3 Ma Basalts (Tb2) 87
Plate 2-68. Structure contours of the top of the Chamita Formation, axial river gravels (Tcar) 88
Plate 2-69. Thickness of the Chamita Formation, axial river gravels (Tcar) 89
Plate 2-70. Structure contours of the bottom of the Chamita Formation, axial river gravels (Tcar) 90
Plate 2-71. Structure contours of the top of the 11.6–13.1 Ma Guaje Canyon Basalt (Tb1) 91
Plate 2-72. Thickness of the 11.6–13.1 Ma Guaje Canyon Basalt (Tb1) 92
Plate 2-73. Structure contours of the bottom of the 11.6–13.1 Ma Guaje Canyon Basalt (Tb1) 93
Plate 2-74. Structure contours of the top of the Tesuque Formation, Chama–El Rito Member (Ttc) 94
Plate 2-75. Thickness of the Tesuque Formation, Chama–El Rito Member (Ttc) 95
Plate 2-76. Structure contours of the bottom of the Tesuque Formation, Chama–El Rito Member (Ttc) 96
Plate 2-77. Structure contours of the top of the Tesuque Formation, lithosome S (fine) (Ttsf) 97
Plate 2-78. Thickness of the Tesuque Formation, lithosome S (fine) (Ttsf) 98
Plate 2-79. Structure contours of the bottom of the Tesuque Formation, lithosome S (fine) (Ttsf) 99
Plate 2-80. Structure contours of the top of the Tesuque Formation, lithosome B (Ttb) 100
Plate 2-81. Thickness of the Tesuque Formation, lithosome B (Ttb) 101
Plate 2-82. Structure contours of the bottom of the Tesuque Formation, lithosome B (Ttb) 102
Plate 2-83. Structure contours of the top of the Galisteo and older units (Bedr) 103
Plate 2-84. Locations of geologic cross-section lines 104
Plate 2-85. Southern east-west cross-sections (N_1735000, N_1745000) 105
Plate 2-86. Central east-west cross-sections (N_1755000, N_1765000) 106
Plate 2-87. Northern east-west cross-sections (N_1775000, N_1785000) 107
Plate 2-88. Western north-south cross-sections (E_1610000, E_1620000) 108
Plate 2-89. West central north-south cross-sections (E_1630000, E_1640000) 109
Plate 2-90. Central north-south cross-sections (E_1650000, E_1660000) 110
Plate 2-91. East central north-south cross-sections (E_1670000, E_1680000) 111
Plate 2-92. Eastern north-south cross-section (E_1690000) 112
Plate 2-93. The atlas portion of the southern Española Basin model—view from the southeast 113
Plate 2-94. The southern Española Basin model—view from the southeast 114
Plate 3-1. Regional water table elevations 115
Plate 3-2. Geology at the water table 116

ABSTRACT

The “2009 Hydrogeologic Site Atlas” describes those portions of the 2009 geologic framework model (GFM) that encompass Los Alamos National Laboratory (the Laboratory) and surrounding area. This atlas is extracted from the 2009 GFM, a major revision and expansion of the previous 2005 GFM, and incorporates a large amount of new subsurface data from an expanded drilling program. The 2009 GFM is a set of three models: the site model (SITE), the southern Española Basin (SEB) model and the Española Basin (EB) model, which provide computational grids for increasingly larger portions of the EB at decreasing resolutions. The 2009 GFM has also been extended to greater depths beneath the Pajarito Plateau through a projection of modeled EB geology to the east and southeast and utilization of new geologic map data from the Valles Caldera to the west and the Cochiti Pueblo region to the south. The atlas incorporates enhanced stratigraphic control to identify additional details of the deeper Santa Fe Group sediments beneath the Laboratory and provides new and/or updated geologic maps, structure contour and thickness maps, and water-table maps, as well as cross-sections and three-dimensional (3-D) visualizations of the geology.

1.0 INTRODUCTION

The Laboratory has produced a series of hydrologic site atlases that document updated models for the Laboratory site (Stone et al. 1999, 064039; Stone et al. 2001, 069830; Cole et al. 2006, 095079). This current document is the latest addition to the atlas series. This document satisfies component 9 as indicated in the 2009 General Facility Information (LANL 2009, 105632).

1.1 Background

The earliest 3-D geologic model for the Laboratory site was produced in the mid-1990s to support compliance with the Laboratory’s Hazardous Waste Facility permit(s), required under the Resource Conservation and Recovery Act. The 1995 site geologic model (Vaniman et al. 1996, 106129) used early-version, ArcInfo software for building the model, and IBM DX-Explorer software for 3-D visualizations. The model consisted of 14 surfaces that were derived from the contouring of triangular integrated networks (TINs) created from limited sets of surface and drill hole control points. The model surfaces did not extend to the Laboratory boundaries and were limited to units/subunits of the Bandelier Tuff, portions of the Cerro Toledo and Puye and Totavi units, and a small piece of the Santa Fe Group. Figures 1-1a and b provide samples of the surfaces and visualizations from this early model of the 3-D geology and the Laboratory site.

Through the ensuing years, there has been an ongoing effort to accelerate the characterization and remediation of the hazardous (release) sites at the Laboratory. This effort has resulted in the installation of many new characterization and monitoring wells and additional surface geologic mapping. The effort has also resulted in the need to extend geologic-based groundwater flow and contaminant transport models past Laboratory boundaries into the surrounding communities. The Laboratory has continued to support the development of 3-D geologic models with updated models produced for 1997 (Cole et al. 1997, 106127), 1998 (Cole et al. 1998, 106128), 1999 (Carey et al. 1999, 066782), 2002 (no report produced), 2003 (partial model, including Area G and Mortandad and Sandia Canyons [Stauffer et al. 2005, 097432]), and 2006 (Cole et al. 2006, 095079). These newer models were developed mainly to support the numerical analysis of groundwater flow and transport.

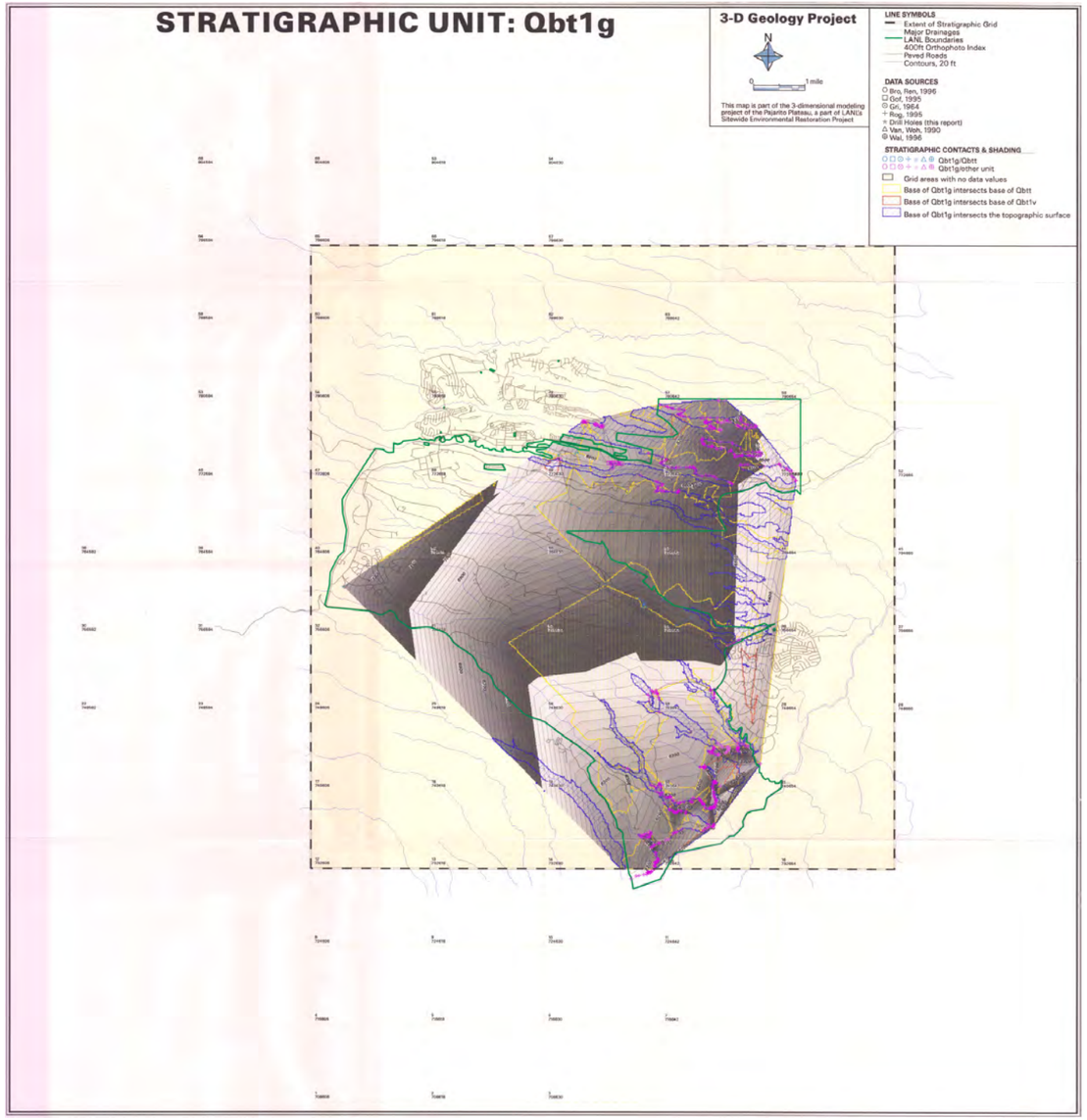
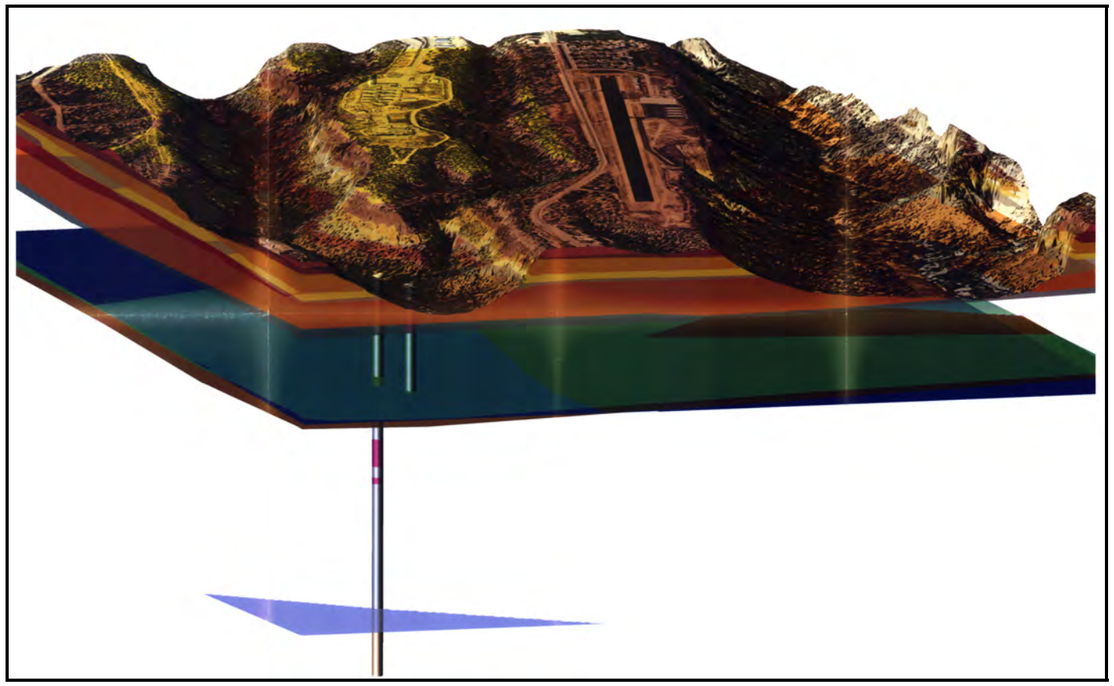


Figure 1-1a. Example of a geologic unit surface (Qbt1g) from the 1995 site geologic model



Source: Vaniman et al. 1996, 106129.

Figure 1-1b. Visualization at TA-21, utilizing the 1995 site geologic model

The earlier geologic models have been expanded in geographical extent to address issues of possible contaminant transport past Laboratory boundaries. The 2002 geologic model was expanded to include the full extent of all four 7.5-min quadrangle maps intersected by the Laboratory boundary. This model was called the “Pajarito Plateau” model in Cole et al. (2006, 095079). The model presented in this atlas includes the SITE model and a portion of the SEB model of the 2009 GFM. Table 1-1 provides a measure of the data support used to create each of the past and present GFMs. The fiscal year (FY) 2003 model provided only a partial coverage of the site and is therefore not included in the comparison.

Table 1-1.
Quantities of Contact Points Available for Past and Present GFMs

Model Year	FY96	FY97	FY98	FY99	FY02	FY06	FY09
Total Number of Data Points	34,989	40,991	43,369	31,624	76,638	121,284	>200,000
Number of Drill Hole Data Points	615	615	703	866	1042	1398	2228

Subsets of the total set of data points, augmented by outcrop maps, are used to develop structure contours. Final digital grids for the unit surfaces are created from the structure contours and “hard” data points reflecting the actual preerosional position of unit surfaces. Increased point counts at the FY02, FY06, and FY09 GFM dates reflect the combined increase in data density, as well as the increased geographical extent of these models.

1.2 Scope

In addition to the Laboratory, a number of government entities have been involved in the development of digital geologic data and geologic-based groundwater models for the region surrounding Los Alamos, including the New Mexico Bureau of Geology and Mineral Resources, the U.S. Geological Survey (USGS), and the City and County of Santa Fe. Development of the 2009 expanded Laboratory GFM incorporates the following:

- voluminous new subsurface (drill hole) data collected to support current characterization and remediation projects at the Laboratory
- new regional geologic information for development of accurate models of deeper, hydrologically significant units beneath the Laboratory (Grauch et. al. 2009, available at http://pubs.usgs.gov/pp/1761/)
- new models by other government agencies, reflecting a communal redefinition of many of the hydrogeologic units for the region (INTERA Incorporated 2006, 106106; Pantea et al. 2009 personal communication)
- revision of many of the geologic quadrangle maps within and along the boundaries of previous Laboratory GFMs
- revision of a large percentage of the geologic quadrangle maps within the EB that provide “boundary constraints” for the numerical flow and transport modeling at the Laboratory

The 2009 GFM was developed at three extents, with two resolutions (cell size) for each extent. The extents of the 2009 3-D geologic model(s) are shown in Figure 1-2. The areal extent of the EB model intersects more than 60 7.5-min quadrangle maps, that of the SEB model incorporates 12 quadrangle maps, and that of the site model consists of the four quadrangle maps encompassing the Laboratory site. The lower resolution for each model version is half the higher resolution and is limited to be no more than a million cells per grid surface. The SITE model has the highest resolution of the three model extents, with the model developed at 50-ft cell center spacing. Additional models of limited extent, including the model presented in this atlas, as well as a local model for Area G at the Laboratory site, represent extraction of data from these larger models and not a regeneration of model surfaces.

The map extent of this atlas encompasses the Laboratory and surrounding area. This region lies mainly within the SITE model but extends into the western portions of the Española and Horcado Ranch quadrangle maps, the northern edges of the Cochiti Dam, Montoso Peak quadrangle maps, and the northwest corner of the Agua Fria quadrangle map. Because the atlas surfaces extend past the SITE model boundary, surfaces were extracted from the lower-resolution (100-ft) SEB model.

The atlas presents a set of maps/plates that provide

1. land ownership and the location of wells that provide constraints for the 3-D geologic model,
2. mapped and modeled surface geology with mapped faults,
3. structure contours for the top of each unit and subunit of the model present within the atlas extent,
4. isochors (vertical thickness contours) for each unit and subunit of the model present within the atlas extent,
5. structure contours for the bottom of each unit of the model present within the atlas extent,
6. elevations of the regional water table produced for this atlas from the currently available data,
7. the geology at the water table,
8. cross-sections of the geology with the water-table position, and
9. locations of the cross-sections.

Basic information for the atlas, including land ownership, roads, and well locations with descriptions is provided in Plates 1-1, 1-2, and 1-3.

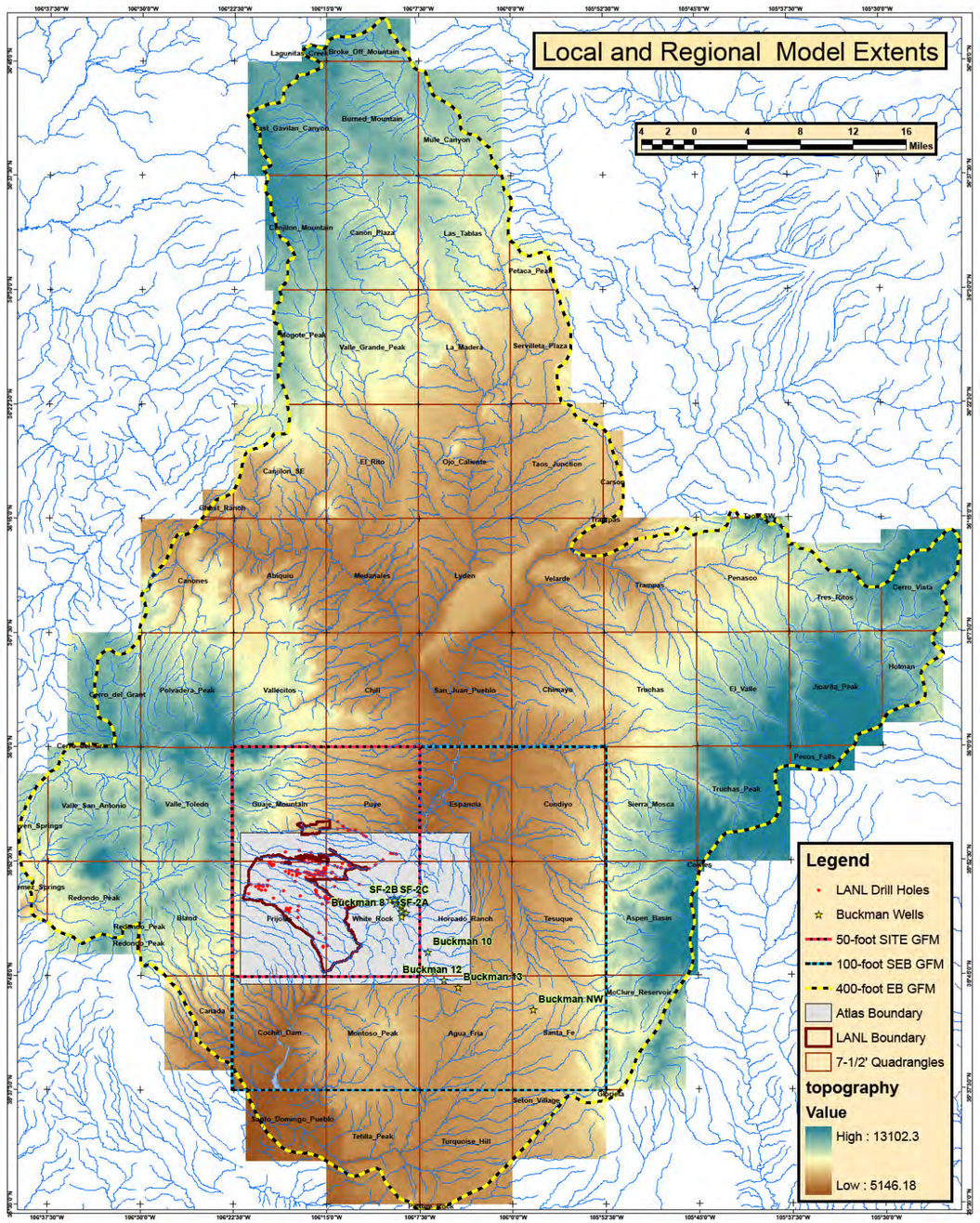


Figure 1-2. Location of the SITE, SEB, and EB models of the 2009 GFM

1.3 Data Sets

Data used to develop the SEB model that encompasses the atlas extent include the following:

- mapped surface geology and associated cross-sections for the following 7.5-min geologic quadrangle maps:
  - Guaje Mountain (Kempter et al. 2007, 106111)
  - Puye (Dethier 2003, 106113)
  - Española (Koning 2002, 105710)
  - Cundiyo (Koning 2002, 105710)
  - Frijoles (Goff et al. 2002, 088776)
  - White Rock (Dethier 1997, 049843)
- professional papers and open file reports for the following 7.5-min geologic quadrangle maps:
  - Horcado Ranch (Read et al. 2005, 105709)
  - Tesuque (Read et al. 2005, 105709)
  - Cochiti Dam (Sawyer et al. 2007, 106130)
  - Montoso Peak (Sawyer et al. 2007, 106130)
  - Agua Fria (Read et al. 2005, 105709)
  - Santa Fe (Read et al. 2005, 105709)
- mapping of subunits of the Bandelier Tuff by Laboratory scientists (Rogers 1995, 054419; Lewis et al. 2002, 073785; Lavine et al. 2003, 092527)
- subsurface geologic contacts from the current Laboratory database (Cole et al. 2006, 095079)

Source data were obtained from digital and analog (paper map) sources and converted to digital contact control points. All geologic unit data were preprocessed to convert (field) mapped units to the set of “regional” units of the model in the appropriate coordinate system. The preprocessed surface geologic map data for the 12-quadrangle map area of the SEB model are shown in “model” units as Figure 1-3.

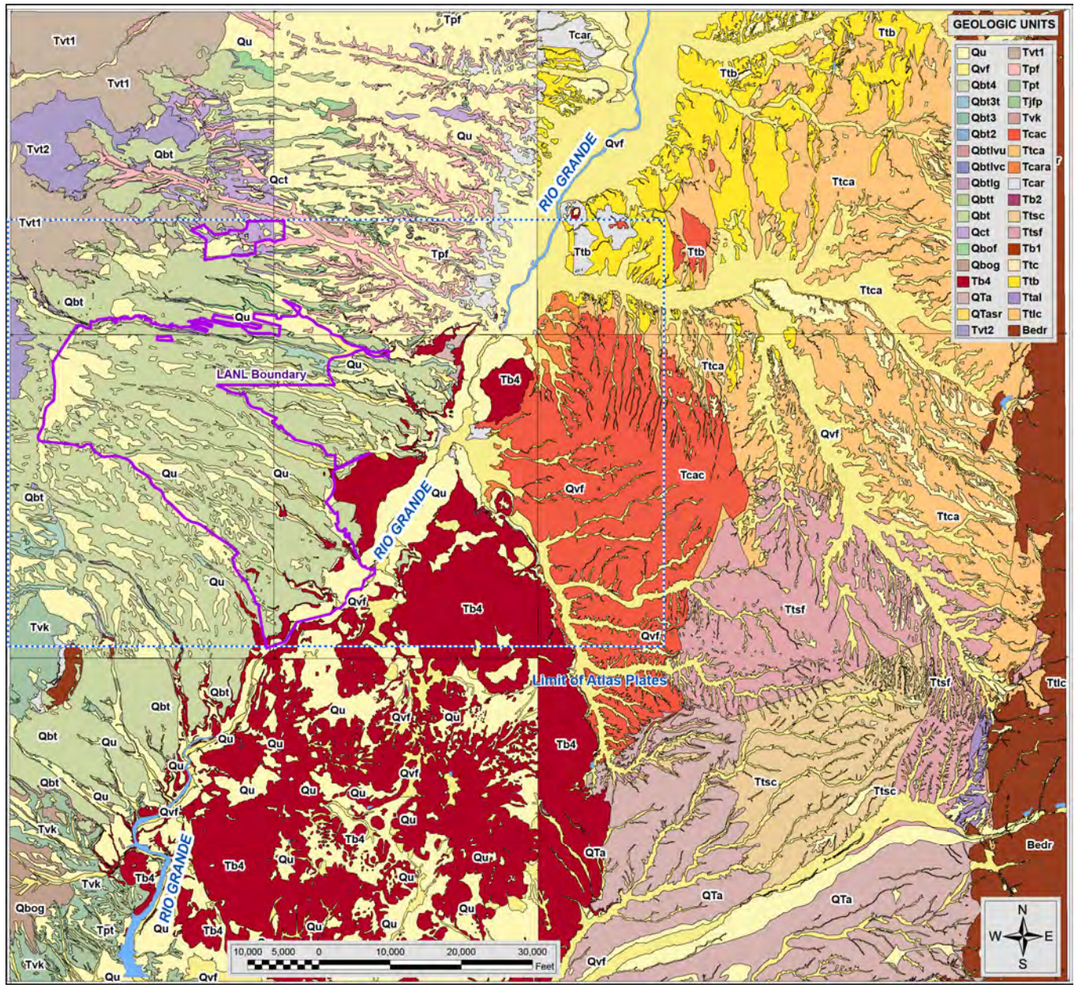
The analog-to-digital conversion process includes

- scanning of contacts from cross-sections and geologic maps,
- extracting points at constant horizontal and/or vertical distances along the lines, and
- obtaining the “third” part of the spatial coordinate through a digital elevation model (for surface maps) or from geometric calculations (for cross-sections).

The conversion process was performed using the R2V digitizing software (Able Software), ArcInfo Geographical Information System (GIS) software and scripts, and utility FORTRAN programs.

2.0 THE 2009 GFM

The 2009 GFM is the latest of a series of 3-D geologic models that have been developed to support environmental cleanup and waste management programs at the Laboratory. This new GFM is unique in that it comprises multiple overlapping models of differing resolutions that allow the highest-resolution model centered on the Laboratory site to be seamlessly joined with lower resolution models at successive distances outside of the Laboratory boundary, with an ultimate model extent of the entire EB. Model resolution, defined by the distance between cell centers on a rectilinear grid, can range from 50 to 800 ft, with possible cell center increments of 50, 100, 200, 400, and 800 ft.



Note: The atlas extent is indicated by the dashed blue-and-white line.

Figure 1-3. Map of geologic unit polygons obtained from the surface geologic maps of the SEB region

The GFM reflects current ideas about the geologic evolution of the model area and depositional processes within the EB, embracing the voluminous amounts of new geologic mapping by the joint USGS and State mapping project, as well as the results of associated geological and geophysical studies. The GFM incorporates a large amount of new, subsurface data, including contact data from borehole logs of more than 100 new wells (through February 2009) that result in a 50% increase of subsurface contact control points. In addition, repositioning of well locations through global positioning system (GPS) techniques and reanalysis of existing geological and geophysical logs have resulted in many changes in the preexisting drill hole database. The locations of wells that provide new or updated contact control data are shown in Plate 1-1.

The 2009 GFM also provides a completely revised definition for the Santa Fe Group units that comprise most of the saturated zone stratigraphy. The GFM incorporates the breakout of geologic units used in the recent geologic remapping of most of the quadrangle maps within the model area.

Surfaces of the new GFM were developed with the ArcInfo software. Digital data sets were obtained from a variety of sources, including

- existing digital grids or digital line data from USGS and the New Mexico Bureau of Geology and Mineral Resources,
- published geologic maps and cross-sections (scanned and digitized),
- "open-source" topographic grids and digital line graphs of the USGS,
- structure contours for unit surfaces developed by the Laboratory, and
- well logs from the Laboratory database as well as off-site logs from other sources, where available.

Quality assurance was provided through comparison of the modeled and actual 3-D position of the input data with emphasis on the fit of subsurface data. USGS topographic data were used rather than the higher-quality, light detection and ranging (LIDAR) elevation data available at the Laboratory (Carey and Cole 2002, 073784). A single-source data set was desired for the GFM, and the LIDAR data do not extend into the SEB and EB portions of the model. Topographic maps (7.5 min) are usually the basis for placement of geologic contacts by field geologists and are the source of the digital line graph (DLG) contour data that are used as the elevation model for the GFM. The subsurface contacts at drill holes are normally positioned relative to high-resolution surface measurements obtained from LIDAR or GPS elevation data and not from the DLG data.

2.1 Geologic Overview

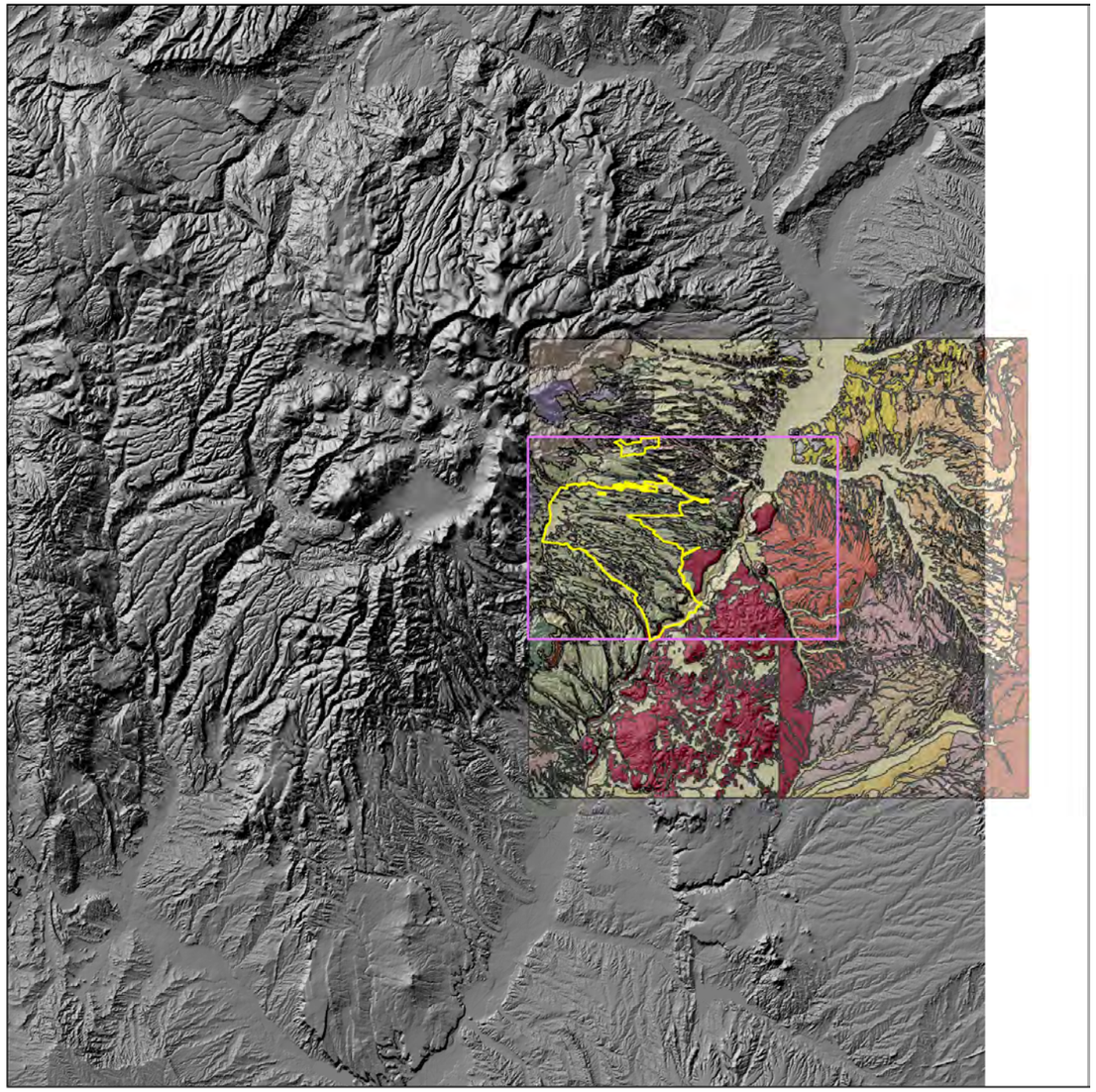
The Laboratory is located on the Pajarito Plateau within the eastern area of the Jemez volcanic field (JVF), along the east-southeastern slope of the Valles Caldera at the western edge of the EB (Figure 2-1).

The stratigraphy of the modeled area reflects the interplay of tectonic and depositional processes within the developing EB, which at the model latitude, is hinged at its eastern edge with major, predominantly downward, displacements at its western margin. This geometry is schematically shown in Figure 2-2.

The tectonically active portion of the western edge of the EB is present within the far western portion of the GFM, at the Pajarito fault system, which exhibits both discrete offsets and distributed strain. Other, poorly defined, north-south faults with major offsets occur west of the model area, within the eastern portion of the Valles Caldera. The volcanic activity began approximately 14 million years ago (Ma) (Goff 2009, 106105), with the most recent major eruptive events creating the Pajarito Plateau. The origin of the upper (above water table) geologic units of the plateau is predominantly volcanic, and these geologic units include dacitic and rhyolitic flows, ash-flow tuffs, and their erosional derivatives. Basaltic flows from sources within and to the east and southeast of the Laboratory are intermixed with this Jemez volcanic material. The units generally tilt to the east and southeast, although downward displacements to the west may offset or reverse the original depositional dips of units, depending on their age.

The JVF material lies on top of EB sedimentary units and extends almost to the currently active position of the Rio Grande, with some intermixing with basin sediments to the east. The EB sedimentary units exposed further east, reflect the erosion of the uplifting Sangre de Cristo Mountains, which form the eastern boundary of the basin, as well as sediment sources farther to the north. The units tilt regionally to the west, reflecting both the depositional attitude as well as their increased downward displacement to the west, along poorly defined north-south trending faults within the basin. Older basin sedimentary units underlie the JVF volcanic material to the west. Figures 2-3 and 2-4 show relationships between the stratigraphic units in the east-west direction between the JVF volcanic and fanglomerate material and the river gravels and other sedimentary material in the EB.

Plates 2-1 and 2-2 show the mapped and modeled geology in greater detail within its extent identified in Figure 2-1. Plate 2-3 provides the observed and inferred geologic structure for this region. Plates 2-84 through 2-91 provide cross-section information for the GFM, which add some reality to the schematic views provided by Figures 2-3 and 2-4. Plates 2-93 and 2-94 provide 3-D views for cutouts of the atlas and SEB model.



Notes: The Laboratory site is outlined in yellow. The purple boundary identifies the geologic extent of this atlas. Geologic units are colored for the extent of the SEB model. The flat, pale-green area running from the north-central to southwest corners of the SEB model identifies the alluvial units of the Rio Grande that approximate the eastern extent of volcanic material of the JVF.

Figure 2-1. The Laboratory setting along the eastern flank of the Valles Caldera

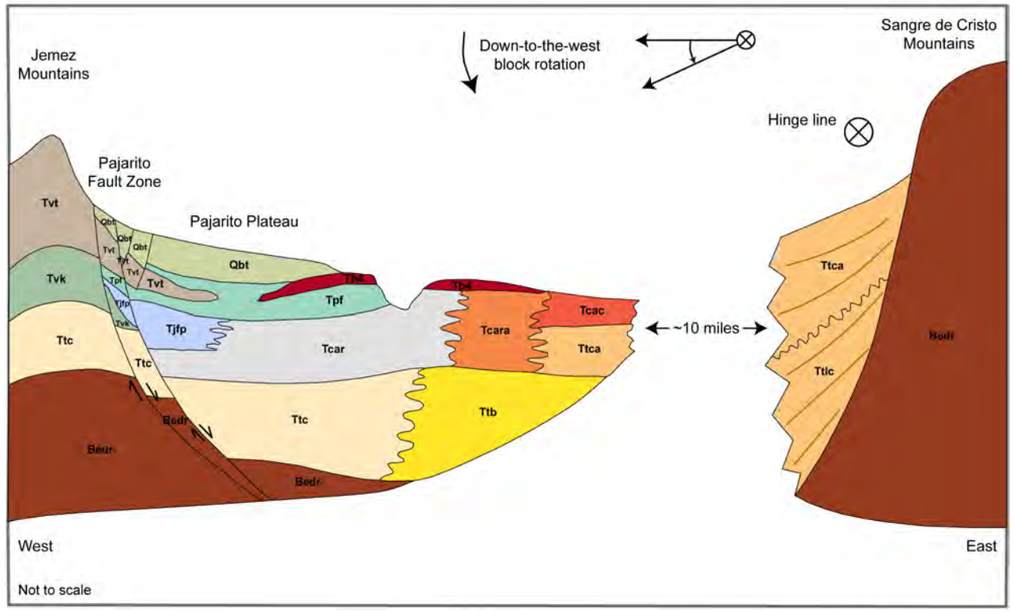
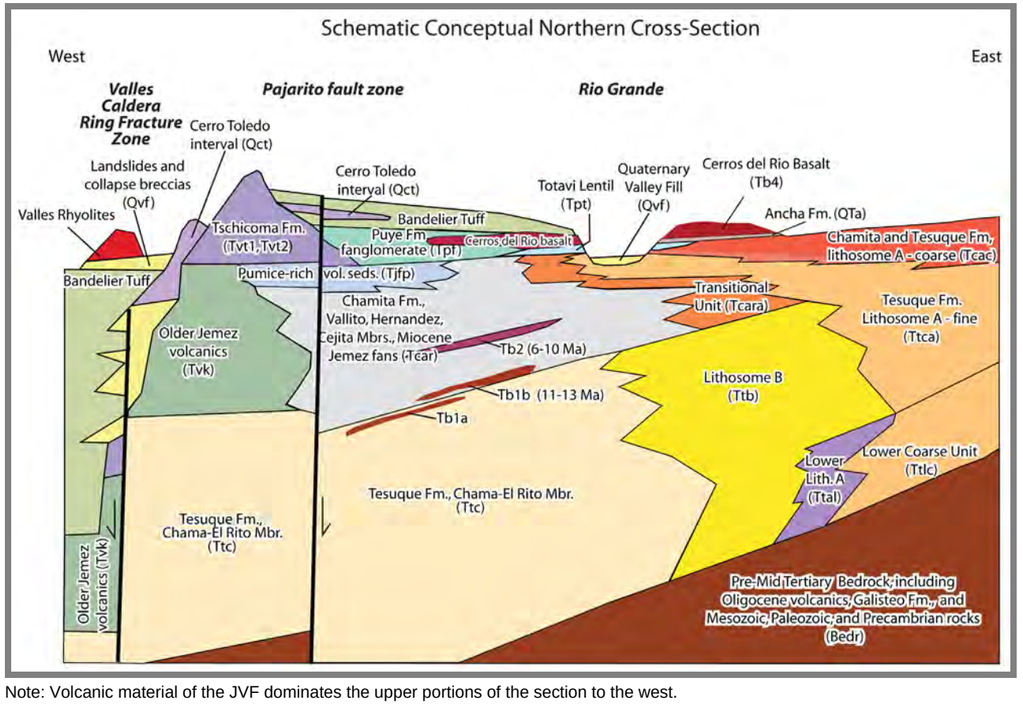
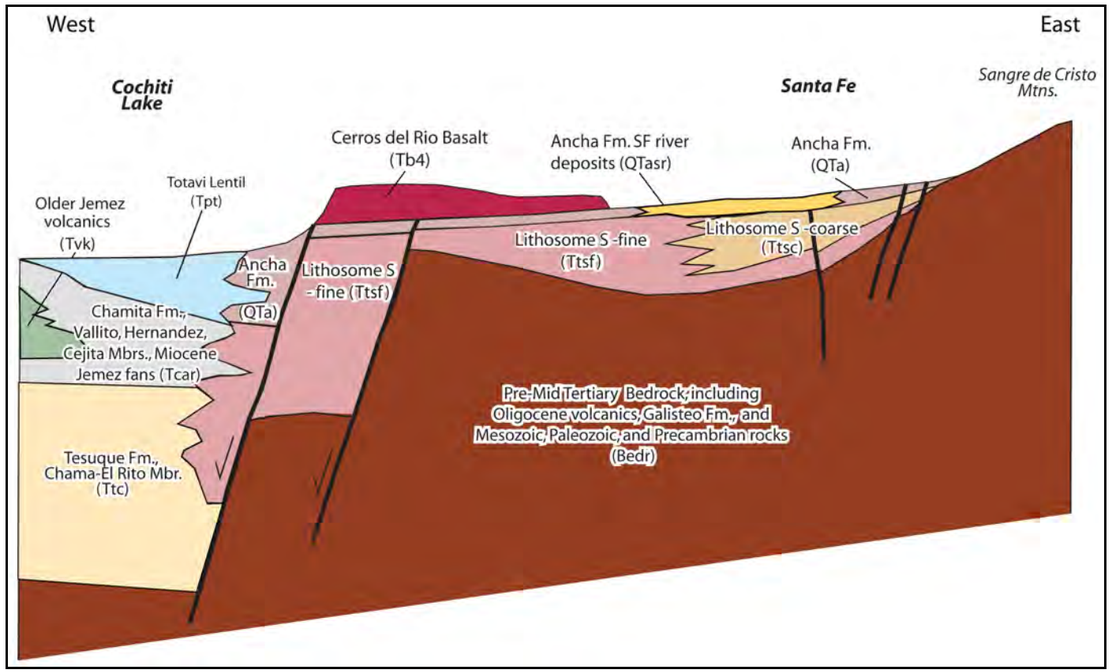


Figure 2-2. Schematic cross-section across the EB



Note: Volcanic material of the JVF dominates the upper portions of the section to the west.

Figure 2-3. Units of the northern portion of the SEB model



Note: The Cerros del Rio Basalts and ancestral Santa Fe River sediments encroach on Jemez volcanic fans to the west.

Figure 2-4. Units of the southern portion of the SEB model

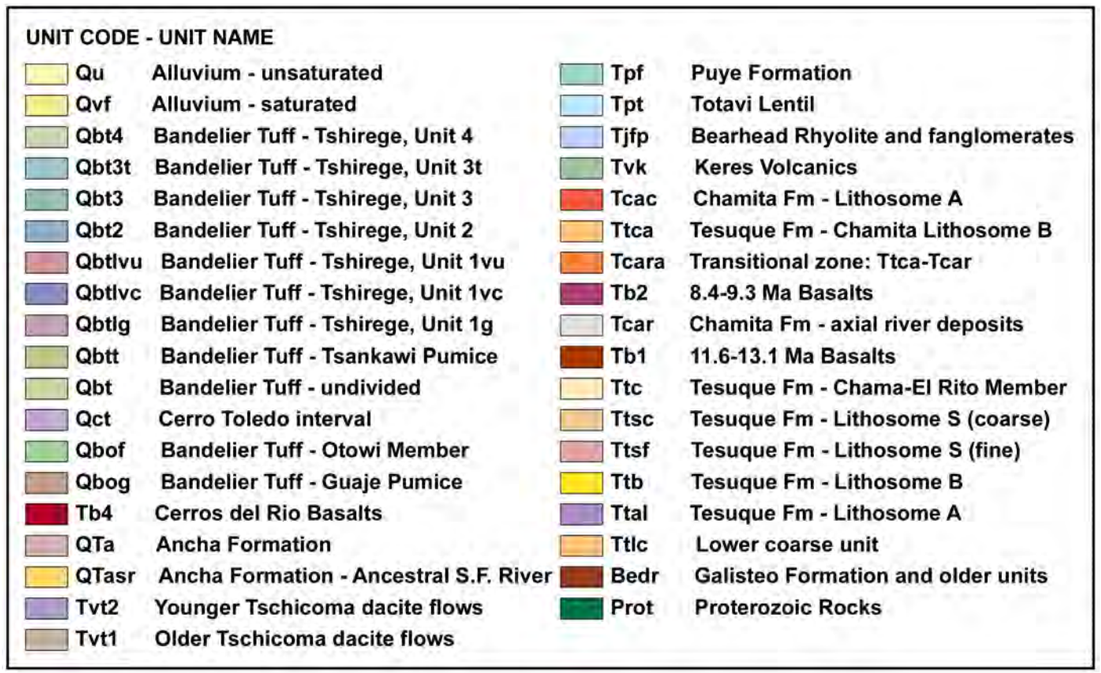


Figure 2-5. Codes and colors used for the GFM units

2.2 Stratigraphic/Geologic Units

The following section describes the modeled geologic units, which include both sedimentary and volcanic units. Figure 2-5 provides the colors and codes that are used in the GFM and on the plates provided in this atlas. Also included are descriptions (and colors) for several units within the SEB that do not extend into the reduced extent of the atlas. Plates showing the top structure and vertical thickness of each unit and the bottom structure of all units, except for the units/subunits of the Tshirege Member of the Bandelier Tuff, are provided as Plates 2-5 through 2-83. The alluvial units are not included in any of the models.

2.2.1 Tshirege Member, Bandelier Tuff (Qbt)

The Tshirege Member is the youngest member of the Bandelier Tuff, a multiple-flow ash-and-pumice unit that erupted from the Valles Caldera at approximately 1.22 Ma (Izett and Obradovich 1994, 048817; Spell et al. 1996, 055542). This is the most widely exposed bedrock unit of the Pajarito Plateau. The Tshirege Member tends to be more strongly welded than the Otowi Member, especially toward the western side of the plateau, closer to the Valles Caldera. Time breaks between the successive emplacements of ash-flow units caused the tuff to cool as several distinct cooling units, resulting in a complex internal stratigraphy that varies laterally as a function of distance from the caldera source. The stratigraphic nomenclature for the subunits of the Tshirege Member has evolved significantly through time (Broxton and Eller 1995, 058207; Broxton and Reneau 1995, 049726; Broxton and Vaniman 2005, 090038). The 2009 GFM follows the Tshirege subdivisions of the 2005 3-D GFM. The Tshirege Member is broken into a basal pumice layer and four overlying cooling units. Two of the cooling units are further subdivided, based on lithologic differences (Cole et al. 2006, 095079).

2.2.1.1 Unit 4 (Qbt4)

Unit 4 is a complex unit consisting of nonwelded to densely welded ash-flow tuffs that crop out in the western part of the Laboratory. Lewis et al. (2002, 073785) divide Qbt4 into local subunits and provide detailed descriptions of this heterogeneous unit. However, for the 3-D GFM, Qbt4 is not subdivided.

2.2.1.2 Unit 3t (Qbt3t)

Unit 3t is a moderately to densely welded ash-flow tuff that has petrographic and geochemical characteristics transitional between unit 3 and unit 4. Unit 3t is present in the western part of the Laboratory (Broxton and Vaniman 2005, 090038) and can impede the downward flow of surface water, creating seasonal springs along canyon walls.

2.2.1.3 Unit 3 (Qbt3)

Unit 3 is a nonwelded to partially welded tuff that forms the cap rock of mesas in the central part of the Pajarito Plateau. This unit and the overlying units Qbt3t and Qbt4 are absent from large areas in the eastern part of the Laboratory where they have been removed by erosion (Broxton and Eller 1995, 058207; Broxton and Reneau 1995, 049726; Broxton and Vaniman 2005, 090038).

2.2.1.4 Unit 2 (Qbt2)

Unit 2 is typically the most strongly welded tuff in the Tshirege Member and is characterized by lower porosity and higher density than the other units. It forms a distinctive medium-brown, vertical cliff that stands out in marked contrast

to the slope-forming, lighter-colored tuffs above and below. Unit 2 contains numerous well-developed, near-vertical fractures (Broxton and Reneau 1995, 049726; Broxton et al. 1995, 058207; Broxton and Vaniman 2005, 090038).

2.2.1.5 Unit 1

Cooling unit 1 of the Tshirege Member is a thick succession of ash-flow tuffs that dips gently east-southeast. This unit is characterized by a lack of welding and has been subdivided into a glassy lower tuff and an upper devitrified, vapor-phase crystallized tuff. The vapor-phase tuff is further divided into a colonnade portion and an upper portion (Broxton and Reneau 1995, 049726; Broxton and Vaniman 2005, 090038).

2.2.1.5.1 Unit 1vu (Qbt1vu)

The upper part of the vapor-phase unit (Qbt1vu) forms a distinctive grayish-white band between the darker colored colonnade tuff (Qbt1vc) below and unit 2 above. The upper vapor-phase unit is generally nonwelded and slope-forming, but in some localities it forms weakly developed cliffs and benches due to slight variations in welding (Broxton and Reneau 1995, 049726; Broxton and Vaniman 2005, 090038).

2.2.1.5.2 Unit 1, Colonnade (Qbt1vc)

The base of this altered vapor-phase unit (Qbt1vc) is a thin, horizontal zone of preferential weathering that forms a marker horizon, often called the vapor-phase notch, which marks the transition from glassy tuffs below to vapor-phase crystallized tuffs above. In some places, the vapor-phase notch grades laterally into a prominent bench developed on top of the glassy tuff. This colonnade vapor-phase tuff has distinctive columnar cooling joints and is a resistant, cliff-forming unit that may be slightly welded (Broxton and Reneau 1995, 049726; Broxton and Vaniman 2005, 090038).

2.2.1.5.3 Unit 1, Glassy (Qbt1g)

The lower part of unit 1 (Qbt1g) is not vapor-phase altered, retaining primary glass in both pumice and ash. Vapor-phase alteration is absent in this and all lower units of the Bandelier Tuff.

2.2.1.5.4 Unit 1 Tsankawi Pumice (Qbtt)

The Tsankawi Pumice Bed is the basal pumice fall of the Tshirege Member. This unit is typically 20 to 100 cm thick. Pumices in the Tsankawi Pumice Bed are mostly of rhyolitic composition, but there is a small (<5%) amount of dacitic pumice as well (Broxton and Reneau 1995, 049726). This pumice fall is vitric and unaltered by vapor-phase processes.

2.2.2 Cerro Toledo Interval (Qct)

The Cerro Toledo interval comprises a stratified sequence of volcaniclastic sediments and tephra and occurs between the two tuff members of the Bandelier Tuff. It is not considered as an integral part of the Bandelier Tuff (Broxton and Eller 1995, 058207; Broxton and Reneau 1995, 049726; Goff 1995, 049682; Broxton and Vaniman 2005, 090038). Structure contours for the base of the Cerro Toledo indicate that this unit fills a broad southeast-draining valley fed by one or more canyons exiting the Sierra de los Valles. The rhyolitic tuffaceous sandstone and tephra within this interval represent the reworked equivalents of Cerro Toledo rhyolitic tephra erupted from the Cerro Toledo and Rabbit Mountain dome complexes located northeast and southeast of the Valles Caldera, respectively. Clast-supported gravel, cobble, and boulder deposits derived from the Tschicoma Formation are interbedded with the tuffaceous rocks. In the western part of the Plateau, the interval also contains tuffaceous sediments that represent reworked Otowi Member of the Bandelier Tuff (Broxton and Vaniman 2005, 090038).

2.2.3 Otowi Member (Qbo)

The Otowi Member includes both the ash-flow (Qbof) and the basal pumice (Qbog).

2.2.3.1 Otowi Member, Bandelier Tuff (Qbof)

The Otowi Member consists of moderately consolidated, porous, nonwelded ash-flow tuffs. The ash-flow tuffs are vitric and contain light gray-to-orange pumice supported in a white to tan ashy matrix of glass shards, broken pumice, crystals, and rock fragments (Broxton et al. 1995, 058207; Goff 1995, 049682). Structure contours indicate that the Otowi Member ash-flow tuffs filled a broad south-draining paleovalley west of the Cerros del Rio basaltic highland and east of the Sierra de los Valles (Broxton and Vaniman 2005, 090038).

2.2.3.2 Guaje Pumice Bed, Otowi Member, Bandelier Tuff (Qbog)

The Guaje Pumice Bed forms the base of the Otowi Member of the Bandelier Tuff, which erupted from the Toledo Caldera at approximately 1.61 Ma (Izett and Obradovich 1994, 048817, Spell et al. 1996, 055542). The Guaje Pumice Bed contains layers of sorted vitric pumice fragments whose mean size varies between 2 and 4 cm. It has an average thickness of ~9 m over much of the Plateau. Geophysical logs show that the Guaje Pumice Bed has a higher porosity than overlying Otowi Member ash-flow tuffs and the underlying Puye Formation (Broxton and Vaniman 2005, 090038).

2.2.4 Puye Formation

The Puye Formation is a large apron of overlapping alluvial and pyroclastic fans that were shed eastward from the JVF into the western EB (Griggs and Hem 1964, 092516; Bailey et al. 1969, 021498). This unit consists of highly stratified, poorly cemented gravels and conglomerates, consisting of subrounded dacitic and andesitic lava clasts in a poorly sorted, sandy to silty matrix. Debris flows, ash beds, pumiceous volcaniclastic sediments, and beds of fluvial sand and silt are interbedded with the gravels and conglomerates. Because its primary source area was volcanic domes in the Sierra de los Valles, the Puye Formation overlaps and postdates the Tschicoma Formation (Broxton and Vaniman 2005, 090038).

2.2.5 Tschicoma Formation

The Tschicoma Formation includes dacitic to low-silica rhyolitic flows.

2.2.5.1 Tschicoma Formation, Pajarito and Caballo Mountains, Cerro Grande (Tvt2)

The Tschicoma Formation of the Polvadera Group consists of thick dacitic to low-silica rhyolitic lava flows that make up the rugged Sierra de los Valles highlands west of Los Alamos. The flows erupted from large overlapping dome complexes. The upper portion of this unit (Tvt2) includes the Pajarito Mountain, Cerro Grande, and Caballo Mountain lobes of the Tschicoma Formation, as well as fine-grained dacites encountered in the subsurface of an unknown source. Lavas from the Pajarito Mountain, Cerro Grande, and Caballo Mountain centers are predominantly dacite, aged between 2.93 and 3.35 Ma (Broxton and Vaniman 2005, 090038).

2.2.5.2 Tschicoma Formation, Rendija Canyon Lobe (Tvt1)

The lower portion of the Tschicoma Formation (Tvt1) consists of the Rendija Canyon lobe and includes low-silica rhyolite erupted from a deeply eroded dome complex in the Rendija Canyon and Guaje Mountain area that has yielded ages between 4.98 and 5.36 Ma (Broxton et al. 2007, 106121).

2.2.6 Cerros del Rio Basalt (Tb4)

The Cerros del Rio volcanic field was active from approximately 4.5 to 2.0 Ma (WoldeGabriel et al. 2001, 092523). These rocks are mostly basalts and basaltic andesites, but subordinate dacite is also present. The Cerros del Rio Basalt is generally composed of thick sequences of stacked lava flows separated by interflow breccia, scoria, sediment, and ash. Outcrops of the Cerros del Rio Basalt cap the Tesuque Formation east of the Rio Grande and the Puye Formation in the vicinity of White Rock. These basalts are buried to increasing depths below the Plateau in the

central portions of the model and may lap onto or interfinger with the Tschicoma flows at isolated locations to the west (Cole et al. 2006, 095079).

2.2.7 Ancha Formation

The Ancha Formation was deposited on an alluvial slope in the Santa Fe area by west-flowing, ephemeral streams (Koning et al. 2002, 105711). It overlies older strata across an angular unconformity. The Ancha Formation contains a coarse-grained and a fine-grained part (Koning et al. 2002, 105711).

2.2.7.1 Ancha Formation (QTa)

Found near the base of the deposit and the mountain front to the east, the coarse-grained part is commonly reddish and consists of sandy pebbles to cobbles. The coarse-grained deposit laterally grades westward into a finer-grained deposit consisting of light yellowish brown to brownish yellow, silty-clayey sand (mostly very fine- to medium-grained). In many places, the Ancha Formation is not saturated. Where it is saturated, groundwater is found near the base of the deposit where the deposit is relatively thick (50–90 m thick). Most of the deposition occurred in the late Pliocene, with aggradation continuing near the mountain-front during the early Pleistocene (Koning et al. 2002, 105711).

2.2.7.2 Ancha Formation, Santa Fe River (QTasr)

An ancestral Santa Fe River was present during Ancha Formation deposition (primarily late Pliocene). The river deposited relatively coarse-grained sediment that interfingers southward and northward into alluvial slope deposits of unit QTa. The sediment of this unit contains sandy gravel (typically cobbles and pebbles) that interfinger with overbank facies of clayey-silty sand. Colors are generally reddish. Near Santa Fe, the unit is inset into lithosome S of the Tesuque Formation (Ttsc).

2.2.8 Totavi Lentil (Tpt)

This unit includes the Totavi Lentil as well as older river gravels. Based on new well data, it appears that the Totavi Lentil river gravels may form lenticular deposits of limited lateral extent and that ancient river deposits in the Pajarito Plateau area are coeval with a variety of stratigraphic units that span a longer time interval than previously recognized (Broxton and Vaniman 2005, 090038). The river gravels probably represent channel deposits of the ancestral Rio Chama/Rio Grande drainages and contain Precambrian and younger cobbles from northern source areas, indicating through-going, north-to-south fluvial systems dating to at least approximately 7.9 Ma (Broxton and Vaniman 2005, 090038; Broxton et al. 2006, 092520).

2.2.9 Bearhead Rhyolite and Fanglomerates (Tjfp)

This unit incorporates the pumiceous Bearhead Rhyolite, vitric pumiceous deposits related to the Peralta Tuff, and older fanglomerate material derived predominantly from erosion of the Keres Group volcanic highlands. These fanglomerates interfinger with Santa Fe Group sands within a north-south trending, troughlike structure in the central portion of the Plateau. This unit does not crop out; its existence and modeled geometry are based solely on well logs and cuttings and surrounding geologic controls. The geometry of this unit suggests deposition within a fault-controlled basin with associated episodic basaltic volcanism (Cole et al. 2006, 095079). This unit tends to be part of the most productive aquifer beneath the Pajarito Plateau (Purtymun 1995, 045344).

2.2.10 Keres Group Volcanics (Tvk)

The Keres Group includes basaltic and rhyolitic rocks that erupted as the JVF began to develop (Gardner et al. 1986, 059104; Goff and Gardner 2004, 092526). These rocks intrude and cover Santa Fe Group rocks along the western edge of the EB (Cole et al. 2006, 095079).

2.2.11 Chamita Formation

The Chamita Formation forms the upper part of the Santa Fe Group.

2.2.11.1 Chamita Formation, Lithosome A (Tcac)

Lithosome A of the Chamita Formation is used to designate strata containing arkosic sand and granite-bearing gravel that were deposited on an alluvial slope by streams draining the west flank of the Sangre de Cristo Mountains south of Truchas Peaks (Cavazza 1986, 105708). Technically, lithosome A extends into the Tesuque Formation east of the Rio Grande (Koning and Aby 2005, 106162).

Lithosome A that is younger than 13.2 Ma is relatively coarser grained (Koning 2002, 105710; Koning et al. 2002, 105711; Koning et al. 2005, 106120), and consists of slightly orange-tan, coarse channel-fill of sandy conglomerate and conglomeratic sandstone, interbedded with subordinate clayey-silty sandstone. Unit Tcac reflects this coarse-grained lithosome A, excluding relatively fine-grained, distal alluvial slope strata. These relatively coarse strata correlate with the Cuarteles Member of the Chamita and Tesuque Formations (Koning and Aby 2005, 106162; Koning et al. 2005, 106120). The Cuarteles Member is considered part of the Tesuque Formation east of the Rio Grande and part of the Chamita Formation west of the Rio Grande. This unit interfingers westward with unit Ttca and gradationally overlies unit Ttca.

2.2.11.2 Chamita and Tesuque Formations, Lithosome A (Ttca)

Unit Ttca includes relatively fine-grained, distal alluvial slope strata that postdates the 13.2 Ma coarsening of Tcac (Koning et al. 2007, 106122). The sediment is a slightly orange-tan to tan, clayey-silty sandstone intercalated with subordinate coarse channel-fills of sandy conglomerate and conglomeratic sandstone. Gravel includes granite with minor, yellowish Paleozoic limestone and siltstone. Minor quartzite clasts are also present. The unit correlates with the fine-grained, distal Cuarteles Member of the Chamita and Tesuque Formations (Koning and Aby 2005, 106162; Koning et al. 2005, 106120) and also correlates with lithosome A sediment of the Pojoaque, Skull Ridge, and Nambe Members of the Tesuque Formation (Cavazza 1986, 105708). This unit grades laterally westward into lithosome B (Ttb) and laterally southward into deposits of the ancestral Santa Fe River (units Ttsc and Ttsf).

2.2.11.3 Transition Zone between Ttca and Tcar (Tcara)

This unit reflects a zone of interfingering and mixing between coarse-grained lithosome A and the axial river deposits of the Chamita Formation. Lithosome A in this zone is typically a slightly orange-tan, silty-clayey sand, interbedded with minor pebbly channel-fills. The axial river deposits include floodplain deposits of claystone, siltstone, and very fine- to medium-grained sandstone that are subequal in proportion to coarse channel-fills of fine- to very coarse-grained sand, pebbly sand, and sandy pebbles-cobbles. Colors of the axial river deposits are generally tannish. This unit interfingers eastward with unit Ttca, and interfingers westward with unit Tcar. It gradationally overlies lithosome B of the Tesuque Formation (Ttb).

2.2.11.4 Chamita Formation, Axial River Deposits (Tcar)

Sediments deposited by the river system flowing south along the basin floor of the EB coarsened after ~13.2 Ma (Koning et al. 2005, 106120; Koning et al. 2007, 106122). This coarser sediment consists primarily of channel-fills of sandstone, gravelly sandstone, and sandy conglomerate. Floodplain deposits of claystone, siltstone, and very fine- to medium-grained sandstone are subequal in proportion to the coarse channel-fills. The gravel of the axial river deposits contains felsic to intermediate volcanic clasts, with lesser quartzite and Paleozoic sedimentary clasts. Tannish colors generally typify the unit. The unit correlates to the Vallito, Hernandez, and Cejita Members of the Chamita Formation (Koning and Aby 2005, 106162). The unit includes sandy channel-fills from a drainage that flowed southeastward in the region that is now the Jemez Mountains. This unit interfingers eastward with unit Tcara and overlies units Ttb and Ttc.

2.2.12 8.4–9.3 Ma Basalts (Tb2)

The Bayo Canyon Basalt is a rift basalt and consists of local, episodic, Miocene basalt to latitic flows that are 8.4 to 9.3 Ma (WoldeGabriel et al. 1996, 054427; WoldeGabriel et al. 2001, 092523) that are interbedded with basin sediments. The flows are intermixed with both Keres Group and Santa Fe Group sedimentary units in a zone that extends from the central plateau east to Bayo Canyon, and south to Ancho Canyon (Cole et al. 2006, 095079). Model boundaries for this unit extend from the bottom of the oldest flow to the top of the youngest flow. Thus, the volume of this unit includes any intercalated sediments.

2.2.13 11.6–13.1 Ma Basalts (Tb1)

The Guaje Canyon Basalt (Tb1) is a thick sequence of basalt flows contained within the Tesuque Formation in the vicinity of Guaje Canyon. The basalts range from 11.55 to 13.1 Ma (WoldeGabriel et al. 1996, 054427; WoldeGabriel et al. 2001, 092523). The Tb1 unit crosses the stratigraphic boundary between the Chamita Formation (Tcar) and the Chama–El Rito Member of the Tesuque Formation (Ttc). The portion of this flow unit within Ttc is designated as Tb1a. The portion of this flow unit within Tcar is designated as Tb1b.

2.2.14 Tesuque Formation

The Tesuque Formation forms the lower part of the Santa Fe Group.

2.2.14.1 Tesuque Formation, Chama–El Rito Member (Ttc)

In the study area, strata assigned to the Chama–El Rito Member are light orange-tan. Sediment consists primarily of very fine- to medium-grained sand, siltstone, and claystone. Pebble beds are very sparse. The unit was deposited on a southward-southeastward alluvial slope environment in the west part of the EB during the early to middle Miocene epoch. The unit includes quartz-rich sand from a southeast-flowing, tributary drainage. This unit gradationally underlies unit Tcar and interfingers eastward with lithosome B of the Tesuque Formation (Ttb).

2.2.14.2 Tesuque Formation, Lithosome S, Coarse-Grained Part (Ttsc)

An ancestral equivalent of the Santa Fe River deposited relatively coarse-grained sediment in the Santa Fe area during the early to middle Miocene epoch. This sediment was named lithosome S by Koning et al. (2004, 106104). Generally reddish, this sediment consists mostly of pebbly sand and sandy pebble channel-fills. Overbank deposits of clay, siltstone, and clayey very fine- to fine-grained sandstone are subordinate. Gravel includes granite with minor, yellowish Paleozoic limestone and siltstone. Minor quartzite clasts are also present. The unit grades northward into lithosomes A and B (units Ttca and Ttb) and westward into finer-grained lithosome S (Ttsf). The unit gradationally overlies the finer-grained part of lithosome S (Ttsf).

2.2.14.3 Tesuque Formation, Lithosome S, Fine-Grained Part (Ttsf)

This unit is also identified as a part of lithosome S by Koning et al. (2004, 106104). Although finer grained than the coarse-grained part of lithosome S (Ttsc), the finer-grained part of lithosome S is still, in an overall sense, coarser grained than lithosomes B and A to the north (units TTb and Ttca). This unit contains relatively abundant, reddish clay, silt, and very fine- to medium-grained sand deposits, which are intercalated with subordinate coarse-grained channel-fills of pebbly sand and sandy pebbles-cobbles. The finer-grained part of lithosome S grades northward into lithosomes A and B (units Ttca and Ttb) and westward into lithosome B (Ttb). The unit gradationally underlies the coarser-grained part of lithosome S (Ttsc).

2.2.14.4 Tesuque Formation, Lithosome B (Ttb)

Lithosome B was deposited on a wide basin floor between approximately 25 and 13 Ma by a drainage system flowing south southwest from the San Luis Basin and Peñasco embayment (Cavazza 1986, 105708; Koning et al. 2005, 106120). Relatively fine-grained, overbank deposits predominate in the SEB model area (Koning 2002, 105710; Koning and Maldonado 2003, 106112). These consist of light gray to light greenish gray clay, silt, and very fine- to medium-grained sand. Subordinate coarse-grained channels contain medium- to very coarse-grained sand, pebbly sand, and sandy pebbles. Gravel includes clasts of Paleozoic sedimentary rocks (limestone, sandstone, and siltstone), in addition to minor quartzite and felsic-intermediate volcanic clasts. This unit grades southward into ancestral Santa Fe River deposits (units Ttsc and Ttsf) and eastward into alluvial slope deposits of lithosome A (Ttca).

2.2.14.5 Tesuque Formation, Lower Lithosome A, Fine Grained (Ttal)

In the Santa Fe area, adjacent to the Sangre de Cristo Mountain front, lies tannish to pinkish sand, clayey sand, and pebbly-cobbly sand. Gravel contains primarily granite clasts, although locally, yellowish Paleozoic limestone-siltstone clasts are present. This unit is well-consolidated and underlies fine-grained lithosome S. It grades northward into the lower, coarse-grained unit (Ttlc).

2.2.14.6 Tesuque Formation, Lower Coarse Unit (Ttlc)

At the base of the Santa Fe Group in the eastern E, lies relatively coarse-grained, alluvial slope deposits. This sediment is tannish to pinkish and contains channel-fills of sandy pebbles-cobbles, pebbly sand, and very fine- to very coarse-grained sand. Overbank beds of clay, silt, and very fine- to fine-grained sand are minor. Gravel contains primarily granite clasts, although the proportion of Paleozoic limestone clasts increases to the south. Near the Rio Tesuque drainage, the proportion of Paleozoic limestone clasts increases down section. This unit grades laterally southward into unit Ttal and is gradationally overlain by unit Ttca. This unit grades laterally westward into lithosome B (unit Ttb).

2.2.15 Bedrock (Bedr)

Underlying the Santa Fe Group are various, typically well-cemented or indurated, formations that we have combined into one unit called “bedrock,” or the Pre-Miocene-Tertiary bedrock. This surface represents the base of the Santa Fe Group, as defined by Grauch et al. (available at http://pubs.usgs.gov/pp/1761/). The combined formations of this unit are described from top to bottom (youngest to oldest). At the top of this unit are lava flows and intercalated, mafic volcaniclastic deposits of the Cieneguilla basanite; this unit is typically dark gray. The Espinaso Formation consists of alluvial fan deposits that were shed away from a volcanic edifice centered near the Cerrillos Hills–La Cienega area. The sediment is composed of latitic to andesitic detritus. There are minor latitic flows intercalated in the well-cemented, light gray to gray alluvial fan deposits. The Galisteo Formation includes red sandstone, pebbly sandstone, and mudstone deposited in a depression formed during the Laramide orogeny. Sand and clasts in the study area are primarily of arkosic and granitic composition, with minor Paleozoic limestone detritus. Mesozoic–Paleozoic strata in the study area mostly consist of interbedded limestone, shale, and sandstone.

The EB model includes an older/deeper unit of Proterozoic rocks that includes pink to red granite and gneiss to the southwest of the model (Goff 2009, 106105), and metasedimentary, metavolcanic, and granitic rocks to the east (Daniel 1995, 106123). This unit is not shown in the atlas because it will be added to the model at a later date when the full basin model is completed. Within the extent of the atlas, this unit is probably located at depths below sea level.

3.0 MAPPING OF THE REGIONAL WATER-TABLE ELEVATION

The regional aquifer beneath the Laboratory is a complex hydrogeological system. The top of the aquifer is predominantly under phreatic (water-table) conditions. However, there are also areas of local confinement that are caused by local hydrogeological conditions. In general, the top of the regional aquifer is defined by the elevation of the regional water table. In the areas of local confinement, there is a regional piezometric surface that represents the elevation of hydraulic heads in the confined zones. In general, the regional piezometric surface can be considered to represent a spatial continuation of the water table in the confined areas. Because the aquifer is predominantly under

phreatic conditions, in the text below, the term “regional water table” is used even though in some areas of the aquifer the term “regional piezometric surface” is more appropriate.

The general shape of the regional water table is predominantly controlled by the areas of regional recharge to the west (flanks of Sierra de los Valles) and discharge to the east (the Rio Grande and the White Rock Canyon Springs). The structure of regional phreatic flow is also expected to be impacted by (1) local infiltration zones (e.g., beneath wet canyons), (2) aquifer properties heterogeneity, and (3) discharge zones (water supply wells and springs).

Information about the elevation of the regional water table is provided by existing data from monitoring wells (water levels) and selected springs (discharge elevations). Well data are predominantly applied to map the elevation of the regional water table; spring discharge elevations are used only in the vicinity of White Rock Canyon to provide additional constraints on the water-table elevation.

Water-table elevations vary in time due to transient effects that include pumping of the water supply wells, and large- and small-scale variability in aquifer recharge. Therefore, water-level maps represent specific periods of time. Based on analysis of 2008 water-level data (Koch and Schmeer 2009, 105181), it has been observed that water levels generally reached recent maxima in March 2008. The March 2008 data are likely to be the least affected by pumping and thus are potentially most representative of ambient flow conditions. Therefore, these data are used, in part, to construct the water-table map.

Monthly averaged water levels for March 2008 are computed for 36 regional aquifer wells and presented in Table 3-1. For the wells, R-7, R-14, R-33, and R-36, water-level data are not available for March 2008 (Table 3-1), and alternative periods of representative measurements have been selected. For five wells, H-19, TW-1, TW-2, TW-3 and TW-4 (Table 3-1), historic water-level data considered to be less certain but important for constraining the water-table map in the northern portion of the Laboratory site are used. New water-level data are also available from a series of recently drilled wells (R-38, R-39, R-40, R-41, R-42, R-43, R-44, R-45, and R-46), but the measurements are difficult to interpret because they are preliminary and for a different time period. Future analysis will address how these data will be incorporated in the water-table mapping. The available preliminary water-level measurements for these wells are listed in Table 3-1 but are not applied in the mapping process.

Inclusion of water-level data that do not represent the March 2008 time period is a source of uncertainty in the mapping process. Differences in the screen placements and local hydrogeologic conditions also complicate the interpretation of the water-level data for the following reasons.

1. Some screens are substantially below the top of regional saturation (more than 60 ft); as a result, the collected water-level data may not be representative of the actual water-table elevations (TW-1, R-10a, R-13, R-18, R-20, R-21, R-24, R-26, R-32, and R-34; 10 wells in total).
2. Some screens are long (more than 50 ft) and may represent composite water levels within the aquifer (DT-5A, DT-9, DT-10, R-8, R-13, and R-15; 6 wells in total).
3. Some screens are potentially under confined conditions and may represent piezometric surface elevations (R-4 and R-24; 2 wells).
4. R-25 is drilled in a complicated hydrogeological setting, and it is uncertain which of the R-25 screens (screen 4 or 5) provides information about the water-table elevation.
5. R-9 is screened in a zone (basalts within Santa Fe Group, Tb2) that is potentially disconnected from the regional aquifer. The regional aquifer screen R-12 is in a similar setting, but this screen has been plugged and abandoned. Water-table screens are located in various hydrostratigraphic units, including sedimentary and volcanic rocks with contrasting hydrogeologic properties (Table 3-1). The structure of the regional water table is probably impacted by groundwater flow within hydrostratigraphic units with contrasting properties. For example, low permeability lava flows may divert the phreatic groundwater flow. Lavas occur at or near the regional water table at R-5, R-9, and R-12 (Miocene basalts [Tb2], and at R-32, R-20, and R-22 [Cerros del Rio Basalts, Tb4]).

Related to issue 5 above, the regional water levels observed at R-9 and at the former R-12 regional screen are substantially lower than water levels observed at nearby wells. (Since December 2007, the regional screen at R-12, screen 3, is abandoned and not monitored; the regional screen of R-12 is replaced by R-36.) The regional screens in both wells are in Miocene basalt (Tb2). R-9 and R-12 monitoring wells are located near water supply wells PM-1 and O-1, and their low water levels might define cones of drawdown around the production wells. However, water levels at R-9 and R-12 do not respond to daily or seasonal changes in municipal water production, suggesting that their low heads are not caused by the water supply pumping. Alternatively, the regional screens at R-9 and R-12 may represent a deep compartmentalized zone within the Santa Fe Group basalt that is in poor hydraulic connection with the rest of the aquifer.

Because of the uncertainties described above, we evaluated a series of alternative conceptual-model assumptions pertaining to the regional groundwater flow and chose the model presented in Plate 3-1.

The process of water-table contouring is theoretically constrained by the following conformity rules (Freeze and Cherry 1979, 088742): (1) the contour lines should be perpendicular to the flow paths and (2) the length and the width of the flow net cells formed by the contour lines between two adjacent flow paths should have the same ratios. These rules are theoretically valid only for the case of a uniform isotropic aquifer with no recharge/discharge sources within flow net cells. Deviations from the conformity rules are caused by aquifer heterogeneity and anisotropy as well as recharge/discharge sources within flow net cells.

The regional water table is contoured by attempting to satisfy three goals simultaneously: (1) to match the water-level data at the monitoring wells, (2) to account for issues of data representativeness, and (3) to preserve flow net conformity. Plate 3-1 is a contour map of the regional water table that attempts to satisfy those three goals. The actual contouring is performed using a combination of manual and automated techniques. (The automated contouring is performed using the standard splining methods.) Table 3-1 lists the deviations between observed and predicted (based on the contoured water-table map) water levels.

The water-level data and the contoured map (Plate 3-1) suggest potential mounding of the regional water table near TW-1, R-8, and R-36 (the water level at R-36 is slightly higher than the water levels of R-28 and R-11). The mounding may result from local recharge of the regional aquifer along Los Alamos, Pueblo, and Sandia Canyons.

The water-level data represented by the contour map indicate that thick lavas near R-32 and R-22 may be the cause of the increased phreatic hydraulic gradients in this area. This may be the result of lower transmissive properties of lava flows compared with the more transmissive Puye Formation and Santa Fe Group sediments. The hydrogeologic properties associated with the lava flows may be also responsible for diverting the flow of phreatic groundwater to the north. The increased hydraulic gradients in the area of R-32 and R-22 may also be an indication of recharge in the lower Pajarito Canyon area that causes local mounding in the lavas, which are expected to be of low storativity when compared with the Puye Formation fanglomerates and Santa Fe Group sediments.

Table 3-1 also lists the differences between observed and contoured water-level elevations displayed in Plate 3-1. Most of the discrepancies are minor and within 3 ft. Substantial deviations are calculated for locations at which the water-level data are uncertain: TW-1, R-5, R-9, R-8, R-10a, and R-25. The table also compares the predicted water levels with recently collected water-level data not included in the mapping. Substantial differences are observed only at R-41 and R-46 where static water-level conditions may not have been achieved. Future analysis will incorporate the water-level data from recently installed monitoring wells.

Plate 3-2 identifies the modeled geologic units present at the regional water table model.

Table 3-1.
Summary of Well-Screen Positions, Water-Level Observations, and Differences between Observed and Contoured Water Levels

Well/Screen Name	Geologic Unit	Surface Elevation (ft)	Screen Top (ft bgs)	Screen Bottom (ft bgs)	Screen Length (ft)	Observed Water-Level Elevation (ft)	Representative Measurement Period	Top of the Screen from the Water Level (ft)	Comments	Differences between Observed and Contoured Water-Level Elevation (ft)
H-19	Tpf	7172	—*	—	—	6228.00	Jan-51	—	Historic observation applied to constrain water-levels in the NW section of LANL site. The data are uncertain	1.47
TW-1	Tcar	6369.19	632.00	642.00	10.00	5855.50	Feb-06	118.31	Historic observation applied to constrain water-levels in the NE section of LANL site. The data are uncertain and potentially affected by well construction problems	35.53
TW-2	Tcar	6648.06	768.00	824.00	56.00	5845.70	Oct-00	-34.36	Historic observation applied to constrain water-levels in the N section of LANL site. The data are uncertain	0.09
TW-3	Tcar	6626.90	805.00	815.00	10.00	5840.10	Feb-06	18.20	Historic observation applied to constrain water-levels in the N section of LANL site. The data are uncertain	0.74
TW-4	Tvt1	7244.56	1195.00	1205.00	10.00	6071.50	Feb-06	21.94	Historic observation applied to constrain water-levels in the NW corner of LANL site. The data are uncertain	1.79
CdV-16-3i	Tvt2	7486.40	—	—	—	6136.75	Oct-05	—	Open borehole. The data are uncertain	2.17
CdV-R-15-3#4	Tpf	7258.90	1235.10	1278.90	43.80	6019.50	Mar-08	-4.30	No comment	-1.17
CdV-R-37-2#2	Tvt2	7330.60	1188.70	1213.80	25.10	6137.00	Mar-08	-4.90	No comment	0.62
DT-10	Tb4/Tpf/Tcar	7019.00	1080.00	1408.00	328.00	5918.70	Mar-08	-20.30	Long screen; Composite water-level expected	1.31
DT-5A	Tb4/Tpf/Tcar	7144.20	1172.00	1821.00	649.00	5958.08	Mar-08	-14.12	Long screen; Composite water-level expected	0.10
DT-9	Tb4/Tpf/Tcar	6936.00	1040.00	1501.00	461.00	5915.12	Mar-08	19.12	Long screen; Composite water-level expected	0.71
R-1	Tjfp	6881.21	1031.12	1057.42	26.30	5878.27	Mar-08	28.18	No comment	-0.44
R-2	Tcar	6770.38	906.45	929.57	23.12	5870.65	Mar-08	6.72	No comment	-0.46
R-4	Tcar	6577.49	792.90	816.00	23.10	5830.83	Mar-08	46.24	Hydrogeologic data suggest confined conditions	-0.84
R-5#3	Tcar	6472.60	676.90	720.30	43.40	5766.75	Mar-08	-28.95	No comment	-42.83
R-6	Tcar	6995.80	1205.00	1228.00	23.00	5838.44	Mar-08	47.64	Screen significantly below water table	-0.82
R-7#3	Tjfp	6779.20	895.50	937.40	41.90	5877.25	Apr-08	-6.45	Water-level data missing for Mar 2008	-0.91
R-8#1	Tcar	6544.74	705.31	755.70	50.39	5853.22	Mar-08	13.79	Long screen below water table	7.29
R-9	Tb2	6382.80	683.00	748.50	65.50	5691.52	Mar-08	-8.28	Water-level may be not representative of the regional water-table due to local aquifer heterogeneities	-108.48
R-10a	Tcar	6363.74	690.00	700.00	10.00	5740.49	Mar-08	66.75	Screen significantly below water table	-3.65
R-11	Tjfp	6673.72	855.00	877.90	22.90	5837.78	Mar-08	19.06	No comment	0.19
R-13	Tpf/Tjfp	6673.05	958.33	1018.72	60.39	5836.08	Mar-08	121.36	Long screen significantly below water table	0.18
R-14#1	Tpf/Tjfp	7062.08	1200.60	1233.20	32.60	5880.19	Feb-08	18.71	Water-level data missing for Mar 2008	0.00
R-15	Tpf/Tjfp	6820.00	958.60	1020.30	61.70	5850.65	Mar-08	-10.75	Long screen; Compsite water-level expected	-0.41
R-16r	Tpt	6256.97	600.00	617.60	17.60	5692.58	Mar-08	35.61	No comment	-0.08
R-17#1	Tpf	6921.51	1057	1080	23.00	5884.77	Mar-08	20.26	No comment	-0.05
R-18	Tpf	7404.83	1358.00	1381.00	23.00	6117.11	Mar-08	70.28	Screen significantly below water table	-0.93
R-19#3	Tpf	7066.30	1171.40	1215.40	44.00	5887.40	Mar-08	-7.50	No comment	-0.73
R-20#1	Tb4	6694.35	904.60	912.20	7.60	5864.60	Mar-08	74.85	Screen significantly below water table	1.26
R-21	Tpf	6656.24	888.80	906.80	18.00	5854.53	Mar-08	87.09	Screen significantly below water table	0.19
R-22#1	Tb4	6650.50	872.30	914.20	41.90	5755.00	Mar-08	-23.20	No comment	0.28

Table 3-1. (continued)

Well/Screen Name	Geologic Unit	Surface Elevation (ft)	Screen Top (ft bgs)	Screen Bottom (ft bgs)	Screen Length (ft)	Observed Water-Level Elevation (ft)	Representative Measurement Period	Top of the Screen from the Water Level (ft)	Comments	Differences between Observed and Contoured Water-Level Elevation (ft)
R-23	Tcar	6527.75	816.00	873.20	57.20	5697.41	Mar-08	-14.34	No comment	0.09
R-24	Tcar	6547.38	825.00	848.00	23.00	5830.04	Mar-08	107.66	Hydrogeologic data suggest confined conditions	-1.17
R-25#5	Tpf	7516.10	1294.70	1304.70	10.00	6234.27	Mar-08	12.87	Uncertain which of the R-25 screens characterizes water-table elevation (4 or 5)	-4.15
R-26#2	Tpf	7641.69	1422.00	1445.00	23.00	6538.00	Mar-08	318.31	Screen significantly below water table	-2.20
R-27	Tpf	6713.72	852	875	23.00	5898.21	Mar-08	36.49	No comment	-0.79
R-28	Tpf/Tjfp	6728.61	934.30	958.10	23.80	5838.31	Mar-08	44.00	Screen significantly below water table	1.13
R-31#2	Tb4	6362.50	515.00	545.70	30.70	5827.44	Mar-08	-20.06	No comment	0.29
R-32#1	Tb4/Tpt	6637.63	867.50	875.20	7.70	5852.74	Mar-08	82.61	Hydrogeologic data suggest confined conditions	0.19
R-33#1	Tjfp	6853.33	995.50	1018.50	23.00	5871.20	Jun-08	13.37	Water-level data missing for Mar 2008	-0.34
R-34	Tcar	6629.99	883.70	906.60	22.90	5834.47	Mar-08	88.18	Screen significantly below water table	0.51
R-35b	Tpf	6625.21	825.40	848.50	23.10	5837.00	Mar-08	37.19	No comment	-0.66
R-36	Tcar	6591.37	766.90	789.90	23.00	5839.47	Apr-08	15.00	Water-level data not available for Mar 2008	1.49
R-38	Tpf	6668.58	821.20	831.20	10.00	5858.73	Jan-09	11.35	Recently installed well. Insufficient water-level record; Hydrogeologic data suggest confined conditions	1.43
R-39	Tb4/Tpf	6580.86	859.00	869.00	10.00	5754.16	Jan-09	32.30	Recently installed well. Insufficient water-level record; Hydrogeologic data suggest confined conditions	-2.85
R-40 # 2	Tpf	6718.00	849.30	870.00	20.70	5864.10	Oct-08	-4.60	Recently installed well. Insufficient water-level record	-2.78
R-41	Tpt	6650.50	965.00	975.00	10.00	5690.37	Mar-09	4.87	Recently installed well. Insufficient water-level record	-72.26
R-42	Tjfp	6759.02	931.80	952.90	21.10	5839.22	Nov-08	12.00	Recently installed well. Insufficient water-level record	0.49
R-43#1	Tcar	6732.65	903.90	924.60	20.70	5839.65	Jan-09	10.90	Recently installed well. Insufficient water-level record	-1.88
R-44#1	Tpf	6714.91	895.00	905.00	10.00	5835.91	Jan-09	16.00	Recently installed well. Insufficient water-level record	-1.25
R-45#1	Tpf	6704.02	880.00	890.00	10.00	5836.12	Jan-09	12.10	Recently installed well. Insufficient water-level record	0.45
R-46	Tpf	7213.33	1340.00	1360.00	20.00	5885.33	Jan-09	12.00	Recently installed well. Insufficient water-level record	-12.17

*— = No data.

4.0 MAP SPECIFICATIONS

All maps are presented in 11- × 17-in. format at a scale of 1:80,000. All map plates include the boundary of the Laboratory and major roads for reference. Unit codes and colors, as defined in Figure 2-5, are consistent for all plates, cross-sections, and 3-D views. The map indices for wells are consistent throughout the set of plates.

Plates mapping the unit surfaces provide well locations only for those wells that contribute exact data to the surface that is mapped. “Exact” is used to mean “hard” data that provide an elevation value. Other wells contain “soft” data that provide “greater than,” “less than,” or “absent” constraints. While this “soft” information is used in the development of the surfaces, well locations for these data are not shown. In some cases, the density of the data prevents identification of all wells with “hard” constraints.

The principal component of an atlas is the set of maps or plates. The maps of this atlas provide the identification and/or definition of surface and subsurface features for the region encompassing the Laboratory and the town of Los Alamos (including White Rock), extending west past the Pajarito Fault zone into the Sierra de los Valles, and east approximately 8 mi past the eastern extent of the Laboratory boundary. The maps are presented using New Mexico state plane (NAD 83) coordinates (in feet). The mapped area, and the reference grid with labels outside of the map area, are extended to the full page size. Placement of map labels, legends, scale, north arrow, and descriptive text are therefore restricted to within the map area, resulting in the masking of some of the map data.

The Laboratory site and most of the volcanic, geologic units are located within the western portion of the map area. For this reason, the sets of tabular data are normally placed within the upper-right (eastern) portions of the map plates. The caption is always located at the lower-right corner, the legend and data credits are normally placed in the lower-left corner, and the map scale and north arrow are usually at the upper-left corner of the plate. Many of the older units are defined only within the eastern portions of the map area.

4.1 Base Map

The base map (Plate 1-1) shows the extent of the Hydrogeologic Site Atlas as well as the locations of R-wells, water supply wells, and other wells or boreholes important in constraining the GFM. The base map also shows the location of the major roads and outlines of Laboratory properties. This map also depicts the surrounding land ownership. Plates 1-2 and 1-3 identify all wells that provide data to the geologic models of the Laboratory. Plate 1-2 identifies the vintage of the well data, highlighting the large amounts of new data that were used in this current GFM.

Plate 1-3 provides a table that lists all wells that contributed to the 2009 GFM, including wells outside of the atlas extent but within the SEB. Where wells on a plate are completely within the extent of Laboratory SITE model, the wells are identified in the legend as Laboratory wells. If the set of wells for a plate consists only of wells outside of the Laboratory boundaries and within the SEB model, they are identified in the legend as SEB wells. The Buckman wells are within the Laboratory SITE model but provide minimal “exact” geologic contact information. These wells are displayed separately as the Buckman wells on selected sets of unit maps where they may be of interest.

4.2 Geology

The geology of the atlas region is presented in a series of plates. Plates 2-1 and 2-2 provide a comparison of the mapped geologic quadrangles, and the surface geology predicted by the modeled geologic unit surfaces. Plate 2-3 provides a compilation of mapped fault trace data within the atlas extent, much of which is inferred. Plates 2-4 through 2-83 provide structure contour maps of the unit surface elevations and isochors (vertical thickness). And finally, Plates 2-93 and 2-94 present a 3-D view for the atlas and that of the encompassing SEB model.

4.2.1 Surface Geology

There are two plates that provide maps of the surface geology. Plate 2-1 provides the merged geologic quadrangle maps identified and referenced in Section 1.3. The unit names have been adjusted to reflect the mapping of source unit names to model unit names. Plate 2-2 provides the surface geologic map defined by the GFM and includes a breakout of the subunits of the Tshirege and Otowi members of the Bandelier Tuff not provided in the geologic quadrangle maps. Plate 2-3 provides fault trace data for the atlas area. The structural block model of the 2005 GFM is shown in the western portion of this plate. The faults to the west (in red) were mapped by the seismic hazards team at the Laboratory. Many of the other fault traces are inferred and/or poorly constrained. The inferred faults are older and do not intersect the Bandelier Tuff. Many of these are inferred based on apparent stratigraphic discontinuities in widely spaced well data. Some of these discontinuities may actually represent paleotopography.

The fault traces can be extruded vertically or with a given dip to provide 3-D structural controls for flow models.

4.2.2 Geologic Unit Morphology

The 3-D morphology and geometry of the geologic units are presented in a series of plates: Plate 2-3 through Plate 2-83. Structure contours of the unit surfaces provide a 3-D definition of the units. Such maps are commonly defined as 2.5-D maps. Maps for the tops, isochors, and bottoms of all units are presented in top-to-bottom order through the set of units. Maps for the top and isochors of the Tshirege subunits are also provided.

Each of these plates also identifies the position of all wells that contributed to the definition of the mapped surface. The number at the well position on the map provides an index to the included map table which shows the well name and the elevation or thickness of the unit at the well. The well numbers also correlate to those of Plates 1-2 and 1-3. For Plate 2-4, there were too many wells to place in a map table, so the user must refer to Plate 1-3 for top elevation values at the wells.

The geologic outcrops can provide critical elevation control points for the surfaces. The geologic contacts are often exposed best in the canyons or regions of rugged topography, while wells intersecting these exposed units are usually located some distance within the Pajarito Plateau. The locations of unit outcrops are therefore identified on all plates, using the modeled color of the units. As these outcrops are often of limited geographical extent, e.g., when on the canyon walls, the structure contours for the top of the unit are clipped at the outcrop/topography so that the outcrop is visible to the map reader. For the Cerros del Rio Basalt, which outcrops over a broad surface area in the south-central portion, these top contours have been reinserted into the plate.

4.3 Cross-Sections

Geologic cross-sections of the GFM are provided for the atlas extent at 10,000-ft intervals in both the north-south and east-west directions. These sections identify both the geologic units and the water table. with a 1.75x vertical exaggeration. The modeled water table is not defined throughout the atlas extent, so the water table may be absent from some lines and represented for only parts of other cross-section lines. The locations of the cross-section lines are shown in Plate 2-84. Plate 2-84 also provides the location of “source” geologic cross-sections that were used in the development of the GFM.

4.4 3-D Views of the GFM

The 3-D views of the GFM, with the southeast quadrant removed, are provided for the atlas extent as Plate 2-93 and for the SEB as Plate 2-94.

4.5 Water-Table Elevation and Geology

Plate 3-1 shows the elevations of the regional water table, highlighting the 100-ft contour interval. Fainter contours at 10- or 20-ft intervals are provided for finer resolution, especially in the central portion of the laboratory. The location of springs and major drainages are also indicated. Topographic contours are provided to allow visual determination of the depth to the water table. Plate 3-2 shows the modeled geology at the water-table surface.

5.0 REFERENCES

The following list includes all documents cited in this report. Parenthetical information following each reference provides the author(s), publication date, and ER ID. This information is also included in text citations. ER IDs are assigned by the Environmental Programs Directorate's Records Processing Facility (RPF) and are used to locate the document at the RPF and, where applicable, in the master reference set.

Copies of the master reference set are maintained at the NMED Hazardous Waste Bureau and the Directorate. The set was developed to ensure that the administrative authority has all material needed to review this document, and it is updated with every document submitted to the administrative authority. Documents previously submitted to the administrative authority are not included.

Bailey, R.A., R.L. Smith, and C.S. Ross, 1969. "Stratigraphic Nomenclature of Volcanic Rocks in the Jemez Mountains, New Mexico," in *Contributions to Stratigraphy*, U.S. Geological Survey Bulletin 1274-P, Washington, D.C. (Bailey at el. 1969, 021498)

Broxton, D., G. WoldeGabriel, L. Peters, J. Budahn, and G. Luedemann, 2007. "Pliocene Volcanic Rocks of the Tschicoma Formation, East-Central Jemez Volcanic Field: Chemistry, Petrography, and Age Constraints," New Mexico Geological Society Guidebook: 58th Field Conference, Geology of the Jemez Mountains Region II, pp. 284–295. (Broxton et al. 2007, 106121)

Broxton, D.E., and P.G. Eller (Eds.), June 1995. "Earth Science Investigations for Environmental Restoration—Los Alamos National Laboratory, Technical Area 21," Los Alamos National Laboratory report LA-12934-MS, Los Alamos, New Mexico. (Broxton and Eller 1995, 058207)

Broxton, D.E., and S.L. Reneau, August 1995. "Stratigraphic Nomenclature of the Bandelier Tuff for the Environmental Restoration Project at Los Alamos National Laboratory," Los Alamos National Laboratory report LA-13010-MS, Los Alamos, New Mexico. (Broxton and Reneau 1995, 049726)

Broxton, D.E., D. Vaniman, G. WoldeGabriel, and G. Cole, March 2006. "Late Miocene Sedimentary Rocks beneath the Central Pajarito Plateau: Results from Recent Borehole Investigations," Geologic and Hydrogeologic Framework of the Española Basin, Proceedings of the 54th Annual Española Basin Workshop, March 7-8, 2006, Santa Fe, New Mexico. (Broxton et al. 2006, 092520)

Broxton, D.E., and D.T. Vaniman, August 2005. "Geologic Framework of a Groundwater System on the Margin of a Rift Basin, Pajarito Plateau, North-Central New Mexico," *Vadose Zone Journal,* Vol. 4, No. 3, pp. 522–550. (Broxton and Vaniman 2005, 090038)

Carey, B., G. Cole, C. Lewis, F. Tsai, R. Warren, and G. WoldeGabriel, 1999. "Revised Site-Wide-Geologic Model for Los Alamos National Laboratory (FY99)," Los Alamos National Laboratory document LA-UR-00-2056, Los Alamos, New Mexico. (Carey et al. 1999, 066782)

Carey, W.J., and G. Cole, January 2002. "Description of the Cerro Grande Fire Laser-Altimetry (LIDAR) Data Set," Los Alamos National Laboratory report LA-13892-MS, Los Alamos, New Mexico. (Carey and Cole 2002, 073784)

Cavazza, W., December 1986. "Miocene Sediment Dispersal in the Central Española Basin, Rio Grande Rift, New Mexico, U.S.A.," *Sedimentary Geology,* Vol. 51, No. 1–2, pp. 119–135. (Cavazza 1986, 105708)

Cole, G., D. Broxton, S. Reneau, and D. Vaniman, 1997. "Revised Site-Wide Geologic Model for Los Alamos National Laboratory (FY97)," Los Alamos National Laboratory document LA-UR-00-2057, Los Alamos, New Mexico. (Cole et al. 1997, 106127)

Cole, G., D. Broxton, S. Reneau, D. Vaniman, R. Warren, and G. WoldeGabriel, 1998. "Revised Site-Wide Geologic Model for Los Alamos National Laboratory (FY98)," Los Alamos National Laboratory document LA-UR-00-2058, Los Alamos, New Mexico. (Cole et al. 1998, 106128)

Cole, G., J.W. Carey, L. Burnette, and T. Miller, 2006. "The 2005 Three-Dimensional Geologic Model of the Pajarito Plateau," Los Alamos National Laboratory document LA-UR-06-3060, Los Alamos, New Mexico. (Cole et al. 2006, 095079)

Cole, G., D. Coblentz, E. Jacobs, D. Koning, D. Broxton, D. Vaniman, F. Goff, and G. WoldeGabriel, 2009. "The 2009 Three-Dimensional Geologic Models of the Los Alamos National Laboratory Site, Southern Española Basin, and Española Basin," Los Alamos National Laboratory document LA-UR-09-3701, Los Alamos, New Mexico. (Cole et al. 2009, 106101)

Daniel, C.G., 1995. "An Overview of the Proterozoic Geology in the Thompson Peak-Glorieta Baldy Area, Santa Fe County, New Mexico," New Mexico Geological Society Guidebook: 46th Field Conference, Geology of the Santa Fe Region, pp. 209–218. (Daniel 1995, 106123)

Dethier, D.P., 1997. "Geology of White Rock Quadrangle, Los Alamos and Santa Fe Counties, New Mexico," Map 73, New Mexico Bureau of Mines and Mineral Resources. (Dethier 1997, 049843)

Dethier, D.P., 2003. "Geologic Map of the Puye Quadrangle, Los Alamos, Rio Arriba, Sandoval, and Santa Fe Counties, New Mexico," U.S. Geologic Survey Miscellaneous Field Studies Map MF-2419, Version 1.0, Washington, D.C. (Dethier 2003, 106113)

Freeze, R.A., and J.A. Cherry, January 1979. *Groundwater*, Prentice-Hall, Inc., Englewood Cliffs, New Jersey. (Freeze and Cherry 1979, 088742)

Gardner, J.N., F.E. Goff, S.R. Garcia, and R.C. Hagan, February 10, 1986. "Stratigraphic Relations and Lithologic Variations in the Jemez Volcanic Field, New Mexico," *Journal of Geophysical Research,* Vol. 91, No. B2, pp. 1763–1778. (Gardner et al. 1986, 059104)

Goff, F., June 1995. "Geologic Map of Technical Area 21," in *Earth Science Investigations for Environmental Restoration—Los Alamos National Laboratory, Technical Area 21*, Los Alamos National Laboratory report LA-12934-MS, Los Alamos, New Mexico, pp. 7–18. (Goff 1995, 049682)

Goff, F., 2009. Excerpted pages from *Valles Caldera*, University of New Mexico Press, Albuquerque, New Mexico. (Goff 2009, 106105)

Goff, F., and J.N. Gardner, 2004. “Late Cenozoic Geochronology of Volcanism and Mineralization in the Jemez Mountains and Valles Caldera, North Central New Mexico,” in *The Geology of New Mexico, A Geologic History*, New Mexico Geologic Society Special Publication 11, New Mexico, pp. 295-312. (Goff and Gardner 2004, 092526)

Goff, F., J.N. Gardner, and S.L. Reneau, June 2002. “Geology of the Frijoles 7.5-minute Quadrangle, Los Alamos and Sandoval Counties, New Mexico,” New Mexico Bureau of Geology and Mineral Resources Open-File Digital Geologic Map OF-GM 42, Socorro, New Mexico. (Goff et al. 2002, 088776)

Griggs, R.L., and J.D. Hem, 1964. “Geology and Ground-Water Resources of the Los Alamos Area, New Mexico,” U.S. Geological Survey Water Supply Paper 1753, Washington, D.C. (Griggs and Hem 1964, 092516)

INTERA Incorporated, September 1, 2006. “Report on Santa Fe County Model Development and Regional Aquifer Evaluation,” Albuquerque, New Mexico. (INTERA Inc. 2006, 106106)

Izett, G.A., and J.D. Obradovich, February 10, 1994. “$^{40}Ar/^{39}Ar$ Age Constraints for the Jaramillo Normal Subchron and the Matuyama-Brunhes Geomagnetic Boundary,” *Journal of Geophysical Research,* Vol. 99, No. B2, pp. 2925-2934. (Izett and Obradovich 1994, 048817)

Kempter, K.A., S. Kelley, J. Gardner, S.L. Reneau, D. Broxton, F. Goff, A. Levine, and C. Lewis, July 2, 2007. “Preliminary Geologic Map of the Guaje Mountain Quadrangle, Los Alamos and Sandoval Counties, New Mexico,” revised, New Mexico Bureau of Geology and Mineral Resources Open-File Digital Geologic Map OF-GM 55, Socorro, New Mexico. (Kempter et al. 2007, 106111)

Koch, R.J., and S. Schmeer, March 2009. “Groundwater Level Status Report for 2008, Los Alamos National Laboratory,” Los Alamos National Laboratory report LA-14397-PR, Los Alamos, New Mexico. (Koch and Schmeer 2009, 105181)

Koning, D.J., May 2002. “Preliminary Geologic Map of the Española 7.5-minute Quadrangle,” New Mexico Bureau of Geology and Mineral Resources Open-File Digital Geologic Map OF-GM 54, Socorro, New Mexico. (Koning 2002, 105710)

Koning, D.J., and S.B. Aby, 2005. “Proposed Members of the Chamita Formation, North-Central New Mexico,” New Mexico Geological Society Guidebook: 56th Field Conference, Geology of the Chama Basin, pp. 258–278. (Koning and Aby 2005, 106162)

Koning, D.J., D. Broxton, D. Sawyer, D. Vaniman, and J. Shomaker, 2007. “Surface and Subsurface Stratigraphy of the Santa Fe Group Near White Rock and the Buckman Areas of the Española Basin, North-Central New Mexico,” New Mexico Geological Society Guidebook: 58th Field Conference, Geology of the Jemez Mountains Region II, pp. 209–224. (Koning et al. 2007, 106122)

Koning, D.J., S.D. Connell, G.S. Morgan, L. Peters, and W.C. McIntosh, 2005. “Stratigraphy and Depositional Trends in the Santa Fe Group Near Española, North-Central New Mexico: Tectonic and Climatic Implications,” New Mexico Geological Society Guidebook: 56th Field Conference, Geology of the Chama Basin, pp. 237–257. (Koning et al. 2005, 106120)

Koning, D.J., S.D. Connell, F.J. Pazzaglia, and W.C. McIntosh, August 2002. “Redefinition of the Ancha Formation and Pliocene-Pleistocene Deposition in the Santa Fe Embayment, North-Central New Mexico,” *New Mexico Geology,* Vol. 24, No. 3, pp. 75–87. (Koning et al. 2002, 105711)

Koning, D.J., and F. Maldonado, October 22, 2003. “Preliminary Geologic Map of the Horcado Ranch 7.5-minute Quadrangle,” revised, New Mexico Bureau of Geology and Mineral Resources Open-File Digital Geologic Map OF-GM 44, Socorro, New Mexico. (Koning and Maldonado 2003, 106112)

Koning, D.J., G. Smith, J. Lyman, and P. Paul, March 2004. “Lithosome S of the Tesuque Formation: Hydrostratigraphic and Tectonic Implications of a Newly Delineated Lithosome in the Southern Española Basin, New Mexico,” Geologic and Hydrogeologic Framework of the Española Basin, Proceedings of the 3rd Annual Española Basin Workshop, March 2–3, 2004, Santa Fe, New Mexico. (Koning et al. 2004, 106104)

LANL (Los Alamos National Laboratory), March 2009. “2009 General Facility Information,” Los Alamos National Laboratory document LA-UR-09-1341, Los Alamos, New Mexico. (LANL 2009, 105632)

Lavine, A., C.J. Lewis, D.K. Katcher, J.N. Gardner, and J. Wilson, June 2003. “Geology of the North-central to Northeastern Portion of Los Alamos National Laboratory, New Mexico,” Los Alamos National Laboratory report LA-14043-MS, Los Alamos, New Mexico. (Lavine et al. 2003, 092527)

Lewis, C.J., A. Lavine, S.L. Reneau, J.N. Gardner, R. Channell, and C.W. Criswell, December 2002. “Geology of the Western Part of Los Alamos National Laboratory (TA-3 to TA-16), Rio Grande Rift, New Mexico,” Los Alamos National Laboratory report LA-13960-MS, Los Alamos, New Mexico. (Lewis et al. 2002, 073785)

Purtymun, W.D., January 1995. “Geologic and Hydrologic Records of Observation Wells, Test Holes, Test Wells, Supply Wells, Springs, and Surface Water Stations in the Los Alamos Area,” Los Alamos National Laboratory report LA-12883-MS, Los Alamos, New Mexico. (Purtymun 1995, 045344)

Read, A.S., D.J. Koning, and P.S. Johnson, March 10, 2005. “Preliminary Geologic Map of the Southern Española Basin, New Mexico,” New Mexico Bureau of Geology and Mineral Resources Open-File Report 481, Version 1.11, on CD, Socorro, New Mexico. (Read et al. 2005, 105709)

Rogers, M.A., 1995. “Geologic Map of the Los Alamos National Laboratory Reservation,” Mara, Inc., Los Alamos, New Mexico. (Rogers 1995, 054419)

Sawyer, D.A., S.A. Minor, R.A. Thompson, R.R. Shroba, G.A. Smith, D.P. Dethier, V.J.S. Grauch, and T.R. Brandt, 2007. “Geologic Map of the Cochiti Pueblo Area, New Mexico,” U.S. Geologic Survey Professional Paper 1720, Plate 2, Reston, Virginia. (Sawyer et al. 2007, 106130)

Spell, T.L., I. McDougall, and A.P. Doulgeris, December 1996. “Cerro Toledo Rhyolite, Jemez Volcanic Field, New Mexico: $^{40}Ar/^{39}Ar$ Geochronology of Eruptions between Two Caldera-Forming Events,” *Geological Society of America Bulletin,* Vol. 108, No. 12, pp. 1549-1566. (Spell et al. 1996, 055542)

Stauffer, P.H., H.S. Viswanathan, B.A. Robinson, C.W. Gable, G.L. Cole, D.E. Broxton, E.P. Springer, and T.G. Schofield, 2005. “Groundwater Pathway Model for the Los Alamos National Laboratory Technical Area 54, Material Disposal Area G,” Los Alamos National Laboratory document LA-UR-05-7393, Los Alamos, New Mexico. (Stauffer et al. 2005, 097432)

Stone, W., G. Cole, B. Carey, and M. Jones, 2001. “Documentation for the Los Alamos National Laboratory Expanded Hydrogeologic Atlas,” Los Alamos National Laboratory document LA-UR-01-70, Los Alamos, New Mexico. (Stone et al. 2001, 069830)

Stone, W., G. Cole, and M. Jones, 1999. “Documentation for the Preliminary Hydrogeology Atlas for Los Alamos National Laboratory,” Los Alamos National Laboratory document LA-UR-99-4619, Los Alamos, New Mexico. (Stone et al. 1999, 064039)

Vaniman, D., G. Cole, J. Gardner, J. Conaway, D. Broxton, S. Reneau, M. Rice, G. WoldeGabriel, J. Blossom, and F. Goff, 1996. “Development of a Site-Wide Geologic Model for Los Alamos National Laboratory (FY96),” on CD, Los Alamos National Laboratory document LA-UR-00-2059, Los Alamos, New Mexico. (Vaniman et al. 1996, 106129)

WoldeGabriel, G., A.W. Laughlin, D.P. Dethier, and M. Heizler, 1996. “Temporal and Geochemical Trends of Lavas in White Rock Canyon and the Pajarito Plateau, Jemez Volcanic Field, New Mexico, USA,” Los Alamos National Laboratory document LA-UR-96-583, Los Alamos, New Mexico. (WoldeGabriel et al. 1996, 054427)

WoldeGabriel, G., R.G. Warren, D. Broxton, D. Vaniman, M.T. Heizler, E.C. Kluk, and L. Peters, 2001. “Episodic Volcanism, Petrology, and Lithostratigraphy of the Pajarito Plateau and Adjacent Areas of the Española Basin and the Jemez Mountains,” *Volcanology in the New Mexico, NM Natural History and Science Bulletin,* Vol. 18, pp. 97-129. (WoldeGabriel et al. 2001, 092523)

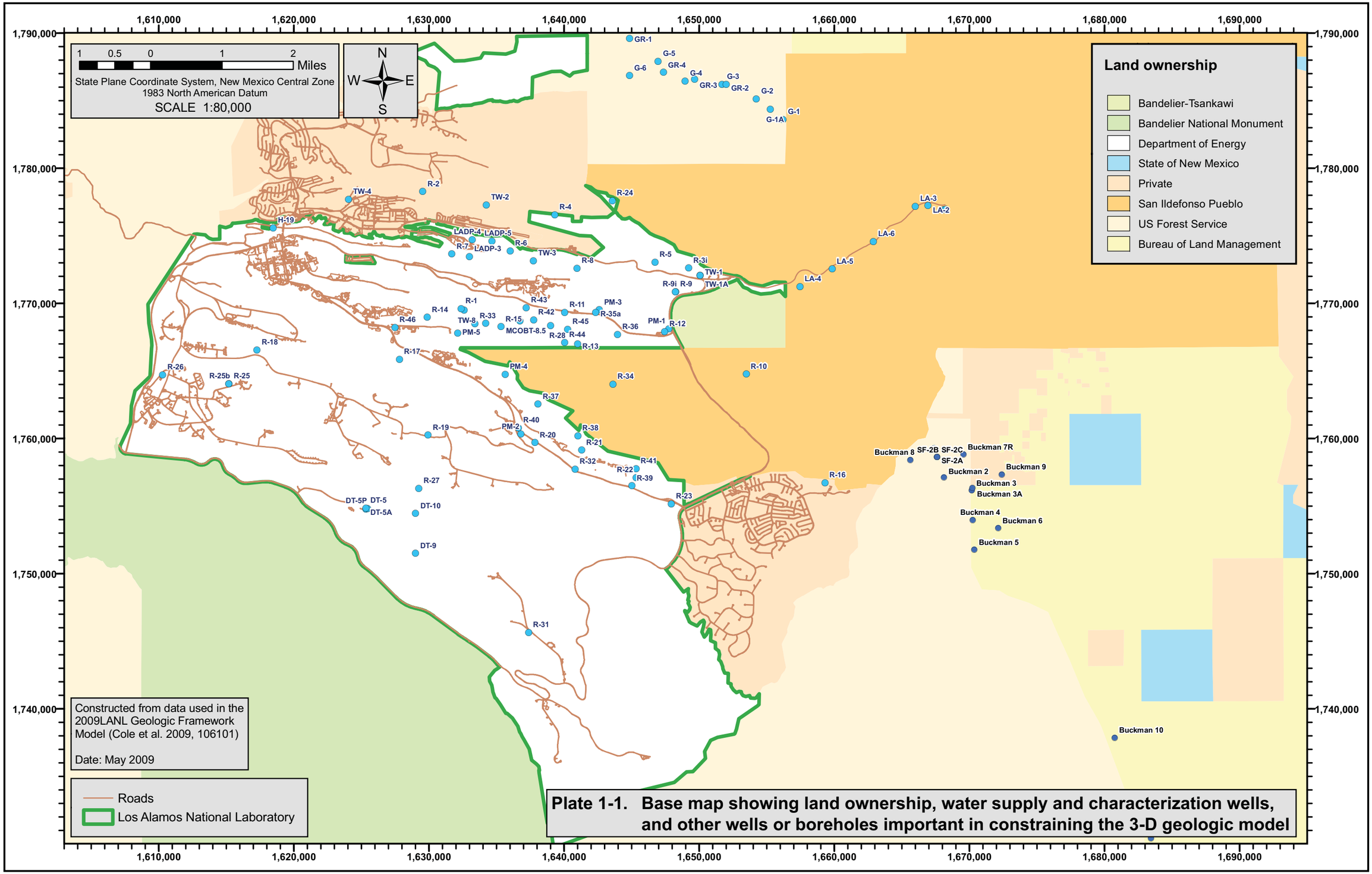


Plate 1-1. Base map showing land ownership, water supply and characterization wells, and other wells or boreholes important in constraining the 3-D geologic model

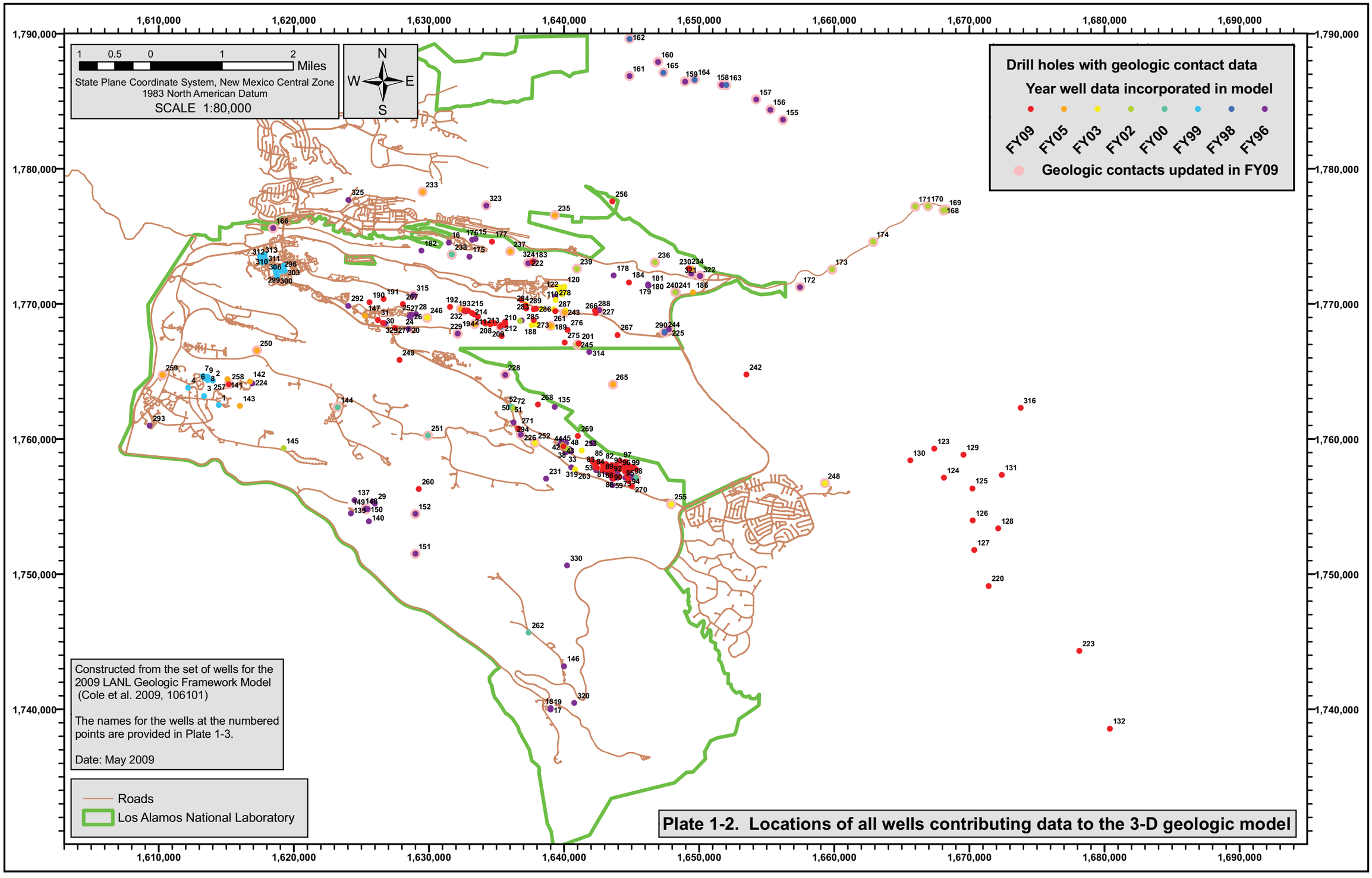
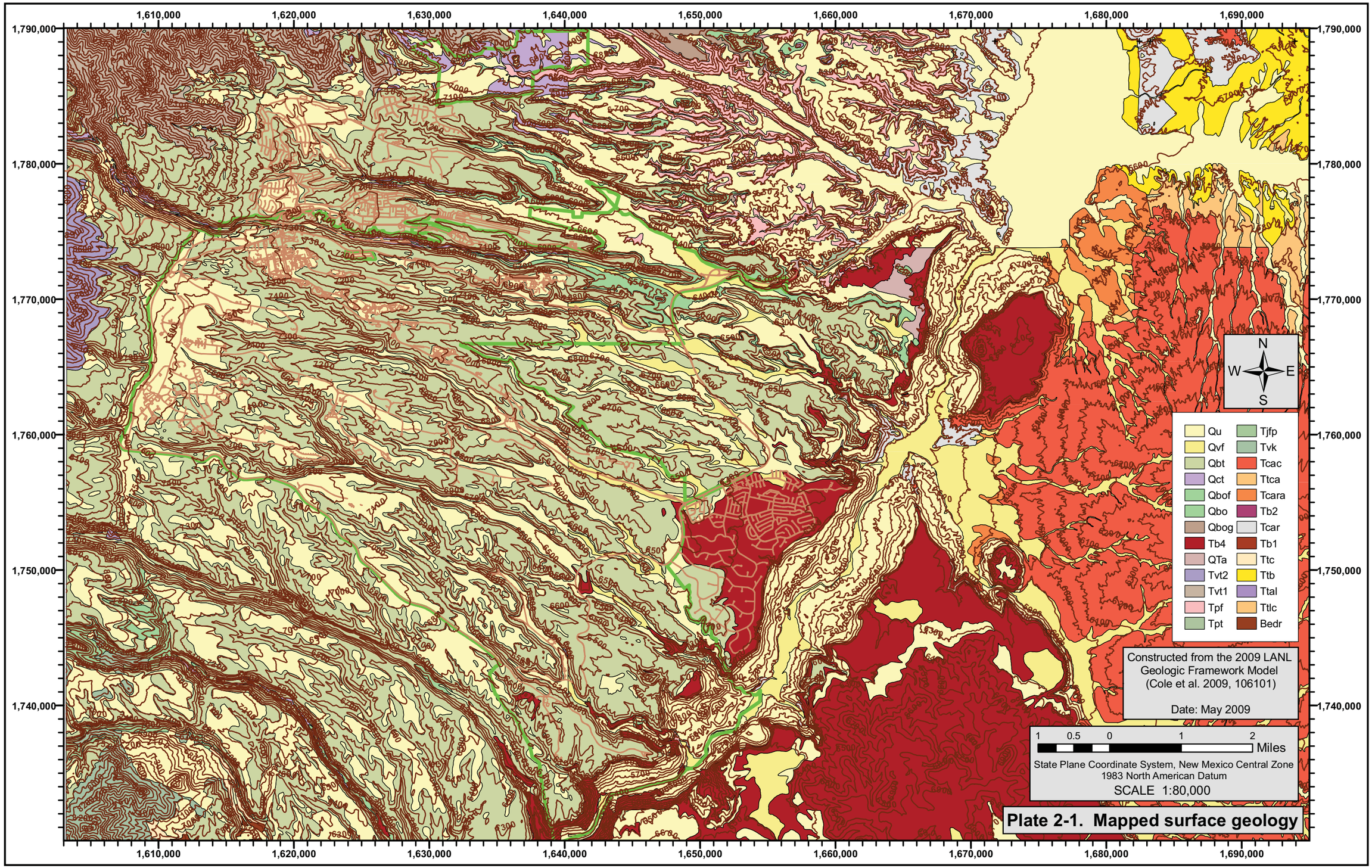


Plate 1-2. Locations of all wells contributing data to the 3-D geologic model

ID	Well name	Top elev.	Bot elev.
1	16-2665	7517.4	7392.4
2	16-2667	7532.0	7325.0
3	16-2668	7556.0	7368.5
4	16-2669	7584.3	7419.3
5	16-2701	7547.0	7462.0
6	16-2702	7535.0	7466.0
7	16-2703	7549.6	7480.0
8	16-2704	7538.9	7469.0
9	16-2706	7530.0	7440.0
10	16-2708	7543.9	7429.5
11	16-2709	7519.8	7486.0
12	16-2711	7521.0	7453.0
13	16-2712	7522.4	7422.0
14	16-2735	7536.5	7446.0
15	21-1811	7032.5	6772.5
16	21-2523	7159.0	6839.0
17	33-1230	6514.0	6284.0
18	33-1231	6516.0	6201.0
19	33-1232	6517.0	6271.0
20	35-2004	7180.2	7080.2
21	35-2005	7170.7	7070.7
22	35-2006	7179.9	7079.9
23	35-2007	7175.5	7082.5
24	35-2008	7172.0	7072.0
25	35-2009	7165.3	7065.3
26	35-2011	7166.8	7066.8
27	35-2013	7171.1	7071.1
28	35-2028	7103.4	6803.4
29	49-2-700-1	7133.9	6433.9
30	50-24769	7240.7	6540.7
31	50-24818	7239.7	6619.7
32	54-1001	6781.7	6499.8
33	54-1002	6789.3	6499.9
34	54-1003	6791.7	6492.7
35	54-1004	6788.2	6448.2
36	54-1005	6778.5	6506.8
37	54-1006	6790.3	6500.3
38	54-1007	6790.3	6640.3
39	54-1008	6796.6	6646.6
40	54-1009	6792.0	6642.0
41	54-1010	6790.6	6748.2
42	54-1011	6792.2	6751.2
43	54-1012	6793.1	6752.1
44	54-1013	6793.6	6752.6
45	54-1014	6793.8	6752.8
46	54-1015	6708.2	6242.4
47	54-1016	6700.4	6177.4
48	54-1018	6787.7	6459.7
49	54-1023	6884.0	6624.3
50	54-1024	6885.0	6795.0
51	54-1025	6889.5	6799.5
52	54-1026	6889.6	6799.6
53	54-1102	6720.6	6656.2
54	54-1105	6710.5	6662.4
55	54-1106	6700.4	6648.4
56	54-1107	6718.1	6588.1
57	54-1108	6701.1	6649.1
58	54-1110(G-3)	6691.2	6588.2
59	54-1111(G-4)	6674.6	6521.6
60	54-1112	6693.2	6632.7
61	54-1114	6667.2	6625.5
62	54-1115	6672.0	6600.5
63	54-1116	6683.0	6593.5
64	54-1117	6679.7	6587.2
65	54-1120	6688.3	6638.8
66	54-1121	6673.5	6525.5
67	54-1123	6665.3	6565.3
68	54-1124	6636.1	6597.6
69	54-1125	6669.4	6605.9
70	54-1126	6655.8	6604.8
71	54-1128	6653.2	6612.0
72	54-15462	6880.0	6580.0
73	54-24360	6670.6	6470.6
74	54-24361/27436	6695.1	6503.6
75	54-24362	6681.6	6492.6
76	54-24363	6692.0	6442.0
77	54-24364	6704.7	6504.7
78	54-24366	6680.7	6430.7
79	54-24367	6692.1	6492.1
80	54-24368	6715.6	6430.6
81	54-24369	6725.0	6475.0
82	54-24370	6726.4	6476.9
83	54-12371	6728.4	6528.4
84	54-24372	6748.5	6498.5
85	54-24373	6746.0	6496.0
86	54-24374	6677.2	6477.2
87	54-243751	6708.9	6703.9
88	54-24375	6638.9	6507.9
89	54-24376	6693.5	6493.5
90	54-24377	6684.0	6484.0
91	54-24378	6684.8	6502.3
92	54-24379	6675.6	6475.6
93	54-24380	6697.6	6501.6
94	54-24381	6660.1	6460.1
95	54-24382	6672.4	6525.4
96	54-24383	6653.7	6506.2
97	54-24384	6605.5	6537.5
98	54-24385	6677.4	6500.4
99	54-24386	6676.8	6475.8
100	54-24387	6616.0	6535.0
101	54-24388	6684.8	6503.8
102	54-24389	6698.2	6498.2
103	54-24390	6704.0	6518.0
104	54-24391	6711.0	6511.0
105	54-24392	6666.4	6466.4
106	54-24393	6717.8	6511.8
107	54-24394	6726.1	6419.6
108	54-24395	6729.3	6529.3
109	54-24396	6684.0	6484.0
110	54-24397	6671.9	6427.6
111	54-24399	6793.0	6133.0
112	54-25105	6709.0	6007.7
113	54-G-2	6694.1	6592.1
114	54-G-5	6699.1	6586.1
115	Archery	7185.0	6032.0
116	BH1	6915.8	6865.8
117	BH2	6914.4	6866.4
118	BH3	6896.4	6846.4
119	BH4	6929.2	6729.2
120	BH5	6913.8	6713.8
121	BH6	6911.9	6711.9
122	BH7	6910.0	6611.0
123	Buckman_1	5510.0	4406.0
124	Buckman_2	5539.0	4066.0
125	Buckman_3A	5619.0	4169.0
126	Buckman_4	5646.0	4211.0
127	Buckman_5	5690.0	4255.0
128	Buckman_6	5718.0	4330.0
129	Buckman_7R	5606.0	4143.0
130	Buckman_8	5514.0	4582.0
131	Buckman_9	5738.0	4303.0
132	Buckman_10	6045.0	4035.0
133	Buckman_11	6155.0	4152.0
134	Buckman_12	6250.0	4318.0
135	CDBM-1	6721.6	6532.6
136	CDBM-2	6634.1	6535.1
137	CH-1	7170.6	6669.6
138	CH-2	7141.3	6634.3
139	CH-3	7169.9	6869.9
140	CH-4	7118.2	6815.2
141	CdV-16-1i	7382.2	6699.2
142	CdV-16-2i	7457.1	6394.1
143	CdV-16-3i	7486.8	6081.8
144	CdV-R-15-3	7258.9	5536.9
145	CdV-R-37-2	7330.6	5666.6
146	DMB-1	6276.1	6152.1
147	DSC-2	7285.0	6880.0
148	DT-5	7144.5	6182.5
149	DT-5A	7144.2	5323.2
150	DT-5P	7136.8	6651.9
151	DT-9	6936.0	5435.0
152	DT-10	7019.0	5610.0
153	EB-35	6930.0	5120.0
154	EB-47	7140.0	5580.0
155	G-1	5978.9	3958.9
156	G-1A	6015.9	3944.9
157	G-2	6057.8	4051.8
158	G-3	6138.8	4142.8
159	G-4	6235.0	4233.0
160	G-5	6309.6	4312.6
161	G-6	6424.4	4419.4
162	GR-1	6416.2	4386.2
163	GR-2	6140.2	4096.2
164	GR-3	6212.2	4202.2
165	GR-4	6299.2	4371.2
166	H-19	7172.0	5172.0
167	Kelly_Fed	6035.0	3332.0
168	LA-1	5624.0	4623.0
169	LA-1B	5622.0	3366.0
170	LA-2	5651.0	4769.0
171	LA-3	5672.0	4762.0
172	LA-4	5970.9	3951.9
173	LA-5	5840.0	3816.0
174	LA-6	5770.0	3740.0
175	LADP-3	6755.6	6406.6
176	LADP-4	7049.7	6249.7
177	LADP-5	7018.1	6298.1
178	LAO-4.5	6479.8	6417.9
179	LAO-5	6427.1	6400.1
180	LAO-6	6423.5	6397.6
181	LAO-6A	6423.8	6408.8
182	LAOI(A)-1.1	6833.2	6510.2
183	LAOI-3.2a	6624.4	6357.5
184	LAOI-7	6458.4	6076.1
185	Las_Campanas	6400.0	4395.0
186	LAWS-01	6304.8	6023.3
187	MC1	6764.6	6580.0
188	MC2	6751.9	6580.0
189	MC3	6726.6	6582.5
190	MCB-1	7150.2	7045.2
191	MCB-2	7076.4	6971.9
192	MCB-5	6895.3	6791.3
193	MCB-6	6875.5	6786.5
194	MCB-7	6852.4	6751.4
195	MCB-8	6824.4	6719.9
196	MCB-9	6824.1	6721.1
197	MCB-10	6805.7	6701.7
198	MCB-11	6805.4	6701.4
199	MCB-12	6805.2	6700.7
200	MCB-14	6827.1	6543.1
201	MCB-16	6670.7	6570.7
202	MCC-8.2	6775.2	6591.2
203	MCM-5.1	6870.8	6759.3
204	MCM-5.9A	6850.2	6656.2
205	MCOBT-4.4	6836.2	6069.2
206	MCOBT-8.5	6780.5	6040.5
207	MCOI-1	7106.2	6263.0
208	MCOI-4	6837.2	6297.2
209	MCOI-5	6819.7	6102.7
210	MCOI-6	6811.1	6091.1
211	MCOI-8	6859.2	6114.2
212	MCOI-10	7034.5	5984.5
213	MCRES-2	6838.2	6638.0
214	MCRES-3	6862.6	6662.6
215	MCRES-4	6870.6	6645.6
216	NAD-64	6635.0	5635.0
217	NAD-63	6415.0	5455.0
218	NAD-60	6225.0	5205.0
219	Northwest	7100.0	5100.0
220	Nuc_Dynamics_34	5683.0	5120.0
221	O-1	6400.9	3791.9
222	O-4	6639.0	3833.0
223	OSE_Devils_Throne	5985.0	3485.0
224	P-12	7451.6	7251.6
225	PM-1	6513.2	4012.2
226	PM-2	6712.0	4112.0
227	PM-3	6610.9	4058.9
228	PM-4	6920.0	4000.0
229	PM-5	7094.0	3974.0
230	POI-4	6372.3	6191.3
231	POTO-4A	6622.0	6448.0
232	R-1	6881.2	5716.2
233	R-2	6770.4	5827.4
234	R-3i	6390.1	6121.9
235	R-4	6577.5	5732.5
236	R-5	6472.6	5570.6
237	R-6	6995.8	5692.8
238	R-7	6779.2	5682.2
239	R-8	6542.9	5520.9
240	R-9	6382.8	5611.8
241	R-9i	6382.8	6060.8
242	R-10	6362.3	5197.3
243	R-11	6672.4	5745.4
244	R-12	6499.6	5613.6
245	R-13	6673.1	5540.1
246	R-14	7062.1	5735.1
247	R-15	6820.0	5713.0
248	R-16	6256.9	4969.9
249	R-17	6921.5	5754.5
250	R-18	7404.8	5974.8
251	R-19	7066.3	5163.8
252	R-20	6694.3	5329.3
253	R-21	6656.2	5661.2
254	R-22	6650.5	5161.5
255	R-23	6527.8	5601.8
256	R-24	6547.4	5666.4
257	R-25	7516.1	5574.1
258	R-25b	7516.0	6376.0
259	R-26	7641.6	6151.1
260	R-27	6713.7	5726.7
261	R-28	6728.5	5723.5
262	R-31	6362.5	5259.5
263	R-32	6637.6	5629.6
264	R-33	6853.3	5723.3
265	R-34	6630.0	5565.0
266	R-35a	6623.1	5481.1
267	R-36	6593.0	5728.0
268	R-37	6860.0	5780.0
269	R-38	6670.0	5760.0
270	R-39	6580.0	5684.0
271	R-40	6718.0	5905.0
272	R-41	6650.0	6650.0
273	R-42	6759.1	5731.1
274	R-43	6730.0	5795.0
275	R-44	6718.0	5624.0
276	R-45	6699.0	5642.0
277	R-46	7212.0	5797.0
278	SC1	6691.5	6578.5
279	SC2	6722.8	6580.0
280	SC3	6701.7	6578.5
281	SC4	6682.1	6578.5
282	SC5	6661.8	6580.0
283	SCC-1	6738.3	6338.3
284	SCC-2	6723.7	6335.1
285	SCC-3	6713.0	6369.0
286	SCC-4	6709.2	6386.2
287	SCC-5	6683.6	6393.6
288	SCC-6	6619.3	6359.8
289	SCI-2	6730.0	5840.0
290	SCOI-3	6499.0	6367.0
291	SF_River	6365.0	4365.0
292	SHB-1	7315.9	6615.9
293	SHB-3	7607.7	6747.7
294	SHB-4	6708.7	6547.7
295	SHB-CMR-1	7402.2	7334.7
296	SHB-CMR-10	7398.4	7338.4
297	SHB-CMR-2	7399.8	7337.3
298	SHB-CMR-3	7398.6	7343.6
299	SHB-CMR-4	7398.4	7346.0
300	SHB-CMR-5	7397.5	7345.0
301	SHB-CMR-6	7392.2	7334.7
302	SHB-CMR-7	7394.9	7337.4
303	SHB-CMR-8	7392.7	7340.2
304	SHB-NISC-1	7439.2	7356.7
305	SHB-NISC-2	7428.1	7345.6
306	SHB-NISC-3	7427.8	7352.8
307	SHB-NISC-4	7439.3	7356.8
308	SHB-NISC-5	7432.5	7347.5
309	SHB-SCC-1	7440.2	7342.7
310	SHB-SCC-2	7430.5	7345.5
311	SHB-SCC-3	7428.1	7343.1
312	SHB-SCC-4	7441.9	7351.9
313	SHB-SCC-5	7435.7	7353.2
314	SIMO	6655.4	6551.4
315	Sigma_Mesa	7209.5	4917.5
316	Skillet	5850.0	3946.0
317	St_Michael	6870.0	4850.0
318	TH-5	6590.7	6327.8
319	TH-6	6642.4	6342.5
320	TH-7	6223.5	6168.5
321	TW-1	6369.9	5727.9
322	TW-1A	6369.8	6144.8
323	TW-2	6646.4	5812.4
324	TW-3	6626.9	5811.9
325	TW-4	7242.7	6037.7
326	TW-8	6875.1	5810.1
327	TestHole6-53	6921.2	6771.2
328	TestHole7-53	6701.0	6621.0
329	USGS-TH	7227.4	7017.4
330	WCO-3	6433.9	6420.0
331	Yates_2	6605.0	2634.0

Constructed from the 2009 LANL Geologic Framework Model (Cole et al. 2009, 106101) Date: May 2009

Plate 1-3. Identification of all wells contributing data to the 3-D geologic model


1,610,000
1,620,000
1,630,000
1,640,000
1,650,000
1,660,000
1,670,000
1,680,000
1,690,000
1,790,000
1,780,000
1,770,000
1,760,000
1,750,000
1,740,000
N
W
E
S
Qu
Qvf
Qbt
Qct
Qbof
Qbo
Qbog
Tb4
QTa
Tvt2
Tvt1
Tpf
Tpt
Tjfp
Tvk
Tcac
Ttca
Tcara
Tb2
Tcar
Tb1
Ttc
Ttb
Ttal
Ttlc
Bedr
Constructed from the 2009 LANL Geologic Framework Model (Cole et al. 2009, 106101)
Date: May 2009
1 0.5 0 1 2
Miles
State Plane Coordinate System, New Mexico Central Zone
1983 North American Datum
SCALE 1:80,000
Plate 2-1. Mapped surface geology

1 0.5 0 1 2 Miles

State Plane Coordinate System, New Mexico Central Zone
1983 North American Datum
SCALE 1:80,000

N W E S

1,610,000 1,620,000 1,630,000 1,640,000 1,650,000 1,660,000 1,670,000 1,680,000 1,690,000

1,790,000 1,780,000 1,770,000 1,760,000 1,750,000 1,740,000

Roads
Los Alamos National Laboratory

Geologic Units

UNIT CODE - UNIT NAME

Qbt4	Bandelier Tuff - Tshirege unit 4
Qbt3t	Bandelier Tuff - Tshirege unit 3t
Qbt3	Bandelier Tuff - Tshirege unit 3
Qbt2	Bandelier Tuff - Tshirege unit 2
Qbt1vu	Bandelier Tuff - Tshirege unit 1vu
Qbt1vc	Bandelier Tuff - Tshirege unit 1vc
Qbt1g	Bandelier Tuff - Tshirege unit 1g
Qbt	Bandelier Tuff - undivided
Qct	Cerro Toledo Interval
Qbof	Bandelier Tuff - Otowi unit
Qbog	Bandelier Tuff - Guaje Pumice
Tb4	Cerros del Rio Basalts
QTa	Ancha Formation
Tvt2	Younger Tschicoma dacite flows
Tvt1	Older Tschicoma dacite flows
Tpf	Puye Formation
Tpt	Totavi Lentil
Tvk	Keres Volcanics
Tcac	Chamita Fm - Lithosome A
Ttca	Tesuque Fm - Chamita Lithosome B
Tcara	Transitional zone: Ttca-Tcar
Tcar	Chamita Fm - axial river deposits
Tb2	8.4-9.3 Ma Basalts
Ttb	Tesuque Fm - Lithosome B

Constructed from the 2009 LANL Geologic Framework Model (Cole et al. 2009, 106101)

Note: Alluvial units: Qu and Qvf will be added to this bedrock model at a later date.

Date: May 2009

Plate 2-2. Modeled surface geology

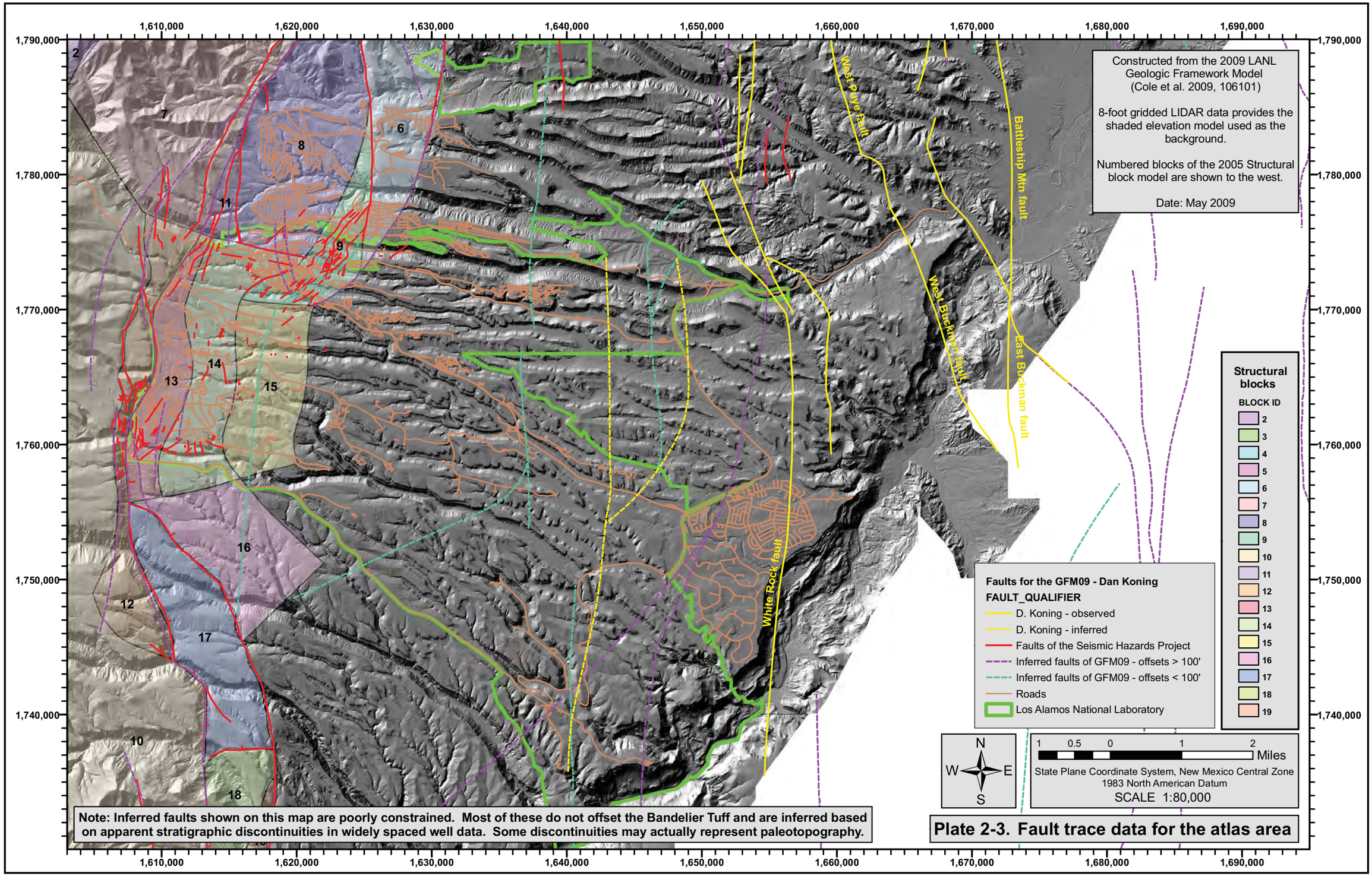


Plate 2-3. Fault trace data for the atlas area

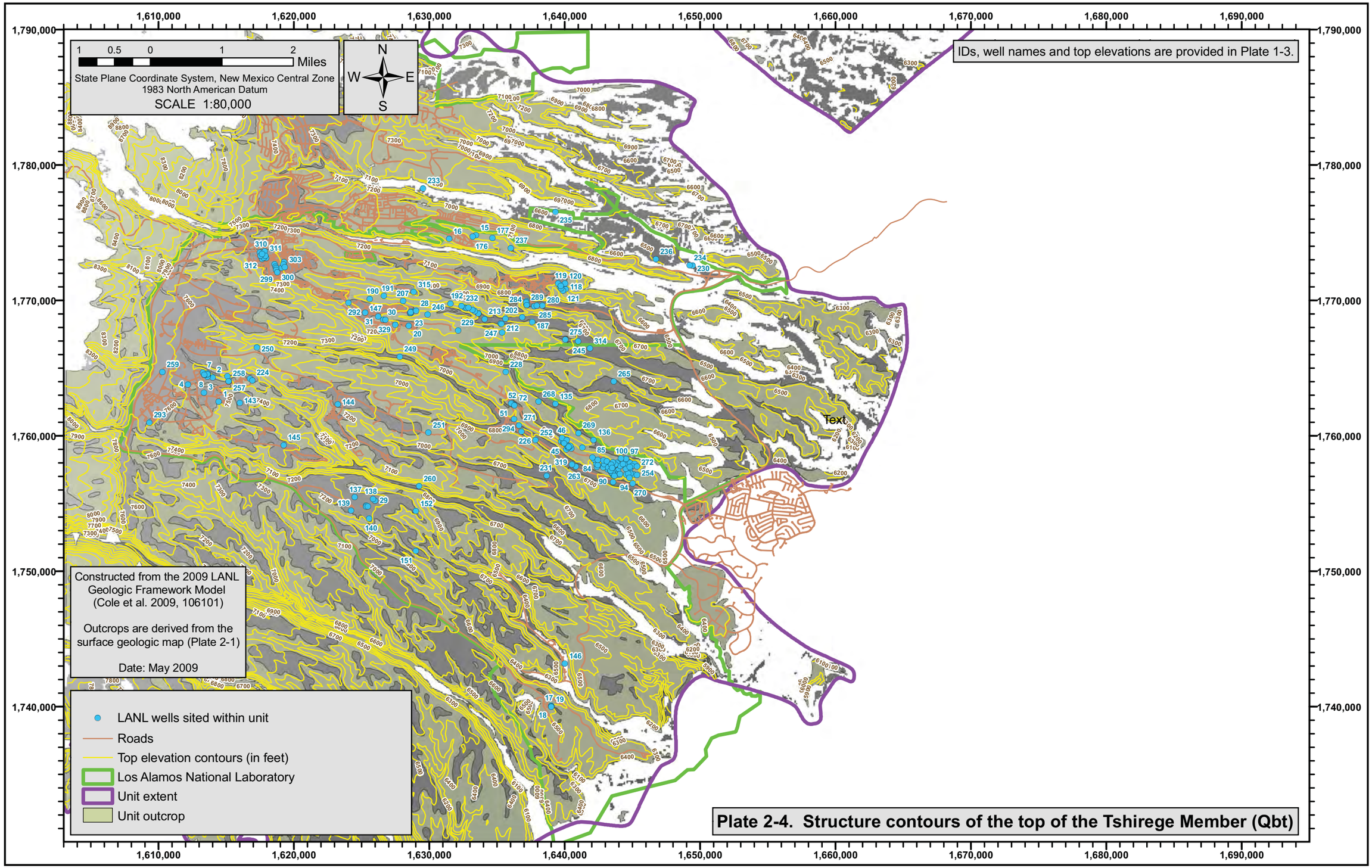
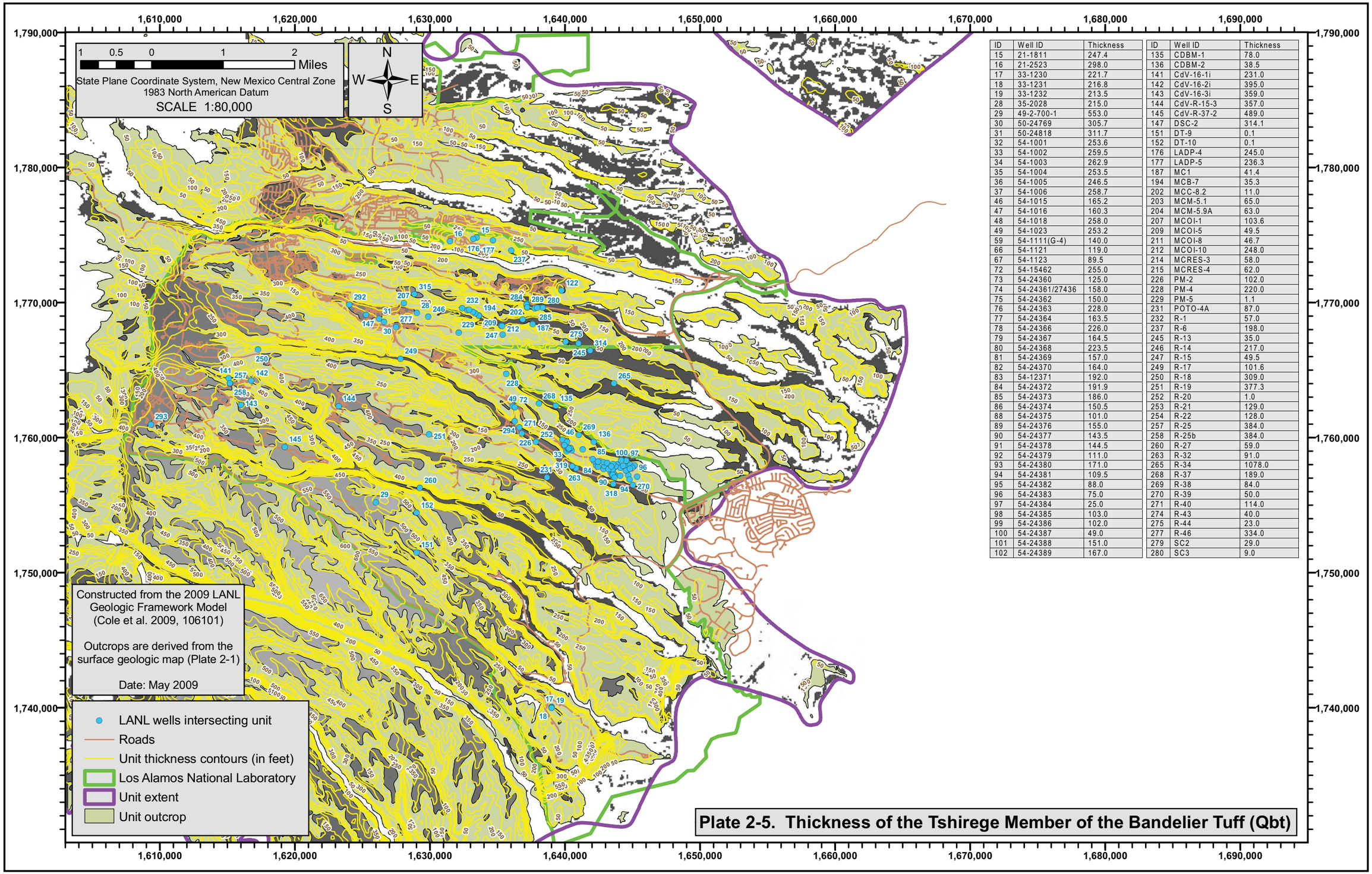


Plate 2-4. Structure contours of the top of the Tshirege Member (Qbt)



ID	Well ID	Thickness
15	21-1811	247.4
16	21-2523	298.0
17	33-1230	221.7
18	33-1231	216.8
19	33-1232	213.5
28	35-2028	215.0
29	49-2-700-1	553.0
30	50-24769	305.7
31	50-24818	311.7
32	54-1001	253.6
33	54-1002	259.5
34	54-1003	262.9
35	54-1004	253.5
36	54-1005	246.5
37	54-1006	258.7
46	54-1015	165.2
47	54-1016	160.3
48	54-1018	258.0
49	54-1023	253.2
59	54-1111(G-4)	140.0
66	54-1121	119.0
67	54-1123	89.5
72	54-15462	255.0
73	54-24360	125.0
74	54-24361/27436	158.0
75	54-24362	150.0
76	54-24363	228.0
77	54-24364	163.5
78	54-24366	226.0
79	54-24367	164.5
80	54-24368	223.5
81	54-24369	157.0
82	54-24370	164.0
83	54-12371	192.0
84	54-24372	191.9
85	54-24373	186.0
86	54-24374	150.5
88	54-24375	101.0
89	54-24376	155.0
90	54-24377	143.5
91	54-24378	144.5
92	54-24379	111.0
93	54-24380	171.0
94	54-24381	109.5
95	54-24382	88.0
96	54-24383	75.0
97	54-24384	25.0
98	54-24385	103.0
99	54-24386	102.0
100	54-24387	49.0
101	54-24388	151.0
102	54-24389	167.0

ID	Well ID	Thickness
135	CDBM-1	78.0
136	CDBM-2	38.5
141	CdV-16-1i	231.0
142	CdV-16-2i	395.0
143	CdV-16-3i	359.0
144	CdV-R-15-3	357.0
145	CdV-R-37-2	489.0
147	DSC-2	314.1
151	DT-9	0.1
152	DT-10	0.1
176	LADP-4	245.0
177	LADP-5	236.3
187	MC1	41.4
194	MCB-7	35.3
202	MCC-8.2	11.0
203	MCM-5.1	65.0
204	MCM-5.9A	63.0
207	MCOI-1	103.6
209	MCOI-5	49.5
211	MCOI-8	46.7
212	MCOI-10	248.0
214	MCRES-3	58.0
215	MCRES-4	62.0
226	PM-2	102.0
228	PM-4	220.0
229	PM-5	1.1
231	POTO-4A	87.0
232	R-1	57.0
237	R-6	198.0
245	R-13	35.0
246	R-14	217.0
247	R-15	49.5
249	R-17	101.6
250	R-18	309.0
251	R-19	377.3
252	R-20	1.0
253	R-21	129.0
254	R-22	128.0
257	R-25	384.0
258	R-25b	384.0
260	R-27	59.0
263	R-32	91.0
265	R-34	1078.0
268	R-37	189.0
269	R-38	84.0
270	R-39	50.0
271	R-40	114.0
274	R-43	40.0
275	R-44	23.0
277	R-46	334.0
279	SC2	29.0
280	SC3	9.0

Plate 2-5. Thickness of the Tshirege Member of the Bandelier Tuff (Qbt)

1 0.5 0 1 2 Miles

State Plane Coordinate System, New Mexico Central Zone
1983 North American Datum
SCALE 1:80,000

N W E S

1,610,000 1,620,000 1,630,000 1,640,000 1,650,000 1,660,000 1,670,000 1,680,000 1,690,000

1,790,000 1,780,000 1,770,000 1,760,000 1,750,000 1,740,000

ID	Well ID	Elevation	ID	Well ID	Elevation
15	21-1811	6778.6	135	CDBM-1	6636.6
16	21-2523	6859.0	136	CDBM-2	6581.6
17	33-1230	6291.0	141	CdV-16-1i	7142.2
18	33-1231	6299.0	142	CdV-16-2i	7062.1
19	33-1232	6302.0	143	CdV-16-3i	7127.8
28	35-2028	6883.9	144	CdV-R-15-3	6896.9
29	49-2-700-1	6572.9	145	CdV-R-37-2	6841.6
30	50-24769	6923.7	147	DSC-2	6970.9
31	50-24818	6923.0	151	DT-9	6474.0
32	54-1001	6527.1	152	DT-10	6541.0
33	54-1002	6527.9	176	LADP-4	6798.7
34	54-1003	6526.7	177	LADP-5	6780.5
35	54-1004	6533.2	187	MC1	6710.6
36	54-1005	6531.1	194	MCB-7	6767.9
37	54-1006	6530.5	202	MCC-8.2	6688.2
46	54-1015	6542.1	203	MCM-5.1	6774.8
47	54-1016	6539.3	204	MCM-5.9A	6749.2
48	54-1018	6528.7	207	MCOI-1	6902.2
49	54-1023	6628.3	209	MCOI-5	6753.7
59	54-1111(G-4)	6534.6	211	MCOI-8	6780.3
66	54-1121	6553.5	212	MCOI-10	6715.5
67	54-1123	6575.8	214	MCRES-3	6778.6
72	54-15462	6625.0	215	MCRES-4	6776.1
73	54-24360	6536.6	226	PM-2	6580.0
74	54-24361/27436	6534.1	228	PM-4	6700.0
75	54-24362	6526.6	229	PM-5	6759.0
76	54-24363	6459.0	231	POTO-4A	6535.0
77	54-24364	6539.2	232	R-1	6791.2
78	54-24366	6450.7	237	R-6	6797.8
79	54-24367	6522.6	245	R-13	6600.1
80	54-24368	6488.1	246	R-14	6842.1
81	54-24369	6544.0	247	R-15	6754.0
82	54-24370	6559.4	249	R-17	6795.2
83	54-12371	6533.4	250	R-18	7095.8
84	54-24372	6546.1	251	R-19	6686.3
85	54-24373	6556.5	252	R-20	6528.3
86	54-24374	6524.2	253	R-21	6510.2
88	54-24375	6537.9	254	R-22	6522.5
89	54-24376	6536.0	257	R-25	7132.1
90	54-24377	6538.0	258	R-25b	7132.0
91	54-24378	6536.3	260	R-27	6633.7
92	54-24379	6558.6	263	R-32	6499.6
93	54-24380	6521.6	265	R-34	5534.0
94	54-24381	6548.1	268	R-37	6631.0
95	54-24382	6577.4	269	R-38	6534.0
96	54-24383	6574.7	270	R-39	6505.0
97	54-24384	6560.5	271	R-40	6564.0
98	54-24385	6568.4	274	R-43	6650.0
99	54-24386	6566.8	275	R-44	6648.0
100	54-24387	6562.0	277	R-46	6868.0
101	54-24388	6530.8	279	SC2	6671.0
102	54-24389	6528.7	280	SC3	6642.0

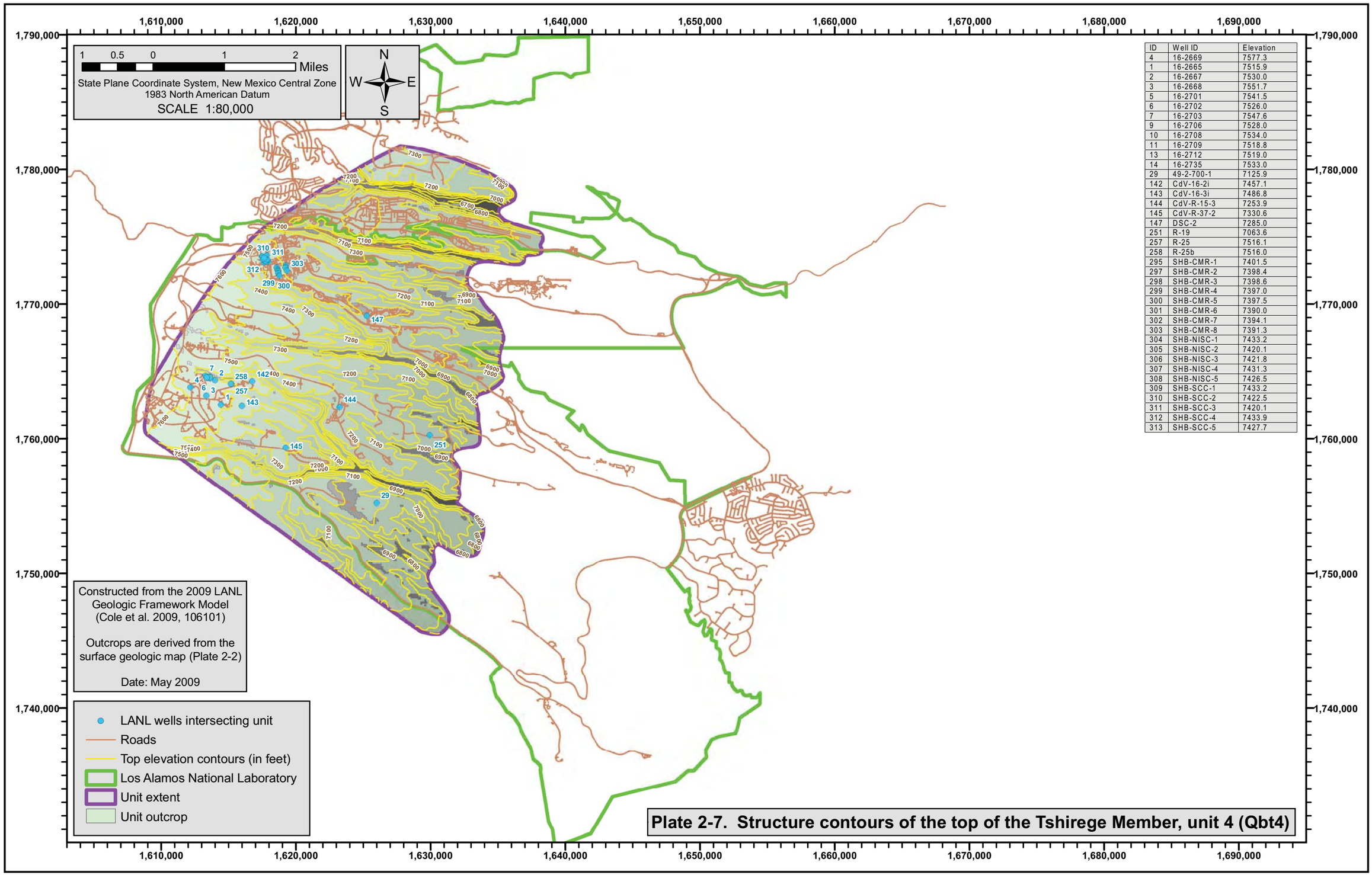
Constructed from the 2009 LANL Geologic Framework Model (Cole et al. 2009, 106101)

Outcrops are derived from the surface geologic map (Plate 2-1)

Date: May 2009

- LANL wells intersecting unit surface
- Roads
- Bottom elevation contours (in feet)
- Los Alamos National Laboratory
- Unit extent
- Unit outcrop

Plate 2-6. Structure contours of the bottom of the Tshirege Member (Qbt)



ID	Well ID	Elevation
4	16-2669	7577.3
1	16-2665	7515.9
2	16-2667	7530.0
3	16-2668	7551.7
5	16-2701	7541.5
6	16-2702	7526.0
7	16-2703	7547.6
9	16-2706	7528.0
10	16-2708	7534.0
11	16-2709	7518.8
13	16-2712	7519.0
14	16-2735	7533.0
29	49-2-700-1	7125.9
142	CdV-16-2i	7457.1
143	CdV-16-3i	7486.8
144	CdV-R-15-3	7253.9
145	CdV-R-37-2	7330.6
147	DSC-2	7285.0
251	R-19	7063.6
257	R-25	7516.1
258	R-25b	7516.0
295	SHB-CMR-1	7401.5
297	SHB-CMR-2	7398.4
298	SHB-CMR-3	7398.6
299	SHB-CMR-4	7397.0
300	SHB-CMR-5	7397.5
301	SHB-CMR-6	7390.0
302	SHB-CMR-7	7394.1
303	SHB-CMR-8	7391.3
304	SHB-NISC-1	7433.2
305	SHB-NISC-2	7420.1
306	SHB-NISC-3	7421.8
307	SHB-NISC-4	7431.3
308	SHB-NISC-5	7426.5
309	SHB-SCC-1	7433.2
310	SHB-SCC-2	7422.5
311	SHB-SCC-3	7420.1
312	SHB-SCC-4	7433.9
313	SHB-SCC-5	7427.7

Plate 2-7. Structure contours of the top of the Tshirege Member, unit 4 (Qbt4)

1 0.5 0 1 2 Miles

State Plane Coordinate System, New Mexico Central Zone
1983 North American Datum
SCALE 1:80,000

N W E S

ID	Well ID	Thickness
4	16-2669	88.0
1	16-2665	99.5
2	16-2667	90.5
3	16-2668	91.0
10	16-2708	98.0
29	49-2-700-1	65.0
142	CdV-16-2i	56.0
143	CdV-16-3i	70.0
144	CdV-R-15-3	29.0
145	CdV-R-37-2	25.0
147	DSC-2	10.1
251	R-19	2.3
257	R-25	84.0
295	SHB-CMR-1	46.5
297	SHB-CMR-2	41.0
298	SHB-CMR-3	39.1
299	SHB-CMR-4	34.8
300	SHB-CMR-5	33.5
301	SHB-CMR-6	45.3
302	SHB-CMR-7	45.7
303	SHB-CMR-8	41.1
304	SHB-NISC-1	69.5
305	SHB-NISC-2	66.9
306	SHB-NISC-3	63.8
307	SHB-NISC-4	63.0
308	SHB-NISC-5	67.4
309	SHB-SCC-1	73.0
310	SHB-SCC-2	71.0
311	SHB-SCC-3	65.6
312	SHB-SCC-4	70.5
313	SHB-SCC-5	68.3

1,610,000 1,620,000 1,630,000 1,640,000 1,650,000 1,660,000 1,670,000 1,680,000 1,690,000

1,790,000 1,780,000 1,770,000 1,760,000 1,750,000 1,740,000

Constructed from the 2009 LANL Geologic Framework Model (Cole et al. 2009, 106101)

Outcrops are derived from the surface geologic map (Plate 2-2)

Date: May 2009

- LANL wells intersecting unit
- Roads
- Unit thickness contours (in feet)
- Los Alamos National Laboratory
- Unit extent
- Unit outcrop

Plate 2-8. Thickness of the Tshirege Member, unit 4 (Qbt4)

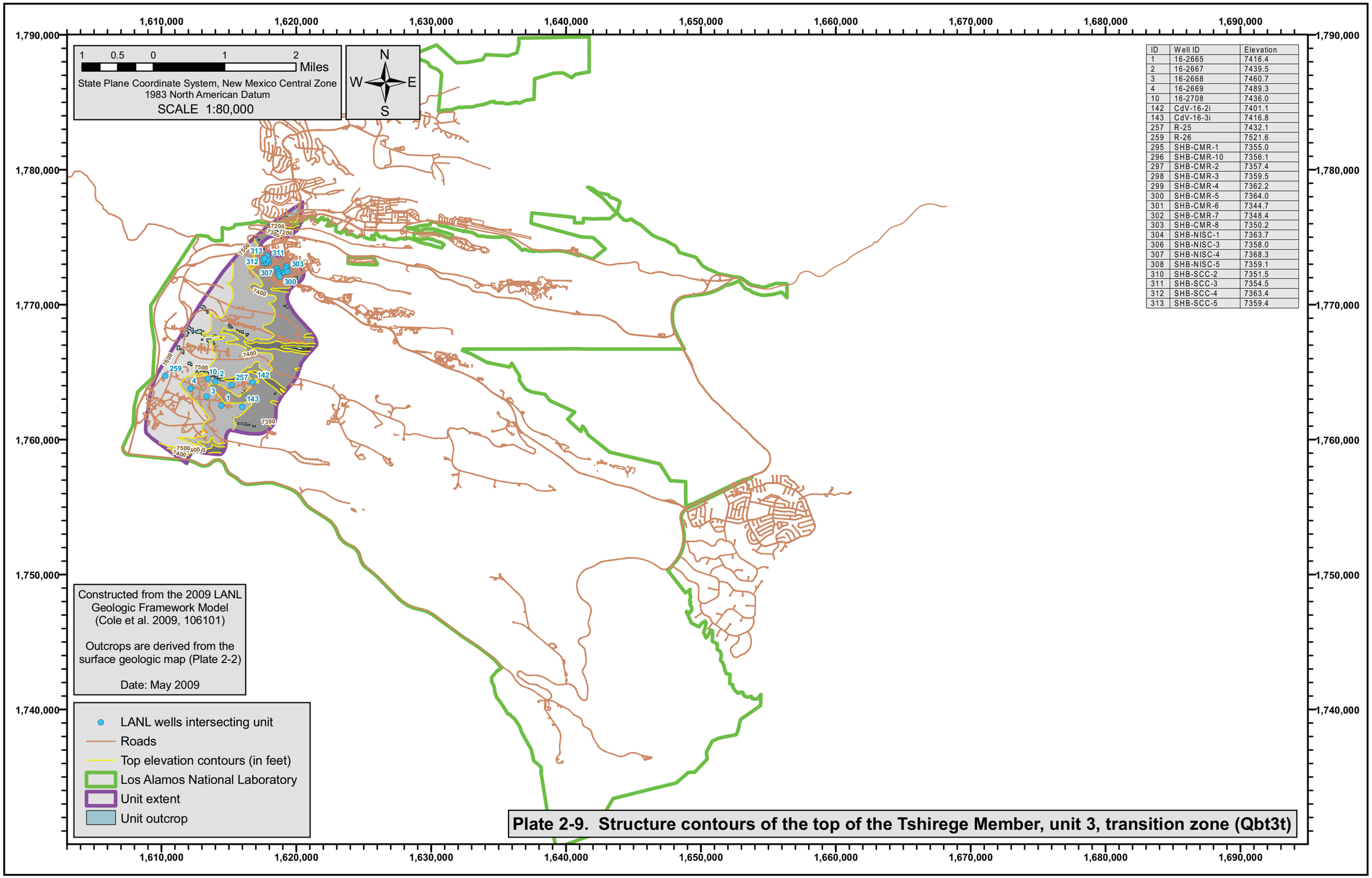


Plate 2-9. Structure contours of the top of the Tshirege Member, unit 3, transition zone (Qbt3t)

1 0.5 0 1 2 Miles

State Plane Coordinate System, New Mexico Central Zone
1983 North American Datum
SCALE 1:80,000

N W E S

ID	Well ID	Thickness
1	16-2665	19.0
2	16-2667	31.7
3	16-2668	22.7
4	16-2669	24.0
142	CdV-16-2i	21.0
143	CdV-16-3i	18.0
257	R-25	71.0
259	R-26	180.0
295	SHB-CMR-1	10.1
296	SHB-CMR-10	7.7
297	SHB-CMR-2	7.8
298	SHB-CMR-3	6.1
299	SHB-CMR-4	7.3
300	SHB-CMR-5	5.6
301	SHB-CMR-6	2.5
302	SHB-CMR-7	6.0
303	SHB-CMR-8	2.5
304	SHB-NISC-1	1.3
306	SHB-NISC-3	4.5
307	SHB-NISC-4	4.0
308	SHB-NISC-5	1.3
310	SHB-SCC-2	0.8
311	SHB-SCC-3	2.4
312	SHB-SCC-4	2.0
313	SHB-SCC-5	1.2

1,610,000 1,620,000 1,630,000 1,640,000 1,650,000 1,660,000 1,670,000 1,680,000 1,690,000

1,790,000 1,780,000 1,770,000 1,760,000 1,750,000 1,740,000

Constructed from the 2009 LANL Geologic Framework Model (Cole et al. 2009, 106101)

Outcrops are derived from the surface geologic map (Plate 2-2)

Date: May 2009

- LANL wells intersecting unit
- Roads
- Unit thickness contours (in feet)
- Los Alamos National Laboratory
- Unit extent
- Unit outcrop

Plate 2-10. Thickness of the Tshirege Member, unit 3, transition zone (Qbt3t)

1 0.5 0 1 2 Miles

State Plane Coordinate System, New Mexico Central Zone
1983 North American Datum
SCALE 1:80,000

N W E S

1,610,000 1,620,000 1,630,000 1,640,000 1,650,000 1,660,000 1,670,000 1,680,000 1,690,000

1,790,000 1,780,000 1,770,000 1,760,000 1,750,000 1,740,000

ID	Well ID	Elevation
1	16-2665	7397.4
2	16-2667	7407.8
3	16-2668	7438.0
4	16-2669	7465.3
29	49-2-700-1	7060.9
142	CdV-16-2i	7380.1
143	CdV-16-3i	7398.8
144	CdV-R-15-3	7224.9
145	CdV-R-37-2	7305.6
147	DSC-2	7274.9
251	R-19	7061.3
257	R-25	7361.1
258	R-25b	7361.0
259	R-26	7341.6
295	SHB-CMR-1	7344.9
296	SHB-CMR-10	7348.4
297	SHB-CMR-2	7349.6
298	SHB-CMR-3	7353.4
299	SHB-CMR-4	7354.9
300	SHB-CMR-5	7358.4
301	SHB-CMR-6	7342.2
302	SHB-CMR-7	7342.4
303	SHB-CMR-8	7347.7
304	SHB-NISC-1	7362.4
305	SHB-NISC-2	7353.3
306	SHB-NISC-3	7353.5
307	SHB-NISC-4	7364.3
308	SHB-NISC-5	7357.8
309	SHB-SCC-1	7360.2
310	SHB-SCC-2	7350.7
311	SHB-SCC-3	7352.1
312	SHB-SCC-4	7361.4
313	SHB-SCC-5	7358.2
16	21-2523	7157.0
18	33-1231	6515.8
19	33-1232	6515.5
22	35-2006	7177.4
25	35-2009	7155.3
28	35-2028	7098.9
31	50-24818	7234.7
116	BH1	6914.2
117	BH2	6914.4
119	BH4	6925.9
120	BH5	6910.4
141	CdV-16-1i	7373.2
176	LADP-4	7043.7
250	R-18	7404.8
277	R-46	7202.0
292	SHB-1	7314.9

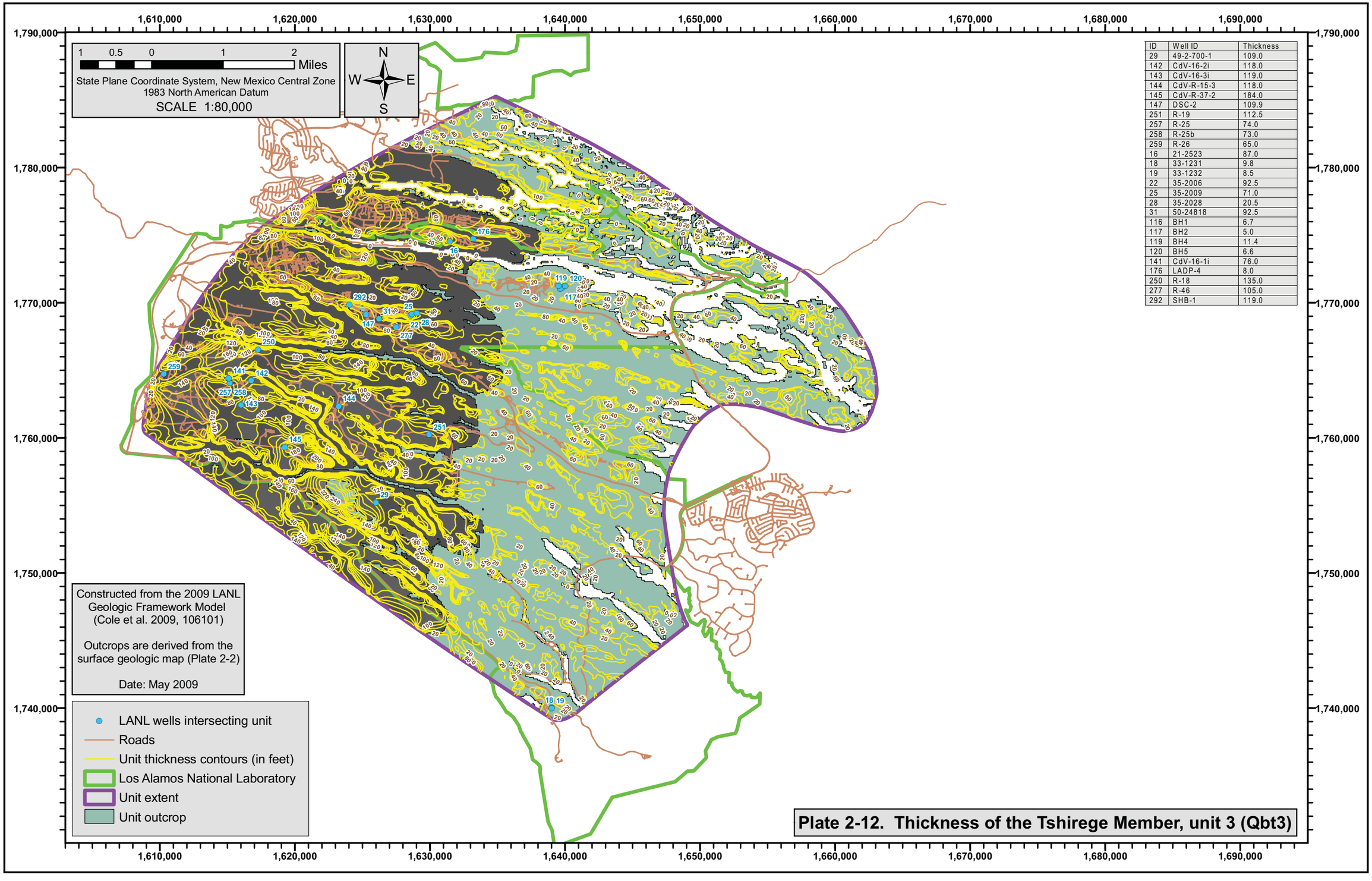
Constructed from the 2009 LANL Geologic Framework Model (Cole et al. 2009, 106101)

Outcrops are derived from the surface geologic map (Plate 2-2)

Date: May 2009

- LANL wells intersecting unit
- Roads
- Top elevation contours (in feet)
- Los Alamos National Laboratory
- Unit extent
- Unit outcrop

Plate 2-11. Structure contours of the top of the Tshirege Member, unit 3 (Qbt3)



ID	Well ID	Thickness
29	49-2-700-1	109.0
142	CdV-16-2i	118.0
143	CdV-16-3i	119.0
144	CdV-R-15-3	118.0
145	CdV-R-37-2	184.0
147	DSC-2	109.9
251	R-19	112.5
257	R-25	74.0
258	R-25b	73.0
259	R-26	65.0
16	21-2523	87.0
18	33-1231	9.8
19	33-1232	8.5
22	35-2006	92.5
25	35-2009	71.0
28	35-2028	20.5
31	50-24818	92.5
116	BH1	6.7
117	BH2	5.0
119	BH4	11.4
120	BH5	6.6
141	CdV-16-1i	76.0
176	LADP-4	8.0
250	R-18	135.0
277	R-46	105.0
292	SHB-1	119.0

Plate 2-12. Thickness of the Tshirege Member, unit 3 (Qbt3)

1 0.5 0 1 2 Miles

State Plane Coordinate System, New Mexico Central Zone
1983 North American Datum
SCALE 1:80,000

N W E S

1,610,000 1,620,000 1,630,000 1,640,000 1,650,000 1,660,000 1,670,000 1,680,000 1,690,000

1,790,000 1,780,000 1,770,000 1,760,000 1,750,000 1,740,000

ID	Well ID	Elevation	ID	Well ID	Elevation
16	21-2523	7070.0	52	54-1026	6888.9
18	33-1231	6506.0	55	54-1106	6699.0
19	33-1232	6507.0	57	54-1108	6699.1
20	35-2004	7094.2	60	54-1112	6690.4
21	35-2005	7082.7	62	54-1115	6671.6
22	35-2006	7084.9	64	54-1117	6675.7
23	35-2007	7083.5	68	54-1124	6635.1
24	35-2008	7082.5	69	54-1125	6668.4
25	35-2009	7084.3	70	54-1126	6655.5
26	35-2011	7082.3	82	54-24370	6723.4
27	35-2013	7085.1	89	54-24376	6691.0
28	35-2028	7078.4	93	54-24380	6692.6
29	49-2-700-1	6951.9	108	54-24395	6725.3
30	50-24769	7138.2	116	BH1	6907.5
31	50-24818	7142.2	117	BH2	6909.4
32	54-1001	6780.7	119	BH4	6914.5
33	54-1002	6787.4	120	BH5	6903.8
34	54-1003	6789.6	141	CdV-16-1i	7297.2
35	54-1004	6786.7	142	CdV-16-2i	7262.1
36	54-1005	6777.6	143	CdV-16-3i	7279.8
37	54-1006	6789.2	144	CdV-R-15-3	7106.9
38	54-1007	6790.2	145	CdV-R-37-2	7121.6
39	54-1008	6795.6	147	DSC-2	7165.0
40	54-1009	6790.5	176	LADP-4	7035.7
41	54-1010	6789.8	224	P-12	7256.6
42	54-1011	6790.4	250	R-18	7269.8
43	54-1012	6791.1	251	R-19	6948.8
44	54-1013	6791.1	257	R-25	7287.1
45	54-1014	6792.7	258	R-25b	7288.0
48	54-1018	6786.7	259	R-26	7276.6
49	54-1023	6881.5	277	R-46	7097.0
50	54-1024	6875.0	292	SHB-1	7195.9
51	54-1025	6886.2	329	USGS-TH	7117.4

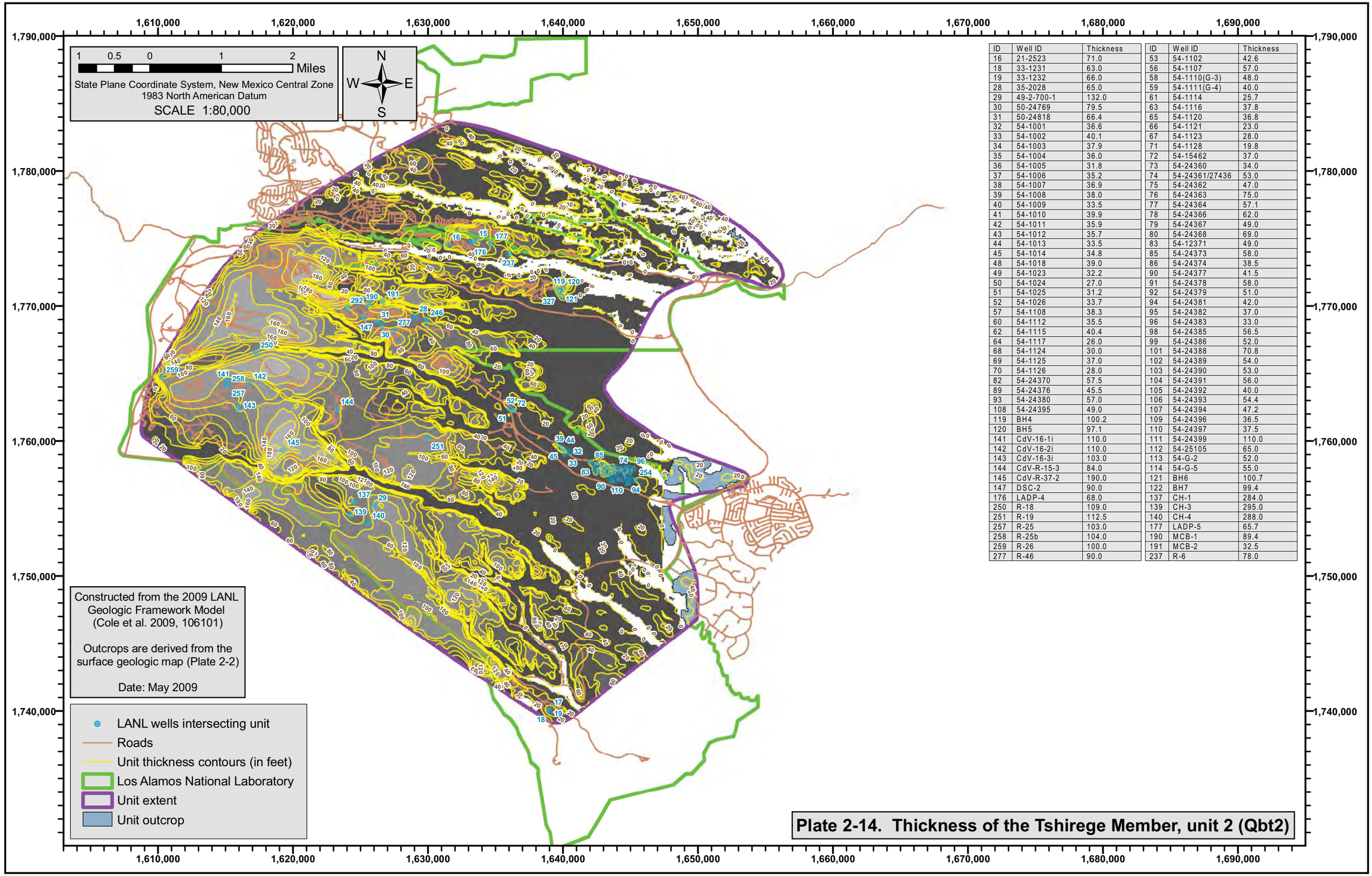
Constructed from the 2009 LANL Geologic Framework Model (Cole et al. 2009, 106101)

Outcrops are derived from the surface geologic map (Plate 2-2)

Date: May 2009

- LANL wells intersecting unit
- Roads
- Top elevation contours (in feet)
- Los Alamos National Laboratory
- Unit extent
- Unit outcrop

Plate 2-13. Structure contours of the top of the Tshirege Member, unit 2 (Qbt2)



ID	Well ID	Thickness
16	21-2523	71.0
18	33-1231	63.0
19	33-1232	66.0
28	35-2028	65.0
29	49-2-700-1	132.0
30	50-24769	79.5
31	50-24818	66.4
32	54-1001	36.6
33	54-1002	40.1
34	54-1003	37.9
35	54-1004	36.0
36	54-1005	31.8
37	54-1006	35.2
38	54-1007	36.9
39	54-1008	38.0
40	54-1009	33.5
41	54-1010	39.9
42	54-1011	35.9
43	54-1012	35.7
44	54-1013	33.5
45	54-1014	34.8
48	54-1018	39.0
49	54-1023	32.2
50	54-1024	27.0
51	54-1025	31.2
52	54-1026	33.7
57	54-1108	38.3
60	54-1112	35.5
62	54-1115	40.4
64	54-1117	26.0
68	54-1124	30.0
69	54-1125	37.0
70	54-1126	28.0
82	54-24370	57.5
89	54-24376	45.5
93	54-24380	57.0
108	54-24395	49.0
119	BH4	100.2
120	BH5	97.1
141	CdV-16-1i	110.0
142	CdV-16-2i	110.0
143	CdV-16-3i	103.0
144	CdV-R-15-3	84.0
145	CdV-R-37-2	190.0
147	DSC-2	90.0
176	LADP-4	68.0
250	R-18	109.0
251	R-19	112.5
257	R-25	103.0
258	R-25b	104.0
259	R-26	100.0
277	R-46	90.0

ID	Well ID	Thickness
53	54-1102	42.6
56	54-1107	57.0
58	54-1110(G-3)	48.0
59	54-1111(G-4)	40.0
61	54-1114	25.7
63	54-1116	37.8
65	54-1120	36.8
66	54-1121	23.0
67	54-1123	28.0
71	54-1128	19.8
72	54-15462	37.0
73	54-24360	34.0
74	54-24361/27436	53.0
75	54-24362	47.0
76	54-24363	75.0
77	54-24364	57.1
78	54-24366	62.0
79	54-24367	49.0
80	54-24368	69.0
83	54-12371	49.0
85	54-24373	58.0
86	54-24374	38.5
90	54-24377	41.5
91	54-24378	58.0
92	54-24379	51.0
94	54-24381	42.0
95	54-24382	37.0
96	54-24383	33.0
98	54-24385	56.5
99	54-24386	52.0
101	54-24388	70.8
102	54-24389	54.0
103	54-24390	53.0
104	54-24391	56.0
105	54-24392	40.0
106	54-24393	54.4
107	54-24394	47.2
109	54-24396	36.5
110	54-24397	37.5
111	54-24399	110.0
112	54-25105	65.0
113	54-G-2	52.0
114	54-G-5	55.0
121	BH6	100.7
122	BH7	99.4
137	CH-1	284.0
139	CH-3	295.0
140	CH-4	288.0
177	LADP-5	65.7
190	MCB-1	89.4
191	MCB-2	32.5
237	R-6	78.0

Plate 2-14. Thickness of the Tshirege Member, unit 2 (Qbt2)

1 0.5 0 1 2 Miles

State Plane Coordinate System, New Mexico Central Zone
1983 North American Datum
SCALE 1:80,000

N W E S

1,610,000 1,620,000 1,630,000 1,640,000 1,650,000 1,660,000 1,670,000 1,680,000 1,690,000

1,790,000 1,780,000 1,770,000 1,760,000 1,750,000 1,740,000

ID	Well ID	Elevation	ID	Well ID	Elevation
15	21-1811	6939.0	86	54-24374	6636.2
16	21-2523	6999.0	88	54-24375	6638.9
17	33-1230	6442.0	89	54-24376	6645.5
18	33-1231	6443.0	90	54-24377	6640.0
19	33-1232	6441.0	91	54-24378	6622.8
28	35-2028	7013.4	92	54-24379	6618.6
29	49-2-700-1	6819.9	93	54-24380	6635.6
30	50-24769	7058.7	94	54-24381	6615.6
31	50-24818	7075.8	95	54-24382	6628.4
32	54-1001	6744.1	96	54-24383	6616.7
33	54-1002	6747.3	98	54-24385	6614.9
34	54-1003	6751.7	99	54-24386	6616.8
35	54-1004	6750.7	101	54-24388	6611.0
36	54-1005	6745.8	102	54-24389	6641.7
37	54-1006	6754.0	103	54-24390	6646.0
38	54-1007	6753.3	104	54-24391	6650.0
39	54-1008	6757.6	105	54-24392	6624.4
40	54-1009	6757.0	106	54-24393	6659.4
41	54-1010	6749.9	107	54-24394	6669.1
42	54-1011	6754.5	108	54-24395	6676.3
43	54-1012	6755.4	109	54-24396	6643.5
44	54-1013	6757.6	110	54-24397	6631.9
45	54-1014	6757.9	111	54-24399	6683.0
48	54-1018	6747.7	112	54-25105	6644.0
49	54-1023	6849.3	113	54-G-2	6642.1
50	54-1024	6848.0	114	54-G-5	6644.1
51	54-1025	6855.0	119	BH4	6814.2
52	54-1026	6855.2	120	BH5	6806.6
53	54-1102	6677.7	121	BH6	6810.3
56	54-1107	6661.1	122	BH7	6810.4
57	54-1108	6660.8	137	CH-1	6886.6
58	54-1110(G-3)	6643.2	138	CH-2	6843.3
59	54-1111(G-4)	6634.6	139	CH-3	6874.9
60	54-1112	6654.9	140	CH-4	6830.2
61	54-1114	6640.8	141	CdV-16-1i	7187.2
62	54-1115	6631.2	142	CdV-16-2i	7152.1
63	54-1116	6644.7	143	CdV-16-3i	7176.8
64	54-1117	6649.7	144	CdV-R-15-3	7022.9
65	54-1120	6650.8	145	CdV-R-37-2	6931.6
66	54-1121	6649.5	147	DSC-2	7075.0
67	54-1123	6637.3	150	DT-5P	6854.8
68	54-1124	6605.1	176	LADP-4	6967.7
69	54-1125	6631.4	177	LADP-5	6951.1
70	54-1126	6627.5	190	MCB-1	7059.7
71	54-1128	6633.2	191	MCB-2	7043.9
72	54-15462	6843.0	207	MCOI-1	7005.7
73	54-24360	6627.6	212	MCOI-10	6904.5
74	54-24361/27436	6639.1	237	R-6	6917.8
75	54-24362	6629.6	246	R-14	6982.1
76	54-24363	6612.0	250	R-18	7160.8
77	54-24364	6645.6	251	R-19	6836.3
78	54-24366	6614.7	254	R-22	6606.5

Constructed from the 2009 LANL Geologic Framework Model (Cole et al. 2009, 106101)

Outcrops are derived from the surface geologic map (Plate 2-2)

Date: May 2009

- LANL wells intersecting unit
- Roads
- Top elevation contours (in feet)
- Los Alamos National Laboratory
- Unit extent
- Unit outcrop

Plate 2-15. Structure contours of the top of the Tshirege Member, unit 1, upper vapor-phase portion (Qbt1vu)

1 0.5 0 1 2 Miles

State Plane Coordinate System, New Mexico Central Zone
1983 North American Datum
SCALE 1:80,000

N W E S

1,610,000 1,620,000 1,630,000 1,640,000 1,650,000 1,660,000 1,670,000 1,680,000 1,690,000

1,790,000 1,780,000 1,770,000 1,760,000 1,750,000 1,740,000

ID	Well ID	Thickness
30	50-24769	40.0
31	50-24818	60.5
32	54-1001	67.6
33	54-1002	74.7
34	54-1003	74.0
35	54-1004	67.5
36	54-1005	58.8
37	54-1006	68.7
38	54-1007	74.0
39	54-1008	69.0
40	54-1009	75.0
48	54-1018	65.0
49	54-1023	94.3
56	54-1107	33.0
58	54-1110(G-3)	22.0
59	54-1111(G-4)	19.0
62	54-1115	24.1
63	54-1116	31.2
64	54-1117	36.0
66	54-1121	42.0
67	54-1123	34.5
70	54-1126	21.0
72	54-15462	93.0
73	54-24360	12.0
74	54-24361/27436	31.0
75	54-24362	23.0
76	54-24363	30.0
77	54-24364	22.9
78	54-24366	19.0
79	54-24367	21.0
80	54-24368	17.0
81	54-24369	28.5

ID	Well ID	Thickness
82	54-24370	24.5
83	54-12371	33.0
84	54-24372	39.0
85	54-24373	23.5
86	54-24374	24.0
88	54-24375	15.0
89	54-24376	22.0
90	54-24377	15.0
91	54-24378	18.0
92	54-24379	21.0
93	54-24380	18.0
94	54-24381	23.5
95	54-24382	6.0
96	54-24383	3.0
98	54-24385	12.5
99	54-24386	8.0
101	54-24388	11.2
102	54-24389	23.5
103	54-24390	32.0
104	54-24391	34.0
105	54-24392	18.0
106	54-24393	21.6
107	54-24394	30.0
108	54-24395	27.0
109	54-24396	29.5
110	54-24397	19.0
119	BH4	30.0
120	BH5	32.9
121	BH6	35.9
122	BH7	37.9
258	R-25b	37.0

Constructed from the 2009 LANL Geologic Framework Model (Cole et al. 2009, 106101)

Outcrops are derived from the surface geologic map (Plate 2-2)

Date: May 2009

- LANL wells intersecting unit
- Roads
- Unit thickness contours (in feet)
- Los Alamos National Laboratory
- Unit extent
- Unit outcrop

Plate 2-16. Thickness of the Tshirege Member, unit 1, upper vapor-phase portion (Qbt1vu)

1 0.5 0 1 2 Miles

State Plane Coordinate System, New Mexico Central Zone
1983 North American Datum
SCALE 1:80,000

N W E S

1,610,000 1,620,000 1,630,000 1,640,000 1,650,000 1,660,000 1,670,000 1,680,000 1,690,000

1,790,000 1,780,000 1,770,000 1,760,000 1,750,000 1,740,000

ID	Well ID	Elevation
30	50-24769	7018.7
31	50-24818	7015.3
32	54-1001	6676.5
33	54-1002	6672.6
34	54-1003	6677.7
35	54-1004	6683.2
36	54-1005	6687.0
37	54-1006	6685.3
38	54-1007	6679.3
39	54-1008	6688.6
40	54-1009	6682.0
46	54-1015	6707.3
47	54-1016	6699.6
48	54-1018	6682.7
49	54-1023	6755.0
56	54-1107	6628.1
58	54-1110(G-3)	6621.2
59	54-1111(G-4)	6615.6
62	54-1115	6607.1
63	54-1116	6613.5
64	54-1117	6613.7
66	54-1121	6607.5
67	54-1123	6602.8
70	54-1126	6606.5
72	54-15462	6750.0
73	54-24360	6615.6
74	54-24361/27436	6608.1
75	54-24362	6606.6
76	54-24363	6582.0
77	54-24364	6622.7
78	54-24366	6595.7
79	54-24367	6617.1

ID	Well ID	Elevation
80	54-24368	6625.6
81	54-24369	6625.0
82	54-24370	6641.4
83	54-12371	6643.4
84	54-24372	6648.5
85	54-24373	6661.0
86	54-24374	6612.2
88	54-24375	6623.9
89	54-24376	6623.5
90	54-24377	6625.0
91	54-24378	6604.8
93	54-24380	6617.6
95	54-24382	6622.4
96	54-24383	6613.7
98	54-24385	6602.4
99	54-24386	6608.8
101	54-24388	6599.8
102	54-24389	6618.2
103	54-24390	6614.0
104	54-24391	6616.0
105	54-24392	6606.4
106	54-24393	6637.8
107	54-24394	6639.1
108	54-24395	6649.3
109	54-24396	6614.0
110	54-24397	6612.9
119	BH4	6784.2
120	BH5	6773.8
121	BH6	6774.4
122	BH7	6772.5
294	SHB-4	6708.7

Constructed from the 2009 LANL Geologic Framework Model (Cole et al. 2009, 106101)

Outcrops are derived from the surface geologic map (Plate 2-2)

Date: May 2009

- LANL wells intersecting unit
- Roads
- Top elevation contours (in feet)
- Los Alamos National Laboratory
- Unit extent
- Unit outcrop

Plate 2-17. Structure contours of the top of the Tshirege Member, unit 1, colonnade vapor-phase portion (Qbt1vc)

1 0.5 0 1 2 Miles

State Plane Coordinate System, New Mexico Central Zone
1983 North American Datum
SCALE 1:80,000

N W E S

1,610,000 1,620,000 1,630,000 1,640,000 1,650,000 1,660,000 1,670,000 1,680,000 1,690,000

1,790,000 1,780,000 1,770,000 1,760,000 1,750,000 1,740,000

ID	Well ID	Thickness
30	50-24769	18.0
31	50-24818	13.6
32	54-1001	20.1
33	54-1002	16.3
34	54-1003	20.0
35	54-1004	26.0
36	54-1005	32.7
37	54-1006	24.1
38	54-1007	20.0
39	54-1008	22.0
40	54-1009	21.5
46	54-1015	37.4
47	54-1016	31.5
48	54-1018	26.0
49	54-1023	17.0
56	54-1107	12.0
58	54-1110(G-3)	15.0
59	54-1111(G-4)	21.0
64	54-1117	15.0
66	54-1121	11.5
67	54-1123	5.0
72	54-15462	16.0
73	54-24360	10.0
74	54-24361/27436	6.0
75	54-24362	10.0
76	54-24363	12.0
77	54-24364	14.0
78	54-24366	32.0
79	54-24367	16.0
80	54-24368	41.0
81	54-24369	15.0
82	54-24370	16.0
83	54-12371	20.0
84	54-24372	13.0
85	54-24373	23.0
86	54-24374	17.0
88	54-24375	19.0
89	54-24376	18.0
90	54-24377	23.0
91	54-24378	7.0
93	54-24380	14.0
95	54-24382	8.0
96	54-24383	11.5
98	54-24385	2.0
99	54-24386	8.5
101	54-24388	8.0
102	54-24389	16.5
103	54-24390	9.0
104	54-24391	8.0
105	54-24392	17.0
106	54-24393	13.5
107	54-24394	20.0

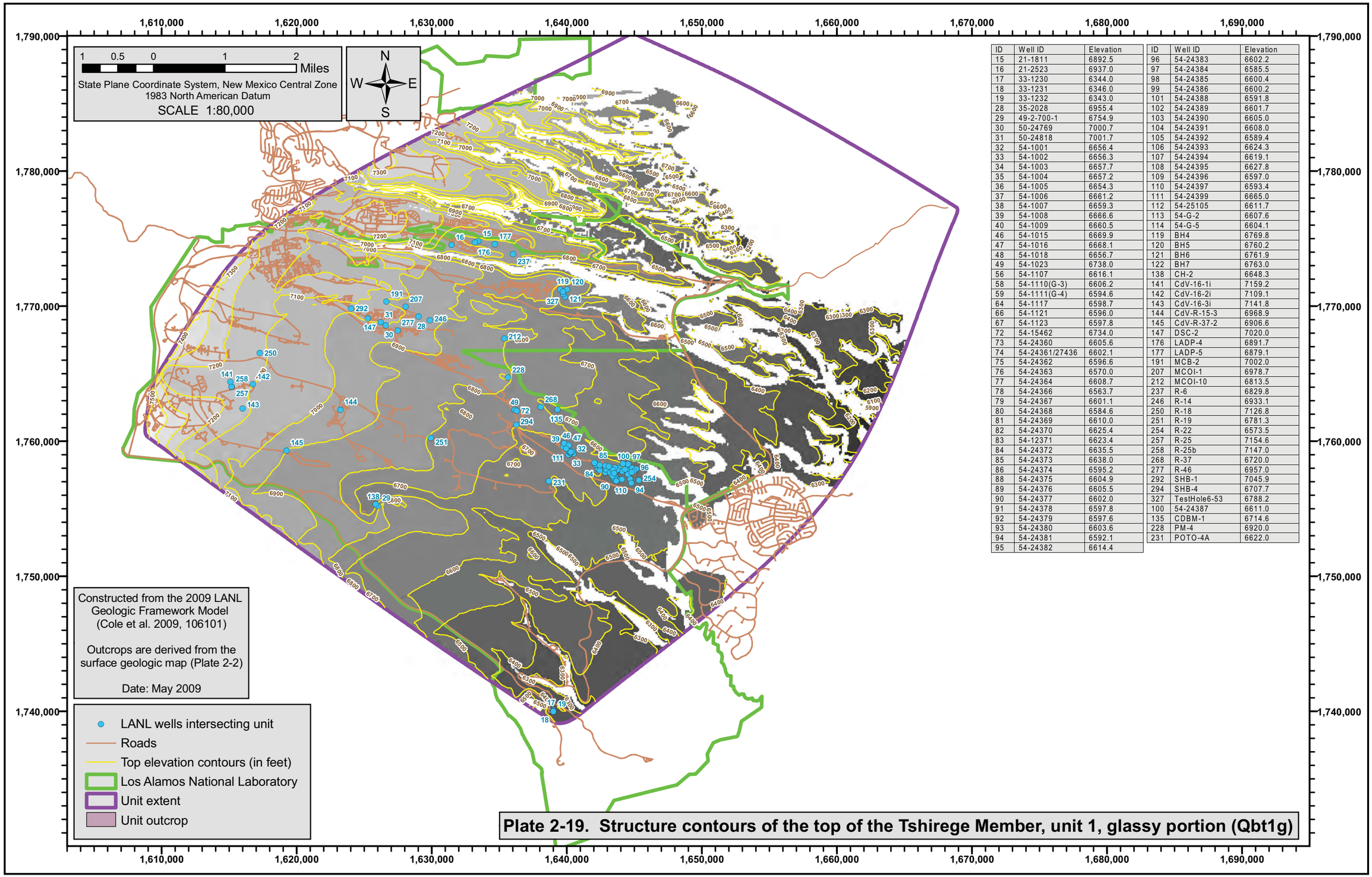
Constructed from the 2009 LANL Geologic Framework Model (Cole et al. 2009, 106101)

Outcrops are derived from the surface geologic map (Plate 2-2)

Date: May 2009

- LANL wells intersecting unit
- Roads
- Unit thickness contours (in feet)
- Los Alamos National Laboratory
- Unit extent
- Unit outcrop

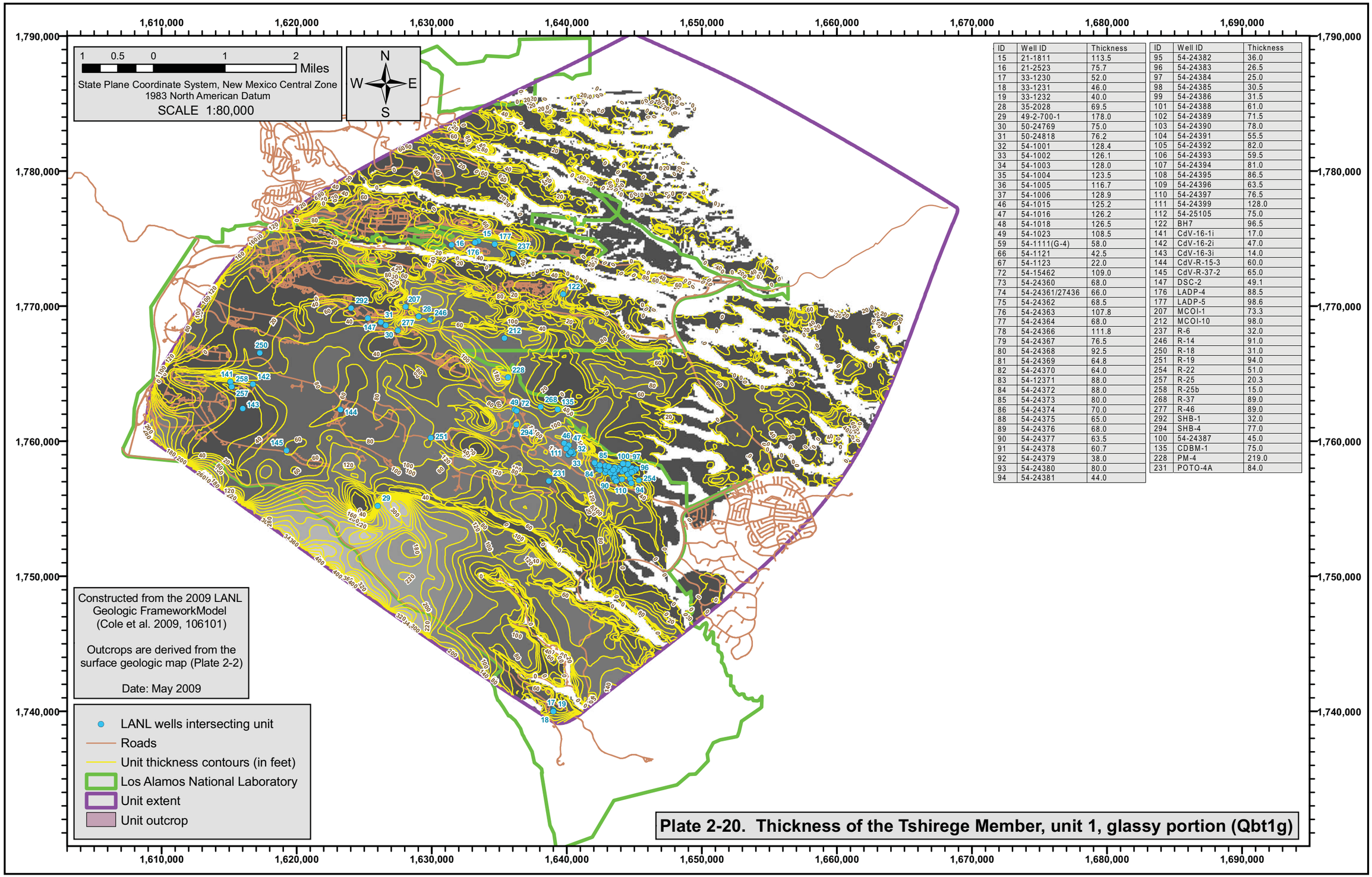
Plate 2-18. Thickness of the Tshirege Member, unit 1, colonnade vapor-phase portion (Qbt1vc)



ID	Well ID	Elevation
15	21-1811	6892.5
16	21-2523	6937.0
17	33-1230	6344.0
18	33-1231	6346.0
19	33-1232	6343.0
28	35-2028	6955.4
29	49-2-700-1	6754.9
30	50-24769	7000.7
31	50-24818	7001.7
32	54-1001	6656.4
33	54-1002	6656.3
34	54-1003	6657.7
35	54-1004	6657.2
36	54-1005	6654.3
37	54-1006	6661.2
38	54-1007	6659.3
39	54-1008	6666.6
40	54-1009	6660.5
46	54-1015	6669.9
47	54-1016	6668.1
48	54-1018	6656.7
49	54-1023	6738.0
56	54-1107	6616.1
58	54-1110(G-3)	6606.2
59	54-1111(G-4)	6594.6
64	54-1117	6598.7
66	54-1121	6596.0
67	54-1123	6597.8
72	54-15462	6734.0
73	54-24360	6605.6
74	54-24361/27436	6602.1
75	54-24362	6596.6
76	54-24363	6570.0
77	54-24364	6608.7
78	54-24366	6563.7
79	54-24367	6601.1
80	54-24368	6584.6
81	54-24369	6610.0
82	54-24370	6625.4
83	54-12371	6623.4
84	54-24372	6635.5
85	54-24373	6638.0
86	54-24374	6595.2
88	54-24375	6604.9
89	54-24376	6605.5
90	54-24377	6602.0
91	54-24378	6597.8
92	54-24379	6597.6
93	54-24380	6603.6
94	54-24381	6592.1
95	54-24382	6614.4

ID	Well ID	Elevation
96	54-24383	6602.2
97	54-24384	6585.5
98	54-24385	6600.4
99	54-24386	6600.2
101	54-24388	6591.8
102	54-24389	6601.7
103	54-24390	6605.0
104	54-24391	6608.0
105	54-24392	6589.4
106	54-24393	6624.3
107	54-24394	6619.1
108	54-24395	6627.8
109	54-24396	6597.0
110	54-24397	6593.4
111	54-24399	6665.0
112	54-25105	6611.7
113	54-G-2	6607.6
114	54-G-5	6604.1
119	BH4	6769.8
120	BH5	6760.2
121	BH6	6761.9
122	BH7	6763.0
138	CH-2	6648.3
141	CdV-16-1i	7159.2
142	CdV-16-2i	7109.1
143	CdV-16-3i	7141.8
144	CdV-R-15-3	6968.9
145	CdV-R-37-2	6906.6
147	DSC-2	7020.0
176	LADP-4	6891.7
177	LADP-5	6879.1
191	MCB-2	7002.0
207	MCOI-1	6978.7
212	MCOI-10	6813.5
237	R-6	6829.8
246	R-14	6933.1
250	R-18	7126.8
251	R-19	6781.3
254	R-22	6573.5
257	R-25	7154.6
258	R-25b	7147.0
268	R-37	6720.0
277	R-46	6957.0
292	SHB-1	7045.9
294	SHB-4	6707.7
327	TestHole6-53	6788.2
100	54-24387	6611.0
135	CDBM-1	6714.6
228	PM-4	6920.0
231	POTO-4A	6622.0

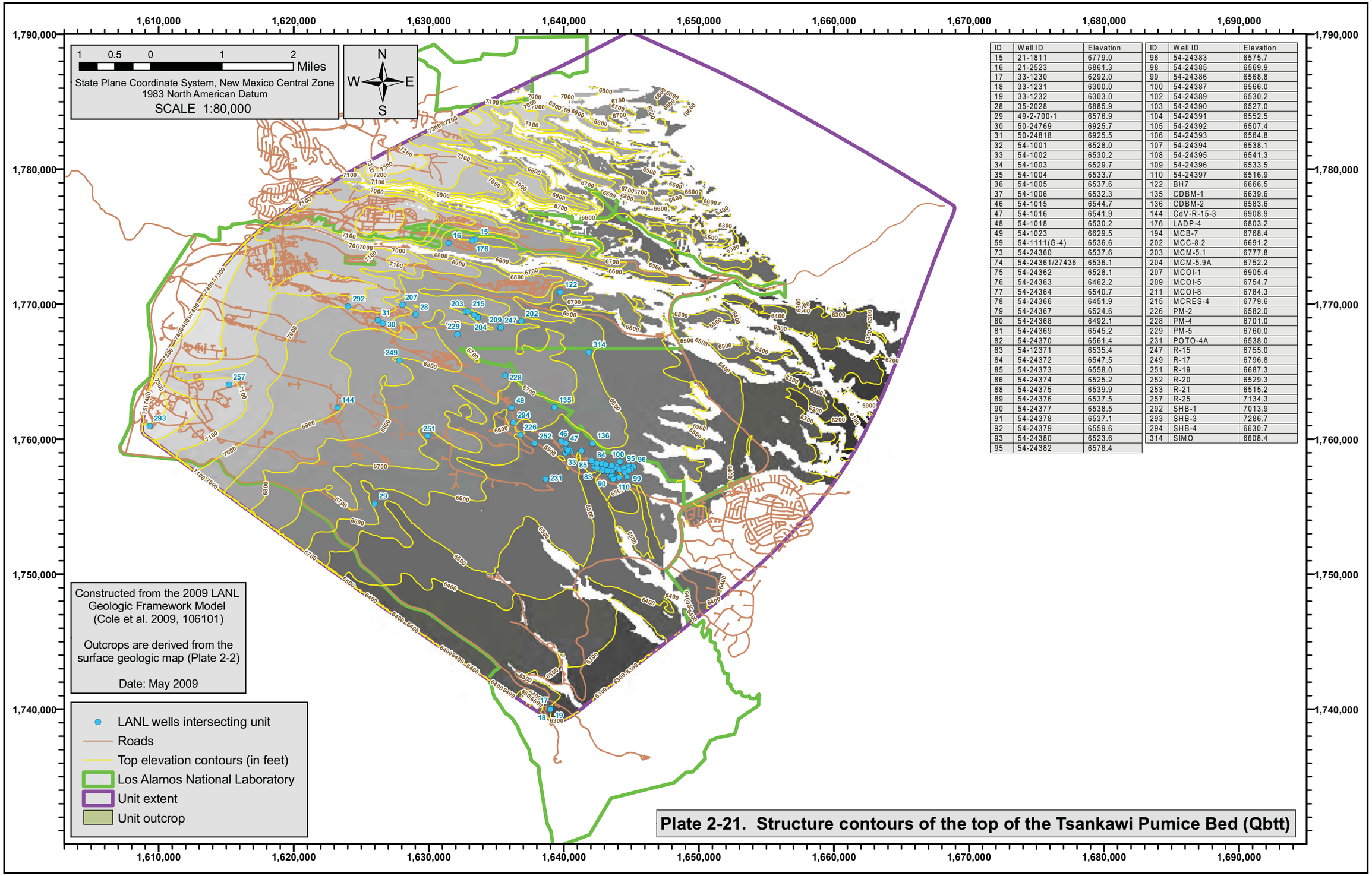
Plate 2-19. Structure contours of the top of the Tshirege Member, unit 1, glassy portion (Qbt1g)



ID	Well ID	Thickness
15	21-1811	113.5
16	21-2523	75.7
17	33-1230	52.0
18	33-1231	46.0
19	33-1232	40.0
28	35-2028	69.5
29	49-2-700-1	178.0
30	50-24769	75.0
31	50-24818	76.2
32	54-1001	128.4
33	54-1002	126.1
34	54-1003	128.0
35	54-1004	123.5
36	54-1005	116.7
37	54-1006	128.9
46	54-1015	125.2
47	54-1016	126.2
48	54-1018	126.5
49	54-1023	108.5
59	54-1111(G-4)	58.0
66	54-1121	42.5
67	54-1123	22.0
72	54-15462	109.0
73	54-24360	68.0
74	54-24361/27436	66.0
75	54-24362	68.5
76	54-24363	107.8
77	54-24364	68.0
78	54-24366	111.8
79	54-24367	76.5
80	54-24368	92.5
81	54-24369	64.8
82	54-24370	64.0
83	54-12371	88.0
84	54-24372	88.0
85	54-24373	80.0
86	54-24374	70.0
88	54-24375	65.0
89	54-24376	68.0
90	54-24377	63.5
91	54-24378	60.7
92	54-24379	38.0
93	54-24380	80.0
94	54-24381	44.0

ID	Well ID	Thickness
95	54-24382	36.0
96	54-24383	26.5
97	54-24384	25.0
98	54-24385	30.5
99	54-24386	31.5
101	54-24388	61.0
102	54-24389	71.5
103	54-24390	78.0
104	54-24391	55.5
105	54-24392	82.0
106	54-24393	59.5
107	54-24394	81.0
108	54-24395	86.5
109	54-24396	63.5
110	54-24397	76.5
111	54-24399	128.0
112	54-25105	75.0
122	BH7	96.5
141	CdV-16-1i	17.0
142	CdV-16-2i	47.0
143	CdV-16-3i	14.0
144	CdV-R-15-3	60.0
145	CdV-R-37-2	65.0
147	DSC-2	49.1
176	LADP-4	88.5
177	LADP-5	98.6
207	MCOI-1	73.3
212	MCOI-10	98.0
237	R-6	32.0
246	R-14	91.0
250	R-18	31.0
251	R-19	94.0
254	R-22	51.0
257	R-25	20.3
258	R-25b	15.0
268	R-37	89.0
277	R-46	89.0
292	SHB-1	32.0
294	SHB-4	77.0
100	54-24387	45.0
135	CDBM-1	75.0
228	PM-4	219.0
231	POTO-4A	84.0

Plate 2-20. Thickness of the Tshirege Member, unit 1, glassy portion (Qbt1g)



ID	Well ID	Elevation
15	21-1811	6779.0
16	21-2523	6861.3
17	33-1230	6292.0
18	33-1231	6300.0
19	33-1232	6303.0
28	35-2028	6885.9
29	49-2-700-1	6576.9
30	50-24769	6925.7
31	50-24818	6925.5
32	54-1001	6528.0
33	54-1002	6530.2
34	54-1003	6529.7
35	54-1004	6533.7
36	54-1005	6537.6
37	54-1006	6532.3
46	54-1015	6544.7
47	54-1016	6541.9
48	54-1018	6530.2
49	54-1023	6629.5
59	54-1111(G-4)	6536.6
73	54-24360	6537.6
74	54-24361/27436	6536.1
75	54-24362	6528.1
76	54-24363	6462.2
77	54-24364	6540.7
78	54-24366	6451.9
79	54-24367	6524.6
80	54-24368	6492.1
81	54-24369	6545.2
82	54-24370	6561.4
83	54-12371	6535.4
84	54-24372	6547.5
85	54-24373	6558.0
86	54-24374	6525.2
88	54-24375	6539.9
89	54-24376	6537.5
90	54-24377	6538.5
91	54-24378	6537.1
92	54-24379	6559.6
93	54-24380	6523.6
95	54-24382	6578.4

ID	Well ID	Elevation
96	54-24383	6575.7
98	54-24385	6569.9
99	54-24386	6568.8
100	54-24387	6566.0
102	54-24389	6530.2
103	54-24390	6527.0
104	54-24391	6552.5
105	54-24392	6507.4
106	54-24393	6564.8
107	54-24394	6538.1
108	54-24395	6541.3
109	54-24396	6533.5
110	54-24397	6516.9
122	BH7	6666.5
135	CDBM-1	6639.6
136	CDBM-2	6583.6
144	CdV-R-15-3	6908.9
176	LADP-4	6803.2
194	MCB-7	6768.4
202	MCC-8.2	6691.2
203	MCM-5.1	6777.8
204	MCM-5.9A	6752.2
207	MCOI-1	6905.4
209	MCOI-5	6754.7
211	MCOI-8	6784.3
215	MCRES-4	6779.6
226	PM-2	6582.0
228	PM-4	6701.0
229	PM-5	6760.0
231	POTO-4A	6538.0
247	R-15	6755.0
249	R-17	6796.8
251	R-19	6687.3
252	R-20	6529.3
253	R-21	6515.2
257	R-25	7134.3
292	SHB-1	7013.9
293	SHB-3	7286.7
294	SHB-4	6630.7
314	SIMO	6608.4

Plate 2-21. Structure contours of the top of the Tsankawi Pumice Bed (Qbtt)

1 0.5 0 1 2 Miles

State Plane Coordinate System, New Mexico Central Zone
1983 North American Datum
SCALE 1:80,000

N W E S

1,610,000 1,620,000 1,630,000 1,640,000 1,650,000 1,660,000 1,670,000 1,680,000 1,690,000

1,790,000 1,780,000 1,770,000 1,760,000 1,750,000 1,740,000

ID	Well ID	Thickness
15	21-1811	0.4
16	21-2523	2.3
17	33-1230	1.0
18	33-1231	1.0
19	33-1232	1.0
28	35-2028	2.0
29	49-2-700-1	4.0
30	50-24769	2.0
31	50-24818	2.5
32	54-1001	0.9
33	54-1002	2.3
34	54-1003	3.0
35	54-1004	0.5
36	54-1005	6.5
37	54-1006	1.8
46	54-1015	2.6
47	54-1016	2.6
48	54-1018	1.5
49	54-1023	1.2
59	54-1111(G-4)	2.0
73	54-24360	1.0
74	54-24361/27436	2.0
75	54-24362	1.5
76	54-24363	3.2
77	54-24364	1.5
78	54-24366	1.2
79	54-24367	2.0
80	54-24368	4.0
81	54-24369	1.2
82	54-24370	2.0
83	54-12371	2.0
84	54-24372	1.4
85	54-24373	1.5
86	54-24374	1.0
88	54-24375	2.0
89	54-24376	1.5
90	54-24377	0.5
91	54-24378	0.8
92	54-24379	1.0
93	54-24380	2.0
95	54-24382	1.0

ID	Well ID	Thickness
96	54-24383	1.0
98	54-24385	1.5
99	54-24386	2.0
100	54-24387	4.0
102	54-24389	1.5
103	54-24390	1.0
104	54-24391	1.5
105	54-24392	2.0
106	54-24393	1.0
107	54-24394	0.5
108	54-24395	1.5
109	54-24396	0.3
110	54-24397	1.5
122	BH7	1.5
135	CDBM-1	3.0
136	CDBM-2	2.0
144	CdV-R-15-3	12.0
176	LADP-4	4.5
194	MCB-7	0.5
202	MCC-8.2	3.0
203	MCM-5.1	3.0
204	MCM-5.9A	3.0
207	MCOI-1	3.2
209	MCOI-5	1.0
211	MCOI-8	4.0
215	MCRES-4	3.5
226	PM-2	2.0
228	PM-4	1.0
229	PM-5	1.0
231	POTO-4A	3.0
247	R-15	1.0
249	R-17	1.6
251	R-19	1.0
252	R-20	1.0
253	R-21	5.0
257	R-25	2.2
292	SHB-1	8.0
293	SHB-3	14.0
294	SHB-4	3.0
314	SIMO	3.0

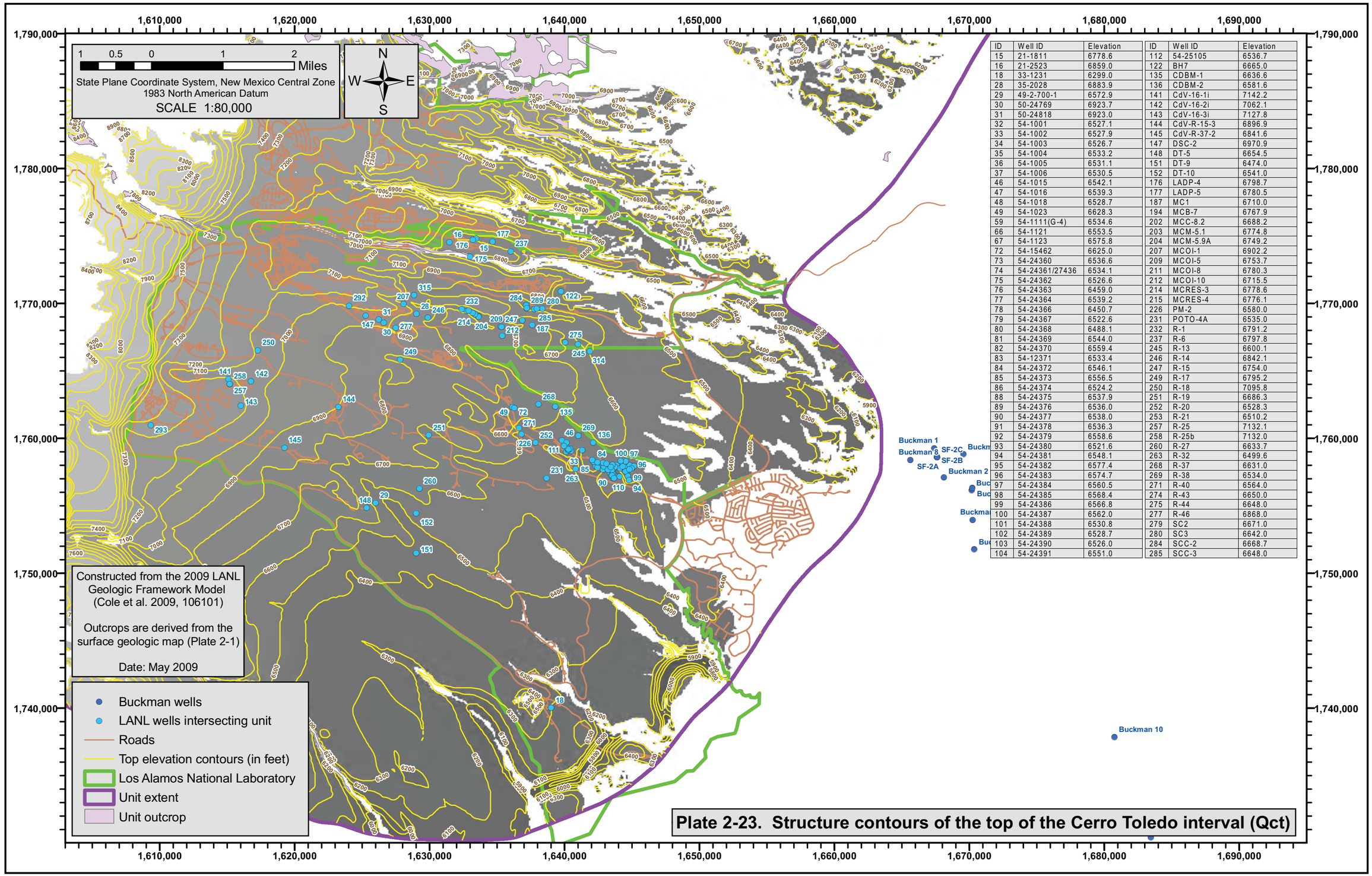
Constructed from the 2009 LANL Geologic Framework Model (Cole et al. 2009, 106101)

Outcrops are derived from the surface geologic map (Plate 2-2)

Date: May 2009

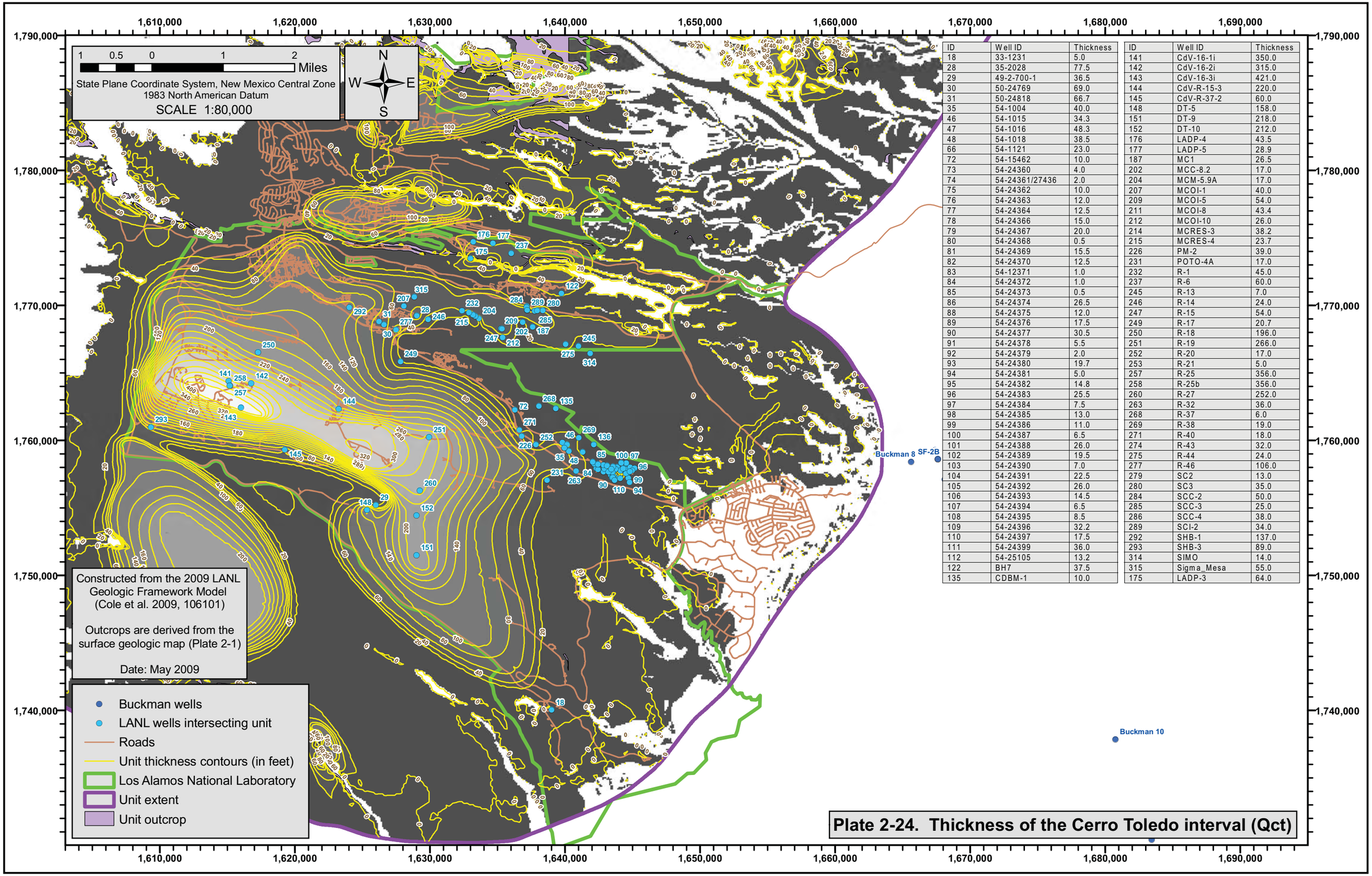
- LANL wells intersecting unit
- Roads
- Unit thickness contours (in feet)
- Los Alamos National Laboratory
- Unit extent
- Unit outcrop

Plate 2-22. Thickness of the Tsankawi Pumice Bed (Qbtt)



ID	Well ID	Elevation	ID	Well ID	Elevation
15	21-1811	6778.6	112	54-25105	6536.7
16	21-2523	6859.0	122	BH7	6665.0
18	33-1231	6299.0	135	CDBM-1	6636.6
28	35-2028	6883.9	136	CDBM-2	6581.6
29	49-2-700-1	6572.9	141	CdV-16-1i	7142.2
30	50-24769	6923.7	142	CdV-16-2i	7062.1
31	50-24818	6923.0	143	CdV-16-3i	7127.8
32	54-1001	6527.1	144	CdV-R-15-3	6896.9
33	54-1002	6527.9	145	CdV-R-37-2	6841.6
34	54-1003	6526.7	147	DSC-2	6970.9
35	54-1004	6533.2	148	DT-5	6654.5
36	54-1005	6531.1	151	DT-9	6474.0
37	54-1006	6530.5	152	DT-10	6541.0
46	54-1015	6542.1	176	LADP-4	6798.7
47	54-1016	6539.3	177	LADP-5	6780.5
48	54-1018	6528.7	187	MC1	6710.0
49	54-1023	6628.3	194	MCB-7	6767.9
59	54-1111(G-4)	6534.6	202	MCC-8.2	6688.2
66	54-1121	6553.5	203	MCM-5.1	6774.8
67	54-1123	6575.8	204	MCM-5.9A	6749.2
72	54-15462	6625.0	207	MCOI-1	6902.2
73	54-24360	6536.6	209	MCOI-5	6753.7
74	54-24361/27436	6534.1	211	MCOI-8	6780.3
75	54-24362	6526.6	212	MCOI-10	6715.5
76	54-24363	6459.0	214	MCRES-3	6778.6
77	54-24364	6539.2	215	MCRES-4	6776.1
78	54-24366	6450.7	226	PM-2	6580.0
79	54-24367	6522.6	231	POTO-4A	6535.0
80	54-24368	6488.1	232	R-1	6791.2
81	54-24369	6544.0	237	R-6	6797.8
82	54-24370	6559.4	245	R-13	6600.1
83	54-12371	6533.4	246	R-14	6842.1
84	54-24372	6546.1	247	R-15	6754.0
85	54-24373	6556.5	249	R-17	6795.2
86	54-24374	6524.2	250	R-18	7095.8
88	54-24375	6537.9	251	R-19	6686.3
89	54-24376	6536.0	252	R-20	6528.3
90	54-24377	6538.0	253	R-21	6510.2
91	54-24378	6536.3	257	R-25	7132.1
92	54-24379	6558.6	258	R-25b	7132.0
93	54-24380	6521.6	260	R-27	6633.7
94	54-24381	6548.1	263	R-32	6499.6
95	54-24382	6577.4	268	R-37	6631.0
96	54-24383	6574.7	269	R-38	6534.0
97	54-24384	6560.5	271	R-40	6564.0
98	54-24385	6568.4	274	R-43	6650.0
99	54-24386	6566.8	275	R-44	6648.0
100	54-24387	6562.0	277	R-46	6868.0
101	54-24388	6530.8	279	SC2	6671.0
102	54-24389	6528.7	280	SC3	6642.0
103	54-24390	6526.0	284	SCC-2	6668.7
104	54-24391	6551.0	285	SCC-3	6648.0

Plate 2-23. Structure contours of the top of the Cerro Toledo interval (Qct)



ID	Well ID	Thickness	ID	Well ID	Thickness
18	33-1231	5.0	141	CdV-16-1i	350.0
28	35-2028	77.5	142	CdV-16-2i	315.0
29	49-2-700-1	36.5	143	CdV-16-3i	421.0
30	50-24769	69.0	144	CdV-R-15-3	220.0
31	50-24818	66.7	145	CdV-R-37-2	60.0
35	54-1004	40.0	148	DT-5	158.0
46	54-1015	34.3	151	DT-9	218.0
47	54-1016	48.3	152	DT-10	212.0
48	54-1018	38.5	176	LADP-4	43.5
66	54-1121	23.0	177	LADP-5	28.9
72	54-15462	10.0	187	MC1	26.5
73	54-24360	4.0	202	MCC-8.2	17.0
74	54-24361/27436	2.0	204	MCM-5.9A	17.0
75	54-24362	10.0	207	MCOI-1	40.0
76	54-24363	12.0	209	MCOI-5	54.0
77	54-24364	12.5	211	MCOI-8	43.4
78	54-24366	15.0	212	MCOI-10	26.0
79	54-24367	20.0	214	MCRES-3	38.2
80	54-24368	0.5	215	MCRES-4	23.7
81	54-24369	15.5	226	PM-2	39.0
82	54-24370	12.5	231	POTO-4A	17.0
83	54-12371	1.0	232	R-1	45.0
84	54-24372	1.0	237	R-6	60.0
85	54-24373	0.5	245	R-13	7.0
86	54-24374	26.5	246	R-14	24.0
88	54-24375	12.0	247	R-15	54.0
89	54-24376	17.5	249	R-17	20.7
90	54-24377	30.5	250	R-18	196.0
91	54-24378	5.5	251	R-19	266.0
92	54-24379	2.0	252	R-20	17.0
93	54-24380	19.7	253	R-21	5.0
94	54-24381	5.0	257	R-25	356.0
95	54-24382	14.8	258	R-25b	356.0
96	54-24383	25.5	260	R-27	252.0
97	54-24384	7.5	263	R-32	36.0
98	54-24385	13.0	268	R-37	6.0
99	54-24386	11.0	269	R-38	19.0
100	54-24387	6.5	271	R-40	18.0
101	54-24388	26.0	274	R-43	32.0
102	54-24389	19.5	275	R-44	24.0
103	54-24390	7.0	277	R-46	106.0
104	54-24391	22.5	279	SC2	13.0
105	54-24392	26.0	280	SC3	35.0
106	54-24393	14.5	284	SCC-2	50.0
107	54-24394	6.5	285	SCC-3	25.0
108	54-24395	8.5	286	SCC-4	38.0
109	54-24396	32.2	289	SCI-2	34.0
110	54-24397	17.5	292	SHB-1	137.0
111	54-24399	36.0	293	SHB-3	89.0
112	54-25105	13.2	314	SIMO	14.0
122	BH7	37.5	315	Sigma_Mesa	55.0
135	CDBM-1	10.0	175	LADP-3	64.0

Plate 2-24. Thickness of the Cerro Toledo interval (Qct)

1 0.5 0 1 2 Miles

State Plane Coordinate System, New Mexico Central Zone
1983 North American Datum
SCALE 1:80,000

N W E S

1,610,000 1,620,000 1,630,000 1,640,000 1,650,000 1,660,000 1,670,000 1,680,000 1,690,000

1,790,000 1,780,000 1,770,000 1,760,000 1,750,000 1,740,000

Buckman 1
Buckman 8
SF-2A
Buckman 10

ID	Well ID	Elevation	ID	Well ID	Elevation
18	33-1231	6294.0	151	DT-9	6256.0
28	35-2028	6806.4	152	DT-10	6329.0
29	49-2-700-1	6536.4	175	LADP-3	6691.6
30	50-24769	6854.7	176	LADP-4	6755.2
31	50-24818	6856.3	177	LADP-5	6751.6
35	54-1004	6493.2	187	MC1	6683.5
46	54-1015	6507.8	188	MC2	6637.0
47	54-1016	6491.0	189	MC3	6623.0
48	54-1018	6490.2	200	MCB-14	6722.1
66	54-1121	6530.5	201	MCB-16	6596.2
72	54-15462	6615.0	202	MCC-8.2	6671.2
73	54-24360	6532.6	204	MCM-5.9A	6732.2
74	54-24361/27436	6532.1	205	MCOBT-4.4	6734.2
75	54-24362	6516.6	207	MCOI-1	6862.2
76	54-24363	6447.0	208	MCOI-4	6732.2
77	54-24364	6526.7	209	MCOI-5	6699.7
78	54-24366	6435.7	210	MCOI-6	6706.1
79	54-24367	6502.6	211	MCOI-8	6736.9
80	54-24368	6487.6	212	MCOI-10	6689.5
81	54-24369	6528.5	213	MCRES-2	6727.8
82	54-24370	6546.9	214	MCRES-3	6740.4
83	54-12371	6532.4	215	MCRES-4	6752.4
84	54-24372	6545.1	226	PM-2	6541.0
85	54-24373	6556.0	231	POTO-4A	6518.0
86	54-24374	6497.7	232	R-1	6746.2
88	54-24375	6525.9	237	R-6	6737.8
89	54-24376	6518.5	244	R-12	6468.3
90	54-24377	6507.5	245	R-13	6593.1
91	54-24378	6530.8	246	R-14	6818.1
92	54-24379	6556.6	247	R-15	6700.0
93	54-24380	6501.9	249	R-17	6774.5
94	54-24381	6543.1	250	R-18	6899.8
95	54-24382	6562.6	251	R-19	6420.3
96	54-24383	6549.2	252	R-20	6511.3
97	54-24384	6553.0	253	R-21	6505.2
98	54-24385	6555.4	257	R-25	6776.1
99	54-24386	6555.8	258	R-25b	6776.0
100	54-24387	6555.5	259	R-26	6776.6
101	54-24388	6504.8	260	R-27	6381.7
102	54-24389	6509.2	263	R-32	6463.6
103	54-24390	6519.0	264	R-33	6763.3
104	54-24391	6528.5	268	R-37	6625.0
105	54-24392	6479.4	269	R-38	6515.0
106	54-24393	6549.3	271	R-40	6546.0
107	54-24394	6531.1	274	R-43	6618.0
108	54-24395	6531.3	275	R-44	6624.0
109	54-24396	6501.0	277	R-46	6762.0
110	54-24397	6497.9	279	SC2	6658.0
111	54-24399	6501.0	280	SC3	6607.0
112	54-25105	6523.5	284	SCC-2	6618.7
122	BH7	6627.5	285	SCC-3	6623.0
135	CDBM-1	6626.6	286	SCC-4	6604.2

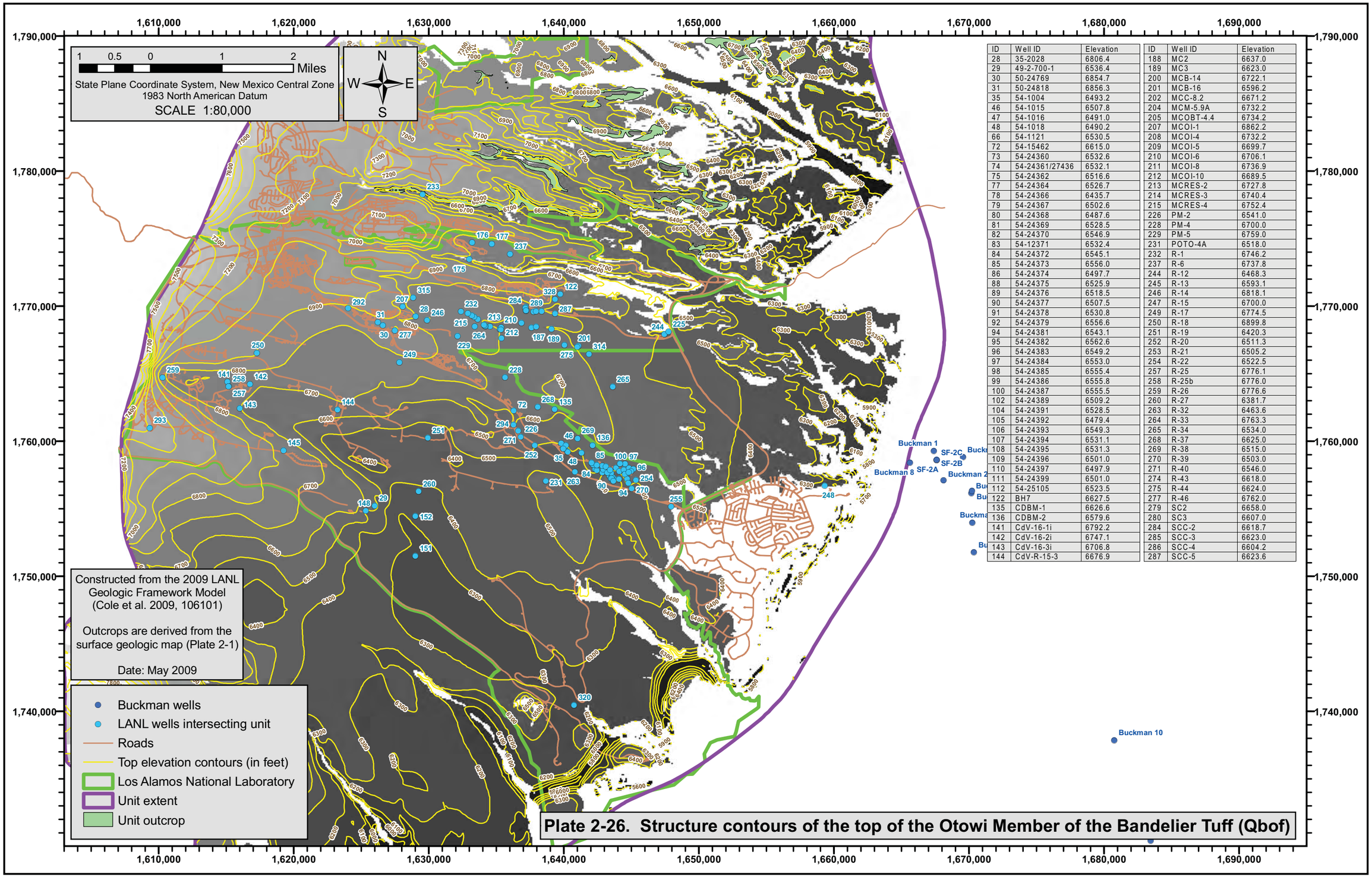
Constructed from the 2009
LANL Geologic Framework Model
(Cole et al. 2009, 106101)

Outcrops are derived from the
surface geologic map (Plate 2-1)

Date: May 2009

- Buckman wells
- LANL wells intersecting unit
- Roads
- Bottom elevation contours (in feet)
- Los Alamos National Laboratory
- Unit extent
- Unit outcrop

Plate 2-25. Structure contours of the bottom of the Cerro Toledo interval (Qct)



ID	Well ID	Elevation
28	35-2028	6806.4
29	49-2-700-1	6536.4
30	50-24769	6854.7
31	50-24818	6856.3
35	54-1004	6493.2
46	54-1015	6507.8
47	54-1016	6491.0
48	54-1018	6490.2
66	54-1121	6530.5
72	54-15462	6615.0
73	54-24360	6532.6
74	54-24361/27436	6532.1
75	54-24362	6516.6
77	54-24364	6526.7
78	54-24366	6435.7
79	54-24367	6502.6
80	54-24368	6487.6
81	54-24369	6528.5
82	54-24370	6546.9
83	54-12371	6532.4
84	54-24372	6545.1
85	54-24373	6556.0
86	54-24374	6497.7
88	54-24375	6525.9
89	54-24376	6518.5
90	54-24377	6507.5
91	54-24378	6530.8
92	54-24379	6556.6
94	54-24381	6543.1
95	54-24382	6562.6
96	54-24383	6549.2
97	54-24384	6553.0
98	54-24385	6555.4
99	54-24386	6555.8
100	54-24387	6555.5
102	54-24389	6509.2
104	54-24391	6528.5
105	54-24392	6479.4
106	54-24393	6549.3
107	54-24394	6531.1
108	54-24395	6531.3
109	54-24396	6501.0
110	54-24397	6497.9
111	54-24399	6501.0
112	54-25105	6523.5
122	BH7	6627.5
135	CDBM-1	6626.6
136	CDBM-2	6579.6
141	CdV-16-1i	6792.2
142	CdV-16-2i	6747.1
143	CdV-16-3i	6706.8
144	CdV-R-15-3	6676.9

ID	Well ID	Elevation
188	MC2	6637.0
189	MC3	6623.0
200	MCB-14	6722.1
201	MCB-16	6596.2
202	MCC-8.2	6671.2
204	MCM-5.9A	6732.2
205	MCOBT-4.4	6734.2
207	MCOI-1	6862.2
208	MCOI-4	6732.2
209	MCOI-5	6699.7
210	MCOI-6	6706.1
211	MCOI-8	6736.9
212	MCOI-10	6689.5
213	MCRES-2	6727.8
214	MCRES-3	6740.4
215	MCRES-4	6752.4
226	PM-2	6541.0
228	PM-4	6700.0
229	PM-5	6759.0
231	POTO-4A	6518.0
232	R-1	6746.2
237	R-6	6737.8
244	R-12	6468.3
245	R-13	6593.1
246	R-14	6818.1
247	R-15	6700.0
249	R-17	6774.5
250	R-18	6899.8
251	R-19	6420.3
252	R-20	6511.3
253	R-21	6505.2
254	R-22	6522.5
257	R-25	6776.1
258	R-25b	6776.0
259	R-26	6776.6
260	R-27	6381.7
263	R-32	6463.6
264	R-33	6763.3
265	R-34	6534.0
268	R-37	6625.0
269	R-38	6515.0
270	R-39	6503.0
271	R-40	6546.0
274	R-43	6618.0
275	R-44	6624.0
277	R-46	6762.0
279	SC2	6658.0
280	SC3	6607.0
284	SCC-2	6618.7
285	SCC-3	6623.0
286	SCC-4	6604.2
287	SCC-5	6623.6

Plate 2-26. Structure contours of the top of the Otowi Member of the Bandelier Tuff (Qbof)

1 0.5 0 1 2 Miles

State Plane Coordinate System, New Mexico Central Zone
1983 North American Datum
SCALE 1:80,000

N W E S

1,610,000 1,620,000 1,630,000 1,640,000 1,650,000 1,660,000 1,670,000 1,680,000 1,690,000

1,790,000 1,780,000 1,770,000 1,760,000 1,750,000 1,740,000

ID	Well ID	Thickness
30	50-24769	224.0
31	50-24818	226.6
46	54-1015	97.8
47	54-1016	57.9
74	54-24361/27436	7.0
75	54-24362	18.0
81	54-24369	47.5
82	54-24370	43.0
88	54-24375	15.0
91	54-24378	27.5
92	54-24379	75.5
95	54-24382	37.0
96	54-24383	37.5
97	54-24384	12.0
98	54-24385	54.0
99	54-24386	61.5
100	54-24387	12.5
106	54-24393	25.9
107	54-24394	96.0
110	54-24397	57.0
111	54-24399	81.0
112	54-25105	9.5
142	CdV-16-2i	92.0
143	CdV-16-3i	114.0
144	CdV-R-15-3	168.0
145	CdV-R-37-2	338.0
175	LADP-3	246.0
176	LADP-4	252.0
177	LADP-5	227.5
205	MCOBT-4.4	356.0
207	MCOI-1	235.5
208	MCOI-4	350.0
209	MCOI-5	323.0
210	MCOI-6	329.4
211	MCOI-8	333.7
212	MCOI-10	328.6
226	PM-2	234.0
228	PM-4	320.0

ID	Well ID	Thickness
229	PM-5	375.0
232	R-1	325.0
237	R-6	233.0
244	R-12	80.7
245	R-13	168.0
246	R-14	278.0
247	R-15	322.0
249	R-17	348.5
250	R-18	150.0
251	R-19	184.0
252	R-20	191.0
253	R-21	64.0
254	R-22	51.0
257	R-25	103.8
258	R-25b	103.0
259	R-26	65.0
260	R-27	188.0
263	R-32	103.0
264	R-33	378.0
265	R-34	38.0
268	R-37	238.0
269	R-38	75.0
270	R-39	62.0
271	R-40	258.0
274	R-43	225.0
275	R-44	202.0
277	R-46	230.0
284	SCC-2	208.0
285	SCC-3	210.0
286	SCC-4	182.0
287	SCC-5	186.0
289	SCI-2	216.0
292	SHB-1	143.0
293	SHB-3	414.0
225	PM-1	120.0
233	R-2	124.0
248	R-16	79.0
255	R-23	20.0

Buckman 8 SF-2B SF-2C SF-2A Buckman 7R Buckman 2 Buckman 9 Buckman 3 Buckman 3A Buckman 4 Buckman 6 Buckman 5 Buckman 10

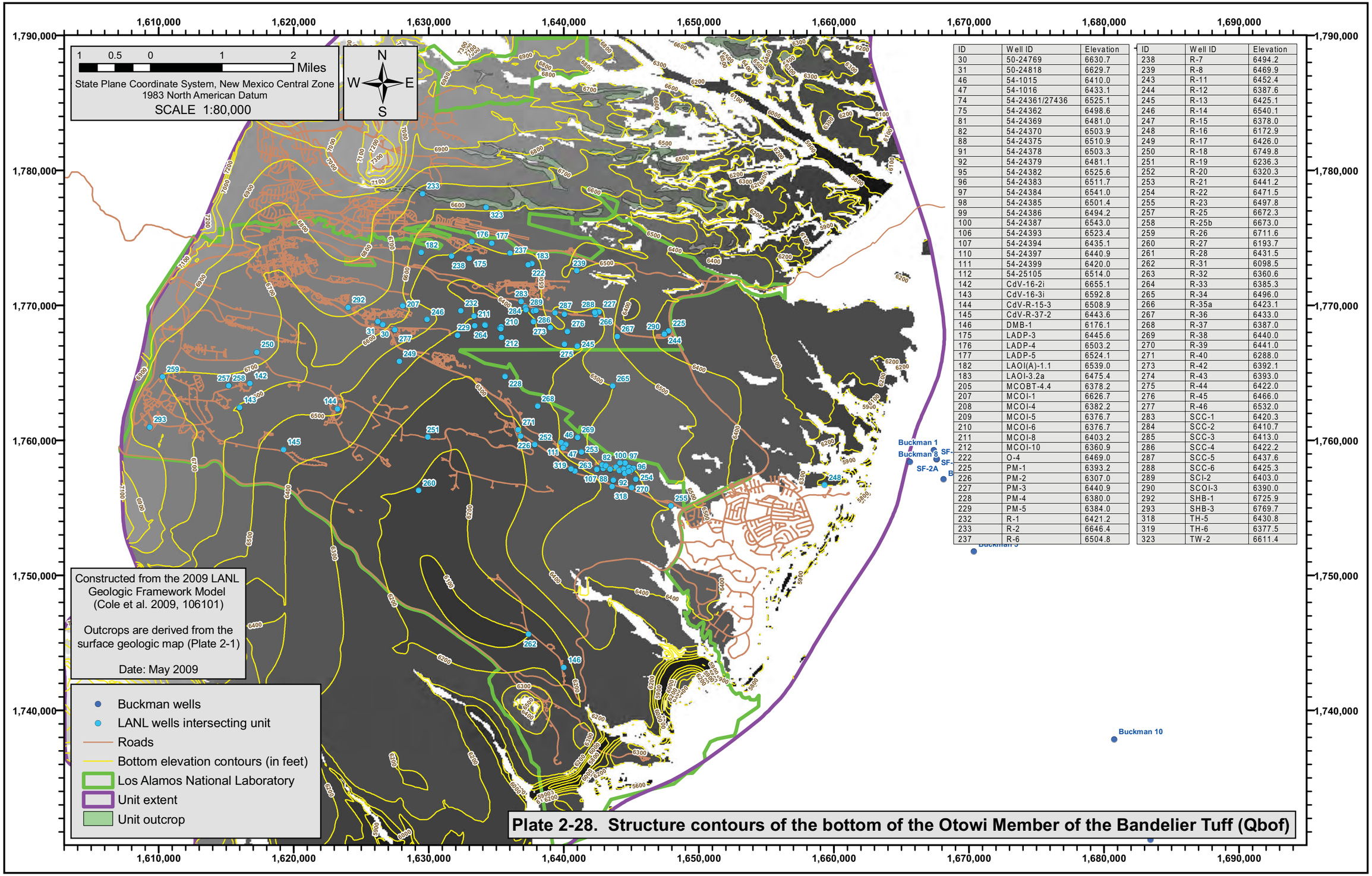
Constructed from the 2009 LANL Geologic Framework Model (Cole et al. 2009, 106101)

Outcrops are derived from the surface geologic map (Plate 2-1)

Date: May 2009

- Buckman wells
- LANL wells intersecting unit
- Roads
- Unit thickness contours (in feet)
- Los Alamos National Laboratory
- Unit extent
- Unit outcrop

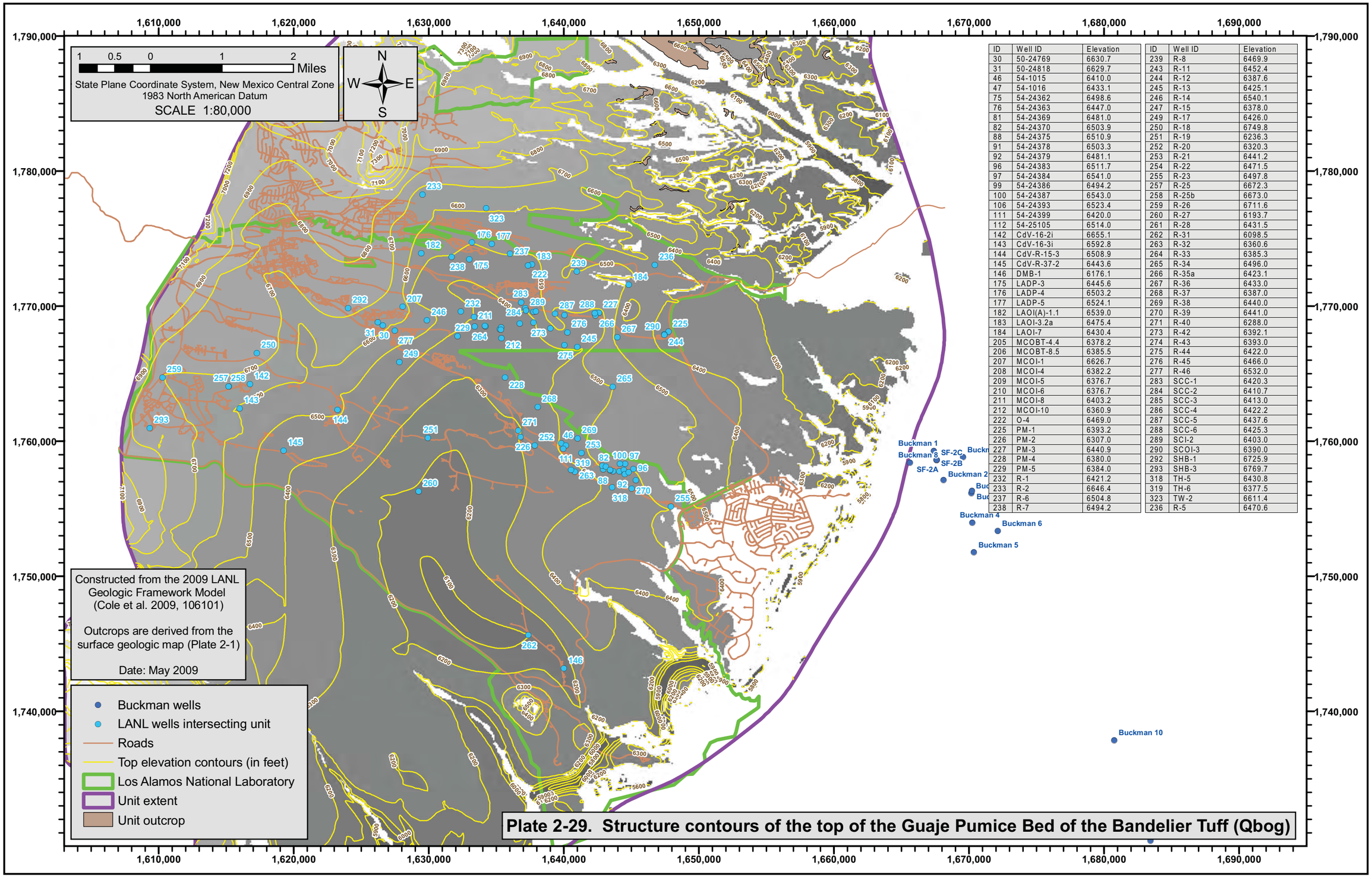
Plate 2-27. Thickness of the Otowi Member of the Bandelier Tuff (Qbof)



ID	Well ID	Elevation
30	50-24769	6630.7
31	50-24818	6629.7
46	54-1015	6410.0
47	54-1016	6433.1
74	54-24361/27436	6525.1
75	54-24362	6498.6
81	54-24369	6481.0
82	54-24370	6503.9
88	54-24375	6510.9
91	54-24378	6503.3
92	54-24379	6481.1
95	54-24382	6525.6
96	54-24383	6511.7
97	54-24384	6541.0
98	54-24385	6501.4
99	54-24386	6494.2
100	54-24387	6543.0
106	54-24393	6523.4
107	54-24394	6435.1
110	54-24397	6440.9
111	54-24399	6420.0
112	54-25105	6514.0
142	CdV-16-2i	6655.1
143	CdV-16-3i	6592.8
144	CdV-R-15-3	6508.9
145	CdV-R-37-2	6443.6
146	DMB-1	6176.1
175	LADP-3	6445.6
176	LADP-4	6503.2
177	LADP-5	6524.1
182	LAOI(A)-1.1	6539.0
183	LAOI-3.2a	6475.4
205	MCOBT-4.4	6378.2
207	MCOI-1	6626.7
208	MCOI-4	6382.2
209	MCOI-5	6376.7
210	MCOI-6	6376.7
211	MCOI-8	6403.2
212	MCOI-10	6360.9
222	O-4	6469.0
225	PM-1	6393.2
226	PM-2	6307.0
227	PM-3	6440.9
228	PM-4	6380.0
229	PM-5	6384.0
232	R-1	6421.2
233	R-2	6646.4
237	R-6	6504.8

ID	Well ID	Elevation
238	R-7	6494.2
239	R-8	6469.9
243	R-11	6452.4
244	R-12	6387.6
245	R-13	6425.1
246	R-14	6540.1
247	R-15	6378.0
248	R-16	6172.9
249	R-17	6426.0
250	R-18	6749.8
251	R-19	6236.3
252	R-20	6320.3
253	R-21	6441.2
254	R-22	6471.5
255	R-23	6497.8
257	R-25	6672.3
258	R-25b	6673.0
259	R-26	6711.6
260	R-27	6193.7
261	R-28	6431.5
262	R-31	6098.5
263	R-32	6360.6
264	R-33	6385.3
265	R-34	6496.0
266	R-35a	6423.1
267	R-36	6433.0
268	R-37	6387.0
269	R-38	6440.0
270	R-39	6441.0
271	R-40	6288.0
273	R-42	6392.1
274	R-43	6393.0
275	R-44	6422.0
276	R-45	6466.0
277	R-46	6532.0
283	SCC-1	6420.3
284	SCC-2	6410.7
285	SCC-3	6413.0
286	SCC-4	6422.2
287	SCC-5	6437.6
288	SCC-6	6425.3
289	SCI-2	6403.0
290	SCOI-3	6390.0
292	SHB-1	6725.9
293	SHB-3	6769.7
318	TH-5	6430.8
319	TH-6	6377.5
323	TW-2	6611.4

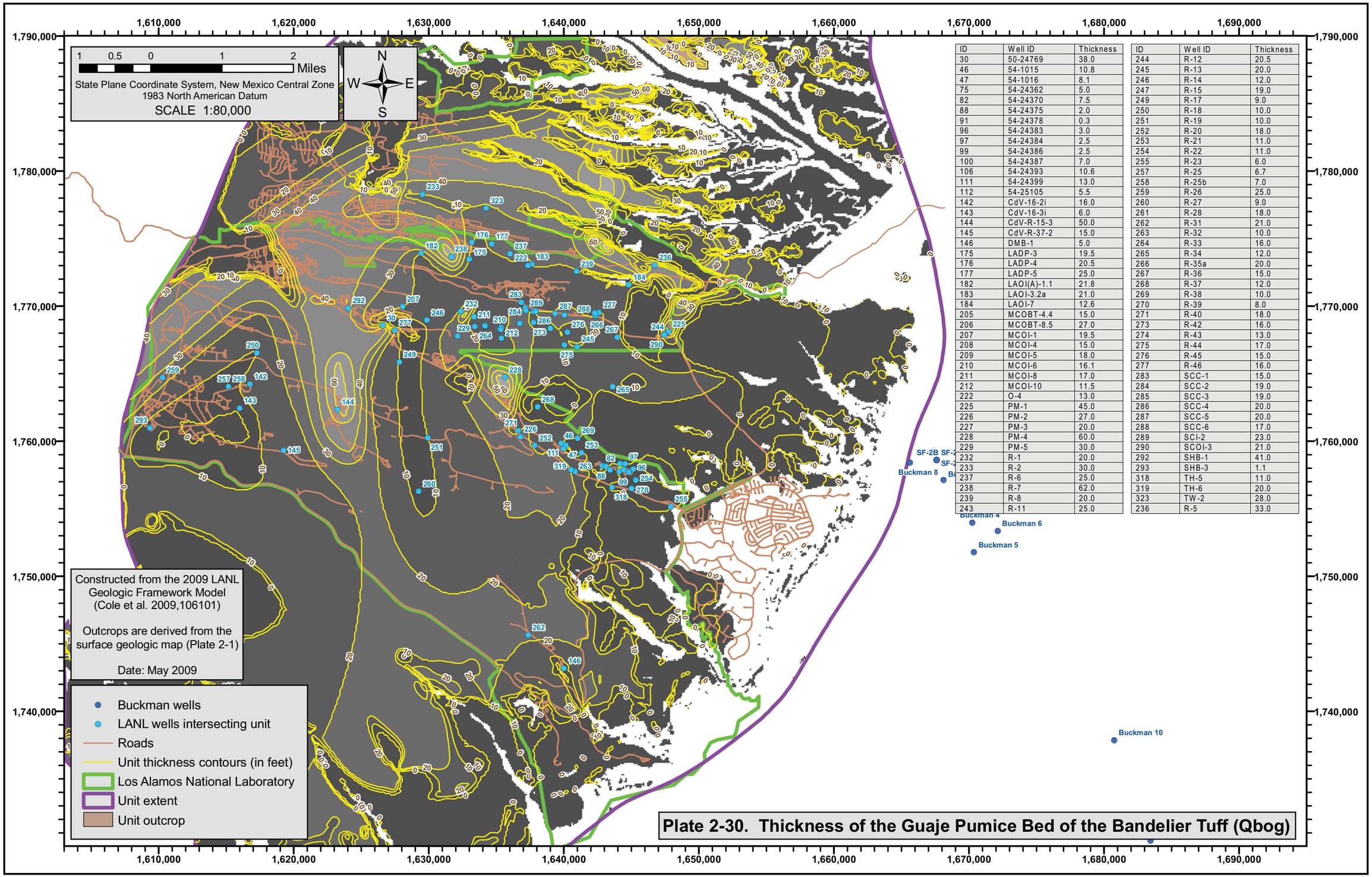
Plate 2-28. Structure contours of the bottom of the Otowi Member of the Bandelier Tuff (Qbof)



ID	Well ID	Elevation
30	50-24769	6630.7
31	50-24818	6629.7
46	54-1015	6410.0
47	54-1016	6433.1
75	54-24362	6498.6
76	54-24363	6447.0
81	54-24369	6481.0
82	54-24370	6503.9
88	54-24375	6510.9
91	54-24378	6503.3
92	54-24379	6481.1
96	54-24383	6511.7
97	54-24384	6541.0
99	54-24386	6494.2
100	54-24387	6543.0
106	54-24393	6523.4
111	54-24399	6420.0
112	54-25105	6514.0
142	CdV-16-2i	6655.1
143	CdV-16-3i	6592.8
144	CdV-R-15-3	6508.9
145	CdV-R-37-2	6443.6
146	DMB-1	6176.1
175	LADP-3	6445.6
176	LADP-4	6503.2
177	LADP-5	6524.1
182	LAOI(A)-1.1	6539.0
183	LAOI-3.2a	6475.4
184	LAOI-7	6430.4
205	MCOBT-4.4	6378.2
206	MCOBT-8.5	6385.5
207	MCOI-1	6626.7
208	MCOI-4	6382.2
209	MCOI-5	6376.7
210	MCOI-6	6376.7
211	MCOI-8	6403.2
212	MCOI-10	6360.9
222	O-4	6469.0
225	PM-1	6393.2
226	PM-2	6307.0
227	PM-3	6440.9
228	PM-4	6380.0
229	PM-5	6384.0
232	R-1	6421.2
233	R-2	6646.4
237	R-6	6504.8
238	R-7	6494.2

ID	Well ID	Elevation
239	R-8	6469.9
243	R-11	6452.4
244	R-12	6387.6
245	R-13	6425.1
246	R-14	6540.1
247	R-15	6378.0
249	R-17	6426.0
250	R-18	6749.8
251	R-19	6236.3
252	R-20	6320.3
253	R-21	6441.2
254	R-22	6471.5
255	R-23	6497.8
257	R-25	6672.3
258	R-25b	6673.0
259	R-26	6711.6
260	R-27	6193.7
261	R-28	6431.5
262	R-31	6098.5
263	R-32	6360.6
264	R-33	6385.3
265	R-34	6496.0
266	R-35a	6423.1
267	R-36	6433.0
268	R-37	6387.0
269	R-38	6440.0
270	R-39	6441.0
271	R-40	6288.0
273	R-42	6392.1
274	R-43	6393.0
275	R-44	6422.0
276	R-45	6466.0
277	R-46	6532.0
283	SCC-1	6420.3
284	SCC-2	6410.7
285	SCC-3	6413.0
286	SCC-4	6422.2
287	SCC-5	6437.6
288	SCC-6	6425.3
289	SCI-2	6403.0
290	SCOI-3	6390.0
292	SHB-1	6725.9
293	SHB-3	6769.7
318	TH-5	6430.8
319	TH-6	6377.5
323	TW-2	6611.4
236	R-5	6470.6

Plate 2-29. Structure contours of the top of the Guaje Pumice Bed of the Bandelier Tuff (Qbog)



ID	Well ID	Thickness
30	50-24769	38.0
46	54-1015	10.8
47	54-1016	8.1
75	54-24362	5.0
82	54-24370	7.5
88	54-24375	2.0
91	54-24378	0.3
96	54-24383	3.0
97	54-24384	2.5
99	54-24386	2.5
100	54-24387	7.0
106	54-24393	10.6
111	54-24399	13.0
112	54-25105	5.5
142	CdV-16-2i	16.0
143	CdV-16-3i	6.0
144	CdV-R-15-3	50.0
145	CdV-R-37-2	15.0
146	DMB-1	5.0
175	LADP-3	19.5
176	LADP-4	20.5
177	LADP-5	25.0
182	LAOI(A)-1.1	21.8
183	LAOI-3.2a	21.0
184	LAOI-7	12.6
205	MCOBT-4.4	15.0
206	MCOBT-8.5	27.0
207	MCOI-1	19.5
208	MCOI-4	15.0
209	MCOI-5	18.0
210	MCOI-6	16.1
211	MCOI-8	17.0
212	MCOI-10	11.5
222	O-4	13.0
225	PM-1	45.0
226	PM-2	27.0
227	PM-3	20.0
228	PM-4	60.0
229	PM-5	30.0
232	R-1	20.0
233	R-2	30.0
237	R-6	25.0
238	R-7	62.0
239	R-8	20.0
243	R-11	25.0

ID	Well ID	Thickness
244	R-12	20.5
245	R-13	20.0
246	R-14	12.0
247	R-15	19.0
249	R-17	9.0
250	R-18	10.0
251	R-19	10.0
252	R-20	18.0
253	R-21	11.0
254	R-22	11.0
255	R-23	6.0
257	R-25	6.7
258	R-25b	7.0
259	R-26	25.0
260	R-27	9.0
261	R-28	18.0
262	R-31	21.0
263	R-32	10.0
264	R-33	16.0
265	R-34	12.0
266	R-35a	20.0
267	R-36	15.0
268	R-37	12.0
269	R-38	10.0
270	R-39	8.0
271	R-40	18.0
273	R-42	16.0
274	R-43	13.0
275	R-44	17.0
276	R-45	15.0
277	R-46	16.0
283	SCC-1	15.0
284	SCC-2	19.0
285	SCC-3	19.0
286	SCC-4	20.0
287	SCC-5	20.0
288	SCC-6	17.0
289	SCI-2	23.0
290	SCOI-3	21.0
292	SHB-1	41.0
293	SHB-3	1.1
318	TH-5	11.0
319	TH-6	20.0
323	TW-2	28.0
236	R-5	33.0

Plate 2-30. Thickness of the Guaje Pumice Bed of the Bandelier Tuff (Qbog)

1 0.5 0 1 2 Miles

State Plane Coordinate System, New Mexico Central Zone
1983 North American Datum
SCALE 1:80,000

N W E S

Constructed from the 2009 LANL Geologic Framework Model (Cole et al. 2009, 106101)

Outcrops are derived from the surface geologic map (Plate 2-1)

Date: May 2009

- Buckman wells
- LANL wells intersecting unit
- Roads
- Bottom elevation contours (in feet)
- Los Alamos National Laboratory
- Unit extent
- Unit outcrop

ID	Well ID	Elevation
30	50-24769	6592.7
46	54-1015	6399.2
47	54-1016	6425.0
75	54-24362	6493.6
82	54-24370	6496.4
88	54-24375	6508.9
91	54-24378	6503.0
96	54-24383	6508.7
97	54-24384	6538.5
99	54-24386	6491.8
100	54-24387	6536.0
106	54-24393	6512.8
111	54-24399	6407.0
112	54-25105	6508.5
142	CdV-16-2i	6639.1
143	CdV-16-3i	6586.8
144	CdV-R-15-3	6458.9
145	CdV-R-37-2	6428.6
146	DMB-1	6171.1
148	DT-5	6204.5
151	DT-9	6086.0
152	DT-10	6155.0
175	LADP-3	6426.1
176	LADP-4	6482.7
177	LADP-5	6499.1
182	LAOI(A)-1.1	6517.2
183	LAOI-3.2a	6454.4
184	LAOI-7	6417.8
205	MCOBT-4.4	6363.2
206	MCOBT-8.5	6358.5
207	MCOI-1	6607.2
208	MCOI-4	6367.2
209	MCOI-5	6358.7
210	MCOI-6	6360.6
211	MCOI-8	6386.2
212	MCOI-10	6349.4
222	O-4	6456.0
225	PM-1	6348.2
226	PM-2	6280.0
227	PM-3	6420.9
228	PM-4	6320.0
229	PM-5	6354.0
232	R-1	6401.2
233	R-2	6616.4
235	R-4	6527.5
236	R-5	6437.6
237	R-6	6479.8
238	R-7	6432.2
239	R-8	6449.9
243	R-11	6427.4

ID	Well ID	Elevation
244	R-12	6367.1
245	R-13	6405.1
246	R-14	6528.1
247	R-15	6359.0
249	R-17	6417.0
250	R-18	6739.8
251	R-19	6226.3
252	R-20	6302.3
253	R-21	6430.2
254	R-22	6460.5
255	R-23	6491.8
256	R-24	6517.4
257	R-25	6665.6
258	R-25b	6666.0
259	R-26	6686.6
260	R-27	6184.7
261	R-28	6413.5
262	R-31	6077.5
263	R-32	6350.6
264	R-33	6369.3
265	R-34	6484.0
266	R-35a	6403.1
267	R-36	6418.0
268	R-37	6375.0
269	R-38	6430.0
270	R-39	6433.0
271	R-40	6270.0
273	R-42	6376.1
274	R-43	6380.0
275	R-44	6405.0
276	R-45	6451.0
277	R-46	6516.0
283	SCC-1	6405.3
284	SCC-2	6391.7
285	SCC-3	6394.0
286	SCC-4	6402.2
287	SCC-5	6417.6
288	SCC-6	6408.3
289	SCI-2	6380.0
290	SCOI-3	6369.0
292	SHB-1	6684.9
293	SHB-3	6768.6
315	Sigma_Mesa	6466.5
318	TH-5	6419.8
319	TH-6	6357.5
320	TH-7	6178.5
323	TW-2	6583.4
325	TW-4	6847.7
326	TW-8	6400.1

Buckman 10

Plate 2-31. Structure contours of the bottom of the Guaje Pumice Bed of the Bandelier Tuff (Qbog)

1 0.5 0 1 2 Miles

State Plane Coordinate System, New Mexico Central Zone
1983 North American Datum
SCALE 1:80,000

N W E S

1,610,000 1,620,000 1,630,000 1,640,000 1,650,000 1,660,000 1,670,000 1,680,000 1,690,000

1,790,000 1,780,000 1,770,000 1,760,000 1,750,000 1,740,000

ID	Well ID	Elevation	ID	Well ID	Elevation
18	33-1231	6294.0	245	R-13	6405.1
19	33-1232	6302.0	246	R-14	6528.1
46	54-1015	6399.2	247	R-15	6359.0
142	CdV-16-2i	6639.1	249	R-17	6417.0
143	CdV-16-3i	6586.8	250	R-18	6739.8
144	CdV-R-15-3	6458.9	251	R-19	6226.3
145	CdV-R-37-2	6428.6	256	R-24	6517.4
146	DMB-1	6171.1	257	R-25	6665.6
148	DT-5	6204.5	258	R-25b	6666.0
149	DT-5A	6214.2	259	R-26	6686.6
151	DT-9	6086.0	260	R-27	6184.7
152	DT-10	6155.0	261	R-28	6413.5
175	LADP-3	6426.1	264	R-33	6369.3
176	LADP-4	6482.7	266	R-35a	6403.1
177	LADP-5	6499.1	267	R-36	6418.0
182	LAOI(A)-1.1	6517.2	269	R-38	6430.0
183	LAOI-3.2a	6454.4	273	R-42	6376.1
184	LAOI-7	6417.8	274	R-43	6380.0
205	MCOBT-4.4	6363.2	275	R-44	6405.0
206	MCOBT-8.5	6358.5	283	SCC-1	6405.3
207	MCOI-1	6607.2	284	SCC-2	6391.7
208	MCOI-4	6367.2	285	SCC-3	6394.0
209	MCOI-5	6358.7	286	SCC-4	6402.2
210	MCOI-6	6360.6	287	SCC-5	6417.6
211	MCOI-8	6386.2	288	SCC-6	6408.3
212	MCOI-10	6349.4	289	SCI-2	6380.0
222	O-4	6456.0	292	SHB-1	6684.9
227	PM-3	6420.9	293	SHB-3	6768.6
232	R-1	6401.2	315	Sigma_Mesa	6466.5
233	R-2	6616.4	319	TH-6	6357.5
235	R-4	6527.5	323	TW-2	6583.4
236	R-5	6437.6	325	TW-4	6847.7
237	R-6	6479.8	326	TW-8	6400.1
238	R-7	6432.2	162	GR-1	6416.2
239	R-8	6449.9	321	TW-1	6369.9
243	R-11	6427.4	322	TW-1A	6369.8

Buckman 8 SF-2B SF-2C Buckman 7R SF-2A Buckman 9 Buckman 2 Buckman 3 Buckman 3A Buckman 4 Buckman 6 Buckman 5 Buckman 10

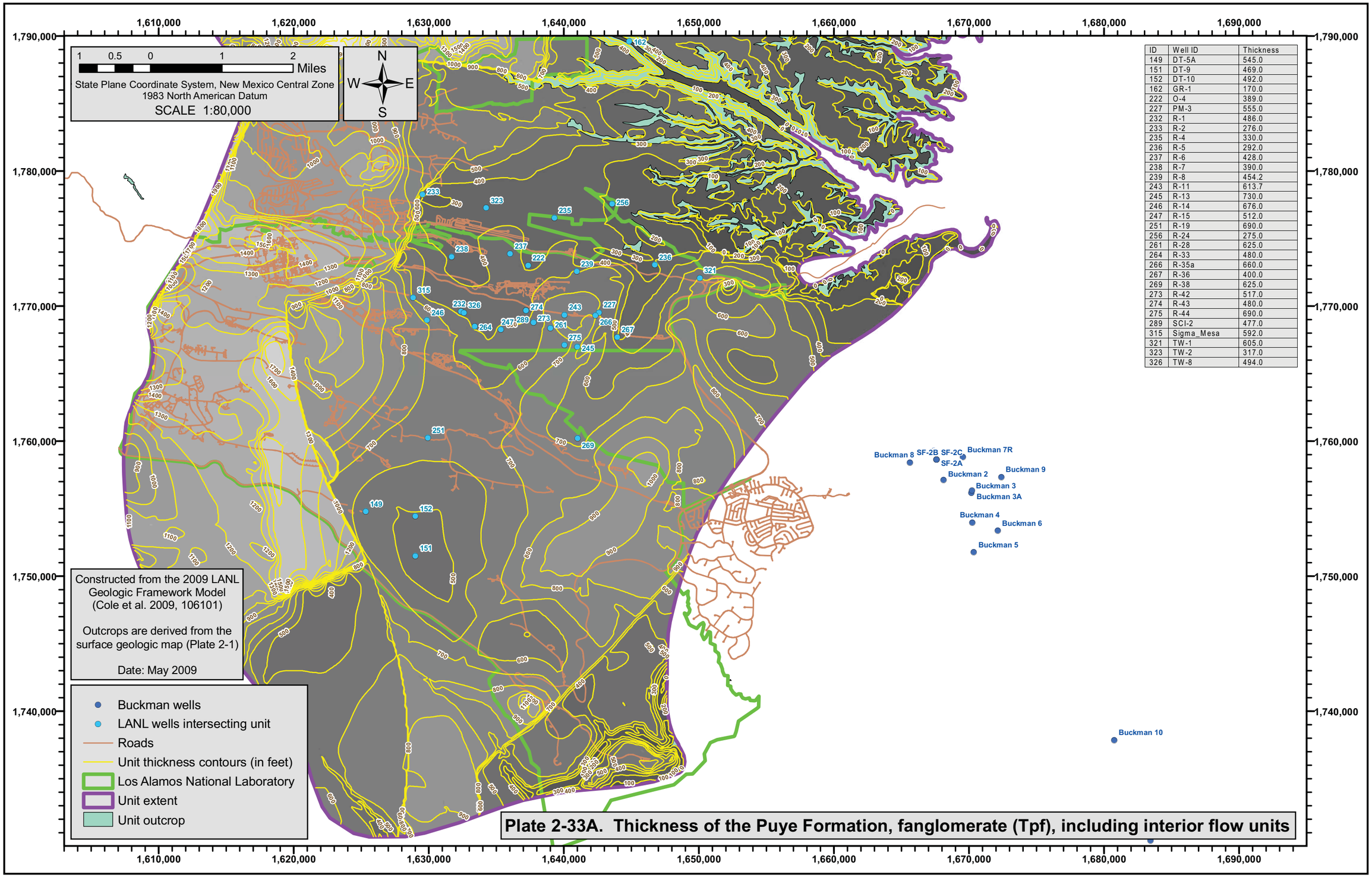
Constructed from the 2009 LANL Geologic Framework Model (Cole et al. 2009, 106101)

Outcrops are derived from the surface geologic map (Plate 2-1)

Date: May 2009

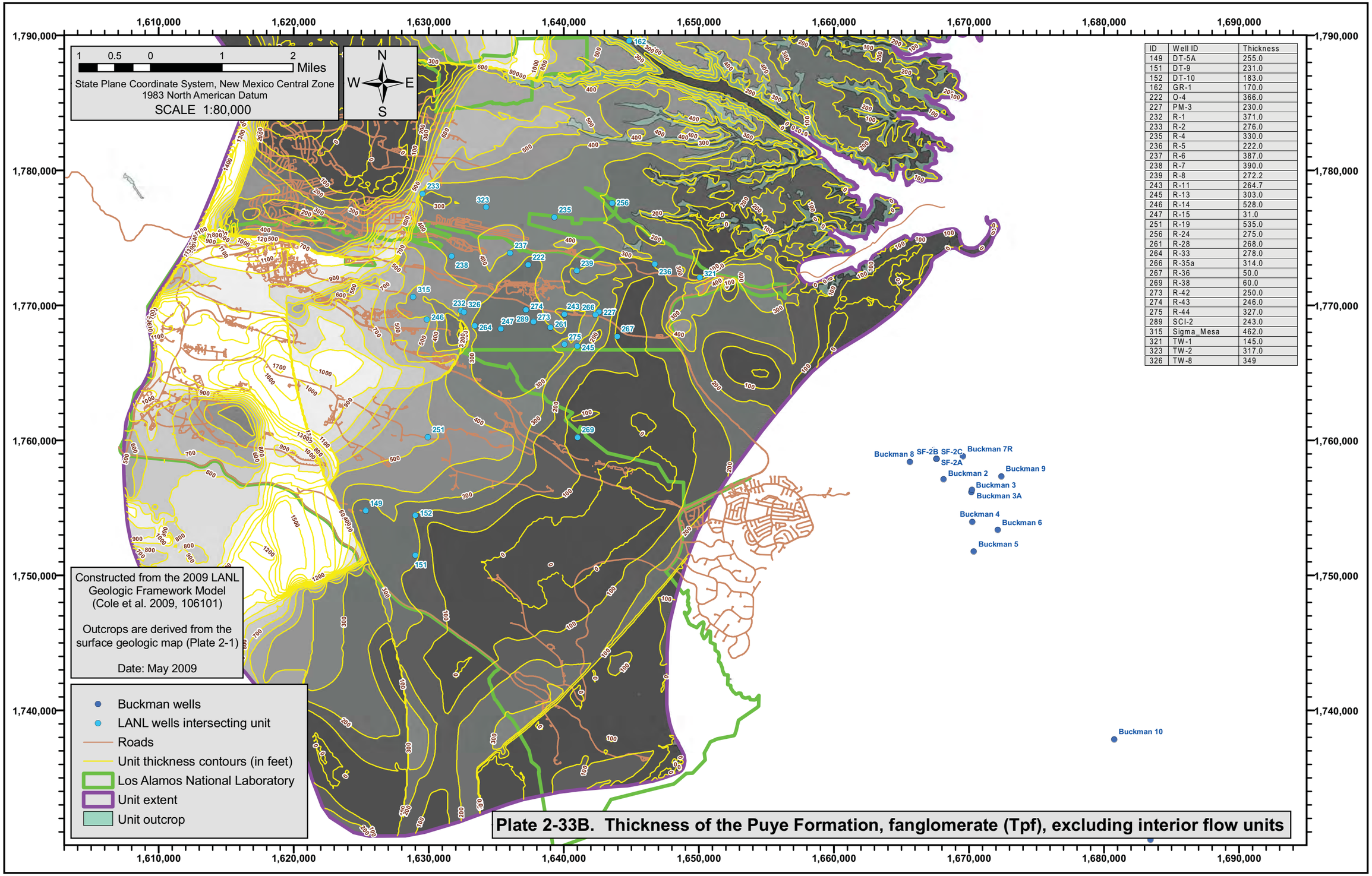
- Buckman wells
- LANL wells intersecting unit
- Roads
- Top elevation contours (in feet)
- Los Alamos National Laboratory
- Unit extent
- Unit outcrop

Plate 2-32. Structure contours of the top of the Puye Formation, fanglomerate (Tpf)



ID	Well ID	Thickness
149	DT-5A	545.0
151	DT-9	469.0
152	DT-10	492.0
162	GR-1	170.0
222	O-4	389.0
227	PM-3	555.0
232	R-1	486.0
233	R-2	276.0
235	R-4	330.0
236	R-5	292.0
237	R-6	428.0
238	R-7	390.0
239	R-8	454.2
243	R-11	613.7
245	R-13	730.0
246	R-14	676.0
247	R-15	512.0
251	R-19	690.0
256	R-24	275.0
261	R-28	625.0
264	R-33	480.0
266	R-35a	660.0
267	R-36	400.0
269	R-38	625.0
273	R-42	517.0
274	R-43	480.0
275	R-44	690.0
289	SCI-2	477.0
315	Sigma_Mesa	592.0
321	TW-1	605.0
323	TW-2	317.0
326	TW-8	494.0

Plate 2-33A. Thickness of the Puye Formation, fanglomerate (Tpf), including interior flow units



ID	Well ID	Thickness
149	DT-5A	255.0
151	DT-9	231.0
152	DT-10	183.0
162	GR-1	170.0
222	O-4	366.0
227	PM-3	230.0
232	R-1	371.0
233	R-2	276.0
235	R-4	330.0
236	R-5	222.0
237	R-6	387.0
238	R-7	390.0
239	R-8	272.2
243	R-11	264.7
245	R-13	303.0
246	R-14	528.0
247	R-15	31.0
251	R-19	535.0
256	R-24	275.0
261	R-28	268.0
264	R-33	278.0
266	R-35a	314.0
267	R-36	50.0
269	R-38	60.0
273	R-42	250.0
274	R-43	246.0
275	R-44	327.0
289	SCI-2	243.0
315	Sigma_Mesa	462.0
321	TW-1	145.0
323	TW-2	317.0
326	TW-8	349

Plate 2-33B. Thickness of the Puye Formation, fanglomerate (Tpf), excluding interior flow units

1 0.5 0 1 2 Miles

State Plane Coordinate System, New Mexico Central Zone
1983 North American Datum
SCALE 1:80,000

N W E S

Constructed from the 2009 LANL Geologic Framework Model (Cole et al. 2009, 106101)

Outcrops are derived from the surface geologic map (Plate 2-1)

Date: May 2009

- Buckman wells
- LANL wells intersecting unit
- Roads
- Bottom elevation contours (in feet)
- Los Alamos National Laboratory
- Unit extent
- Unit outcrop

ID	Well ID	Elevation
149	DT-5A	5669.2
151	DT-9	5617.0
152	DT-10	5663.0
155	G-1	5954.9
156	G-1A	5956.9
157	G-2	6027.8
158	G-3	6080.8
159	G-4	6175.0
161	G-6	6294.4
162	GR-1	6246.2
163	GR-2	6060.2
164	GR-3	6162.2
172	LA-4	5857.9
221	O-1	5860.0
222	O-4	6067.0
225	PM-1	5738.2
226	PM-2	5544.0
227	PM-3	5865.9
228	PM-4	5725.0
229	PM-5	5754.0
232	R-1	5915.2
233	R-2	6340.4
235	R-4	6197.5
236	R-5	6145.6
237	R-6	6051.8
238	R-7	6042.2
239	R-8	5995.7
240	R-9	5843.8
242	R-10	5882.3
243	R-11	5813.7
244	R-12	5833.6
245	R-13	5675.1
246	R-14	5852.1
247	R-15	5847.0
251	R-19	5536.3
252	R-20	5567.3
255	R-23	5706.8
256	R-24	6242.4
261	R-28	5788.5
262	R-31	5582.5
264	R-33	5889.3
266	R-35a	5743.1
267	R-36	6018.0
269	R-38	5805.0
273	R-42	5859.1
274	R-43	5900.0
275	R-44	5715.0
276	R-45	5734.0
277	R-46	5807.0
289	SCI-2	5903.0
315	Sigma_Mesa	5874.5
321	TW-1	5764.9

Plate 2-34. Structure contours of the bottom of the Puye Formation, fanglomerate (Tpf)

1 0.5 0 1 2 Miles

State Plane Coordinate System, New Mexico Central Zone
1983 North American Datum
SCALE 1:80,000

N W E S

1,610,000 1,620,000 1,630,000 1,640,000 1,650,000 1,660,000 1,670,000 1,680,000 1,690,000

1,790,000 1,780,000 1,770,000 1,760,000 1,750,000 1,740,000

Buckman 8 SF-2B SF-2C SF-2A Buckman 7R Buckman 9 Buckman 2 Buckman 3 Buckman 3A Buckman 4 Buckman 6 Buckman 5 Buckman 10

ID	Well ID	Elevation
17	33-1230	6291.0
18	33-1231	6248.0
46	54-1015	6391.8
47	54-1016	6425.0
74	54-24361/27436	6525.1
75	54-24362	6493.6
82	54-24370	6496.4
88	54-24375	6508.9
91	54-24378	6503.0
93	54-24380	6501.9
95	54-24382	6525.6
96	54-24383	6508.7
97	54-24384	6538.5
98	54-24385	6501.4
99	54-24386	6491.8
100	54-24387	6536.0
101	54-24388	6504.8
103	54-24390	6519.0
106	54-24393	6512.8
107	54-24394	6435.1
110	54-24397	6440.9
111	54-24399	6407.0
112	54-25105	6508.5
144	CdV-R-15-3	6295.9
146	DMB-1	6158.6
149	DT-5A	5977.2
151	DT-9	6012.0
152	DT-10	6047.0
178	LAO-4.5	6441.9
183	LAOI-3.2a	6357.9
184	LAOI-7	6383.4
205	MCOBT-4.4	6319.2
206	MCOBT-8.5	6349.5
208	MCOI-4	6317.2
209	MCOI-5	6327.7
210	MCOI-6	6318.1
211	MCOI-8	6324.2
212	MCOI-10	6324.5
221	O-1	6320.9
222	O-4	6349.0
225	PM-1	6348.2
226	PM-2	6280.0
227	PM-3	6395.9
228	PM-4	6320.0
232	R-1	6291.2
236	R-5	6396.6

ID	Well ID	Elevation
237	R-6	6312.8
239	R-8	6362.9
243	R-11	6398.4
244	R-12	6367.1
245	R-13	6370.1
247	R-15	6328.0
248	R-16	6172.9
251	R-19	6141.3
252	R-20	6302.3
253	R-21	6430.2
254	R-22	6460.5
255	R-23	6491.8
260	R-27	6079.7
261	R-28	6410.5
262	R-31	6077.5
263	R-32	6350.6
264	R-33	6324.3
265	R-34	6484.0
266	R-35a	6367.1
267	R-36	6398.0
268	R-37	6375.0
269	R-38	6415.0
270	R-39	6433.0
271	R-40	6270.0
273	R-42	6344.1
274	R-43	6334.0
275	R-44	6374.0
276	R-45	6451.0
283	SCC-1	6347.8
284	SCC-2	6346.7
285	SCC-3	6385.0
286	SCC-4	6387.2
287	SCC-5	6403.1
288	SCC-6	6370.3
289	SCI-2	6334.5
290	SCOI-3	6369.0
318	TH-5	6419.8
320	TH-7	6178.5
321	TW-1	6319.9
322	TW-1A	6319.8
324	TW-3	6360.9
326	TW-8	6295.1
186	LAWS-01	6295.8
240	R-9	6372.8
241	R-9i	6372.8

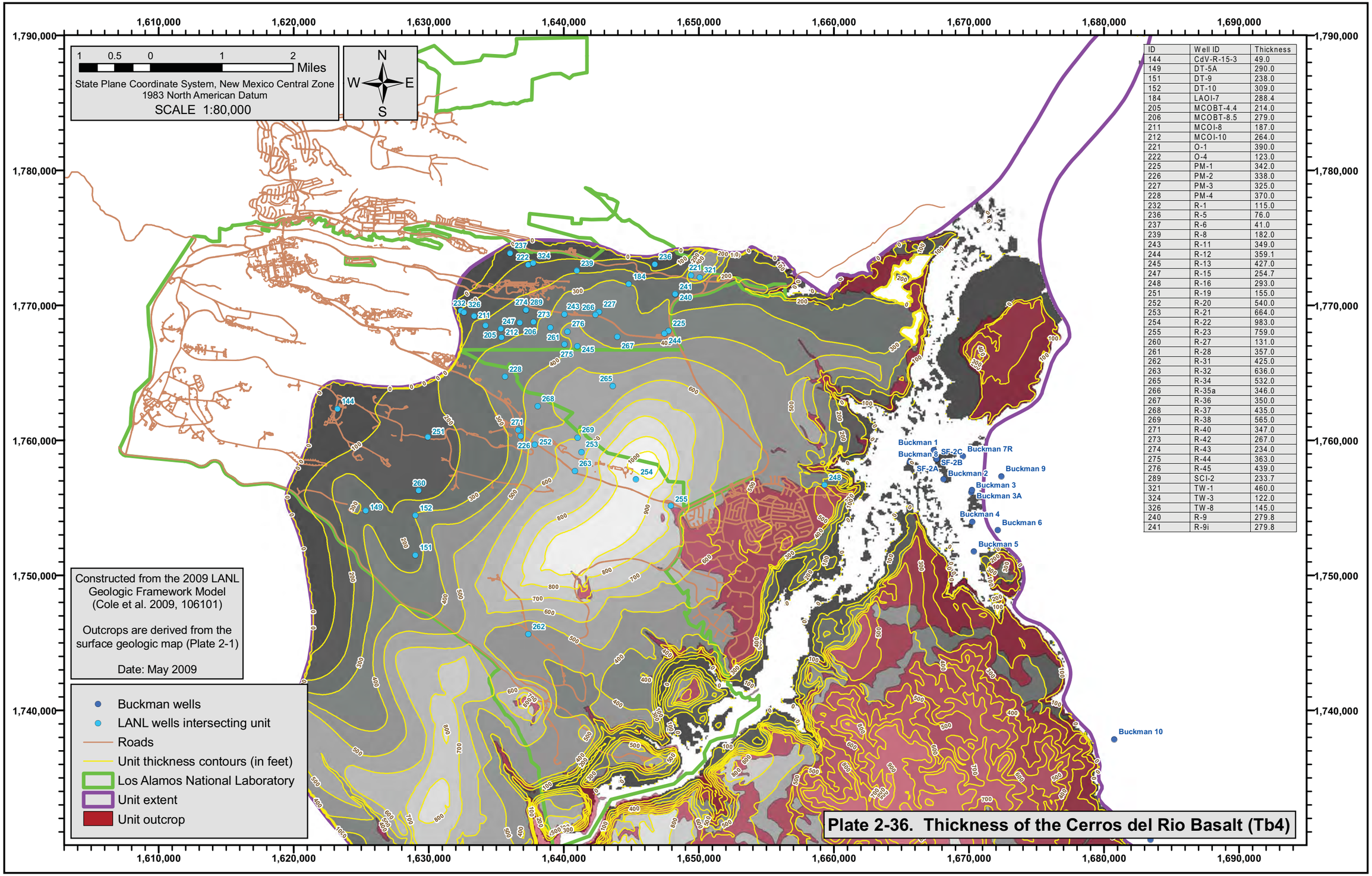
Constructed from the 2009 LANL Geologic Framework Model (Cole et al. 2009, 106101)

Outcrops are derived from the surface geologic map (Plate 2-1)

Date: May 2009

- Buckman wells
- LANL wells intersecting unit
- Roads
- Top elevation contours (in feet)
- Los Alamos National Laboratory
- Unit extent
- Unit outcrop

Plate 2-35. Structure contours of the top of the Cerros del Rio Basalt (Tb4)



ID	Well ID	Thickness
144	CdV-R-15-3	49.0
149	DT-5A	290.0
151	DT-9	238.0
152	DT-10	309.0
184	LAOI-7	288.4
205	MCOBT-4.4	214.0
206	MCOBT-8.5	279.0
211	MCOI-8	187.0
212	MCOI-10	264.0
221	O-1	390.0
222	O-4	123.0
225	PM-1	342.0
226	PM-2	338.0
227	PM-3	325.0
228	PM-4	370.0
232	R-1	115.0
236	R-5	76.0
237	R-6	41.0
239	R-8	182.0
243	R-11	349.0
244	R-12	359.1
245	R-13	427.0
247	R-15	254.7
248	R-16	293.0
251	R-19	155.0
252	R-20	540.0
253	R-21	664.0
254	R-22	983.0
255	R-23	759.0
260	R-27	131.0
261	R-28	357.0
262	R-31	425.0
263	R-32	636.0
265	R-34	532.0
266	R-35a	346.0
267	R-36	350.0
268	R-37	435.0
269	R-38	565.0
271	R-40	347.0
273	R-42	267.0
274	R-43	234.0
275	R-44	363.0
276	R-45	439.0
289	SCI-2	233.7
321	TW-1	460.0
324	TW-3	122.0
326	TW-8	145.0
240	R-9	279.8
241	R-9i	279.8

Plate 2-36. Thickness of the Cerros del Rio Basalt (Tb4)

1 0.5 0 1 2 Miles

State Plane Coordinate System, New Mexico Central Zone
1983 North American Datum
SCALE 1:80,000

N W E S

ID	Well ID	Elevation
144	CdV-R-15-3	6246.9
149	DT-5A	5687.2
151	DT-9	5774.0
152	DT-10	5738.0
184	LAOI-7	6095.0
205	MCOBT-4.4	6105.2
206	MCOBT-8.5	6070.5
211	MCOI-8	6137.2
212	MCOI-10	6060.5
221	O-1	5930.9
222	O-4	6226.0
225	PM-1	6006.2
226	PM-2	5942.0
227	PM-3	6070.9
228	PM-4	5950.0
232	R-1	6176.2
236	R-5	6320.6
237	R-6	6271.8
239	R-8	6180.9
240	R-9	6093.0
241	R-9i	6093.0
242	R-10	5904.3
243	R-11	6049.4
244	R-12	6008.0
245	R-13	5943.1
247	R-15	6073.3
248	R-16	5879.9
251	R-19	5986.3
252	R-20	5762.3
253	R-21	5766.2
254	R-22	5477.5
255	R-23	5732.8
260	R-27	5948.7
261	R-28	6053.5
262	R-31	5652.5
263	R-32	5714.6
265	R-34	5952.0
266	R-35a	6021.1
267	R-36	6048.0
268	R-37	5940.0
269	R-38	5850.0
271	R-40	5923.0
273	R-42	6077.1
274	R-43	6100.0
275	R-44	6011.0
276	R-45	6012.0
289	SCI-2	6100.8
321	TW-1	5859.9
324	TW-3	6238.9
326	TW-8	6150.1

Constructed from the 2009 LANL Geologic Framework Model (Cole et al. 2009, 106101)

Outcrops are derived from the surface geologic map (Plate 2-1)

Date: May 2009

- Buckman wells
- LANL wells intersecting unit
- Roads
- Bottom elevation contours (in feet)
- Los Alamos National Laboratory
- Unit extent
- Unit outcrop

Buckman 8, SF-2B, SF-2C, Buckman 7R, SF-2A, Buckman 2, Buckman 3, Buckman 9, Buckman 3A, Buckman 4, Buckman 6, Buckman 5, Buckman 10

Plate 2-37. Structure contours of the bottom of the Cerros del Rio Basalt (Tb4)

1 0.5 0 1 2 Miles

State Plane Coordinate System, New Mexico Central Zone
1983 North American Datum
SCALE 1:80,000

N W E S

1,610,000 1,620,000 1,630,000 1,640,000 1,650,000 1,660,000 1,670,000 1,680,000 1,690,000

1,790,000 1,780,000 1,770,000 1,760,000 1,750,000 1,740,000

Buckman 8 SF-2B SF-2C Buckman 7R SF-2A Buckman 2 Buckman 9 Buckman 3 Buckman 3A Buckman 4 Buckman 6 Buckman 5 Buckman 10

5200 5500 5600 6000 6200

Constructed from the 2009 LANL Geologic Framework Model (Cole et al. 2009, 106101)

Outcrops are derived from the surface geologic map (Plate 2-1)

Date: May 2009

- Buckman wells
- LANL wells intersecting unit
- Roads
- Top elevation contours (in feet)
- Los Alamos National Laboratory
- Unit extent
- Unit outcrop

Plate 2-38. Structure contours of the top of the Ancha Formation (Qta)

1 0.5 0 1 2 Miles

State Plane Coordinate System, New Mexico Central Zone
1983 North American Datum
SCALE 1:80,000

N W E S

1,610,000 1,620,000 1,630,000 1,640,000 1,650,000 1,660,000 1,670,000 1,680,000 1,690,000

1,790,000 1,780,000 1,770,000 1,760,000 1,750,000 1,740,000

Buckman 8 SF-2B SF-2C Buckman 7R SF-2A Buckman 2 Buckman 9 Buckman 3 Buckman 3A Buckman 6 Buckman 4 Buckman 5 Buckman 10

Constructed from the 2009 LANL Geologic Framework Model (Cole et al. 2009, 106101)

Outcrops are derived from the surface geologic map (Plate 2-1)

Date: May 2009

- Buckman wells
- LANL wells intersecting unit
- Roads
- Unit thickness contours (in feet)
- Los Alamos National Laboratory
- Unit extent
- Unit outcrop

Plate 2-39. Thickness of the Ancha Formation (Qta)

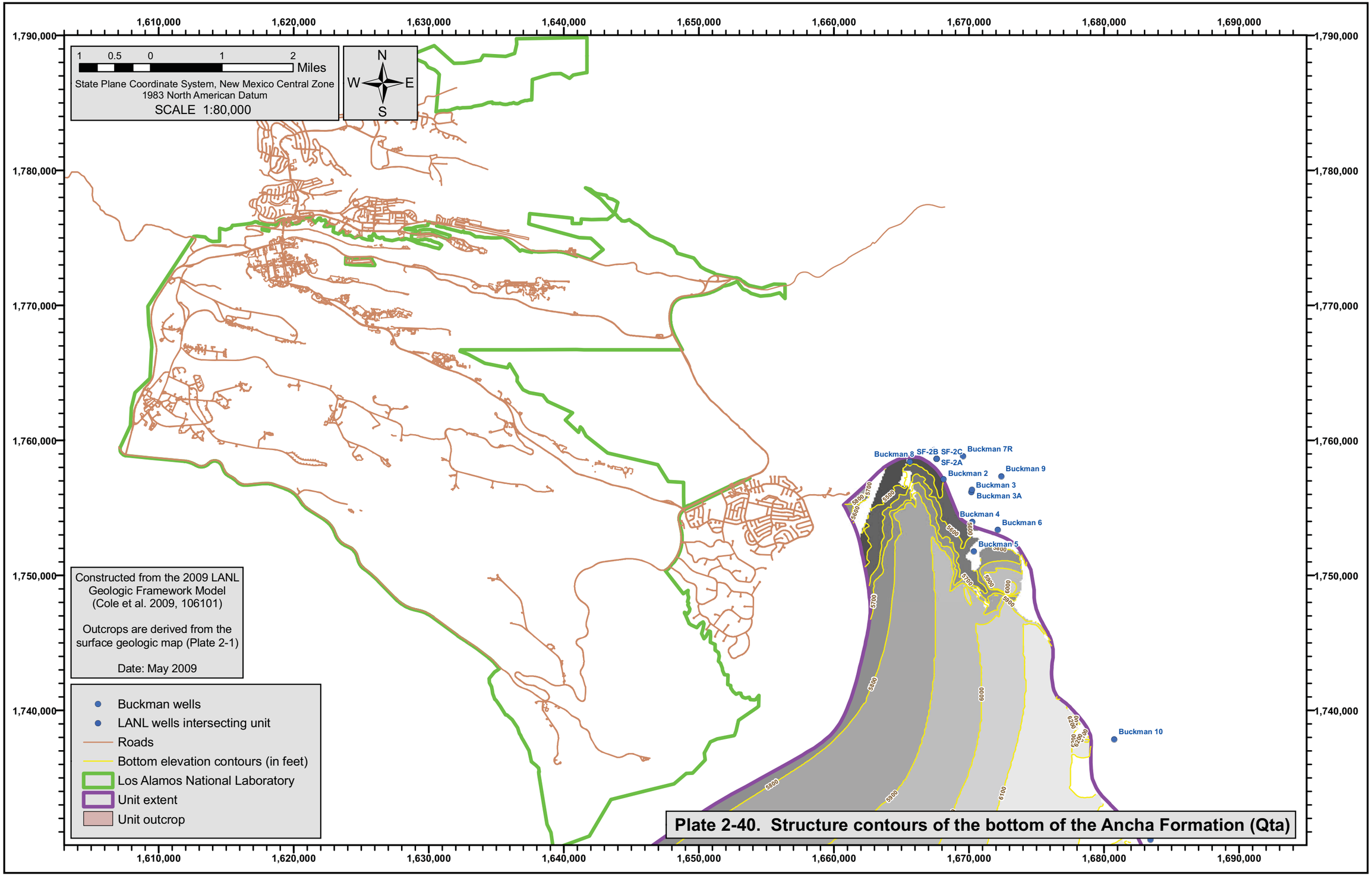


Plate 2-40. Structure contours of the bottom of the Ancha Formation (Qta)

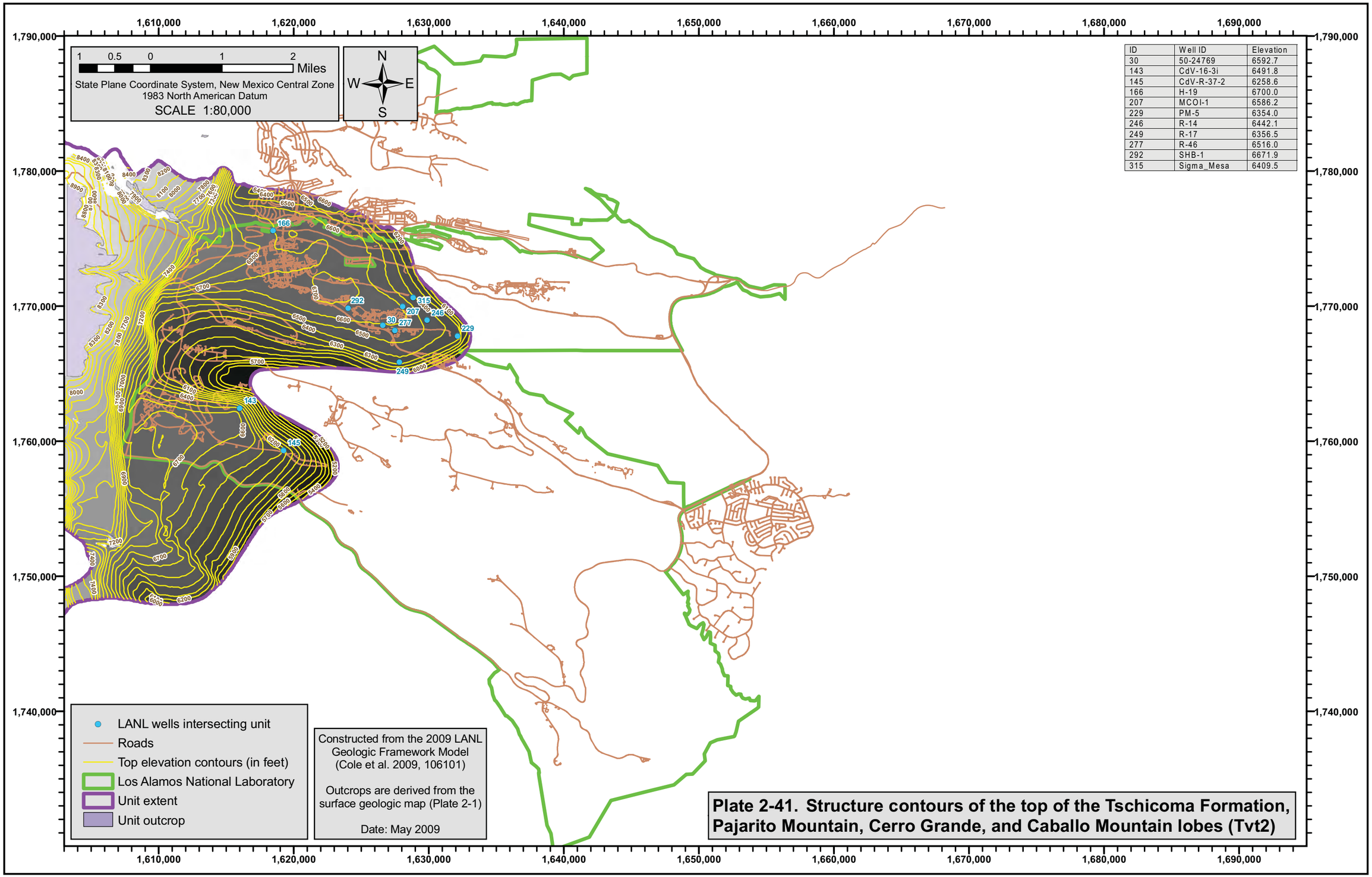


Plate 2-41. Structure contours of the top of the Tschicoma Formation, Pajarito Mountain, Cerro Grande, and Caballo Mountain lobes (Tvt2)

1 0.5 0 1 2 Miles

State Plane Coordinate System, New Mexico Central Zone
1983 North American Datum
SCALE 1:80,000

N
W E
S

ID	Well ID	Thickness
166	H-19	347.0
207	MCOI-1	314.8
229	PM-5	405.0
246	R-14	148.0
249	R-17	175.0
277	R-46	244.0
315	Sigma_Mesa	130.0

1,610,000 1,620,000 1,630,000 1,640,000 1,650,000 1,660,000 1,670,000 1,680,000 1,690,000

1,790,000 1,780,000 1,770,000 1,760,000 1,750,000 1,740,000

LANL wells intersecting unit
Roads
Unit thickness contours (in feet)
Los Alamos National Laboratory
Unit extent
Unit outcrop

Constructed from the 2009 LANL Geologic Framework Model (Cole et al. 2009, 106101)

Outcrops are derived from the surface geologic map (Plate 2-1)

Date: May 2009

Plate 2-42. Thickness of the Tschicoma Formation, Pajarito Mountain, Cerro Grande, and Caballo Mountain lobes (Tvt2)

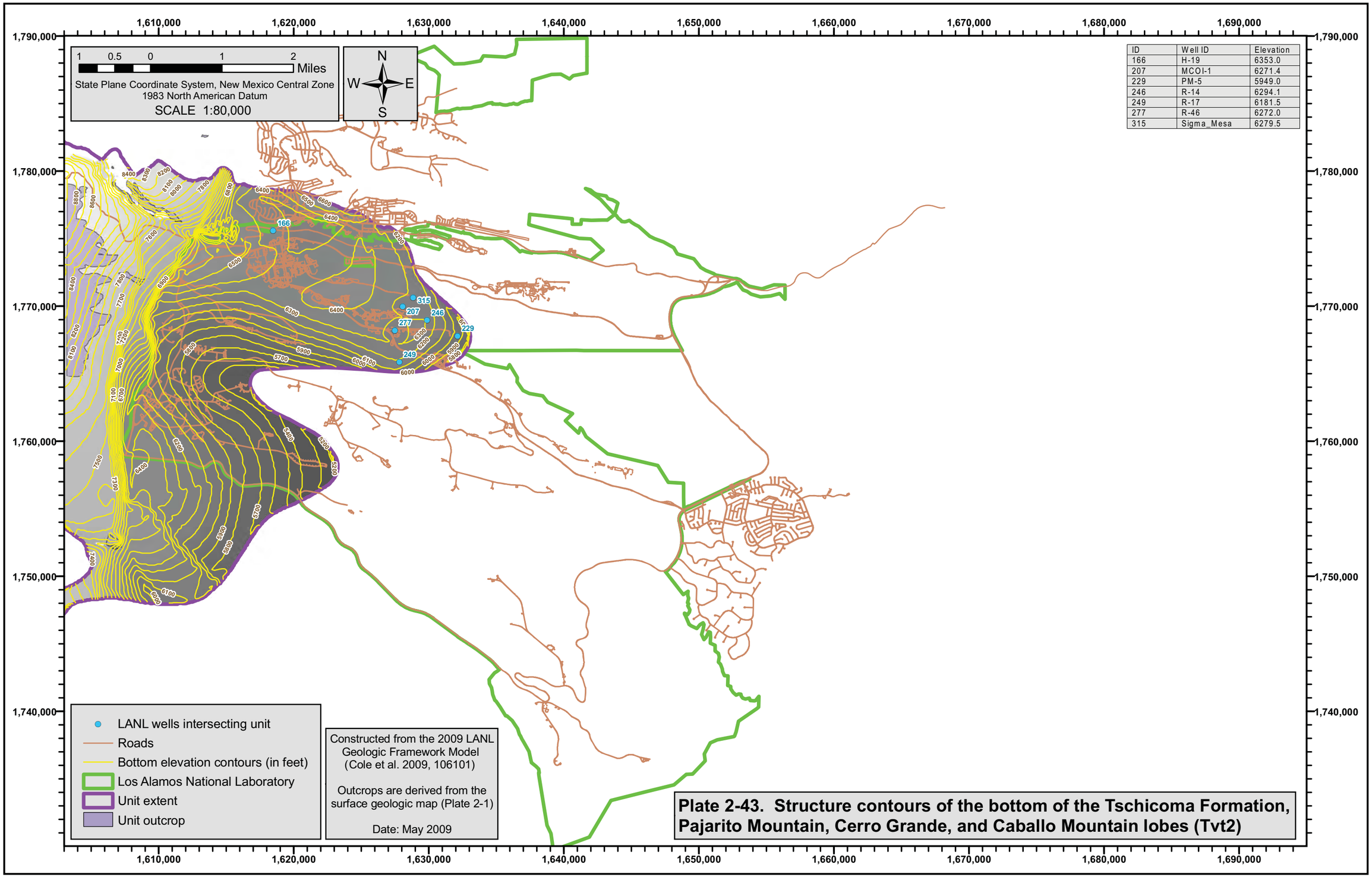


Plate 2-43. Structure contours of the bottom of the Tschicoma Formation, Pajarito Mountain, Cerro Grande, and Caballo Mountain lobes (Tvt2)

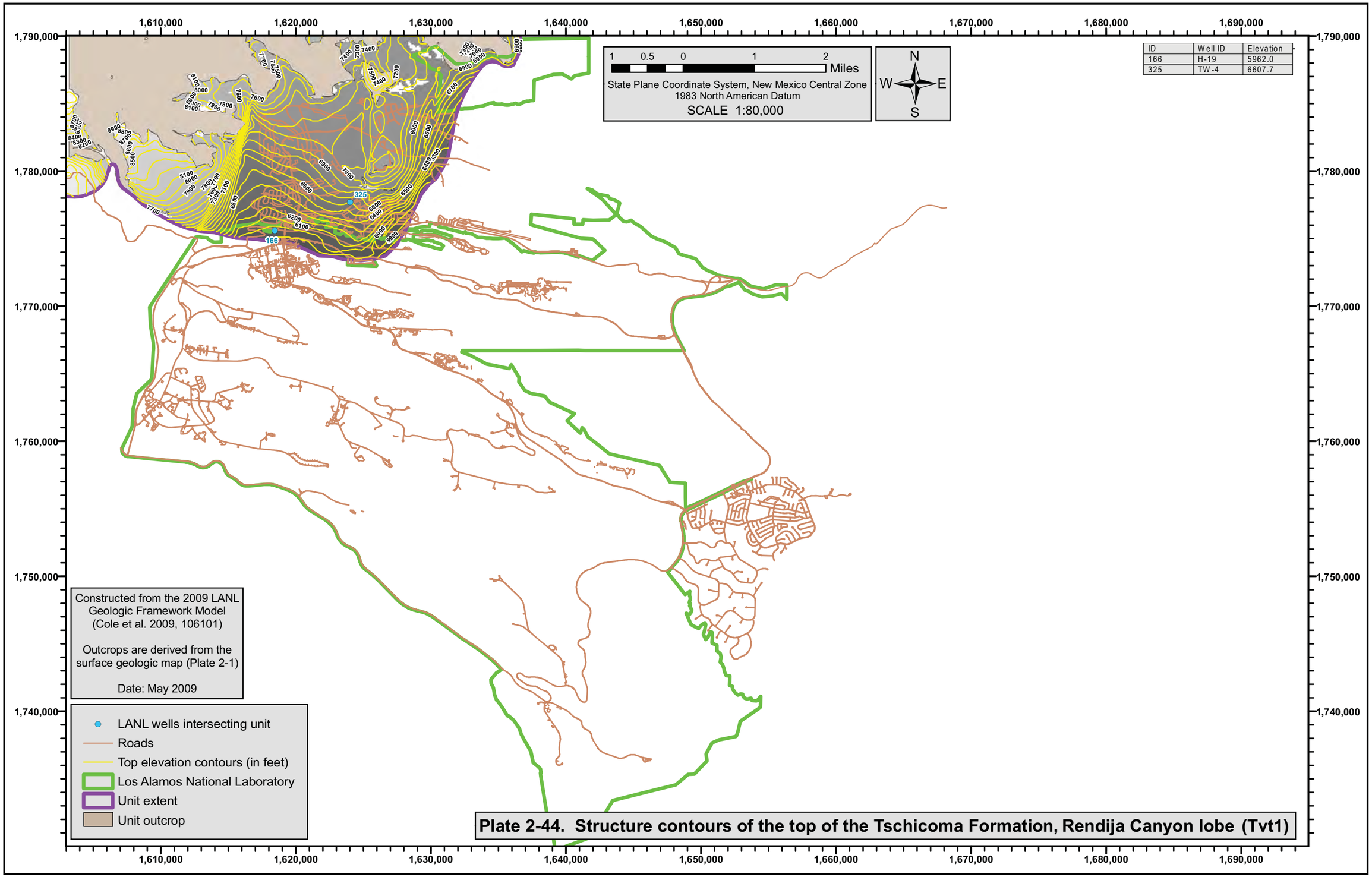


Plate 2-44. Structure contours of the top of the Tschicoma Formation, Rendija Canyon lobe (Tvt1)

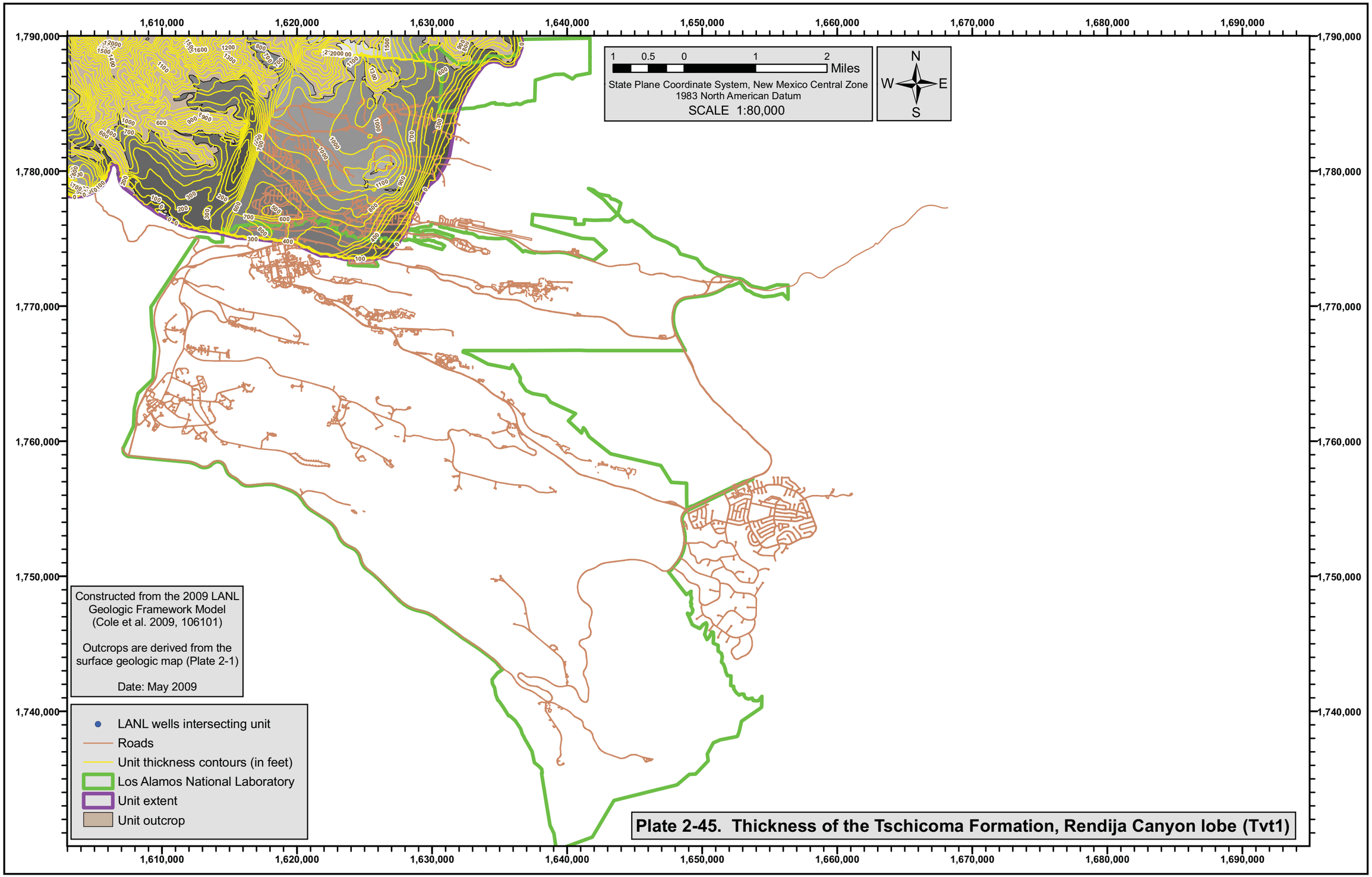


Plate 2-45. Thickness of the Tschicoma Formation, Rendija Canyon lobe (Tvt1)

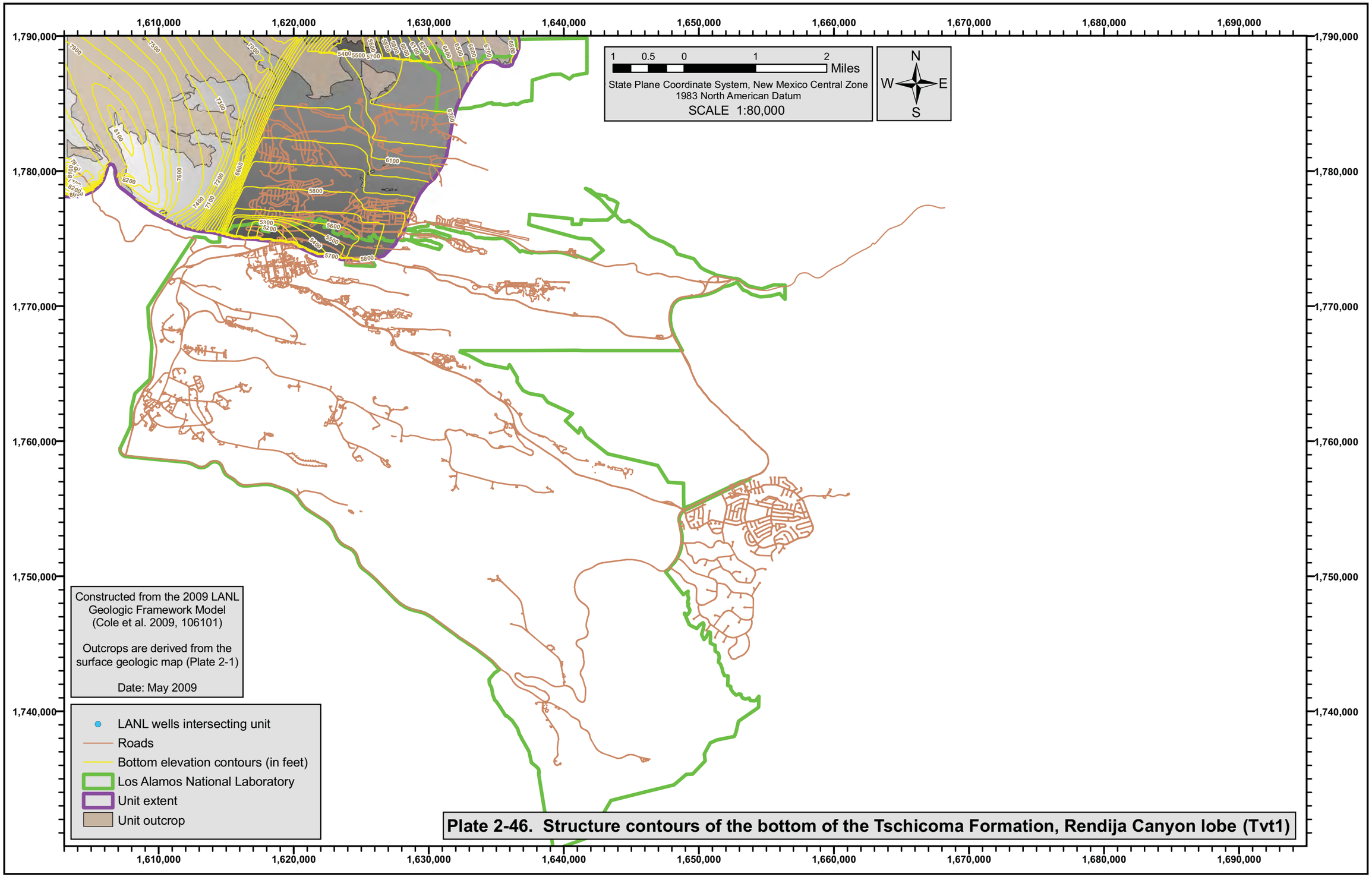


Plate 2-46. Structure contours of the bottom of the Tschicoma Formation, Rendija Canyon lobe (Tvt1)

1 0.5 0 1 2 Miles

State Plane Coordinate System, New Mexico Central Zone
1983 North American Datum
SCALE 1:80,000

N W E S

ID	Well ID	Elevation
172	LA-4	5857.9
248	R-16	5879.9
262	R-31	5582.5

1,610,000 1,620,000 1,630,000 1,640,000 1,650,000 1,660,000 1,670,000 1,680,000 1,690,000

1,790,000 1,780,000 1,770,000 1,760,000 1,750,000 1,740,000

Buckman 8 SF-2B SF-2C Buckman 7R SF-2A Buckman 2 Buckman 9 Buckman 3 Buckman 3A Buckman 4 Buckman 6 Buckman 5 Buckman 10

Constructed from the 2009 LANL Geologic Framework Model (Cole et al. 2009)

Outcrops are derived from the surface geologic map (Plate 2-1)

Date: May 2009

- Buckman wells
- LANL wells intersecting unit
- Roads
- Top elevation contours (in feet)
- Los Alamos National Laboratory
- Unit extent
- Unit outcrop

Plate 2-47. Structure contours of the top of the Totavi Lentil (Tpt)

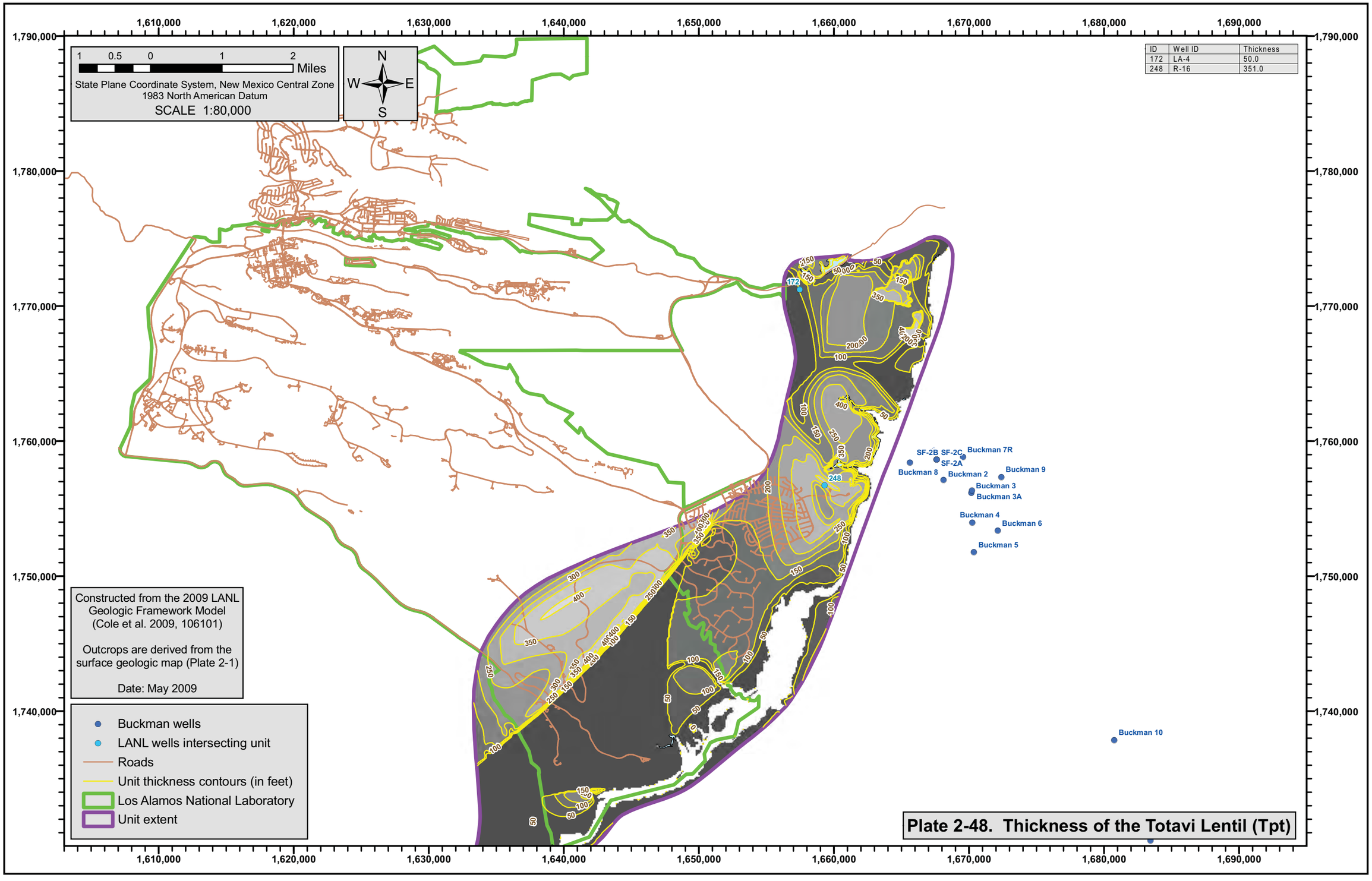


Plate 2-48. Thickness of the Totavi Lentil (Tpt)

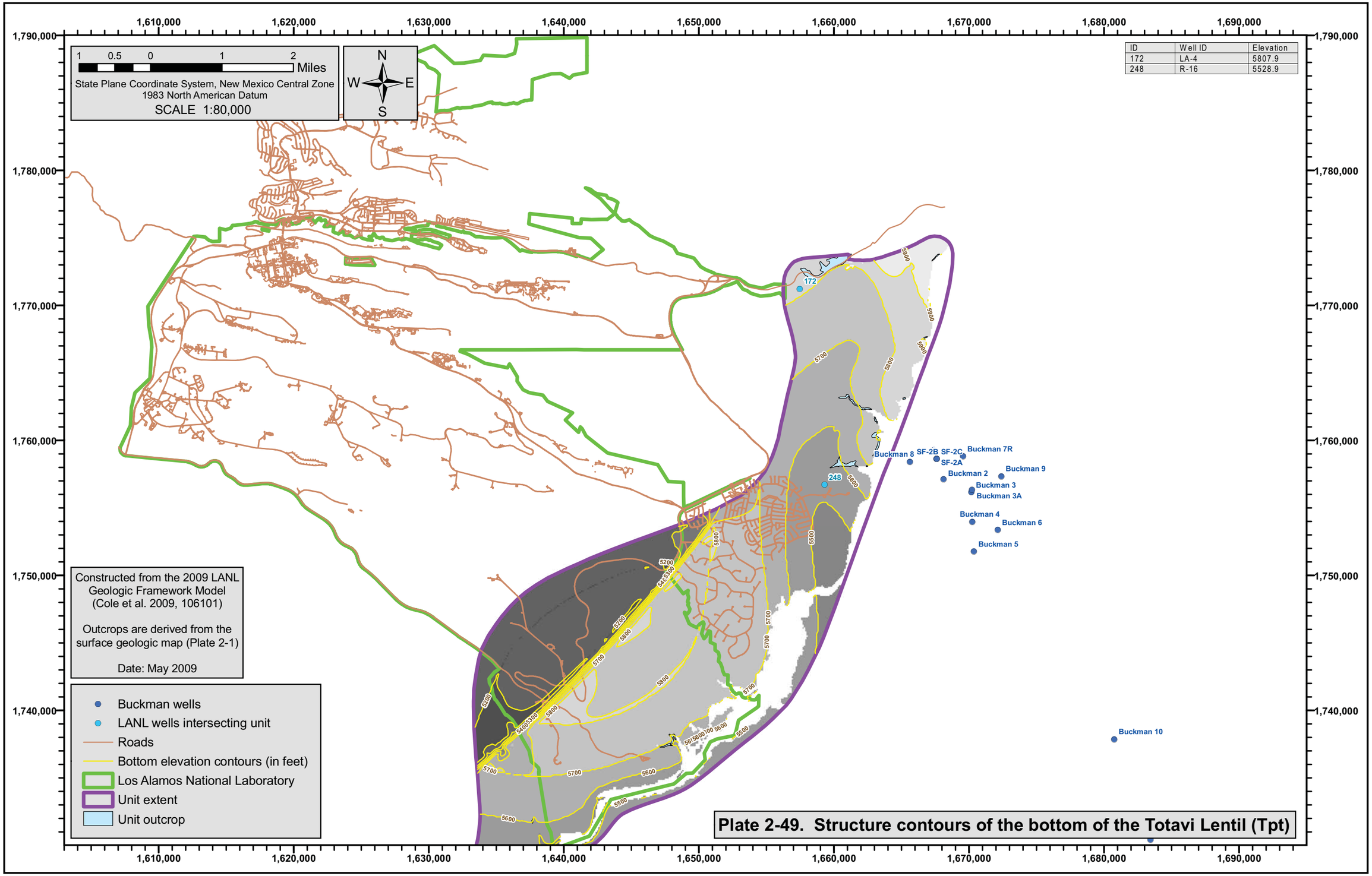


Plate 2-49. Structure contours of the bottom of the Totavi Lentil (Tpt)

ID	Well ID	Elevation
222	O-4	6067.0
226	PM-2	5544.0
228	PM-4	5725.0
229	PM-5	5754.0
232	R-1	5915.2
233	R-2	6340.4
235	R-4	6197.5
237	R-6	6051.8
238	R-7	6042.2
243	R-11	5813.7
245	R-13	5675.1
246	R-14	5852.1
247	R-15	5847.0
251	R-19	5536.3
252	R-20	5567.3
261	R-28	5788.5
264	R-33	5889.3
273	R-42	5859.1
274	R-43	5900.0
275	R-44	5715.0
276	R-45	5734.0
277	R-46	5807.0
289	SCI-2	5903.0
315	Sigma_Mesa	5874.5
323	TW-2	6266.4
324	TW-3	6096.9
326	TW-8	5906.1

1 0.5 0 1 2 Miles

State Plane Coordinate System, New Mexico Central Zone
1983 North American Datum
SCALE 1:80,000

N W E S

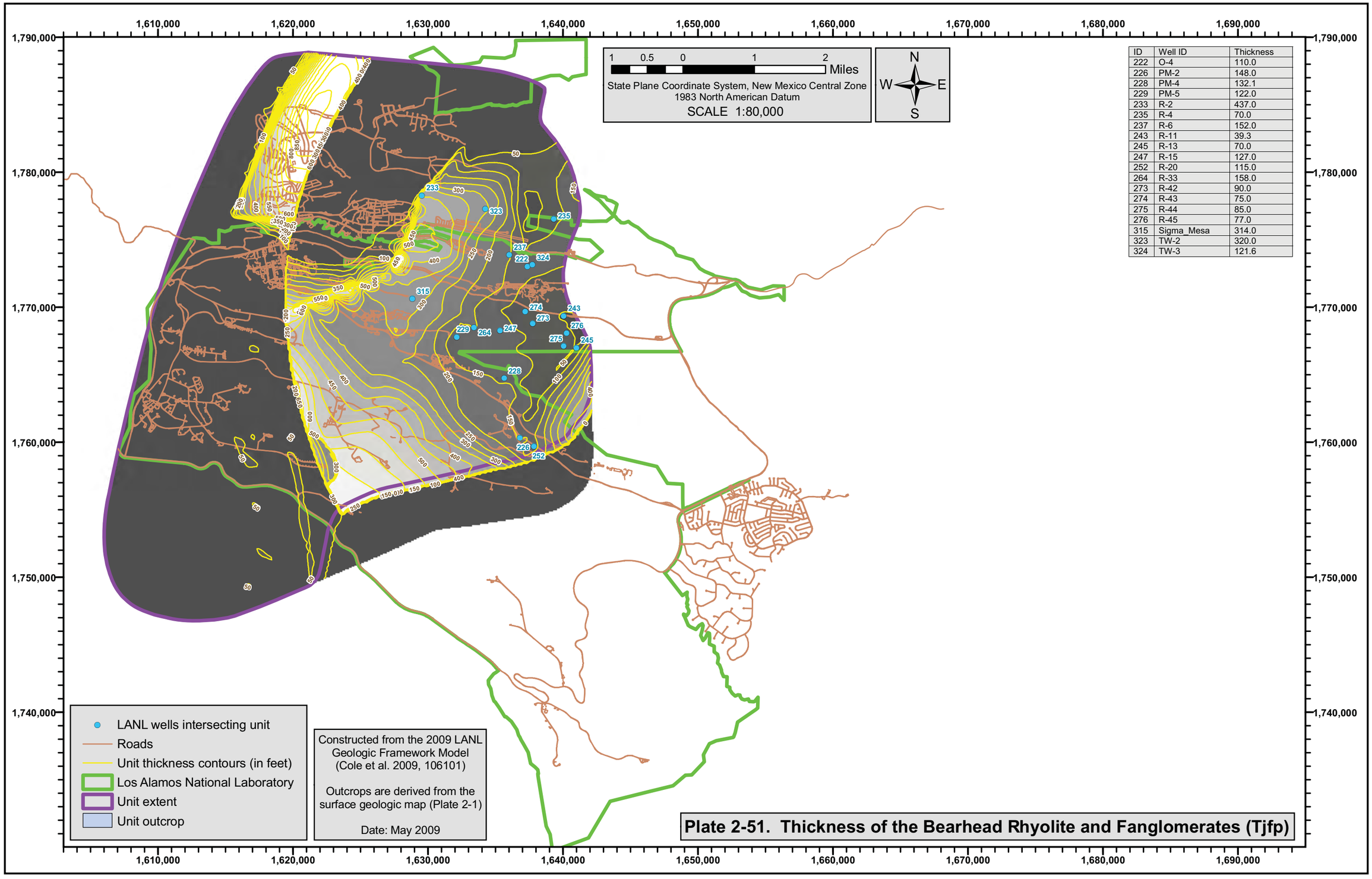
LANL wells intersecting unit
Roads
Top elevation contours (in feet)
Los Alamos National Laboratory
Unit extent
Unit outcrop

Constructed from the 2009 LANL Geologic Framework Model (Cole et al. 2009, 106101)

Outcrops are derived from the surface geologic map (Plate 2-1)

Date: May 2009

Plate 2-50. Structure contours of the top of the Bearhead Rhyolite and Fanglomerates (Tjfp)



ID	Well ID	Thickness
222	O-4	110.0
226	PM-2	148.0
228	PM-4	132.1
229	PM-5	122.0
233	R-2	437.0
235	R-4	70.0
237	R-6	152.0
243	R-11	39.3
245	R-13	70.0
247	R-15	127.0
252	R-20	115.0
264	R-33	158.0
273	R-42	90.0
274	R-43	75.0
275	R-44	85.0
276	R-45	77.0
315	Sigma_Mesa	314.0
323	TW-2	320.0
324	TW-3	121.6

Plate 2-51. Thickness of the Bearhead Rhyolite and Fanglomerates (Tjfp)

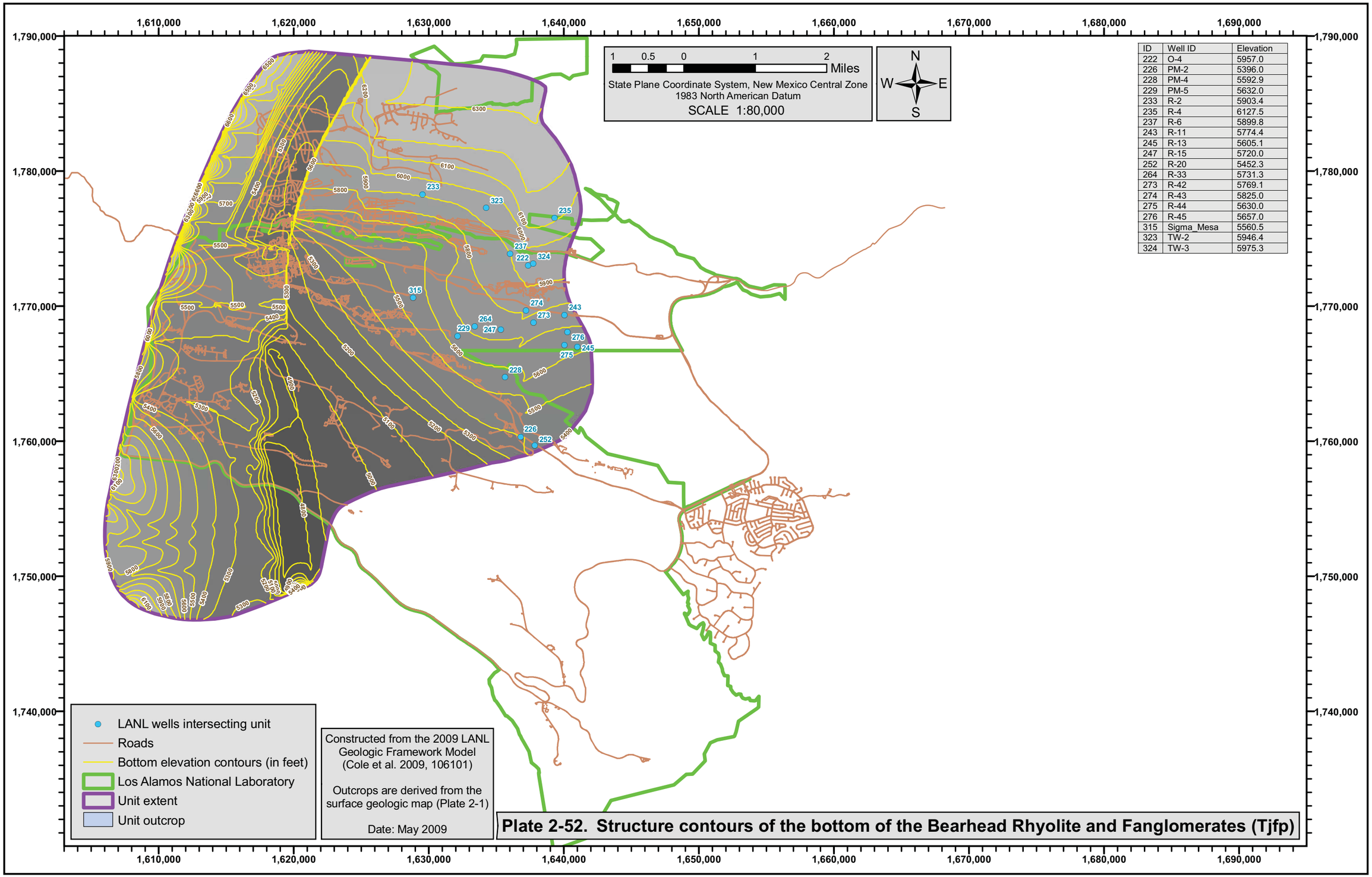


Plate 2-52. Structure contours of the bottom of the Bearhead Rhyolite and Fanglomerates (Tjfp)

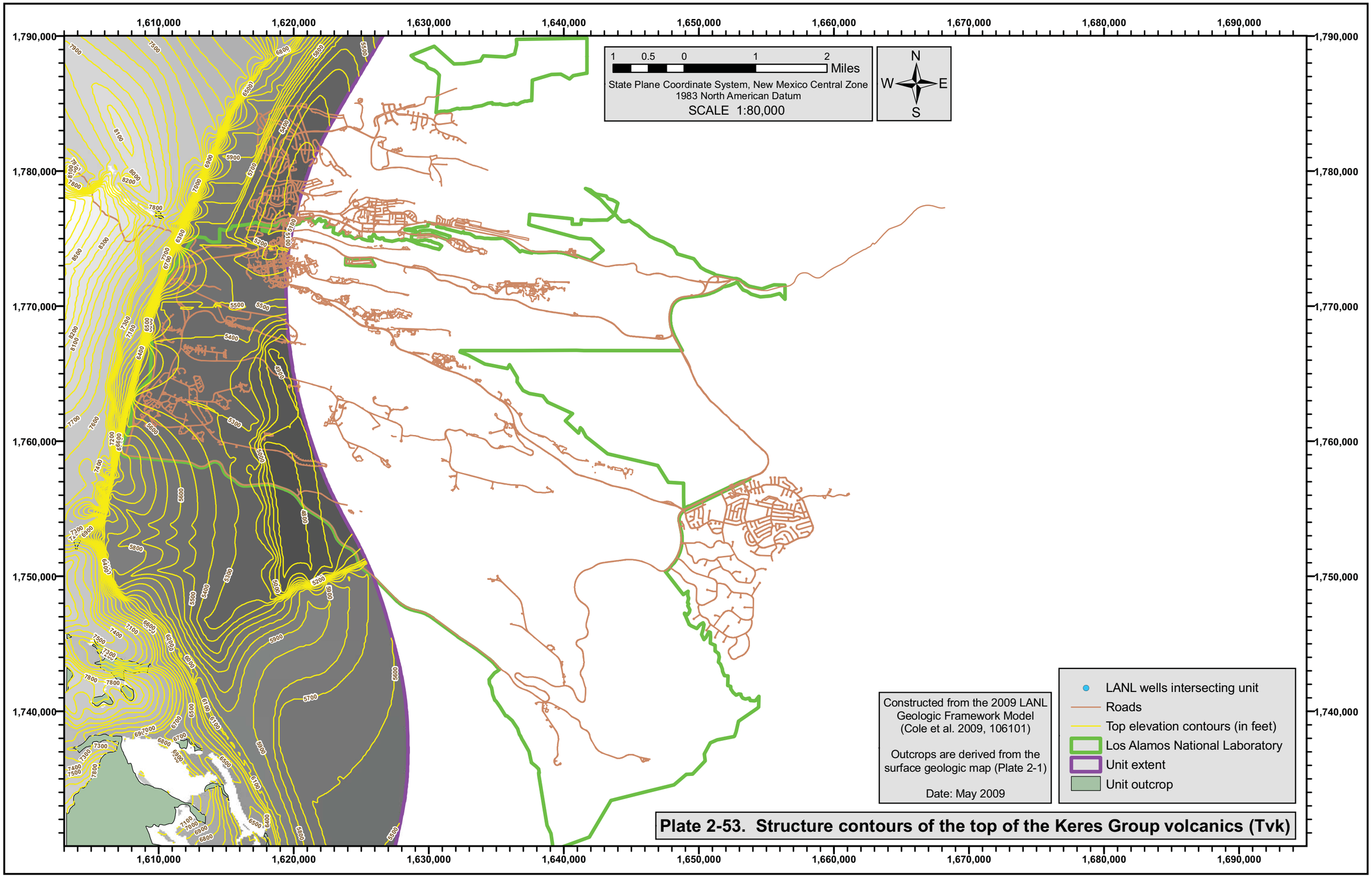
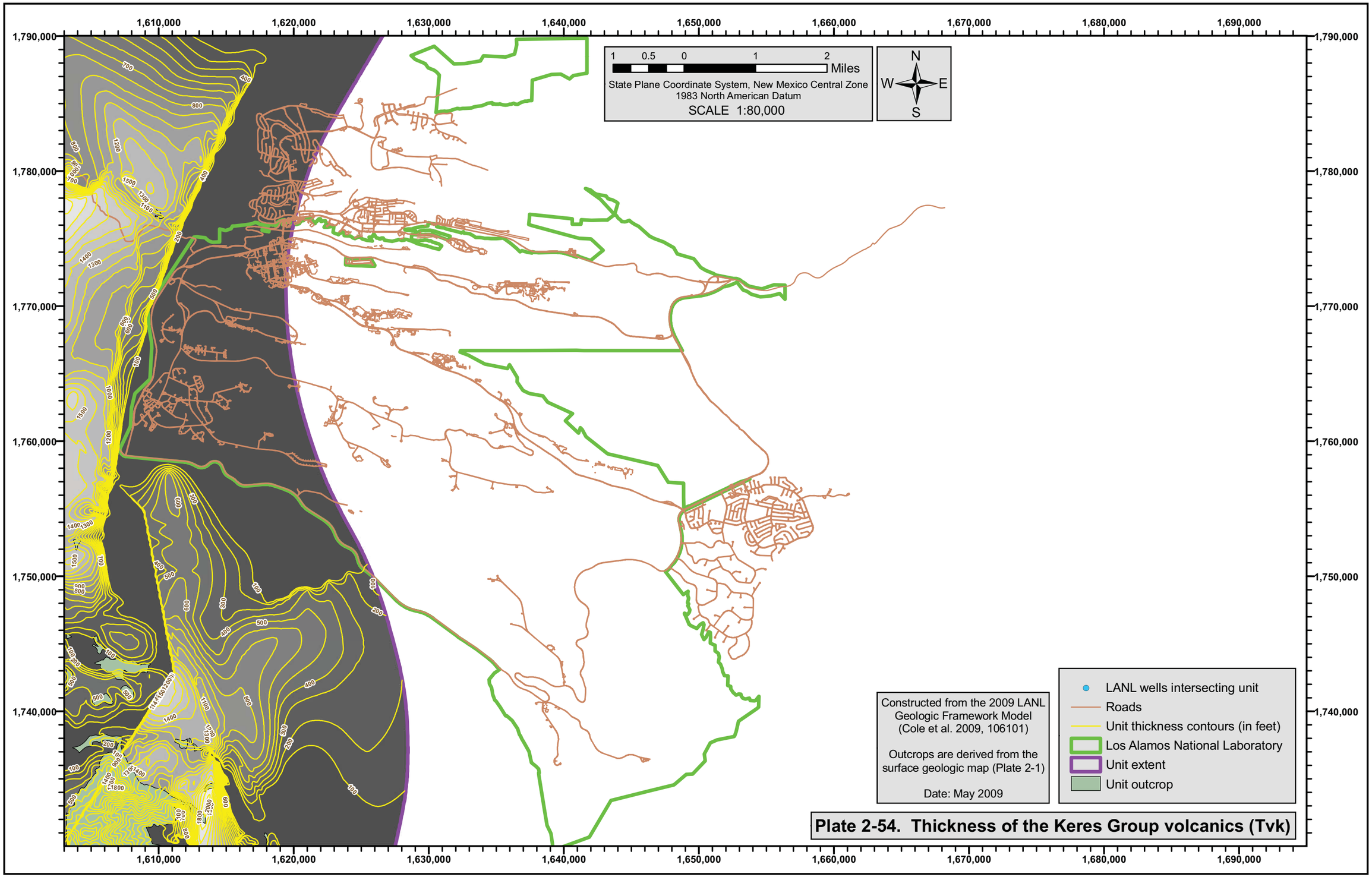


Plate 2-53. Structure contours of the top of the Keres Group volcanics (Tvk)


1,610,000
1,620,000
1,630,000
1,640,000
1,650,000
1,660,000
1,670,000
1,680,000
1,690,000
1,790,000
1,780,000
1,770,000
1,760,000
1,750,000
1,740,000
1 0.5 0 1 2 Miles
State Plane Coordinate System, New Mexico Central Zone
1983 North American Datum
SCALE 1:80,000
N
W E
S
Constructed from the 2009 LANL Geologic Framework Model (Cole et al. 2009, 106101)
Outcrops are derived from the surface geologic map (Plate 2-1)
Date: May 2009
LANL wells intersecting unit
Roads
Unit thickness contours (in feet)
Los Alamos National Laboratory
Unit extent
Unit outcrop
Plate 2-54. Thickness of the Keres Group volcanics (Tvk)

1 0.5 0 1 2 Miles

State Plane Coordinate System, New Mexico Central Zone
1983 North American Datum
SCALE 1:80,000

N W E S

1,610,000 1,620,000 1,630,000 1,640,000 1,650,000 1,660,000 1,670,000 1,680,000 1,690,000

1,790,000 1,780,000 1,770,000 1,760,000 1,750,000 1,740,000

Constructed from the 2009 LANL Geologic Framework Model (Cole et al. 2009, 106101)

Outcrops are derived from the surface geologic map (Plate 2-1)

Date: May 2009

- LANL wells intersecting unit
- Roads
- Bottom elevation contours (in feet)
- Los Alamos National Laboratory
- Unit extent
- Unit outcrop

Plate 2-55. Structure contours of the bottom of the Keres Group volcanics (Tvk)

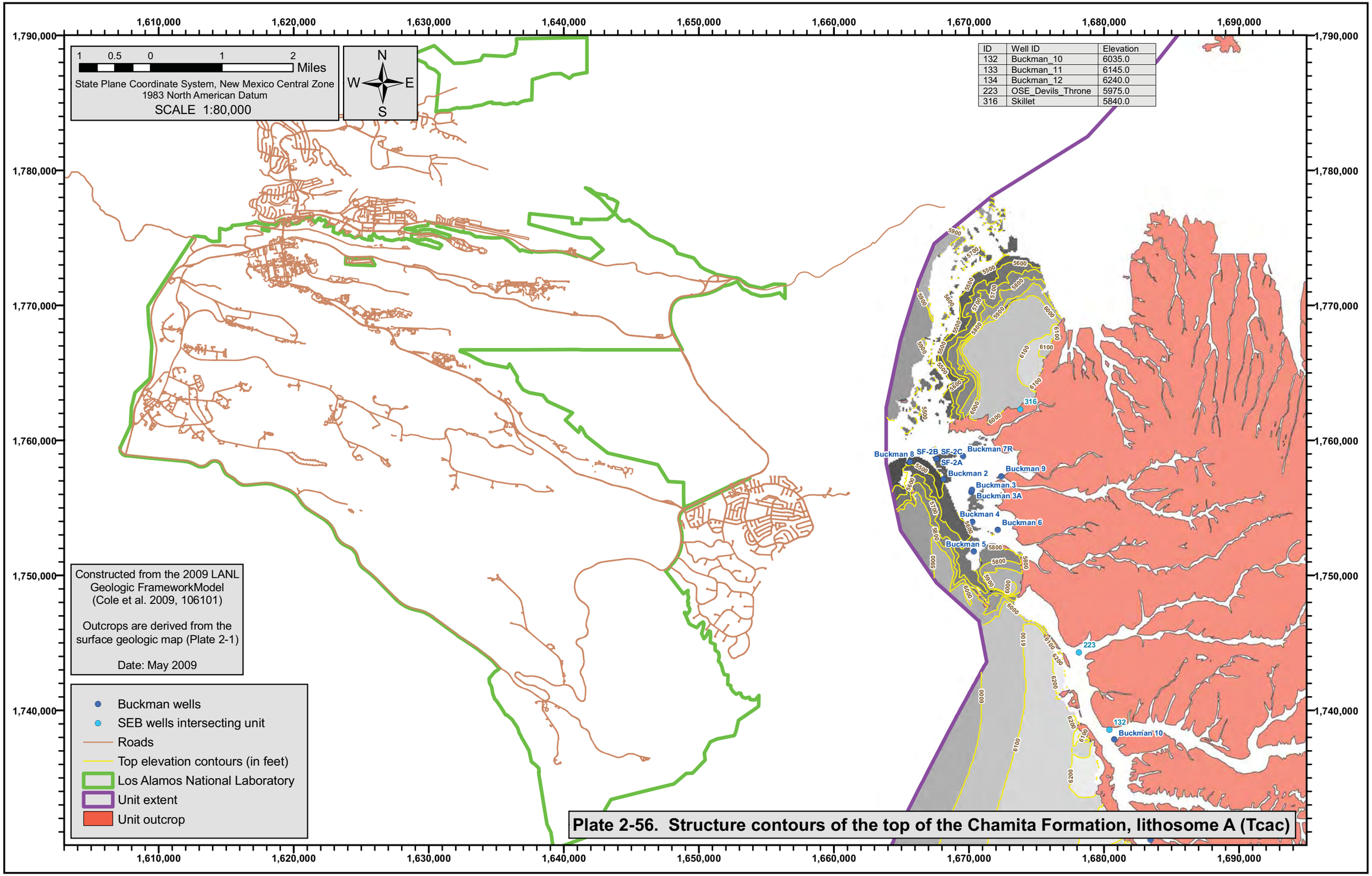


Plate 2-56. Structure contours of the top of the Chamita Formation, lithosome A (Tcac)

1 0.5 0 1 2 Miles

State Plane Coordinate System, New Mexico Central Zone
1983 North American Datum
SCALE 1:80,000

N W E S

ID	Well ID	Thickness
132	Buckman_10	970.0
133	Buckman_11	634.0
134	Buckman_12	604.0
223	OSE_Devils_Throne	65.0
316	Skillet	174.0

Constructed from the 2009 LANL Geologic Framework Model (Cole et al. 2009, 106101)

Outcrops are derived from the surface geologic map (Plate 2-1)

Date: May 2009

- Buckman wells
- SEB wells intersecting unit
- Roads
- Unit thickness contours (in feet)
- Los Alamos National Laboratory
- Unit extent
- Unit outcrop

SF-2B SF-2C
SF-2A
Buckman 7R
Buckman 8
Buckman 2
Buckman 9
Buckman 3
Buckman 3A
Buckman 4
Buckman 6
Buckman 5
316
223
132
Buckman 10

Plate 2-57. Thickness of the Chamita Formation, lithosome A (Tcac)

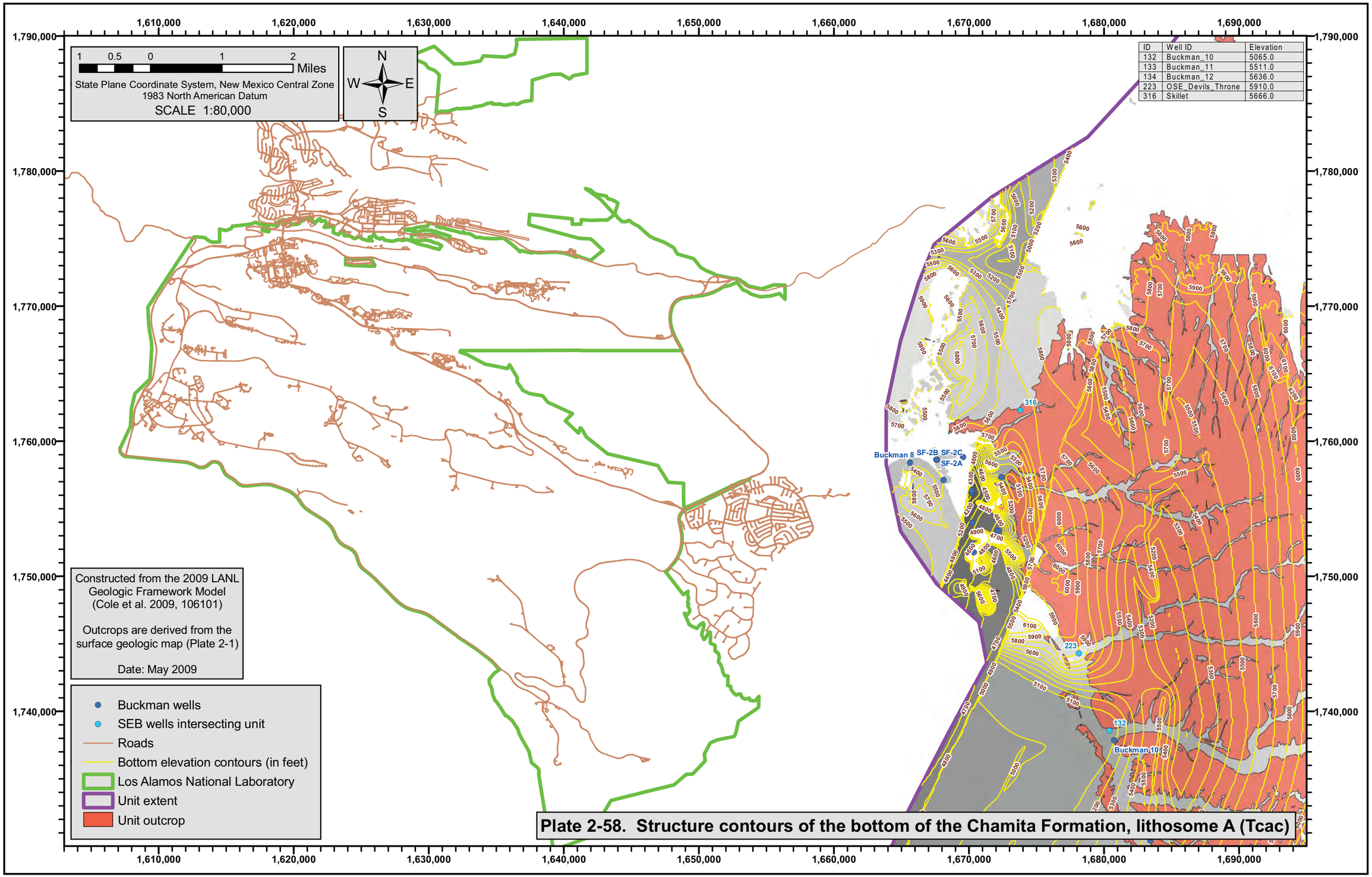


Plate 2-58. Structure contours of the bottom of the Chamita Formation, lithosome A (Tcac)

1 0.5 0 1 2 Miles

State Plane Coordinate System, New Mexico Central Zone
1983 North American Datum
SCALE 1:80,000

N W E S

ID	Well ID	Elevation
132	Buckman_10	5065.0
133	Buckman_11	5511.0
134	Buckman_12	5636.0
223	OSE_Devils_Throne	5910.0
131	Buckman_9	5728.0
167	Kelly_Fed	6025.0
217	NAD-63	6405.0
218	NAD-60	6215.0

Constructed from the 2009 LANL Geologic Framework Model (Cole et al. 2009, 106101)

Outcrops are derived from the surface geologic map (Plate 2-1)

Date: May 2009

- Buckman wells
- SEB wells intersecting unit
- Roads
- Top elevation contours (in feet)
- Los Alamos National Laboratory
- Unit extent
- Unit outcrop

Buckman 8, SF-2B, SF-2C, Buckman 7R, SF-2A, Buckman 2, 131, Buckman 9, Buckman 3, Buckman 3A, Buckman 4, Buckman 6, Buckman 5, 223, 132, Buckman 10, Buckman 11

Plate 2-59. Structure contours of the top of the Tesuque Formation, Chamita lithosome B (Ttca)

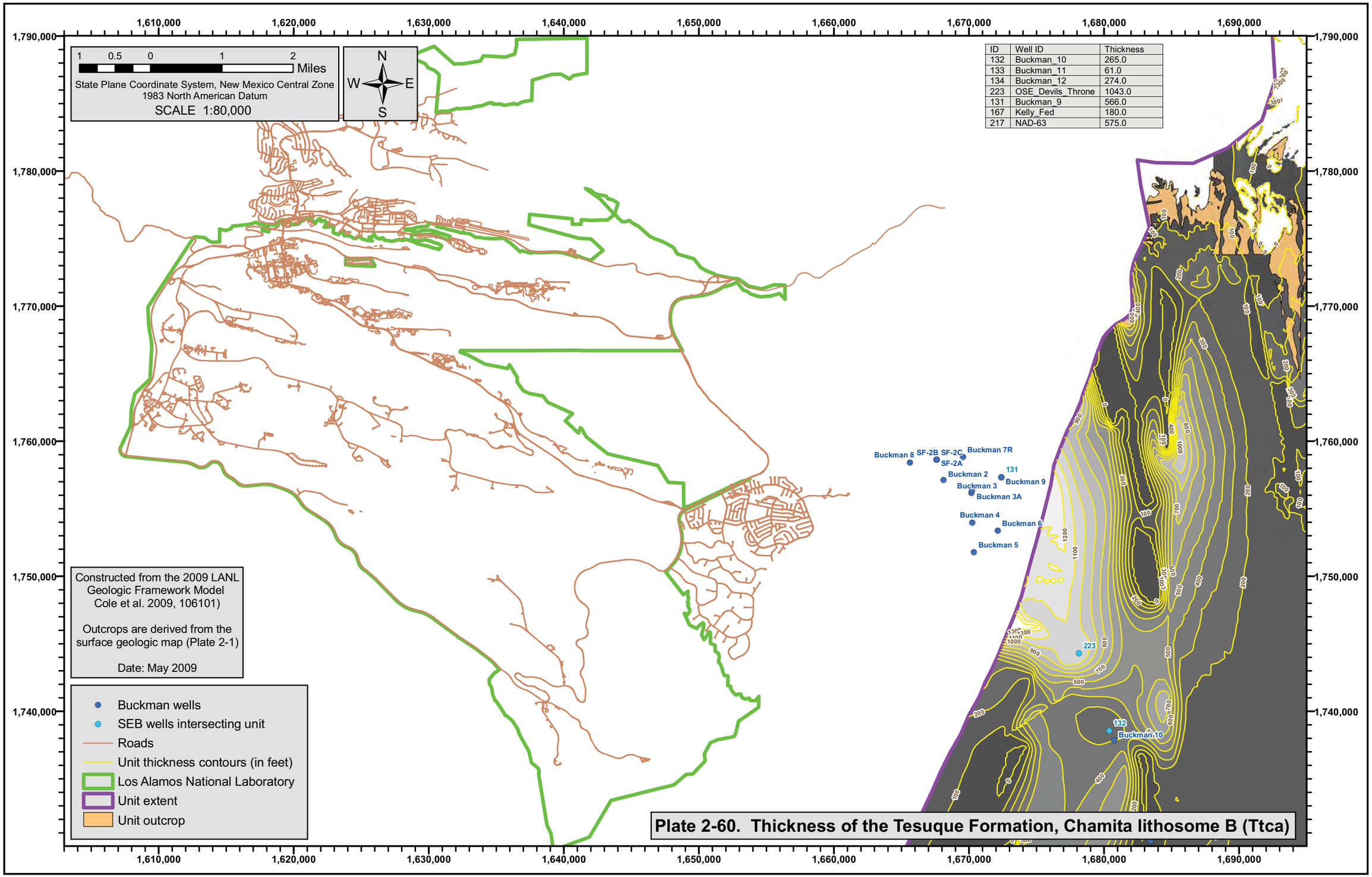


Plate 2-60. Thickness of the Tesuque Formation, Chamita lithosome B (Ttca)

1 0.5 0 1 2 Miles

State Plane Coordinate System, New Mexico Central Zone
1983 North American Datum
SCALE 1:80,000

N
W E
S

ID	Well ID	Elevation
131	Buckman_9	5162.0
132	Buckman_10	4800.0
133	Buckman_11	5450.0
134	Buckman_12	5362.0
167	Kelly_Fed	5845.0
217	NAD-63	5830.0
223	OSE_Devils_Throne	4867.0

Constructed from the 2009 LANL Geologic Framework Model (Cole et al. 2009, 106101)

Outcrops are derived from the surface geologic map (Plate 2-1)

Date: May 2009

- Buckman wells
- SEB wells intersecting unit
- Roads
- Bottom elevation contours (in feet)
- Los Alamos National Laboratory
- Unit extent
- Unit outcrop

Buckman 8 SF-2B SF-2C Buckman 7R SF-2A Buckman 2 131 Buckman 9 Buckman 3 Buckman 3A Buckman 4 Buckman 6 Buckman 5 223 132 Buckman 10

Plate 2-61. Structure contours of the bottom of the Tesuque Formation, Chamita lithosome B (Ttca)

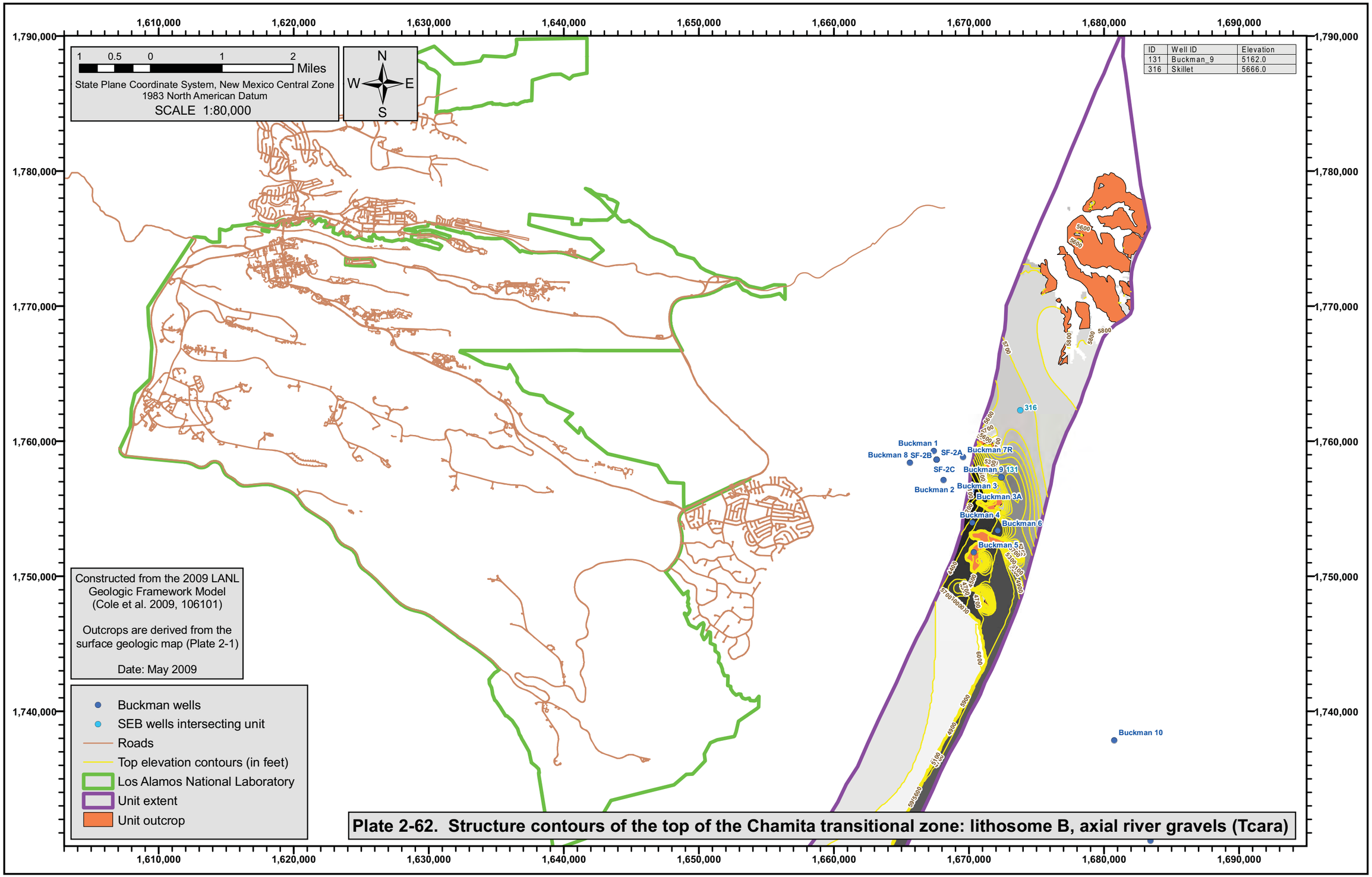


Plate 2-62. Structure contours of the top of the Chamita transitional zone: lithosome B, axial river gravels (Tcara)

1 0.5 0 1 2 Miles

State Plane Coordinate System, New Mexico Central Zone
1983 North American Datum
SCALE 1:80,000

N
W E
S

ID	Well ID	Thickness
131	Buckman_9	757.0
316	Skillet	1191.0

Constructed from the 2009 LANL Geologic Framework Model (Cole et al. 2009, 106101)

Outcrops are derived from the surface geologic map (Plate 2-1)

Date: May 2009

- Buckman wells
- SEB wells intersecting unit
- Roads
- Unit thickness contours (in feet)
- Los Alamos National Laboratory
- Unit extent
- Unit outcrop

Buckman 8, SF-2B, SF-2C, SF-2A, Buckman 7R, Buckman 2, 131, Buckman 9, Buckman 3, Buckman 3A, Buckman 4, Buckman 6, Buckman 5, 316, Buckman 10

Plate 2-63. Thickness of the Chamita transitional zone: lithosome B, axial river gravels (Tcara)

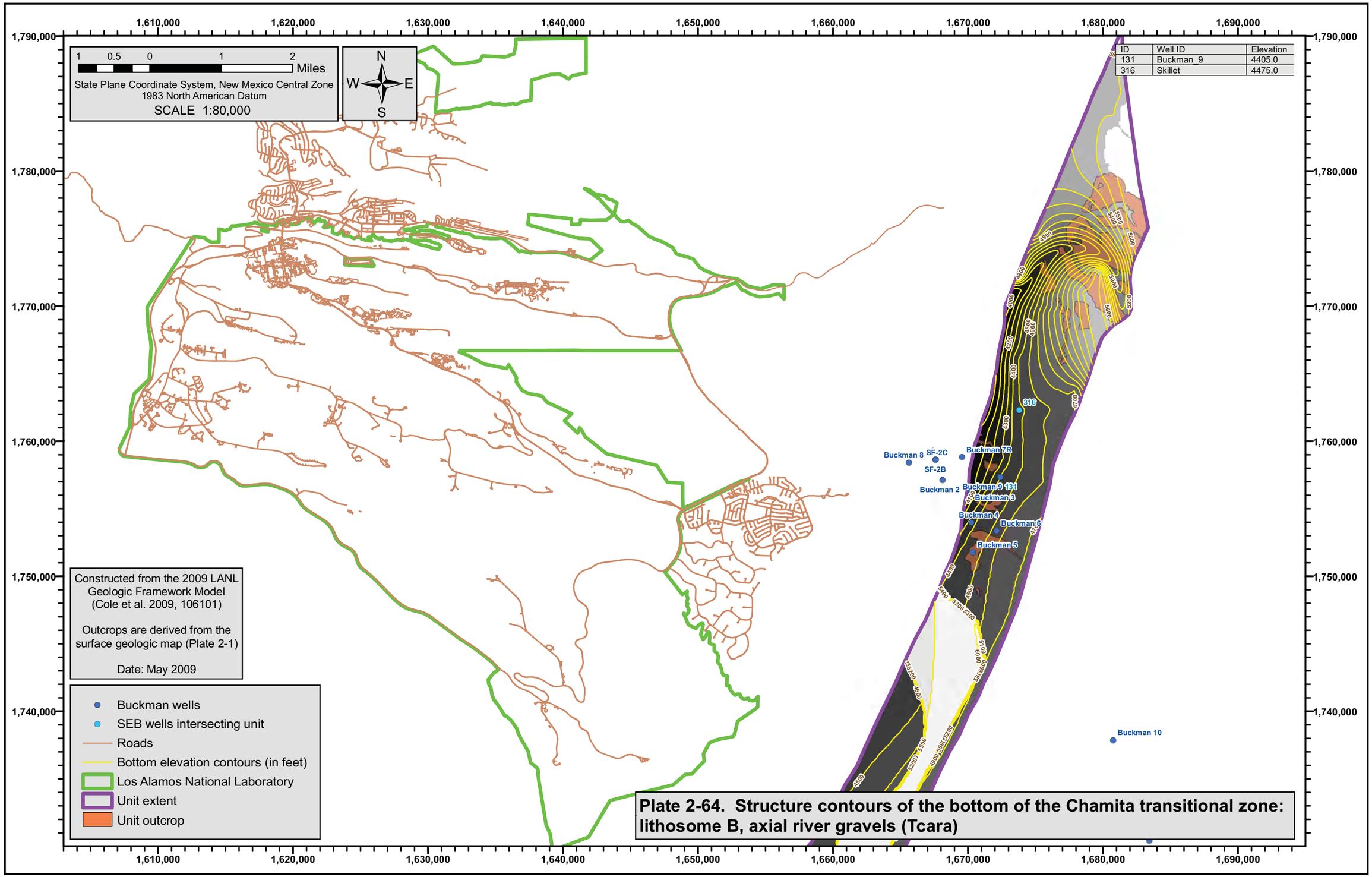


Plate 2-64. Structure contours of the bottom of the Chamita transitional zone: lithosome B, axial river gravels (Tcara)

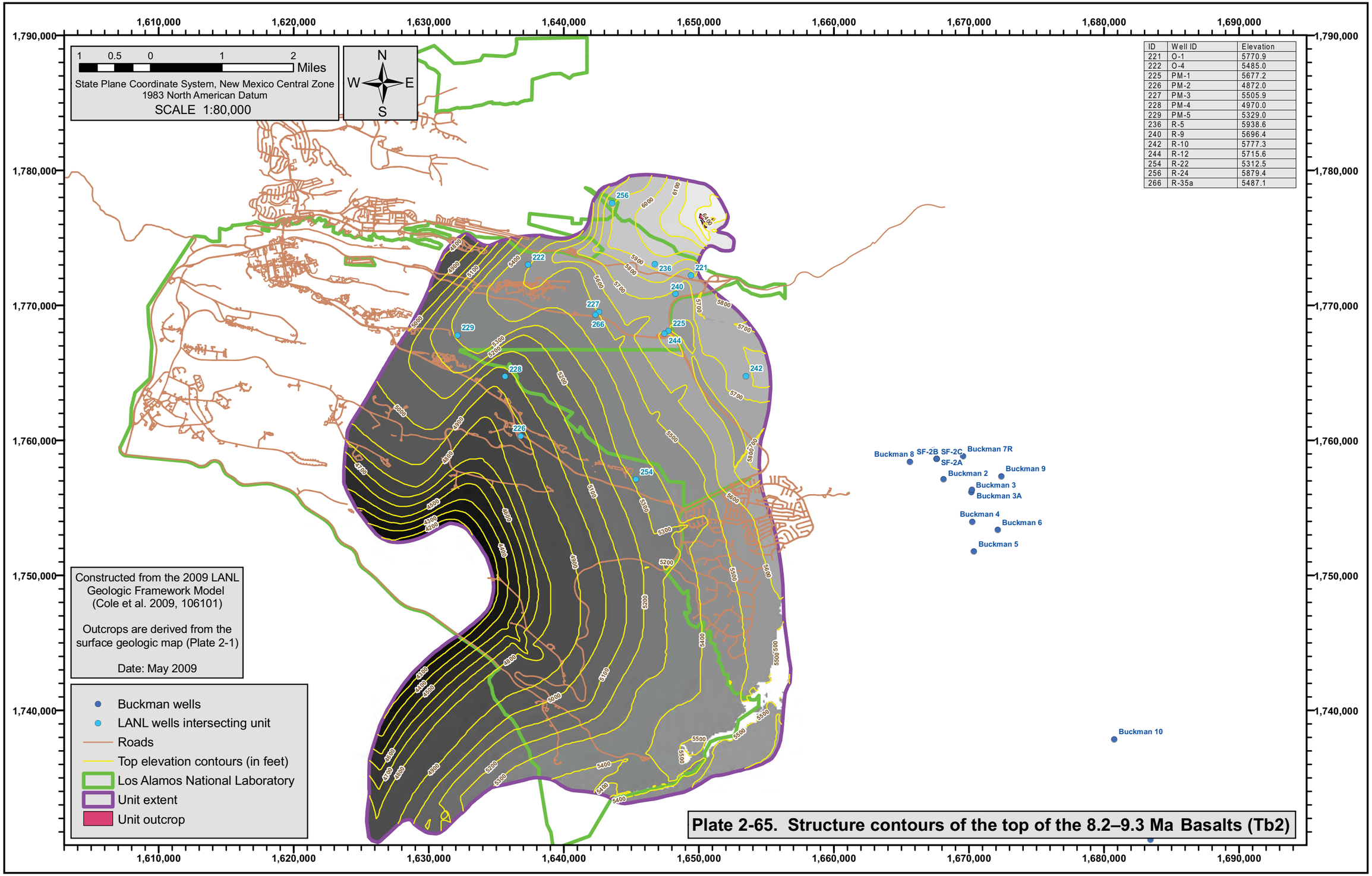


Plate 2-65. Structure contours of the top of the 8.2–9.3 Ma Basalts (Tb2)

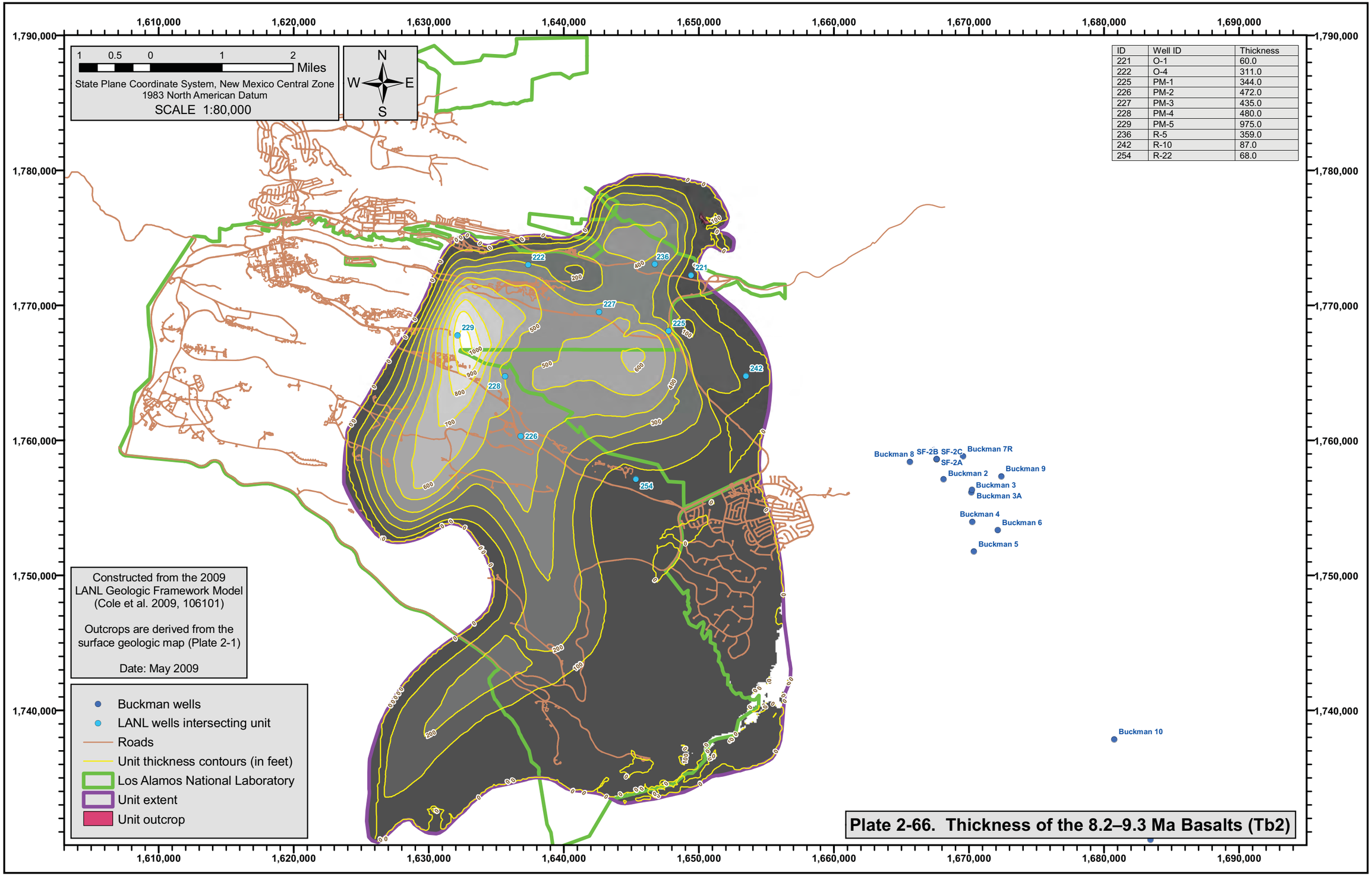


Plate 2-66. Thickness of the 8.2–9.3 Ma Basalts (Tb2)

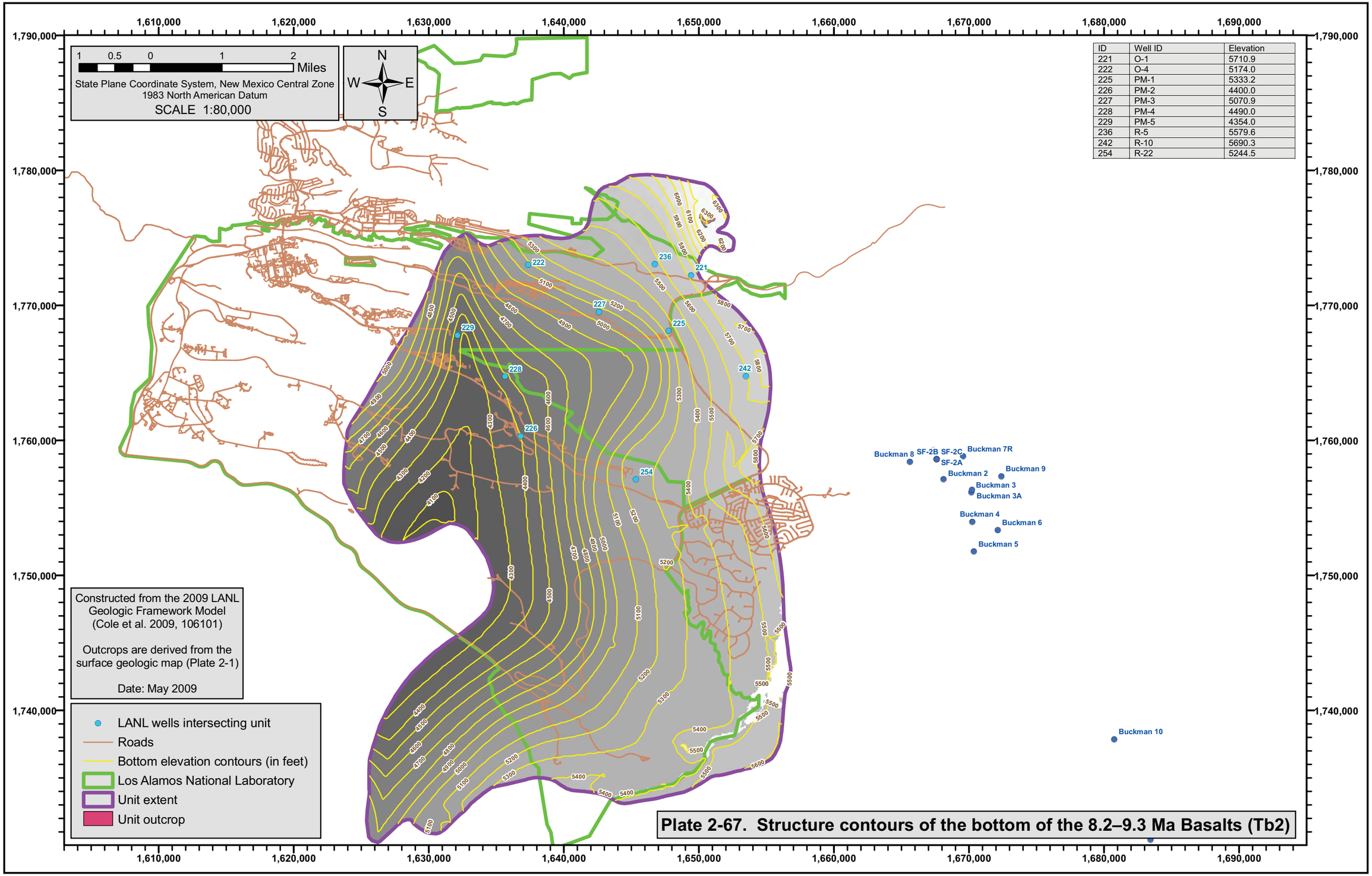


Plate 2-67. Structure contours of the bottom of the 8.2–9.3 Ma Basalts (Tb2)

1 0.5 0 1 2 Miles

State Plane Coordinate System, New Mexico Central Zone
1983 North American Datum
SCALE 1:80,000

N W E S

1,610,000 1,620,000 1,630,000 1,640,000 1,650,000 1,660,000 1,670,000 1,680,000 1,690,000

1,790,000 1,780,000 1,770,000 1,760,000 1,750,000 1,740,000

ID	Well ID	Elevation
149	DT-5A	5669.2
151	DT-9	5617.0
152	DT-10	5663.0
155	G-1	5954.9
156	G-1A	5956.9
157	G-2	6027.8
158	G-3	6080.8
159	G-4	6175.0
161	G-6	6294.4
162	GR-1	6246.2
163	GR-2	6060.2
164	GR-3	6162.2
172	LA-4	5807.9
221	O-1	5860.0
222	O-4	5957.0
225	PM-1	5738.2
226	PM-2	5396.0
227	PM-3	5865.9
228	PM-4	5592.9
229	PM-5	5632.0
233	R-2	5903.4
235	R-4	6127.5
236	R-5	6145.6
237	R-6	5899.8
239	R-8	5995.7
240	R-9	5843.8
242	R-10	5882.3
243	R-11	5774.4
244	R-12	5833.6
245	R-13	5605.1
247	R-15	5720.0
248	R-16	5528.9
252	R-20	5452.3
254	R-22	5477.5
255	R-23	5706.8
256	R-24	6242.4
264	R-33	5731.3
265	R-34	5952.0
266	R-35a	5743.1
267	R-36	6018.0
269	R-38	5805.0
273	R-42	5769.1
274	R-43	5825.0
275	R-44	5630.0
276	R-45	5657.0
315	Sigma_Mesa	5560.5
321	TW-1	5764.9
323	TW-2	5946.4
324	TW-3	5975.3
123	Buckman_1	5500.0
124	Buckman_2	5529.0
125	Buckman_3A	5609.0

Buckman 1 123
Buckman 8 130
SF-2C 124
Buckman 2 125
Buckman 3
Buckman 4 126
Buckman 9
128
Buckman 6
127
Buckman 5
129
220

Constructed from the 2009 LANL Geologic Framework Model (Cole et al. 2009, 106101)

Outcrops are derived from the surface geologic map (Plate 2-1)

Date: May 2009

- Buckman wells
- LANL/SEB wells intersecting unit
- Roads
- Top elevation contours (in feet)
- Los Alamos National Laboratory
- Unit extent
- Unit outcrop

Plate 2-68. Structure contours of the top of the Chamita Formation, axial river gravels (Tcar)

1 0.5 0 1 2 Miles

State Plane Coordinate System, New Mexico Central Zone
1983 North American Datum
SCALE 1:80,000

N W E S

ID	Well ID	Thickness
157	G-2	1637.8
158	G-3	1473.8
159	G-4	1480.0
161	G-6	1604.4
162	GR-1	1496.2
163	GR-2	1453.0
164	GR-3	1440.0
126	Buckman_4	1296.0
127	Buckman_5	1228.0
128	Buckman_6	1163.0
160	G-5	1616.6

Constructed from the 2009 LANL Geologic Framework Model (Cole et al. 2009, 106101)

Outcrops are derived from the surface geologic map (Plate 2-1)

Date: May 2009

- Buckman wells
- LANL/SEB wells intersecting unit
- Roads
- Unit thickness contours (in feet)
- Los Alamos National Laboratory
- Unit extent
- Unit outcrop

Plate 2-69. Thickness of the Chamita Formation, axial river gravels (Tcar)

1 0.5 0 1 2 Miles

State Plane Coordinate System, New Mexico Central Zone
1983 North American Datum
SCALE 1:80,000

N W E S

ID	Well ID	Elevation
126	Buckman_4	4340.0
127	Buckman_5	4452.0
128	Buckman_6	4545.0
157	G-2	4390.0
158	G-3	4607.0
159	G-4	4695.0
160	G-5	4685.0
161	G-6	4690.0
162	GR-1	4750.0
163	GR-2	4607.2
164	GR-3	4722.2
165	GR-4	4681.2
169	LA-1B	4010.0
174	LA-6	3950.0

Constructed from the 2009 LANL Geologic Framework Model (Cole et al. 2009, 106101)

Outcrops are derived from the surface geologic map (Plate 2-1)

Date: May 2009

- Buckman wells
- LANL/SEB wells intersecting unit
- Roads
- Bottom elevation contours (in feet)
- Los Alamos National Laboratory
- Unit extent
- Unit outcrop

Plate 2-70. Structure contours of the bottom of the Chamita Formation, axial river gravels (Tcar)

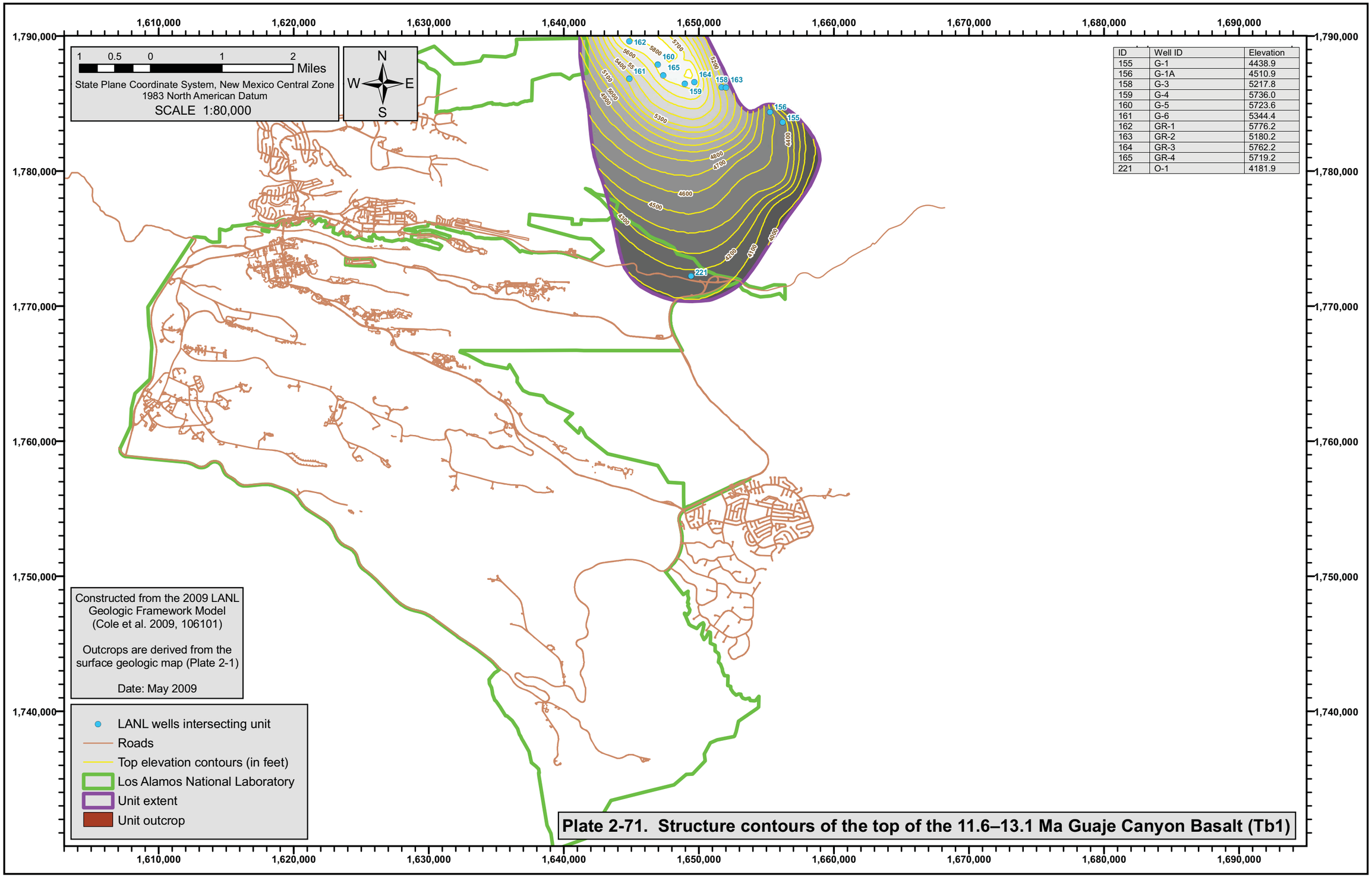


Plate 2-71. Structure contours of the top of the 11.6–13.1 Ma Guaje Canyon Basalt (Tb1)

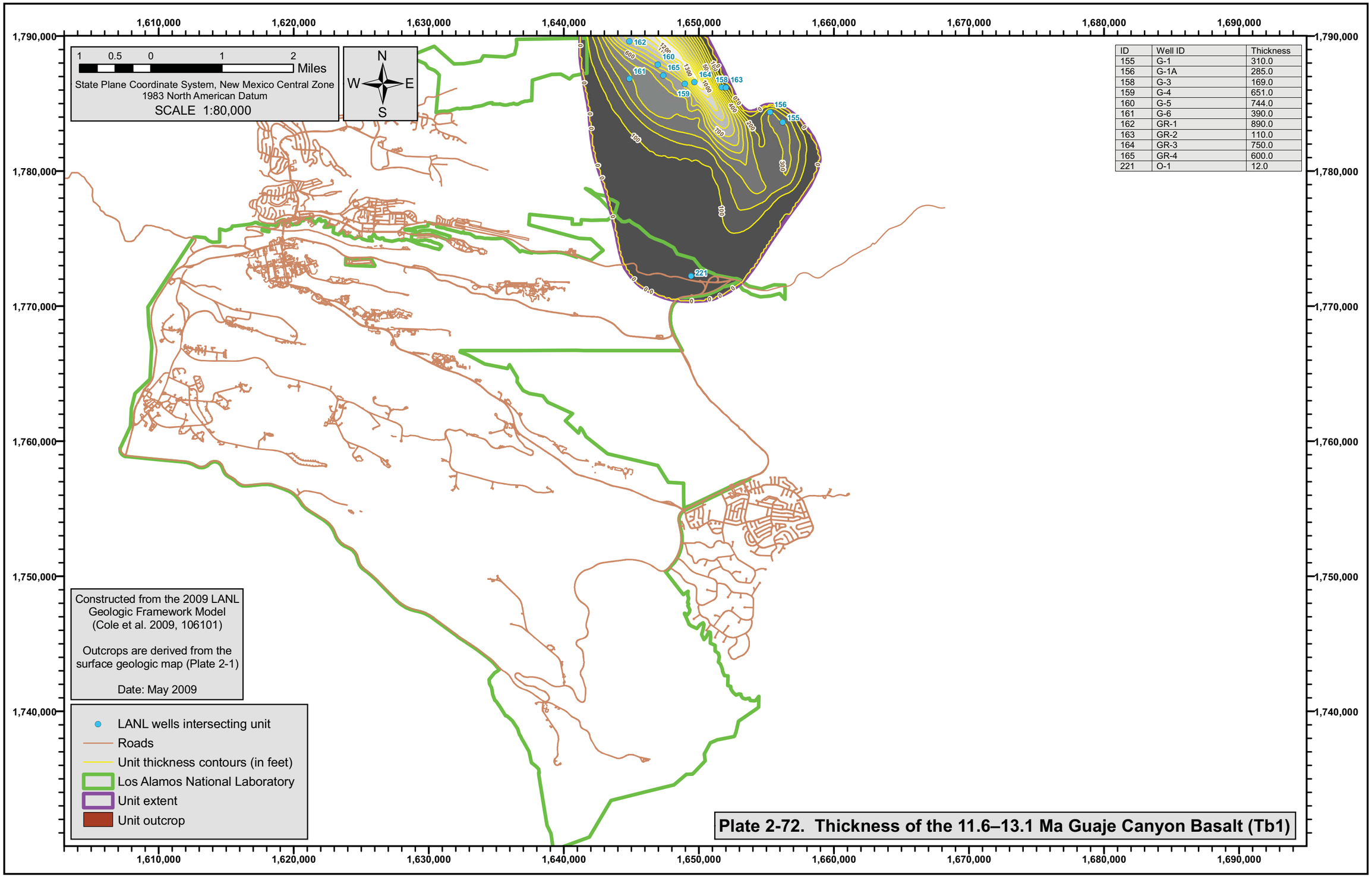


Plate 2-72. Thickness of the 11.6–13.1 Ma Guaje Canyon Basalt (Tb1)

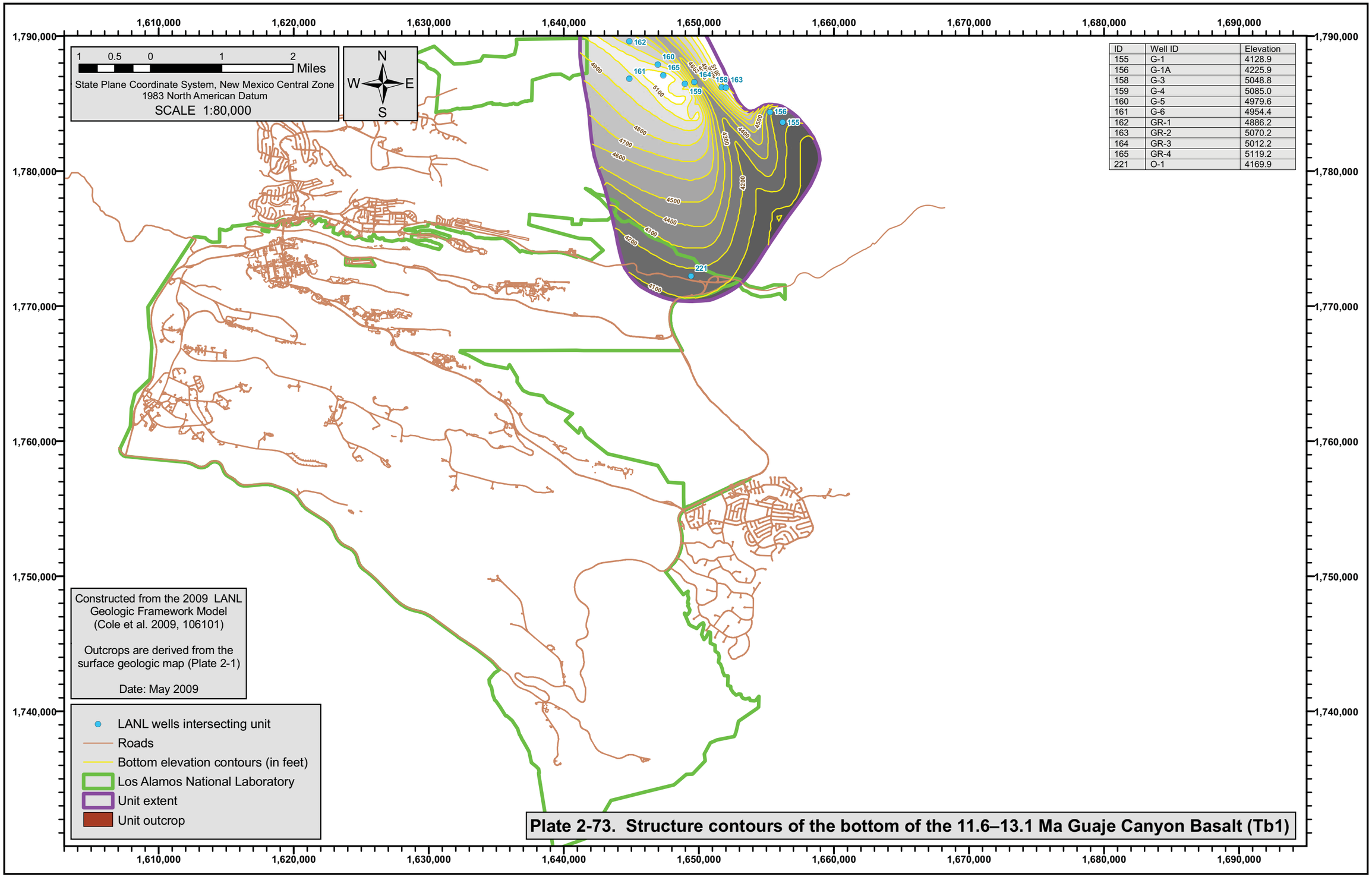


Plate 2-73. Structure contours of the bottom of the 11.6–13.1 Ma Guaje Canyon Basalt (Tb1)

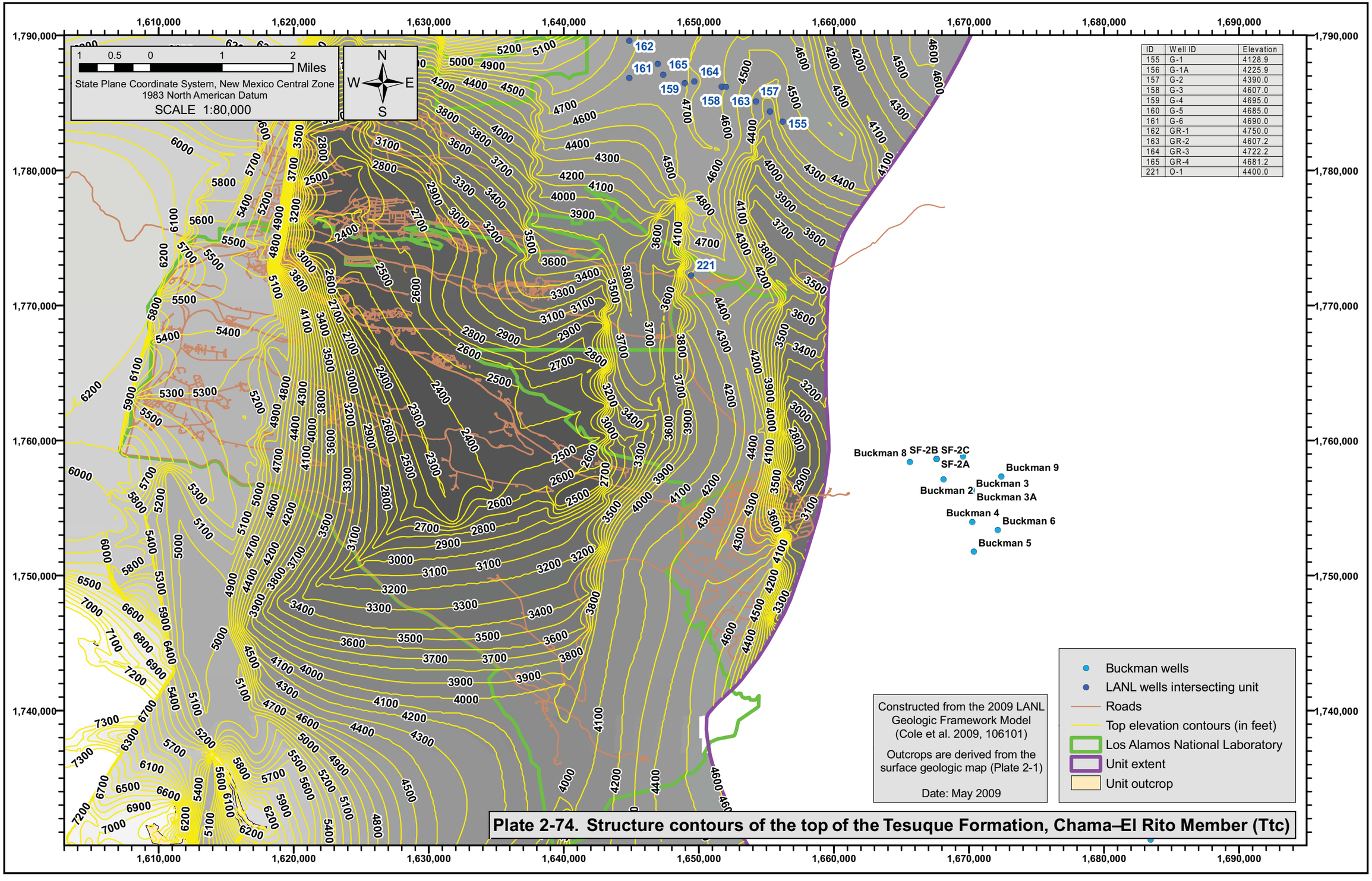


Plate 2-74. Structure contours of the top of the Tesuque Formation, Chama–El Rito Member (Ttc)

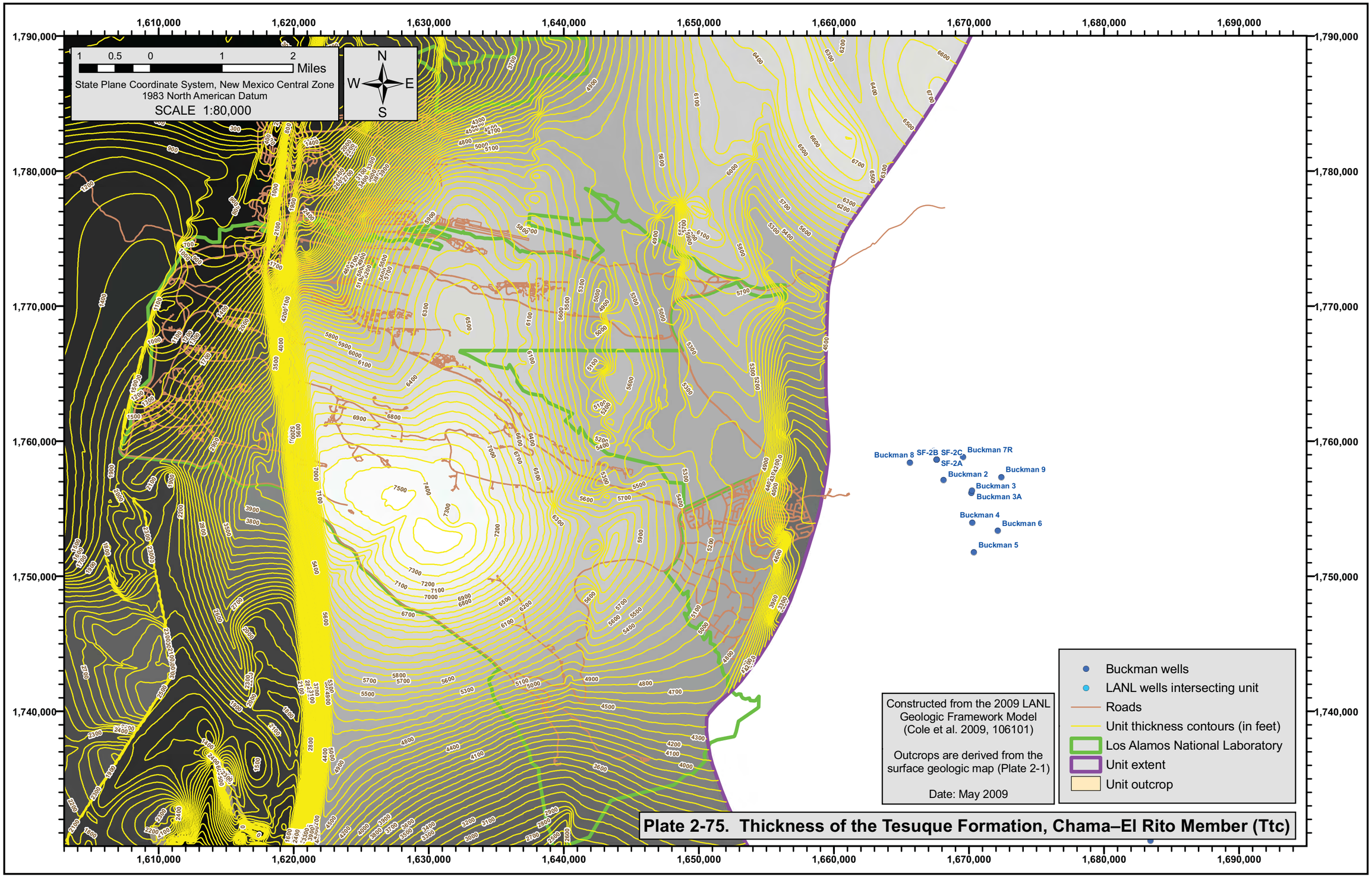


Plate 2-75. Thickness of the Tesuque Formation, Chama–El Rito Member (Ttc)

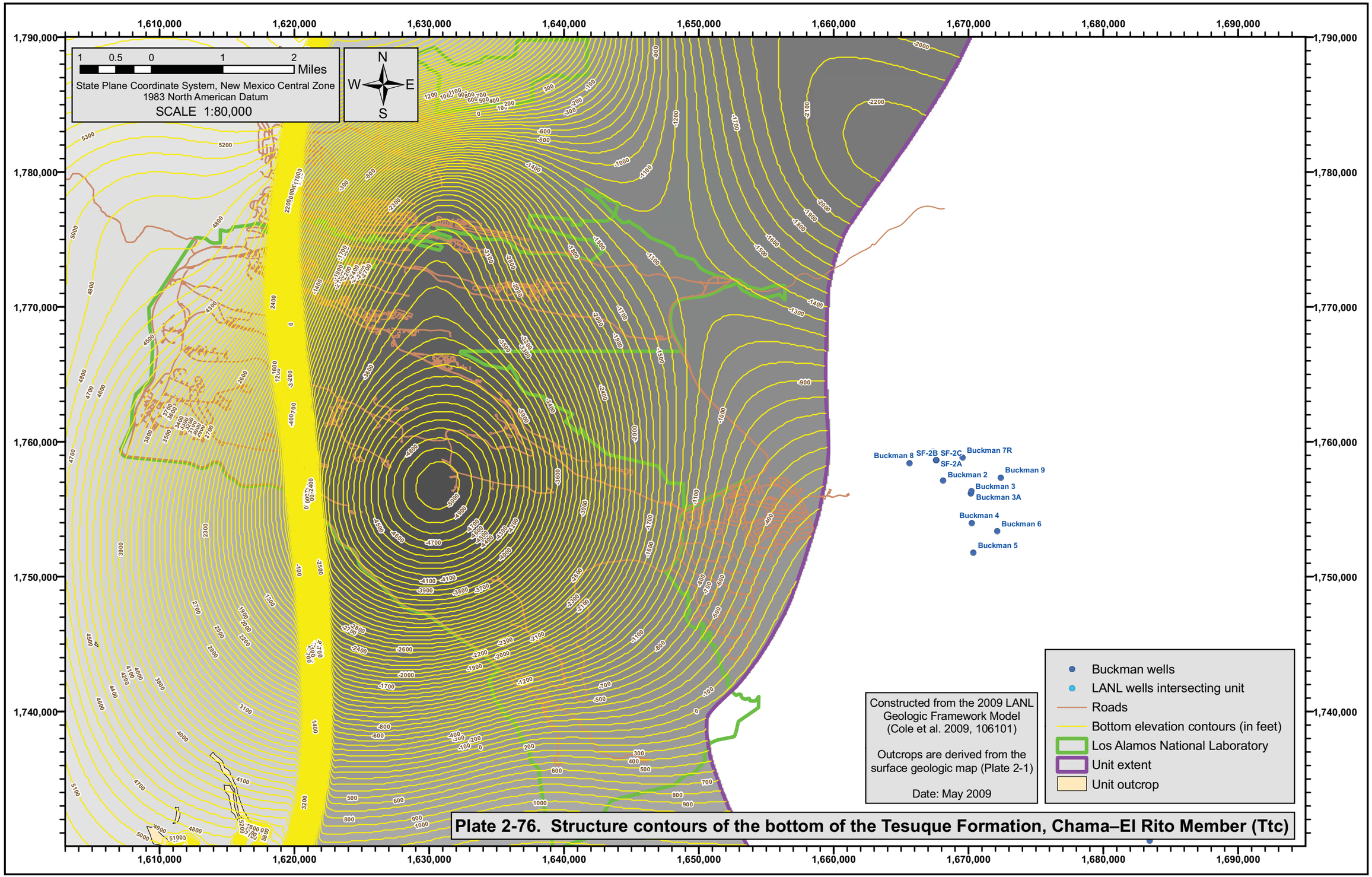


Plate 2-76. Structure contours of the bottom of the Tesuque Formation, Chama–El Rito Member (Ttc)

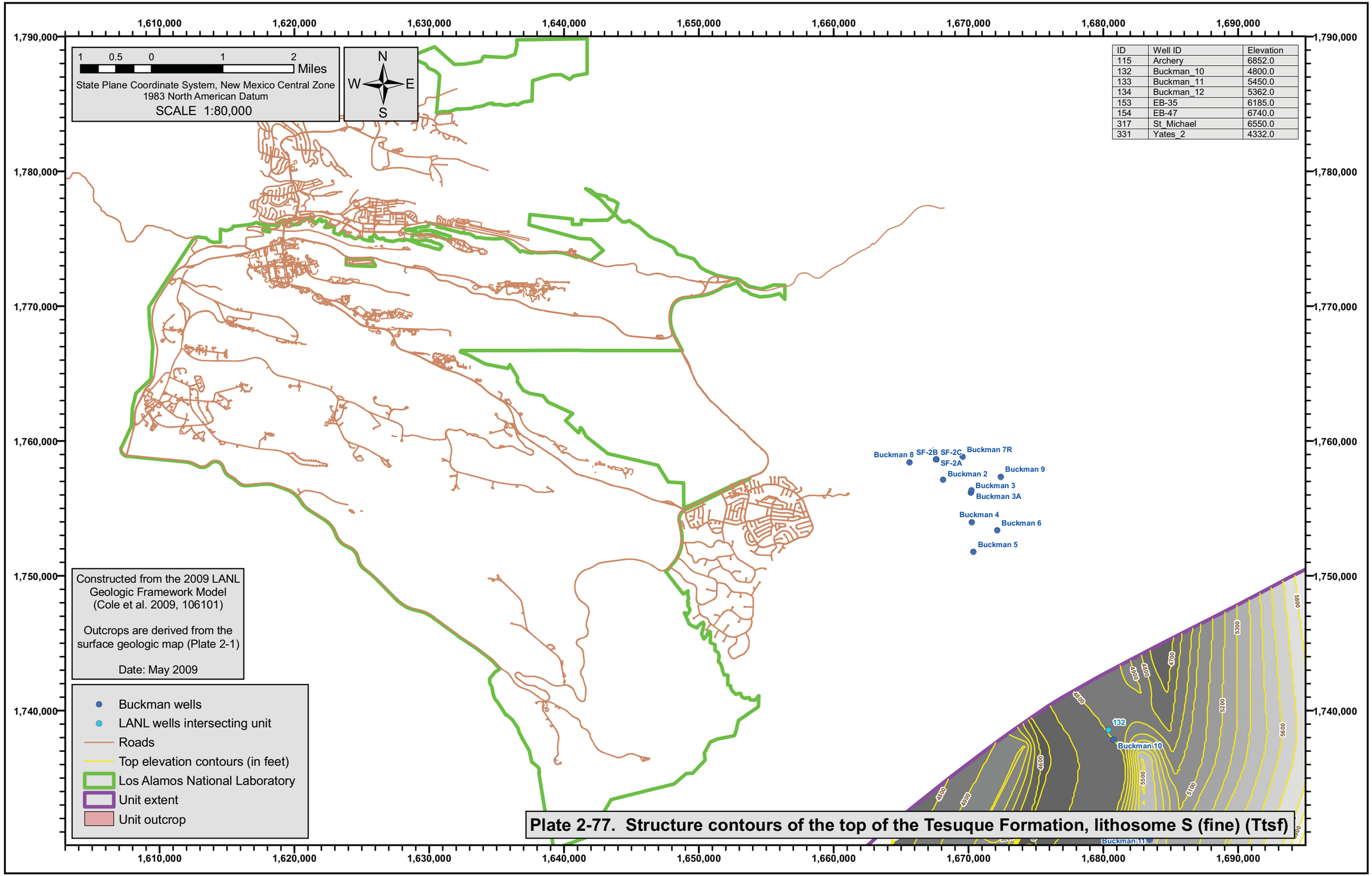


Plate 2-77. Structure contours of the top of the Tesuque Formation, lithosome S (fine) (Ttsf)

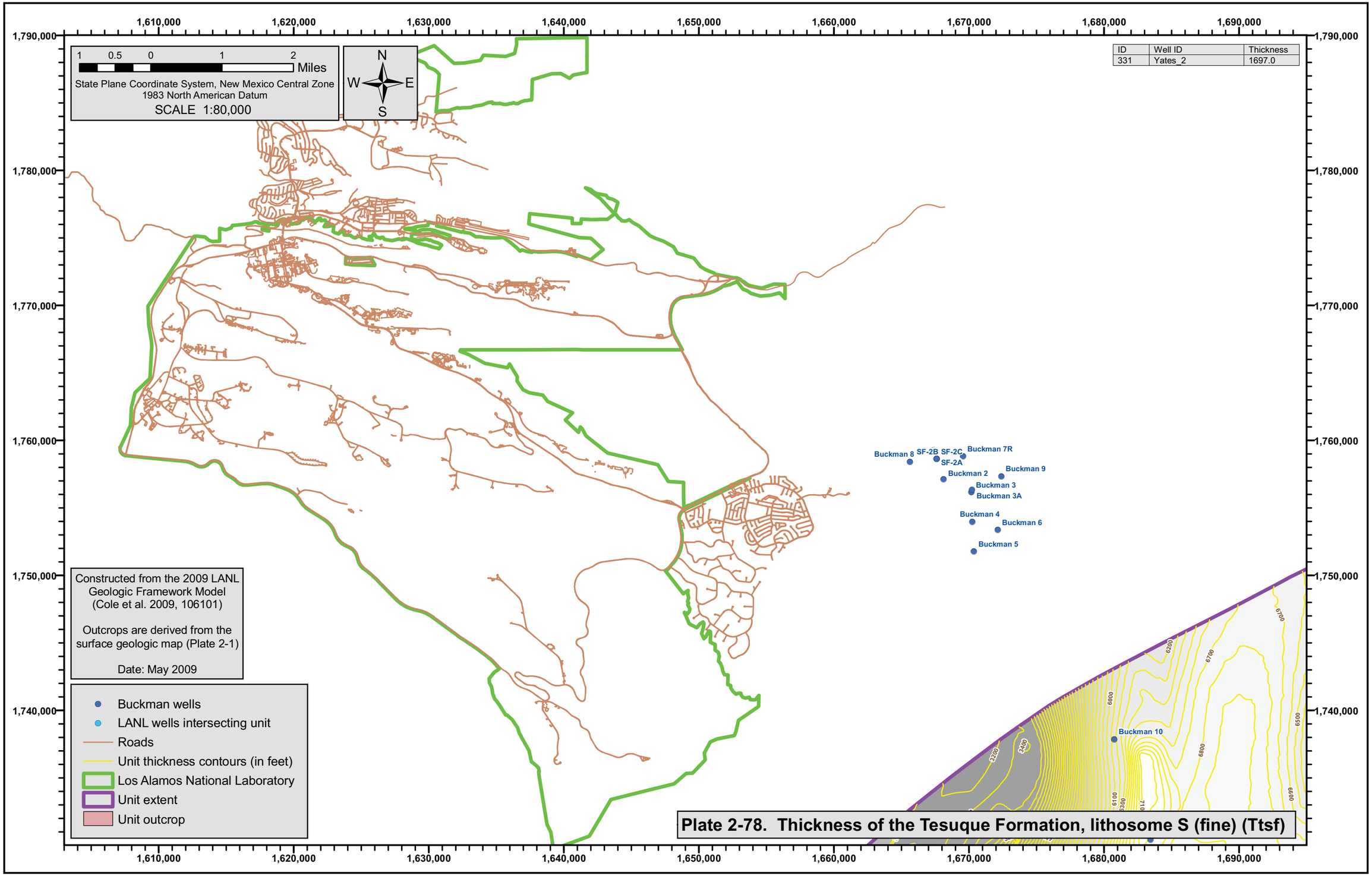


Plate 2-78. Thickness of the Tesuque Formation, lithosome S (fine) (Ttsf)

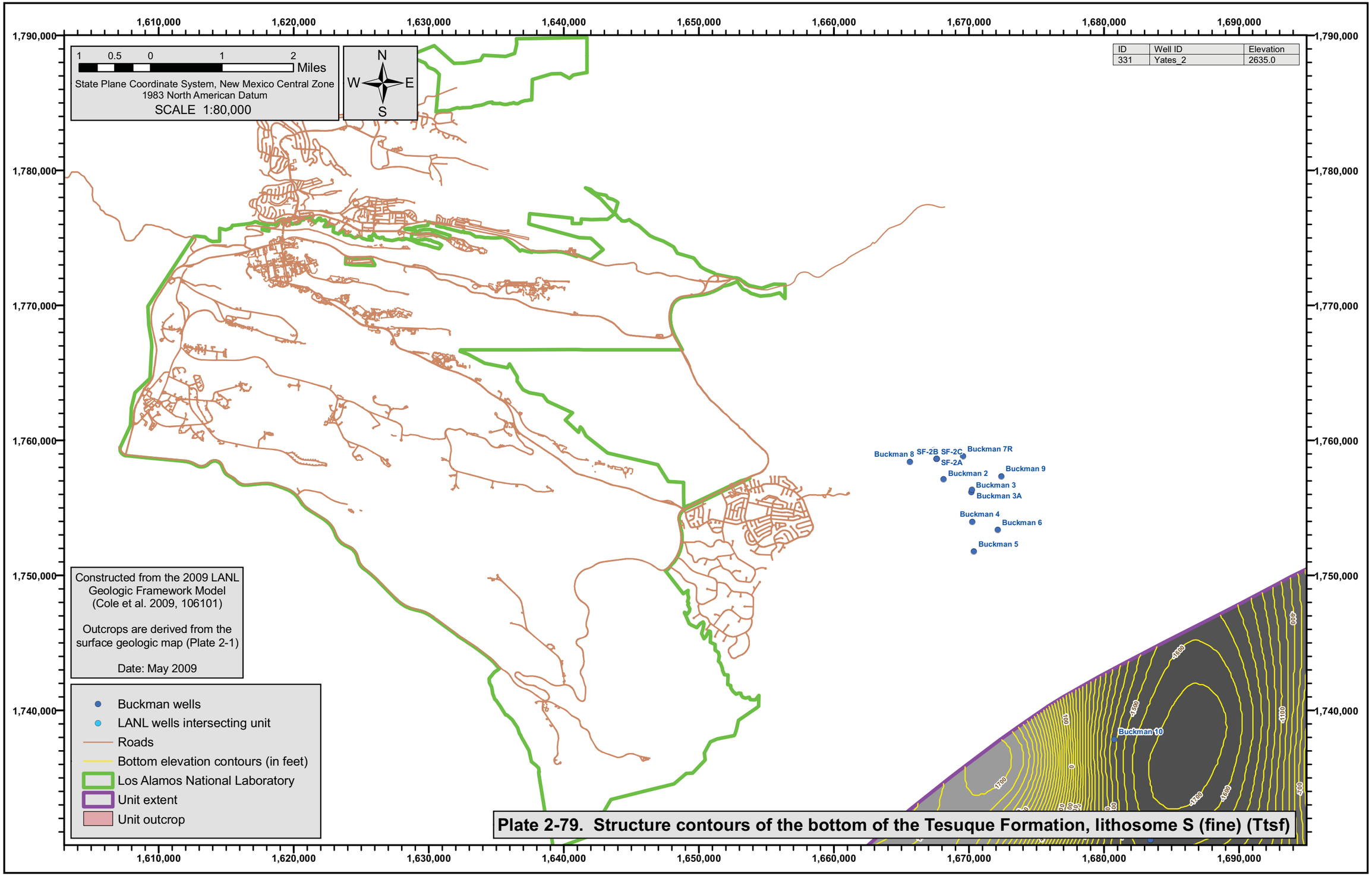


Plate 2-79. Structure contours of the bottom of the Tesuque Formation, lithosome S (fine) (Ttsf)

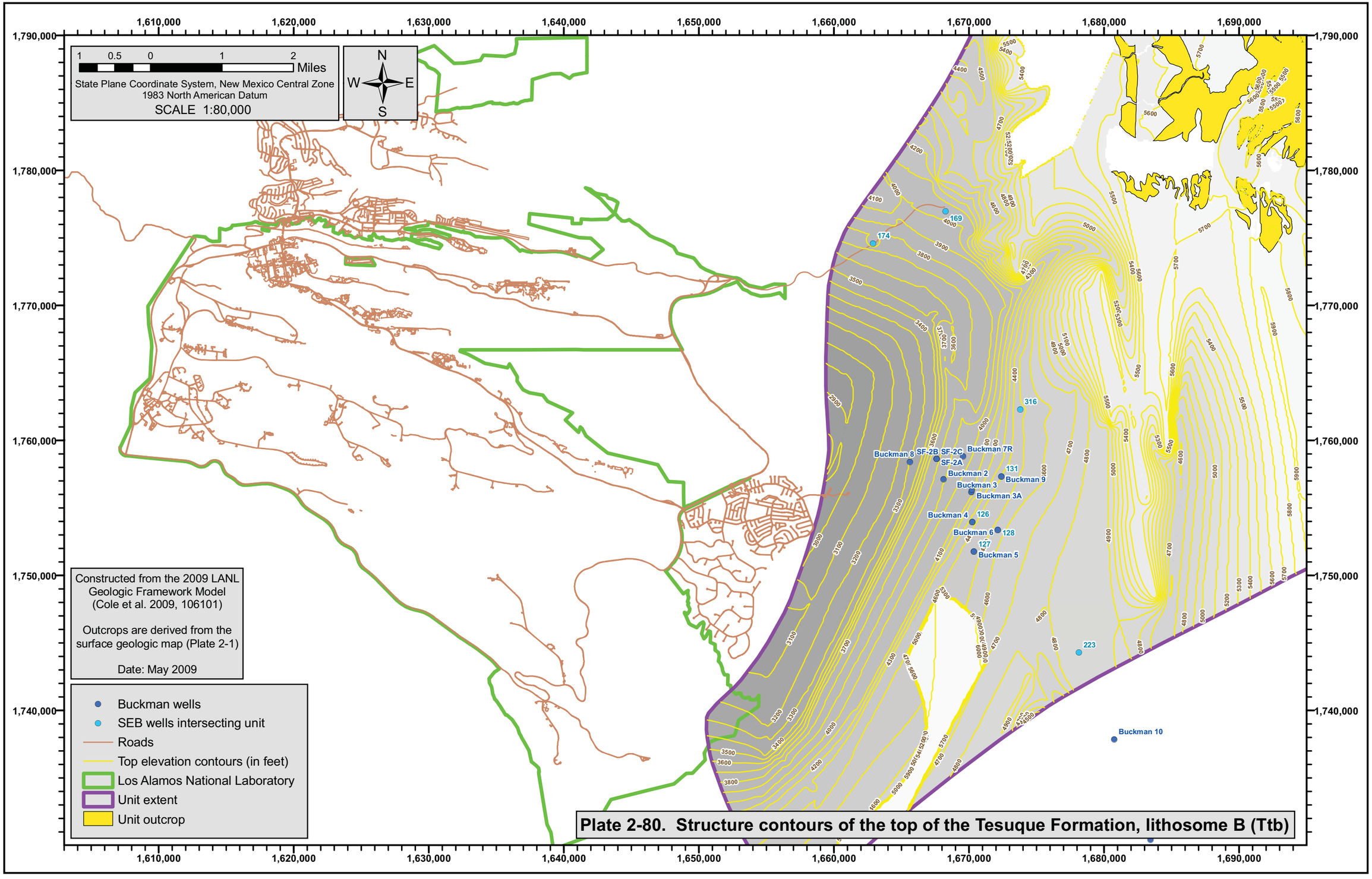


Plate 2-80. Structure contours of the top of the Tesuque Formation, lithosome B (Ttb)

1 0.5 0 1 2 Miles

State Plane Coordinate System, New Mexico Central Zone
1983 North American Datum
SCALE 1:80,000

N W E S

1,610,000 1,620,000 1,630,000 1,640,000 1,650,000 1,660,000 1,670,000 1,680,000 1,690,000

1,790,000 1,780,000 1,770,000 1,760,000 1,750,000 1,740,000

Buckman 8 SF-2B SF-2C Buckman 7R SF-2A Buckman 9 Buckman 2 Buckman 3 Buckman 3A Buckman 4 Buckman 6 Buckman 5 Buckman 10

Constructed from the 2009 LANL Geologic Framework Model (Cole et al. 2009, 106101)

Outcrops are derived from the surface geologic map (Plate 2-1)

Date: May 2009

- Buckman wells
- LANL wells intersecting unit
- Roads
- Unit thickness contours (in feet)
- Los Alamos National Laboratory
- Unit extent
- Unit outcrop

Plate 2-81. Thickness of the Tesuque Formation, lithosome B (Ttb)

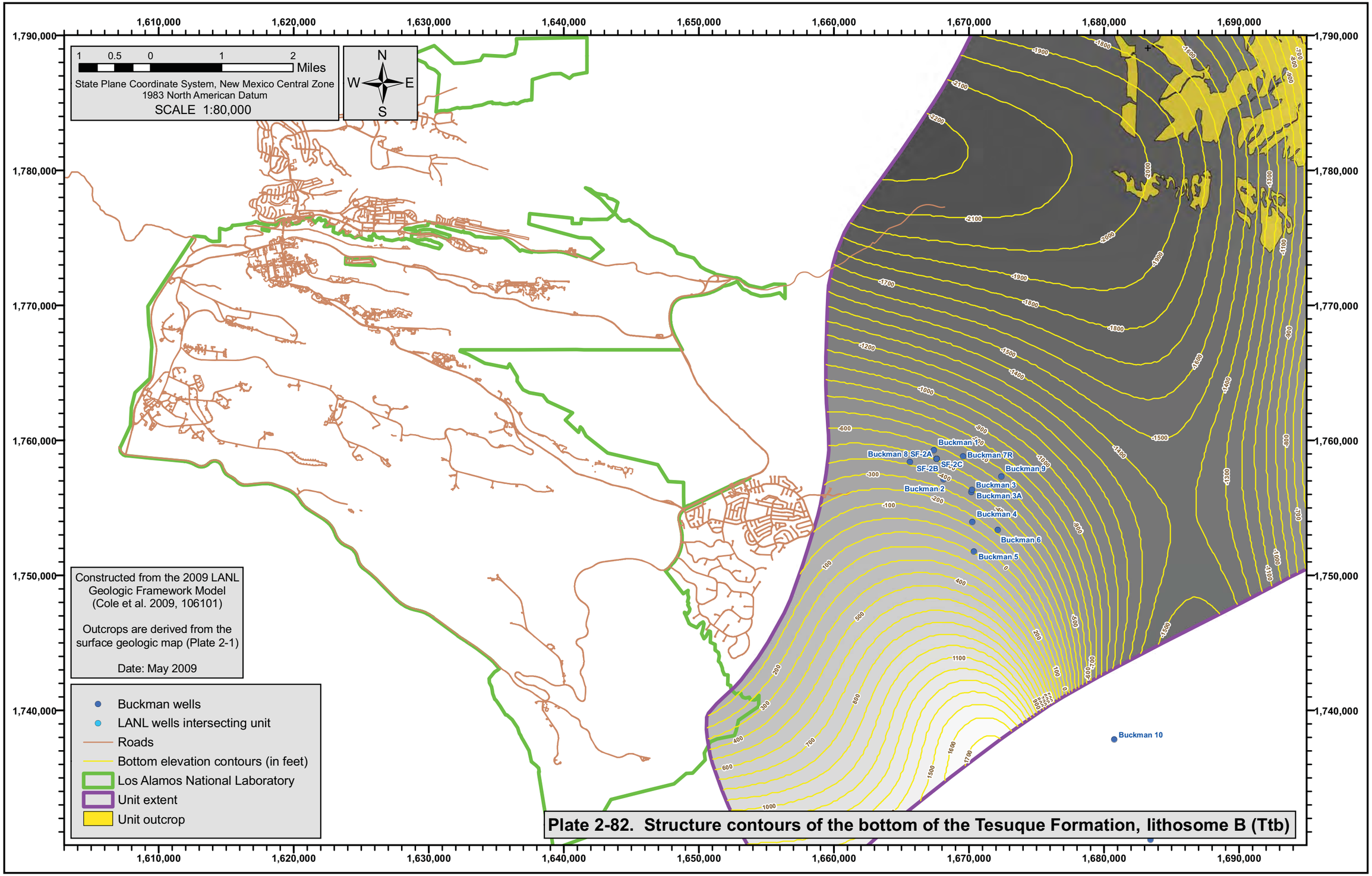


Plate 2-82. Structure contours of the bottom of the Tesuque Formation, lithosome B (Ttb)

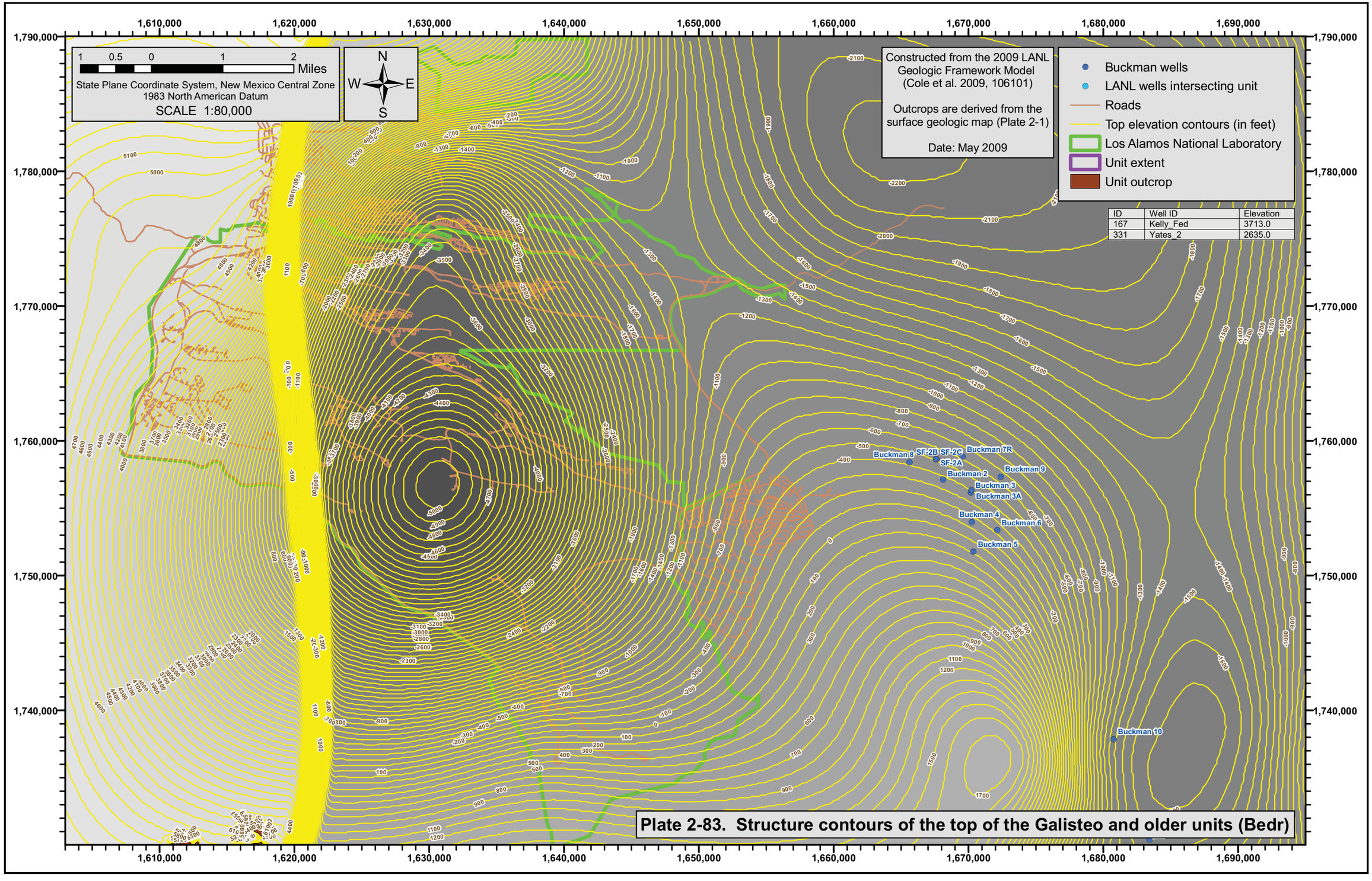
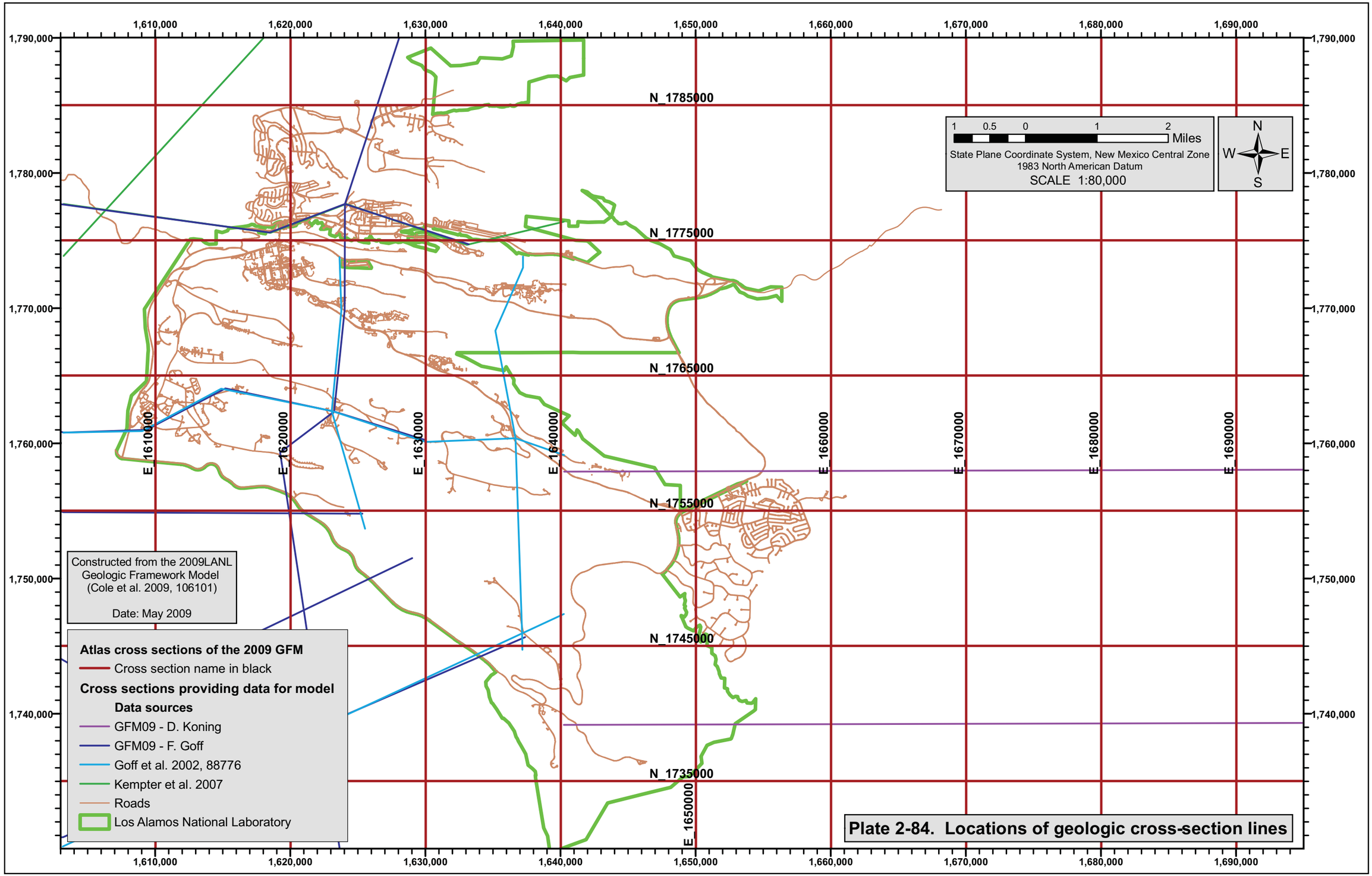
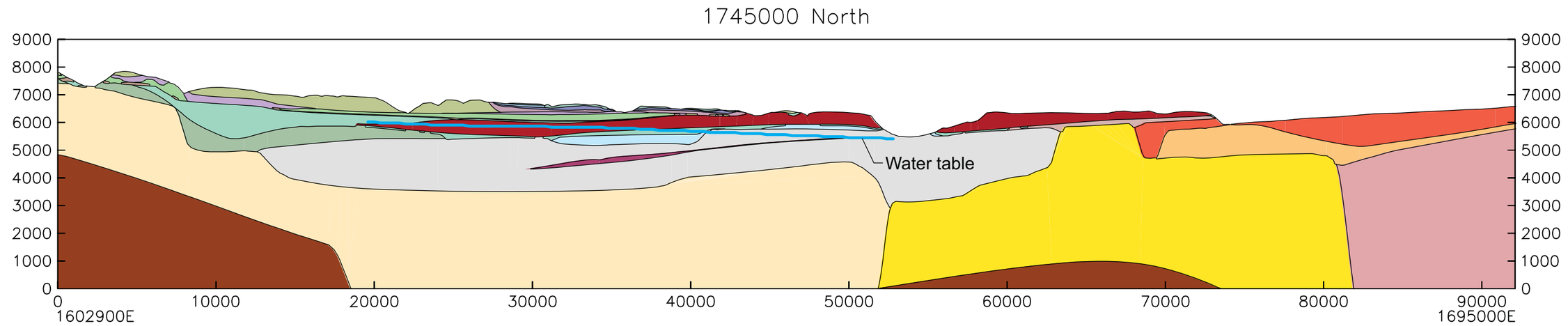
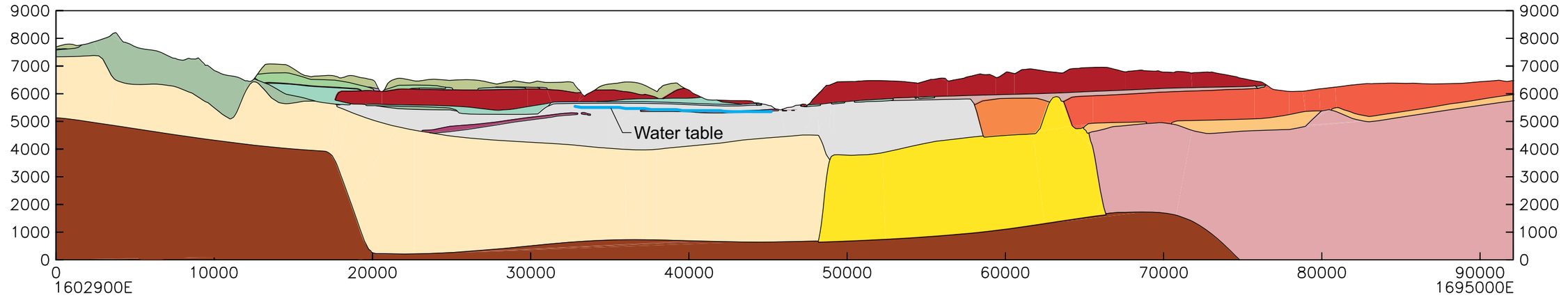
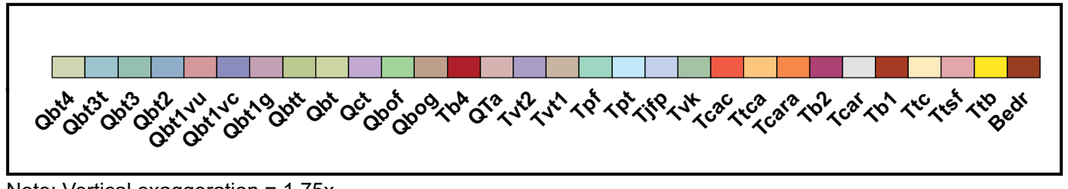


Plate 2-83. Structure contours of the top of the Galisteo and older units (Bedr)


1,610,000
1,620,000
1,630,000
1,640,000
1,650,000
1,660,000
1,670,000
1,680,000
1,690,000
1,790,000
1,780,000
1,770,000
1,760,000
1,750,000
1,740,000
N_1785000
N_1775000
N_1765000
N_1755000
N_1745000
N_1735000
E_1610000
E_1620000
E_1630000
E_1640000
E_1650000
E_1660000
E_1670000
E_1680000
E_1690000
1 0.5 0 1 2 Miles
State Plane Coordinate System, New Mexico Central Zone
1983 North American Datum
SCALE 1:80,000
N
W E
S
Constructed from the 2009LANL Geologic Framework Model (Cole et al. 2009, 106101)
Date: May 2009
Atlas cross sections of the 2009 GFM
Cross section name in black
Cross sections providing data for model
Data sources
GFM09 - D. Koning
GFM09 - F. Goff
Goff et al. 2002, 88776
Kempter et al. 2007
Roads
Los Alamos National Laboratory
Plate 2-84. Locations of geologic cross-section lines



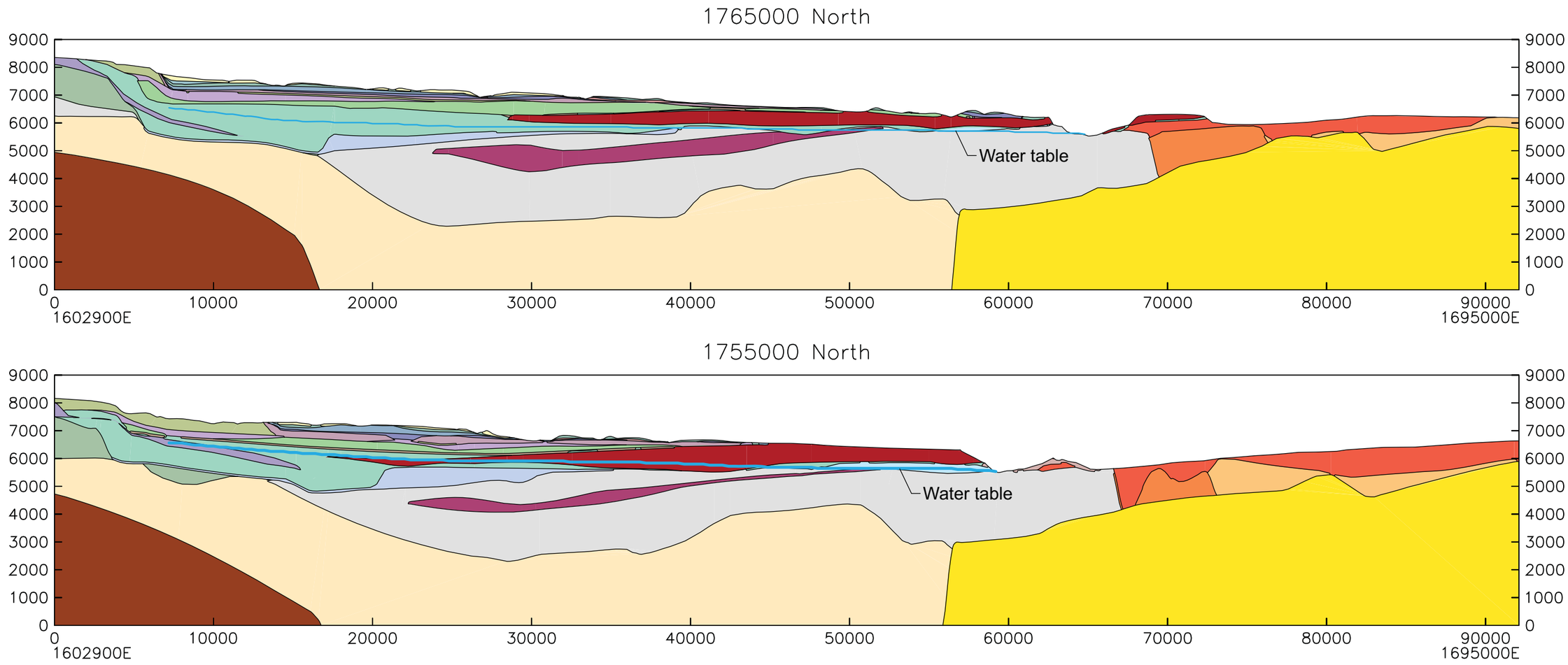




Note: Vertical exaggeration = 1.75x.

Constructed from the 2009 LANL Geologic Framework Model (Cole et al. 2009, 106101) Date: May 2009

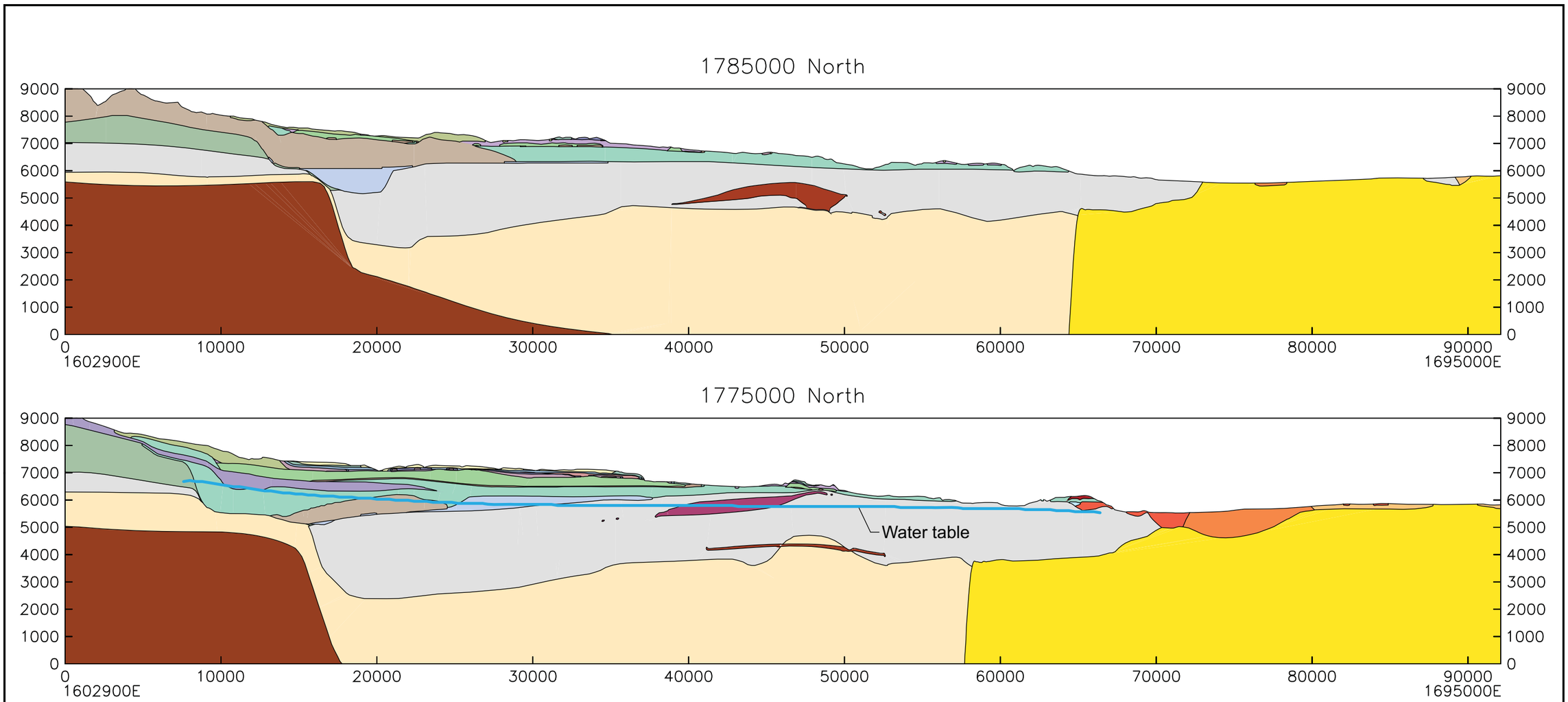
Plate 2-85. Southern east-west cross-sections (N_1735000, N_1745000)



Note: Vertical exaggeration = 1.75x.

Constructed from the 2009 LANL Geologic Framework Model (Cole et al. 2009, 106101) Date: May 2009

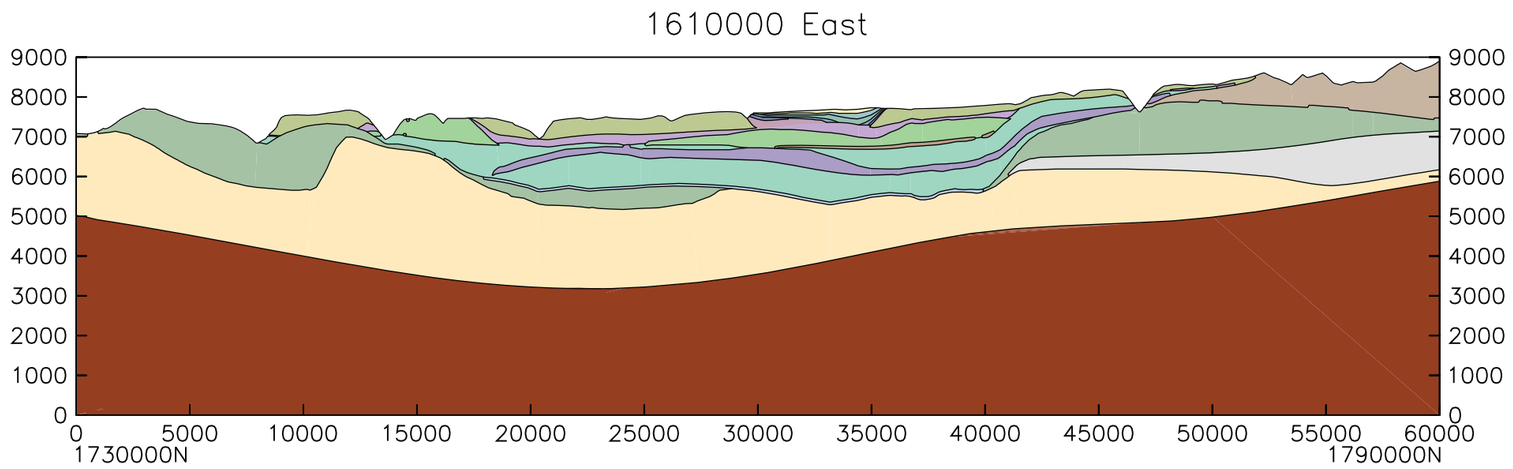
Plate 2-86. Central east-west cross-sections (N_1755000, N_1765000)

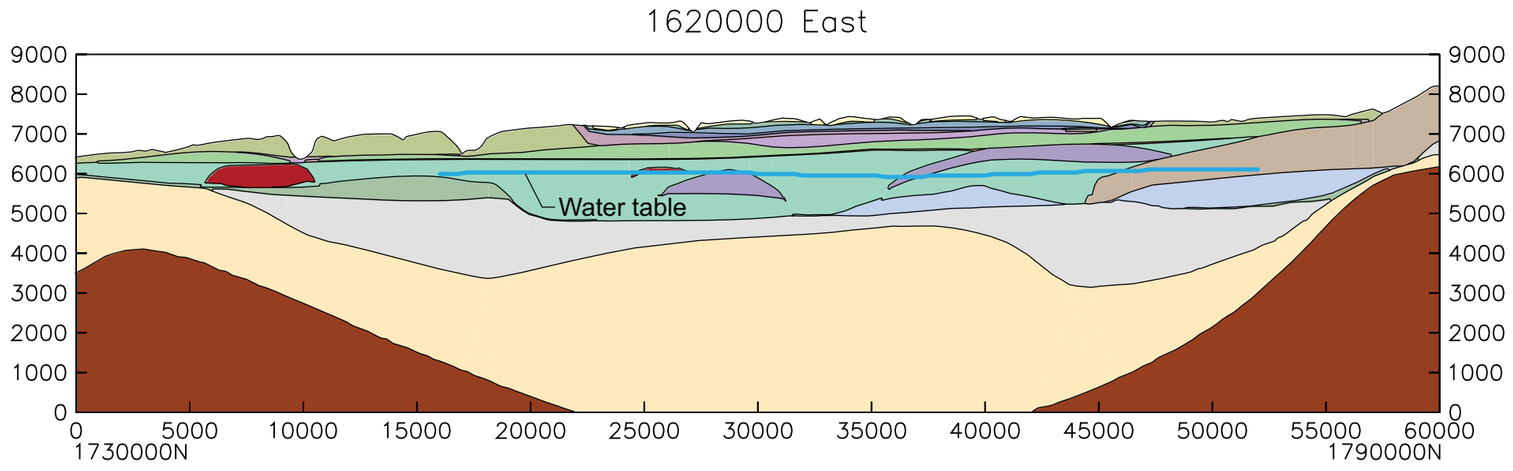


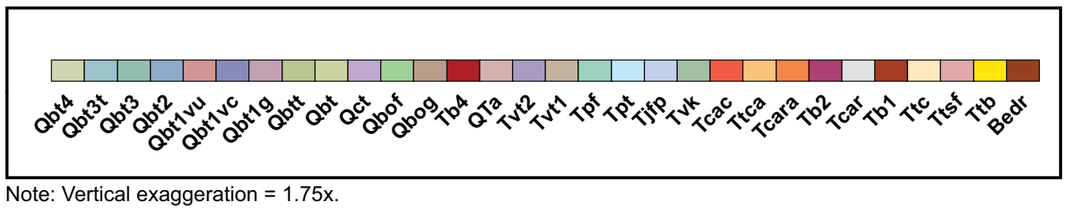
Note: Vertical exaggeration = 1.75x.

Constructed from the 2009 LANL Geologic Framework Model (Cole et al. 2009, 106101) Date: May 2009

Plate 2-87. Northern east-west cross-sections (N_1775000, N_1785000)



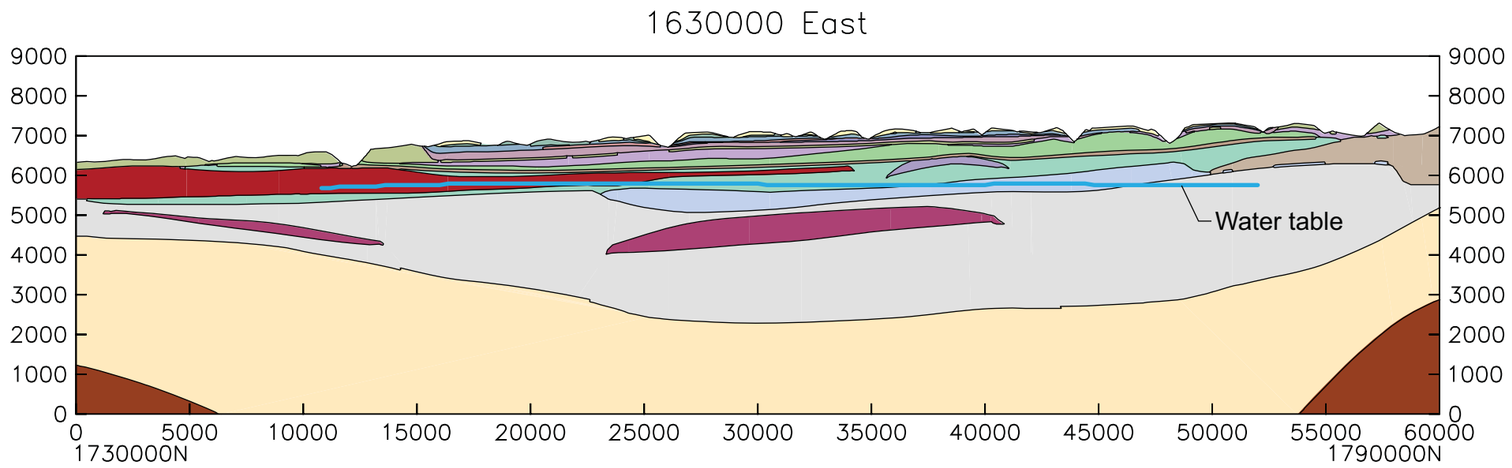


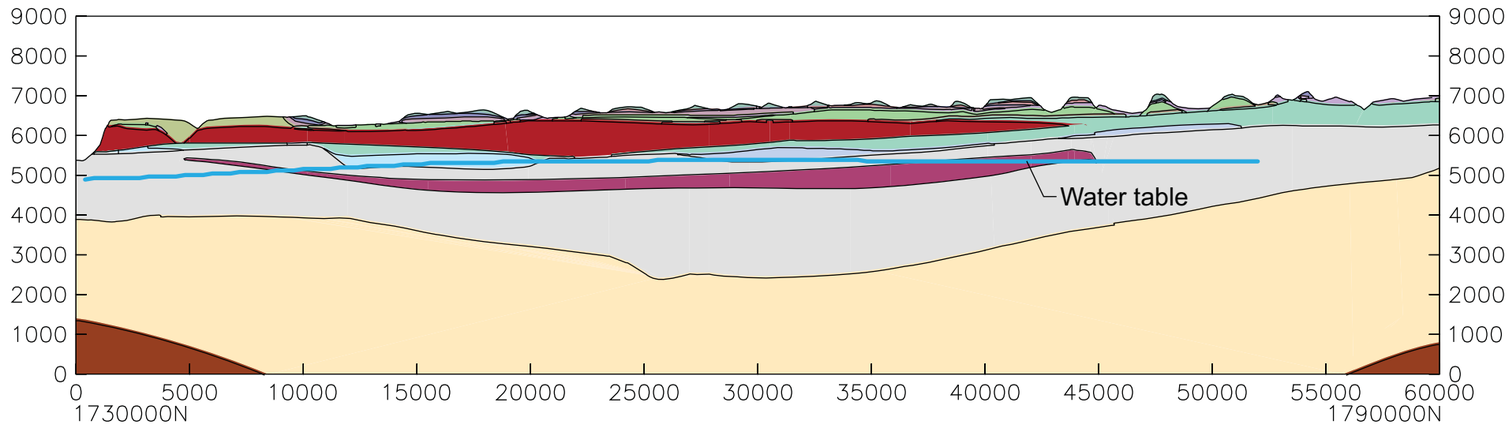


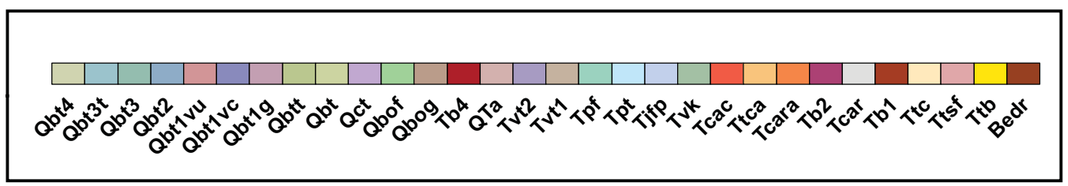
Note: Vertical exaggeration = 1.75x.

Constructed from the 2009 LANL Geologic Framework Model (Cole et al. 2009, 106101) Date: May 2009

Plate 2-88. Western north-south cross-sections (E_1610000, E_1620000)



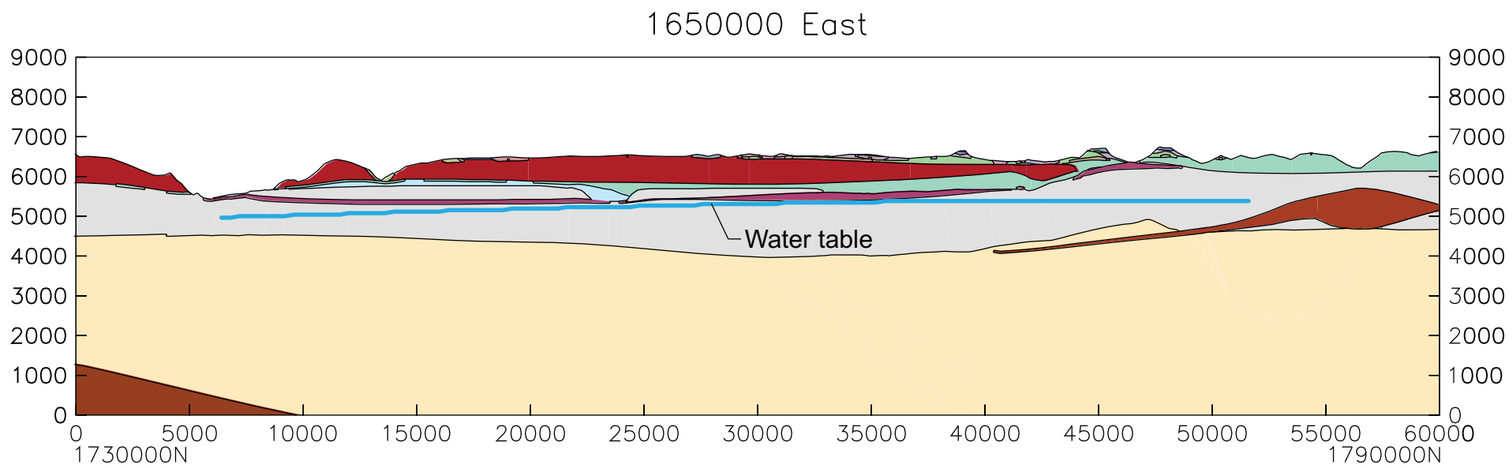


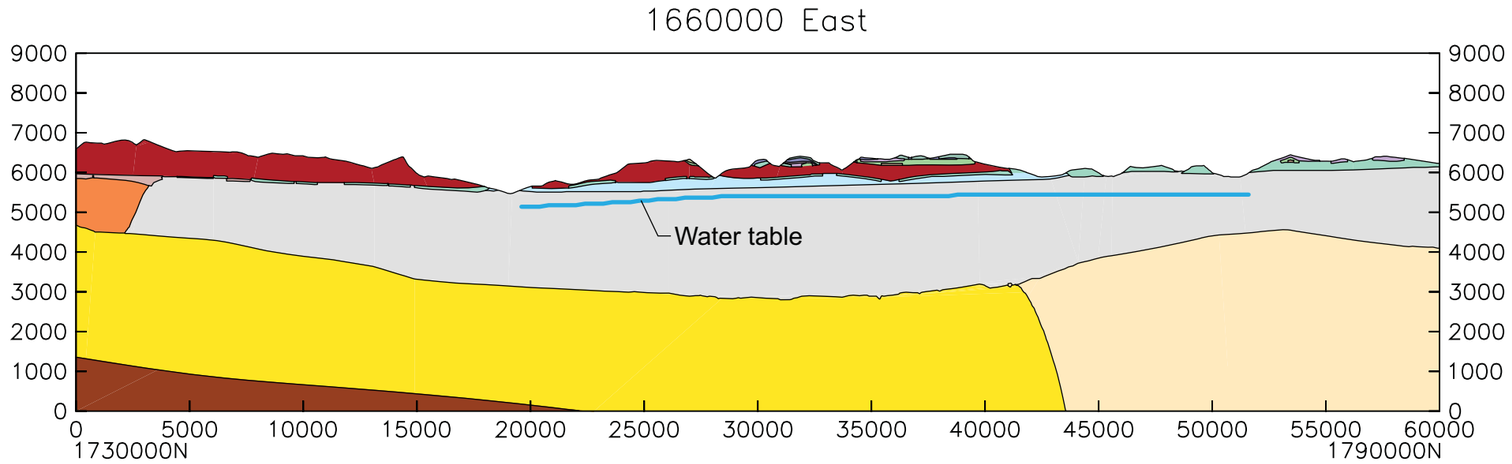


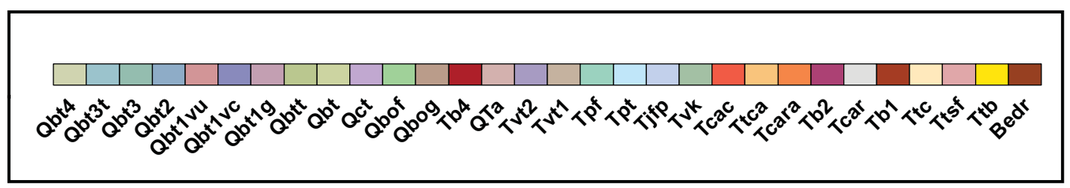
Note: Vertical exaggeration = 1.75x.

Constructed from the 2009 LANL Geologic Framework Model (Cole et al. 2009, 106101) Date: May 2009

Plate 2-89. West central north-south cross-sections (E_1630000, E_1640000)



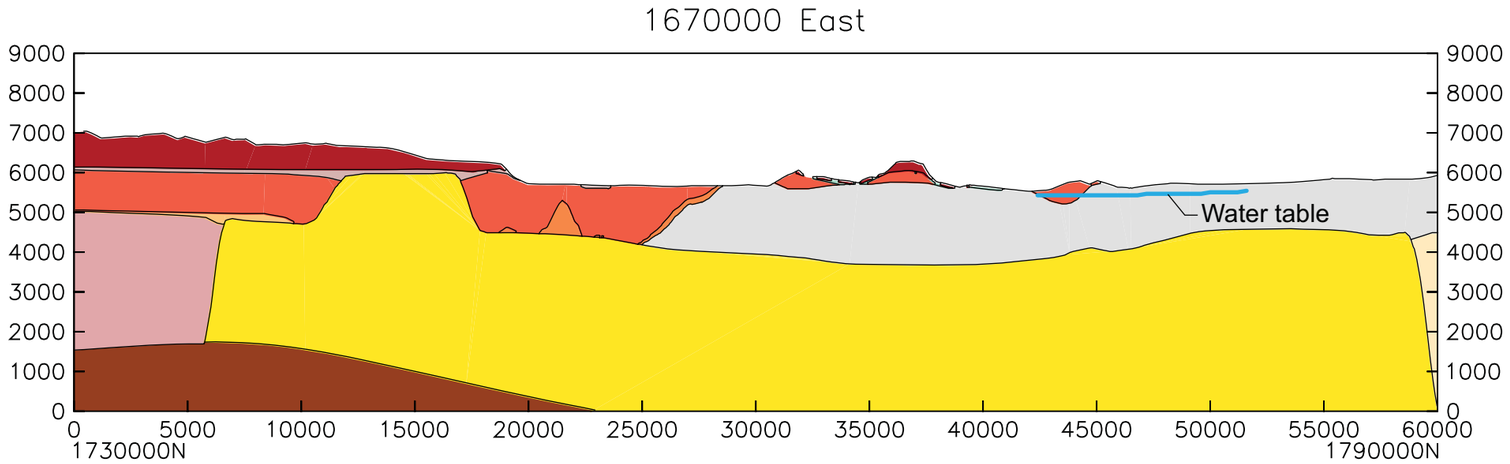


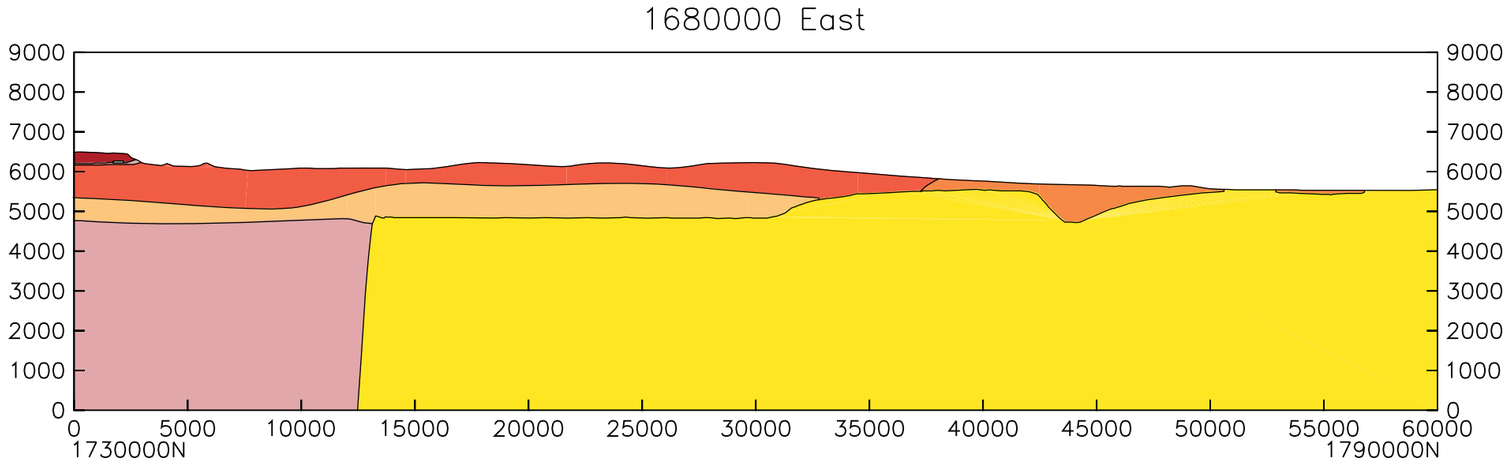


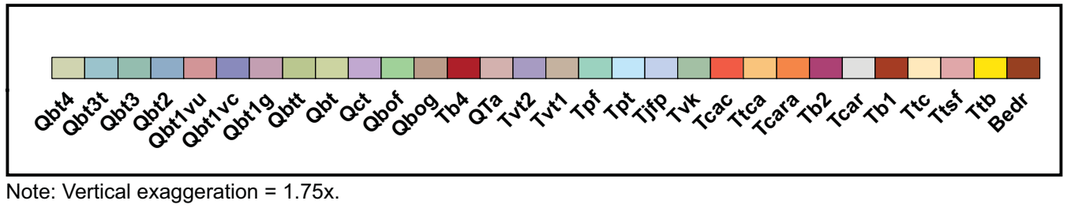
Note: Vertical exaggeration = 1.75x.

Constructed from the 2009 LANL Geologic Framework Model (Cole et al. 2009, 106101) Date: May 2009

Plate 2-90. Central north-south cross-sections (E_1650000, E_1660000)



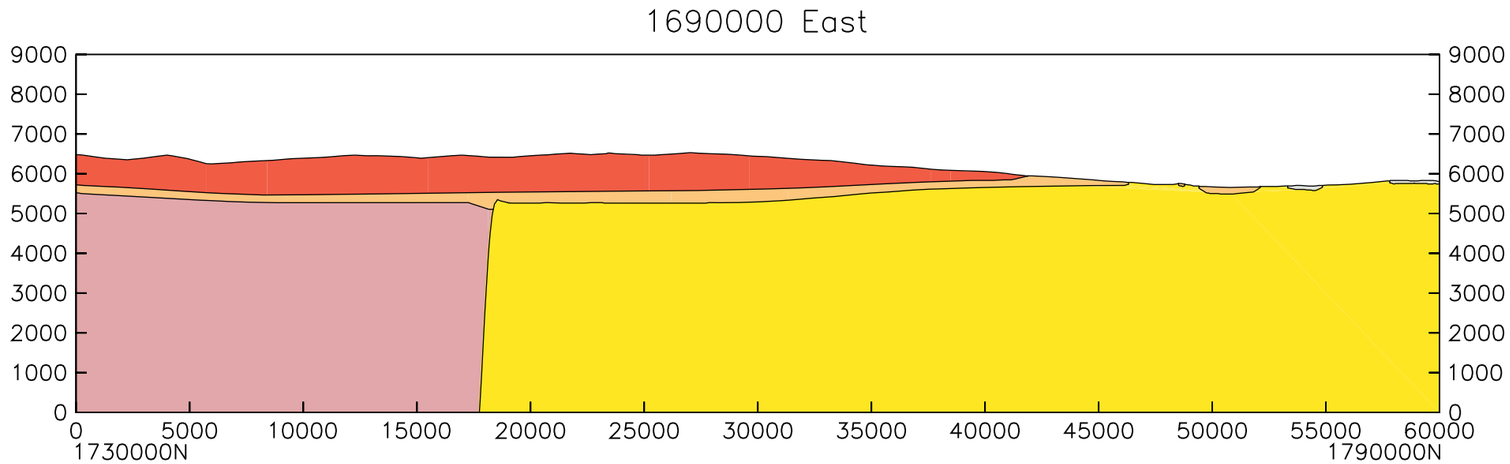


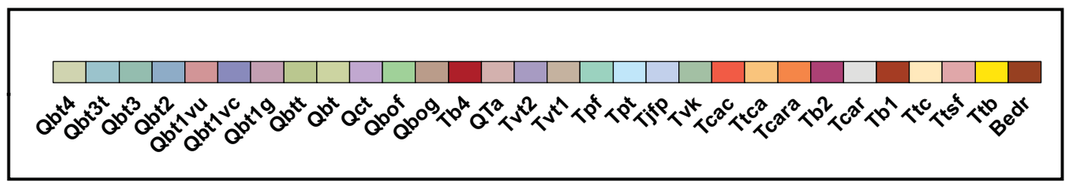


Note: Vertical exaggeration = 1.75x.

Constructed from the 2009 LANL Geologic Framework Model (Cole et al. 2009, 106101) Date: May 2009

Plate 2-91. East central north-south cross-sections (E_1670000, E_1680000)

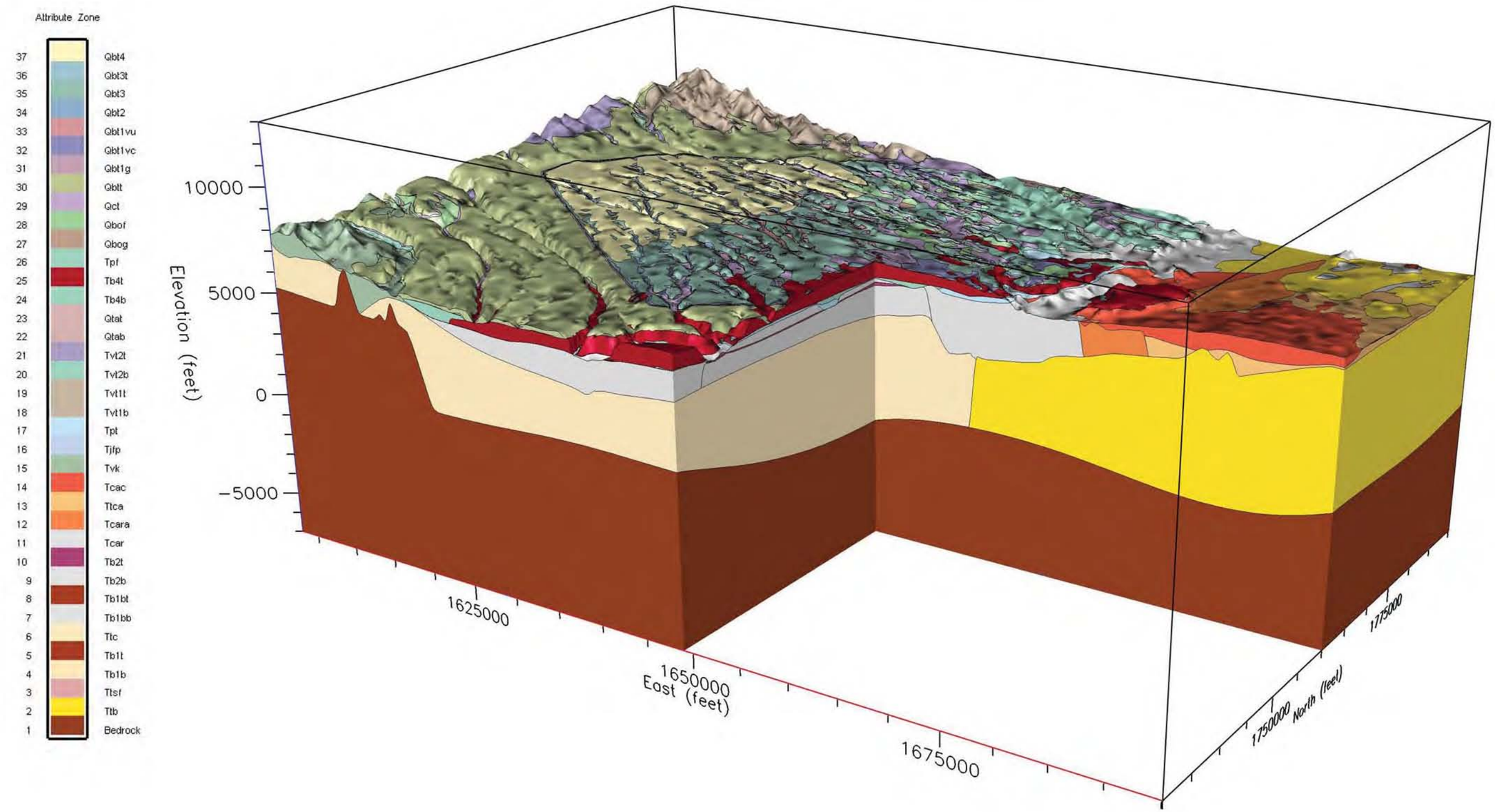




Note: Vertical exaggeration = 1.75x.

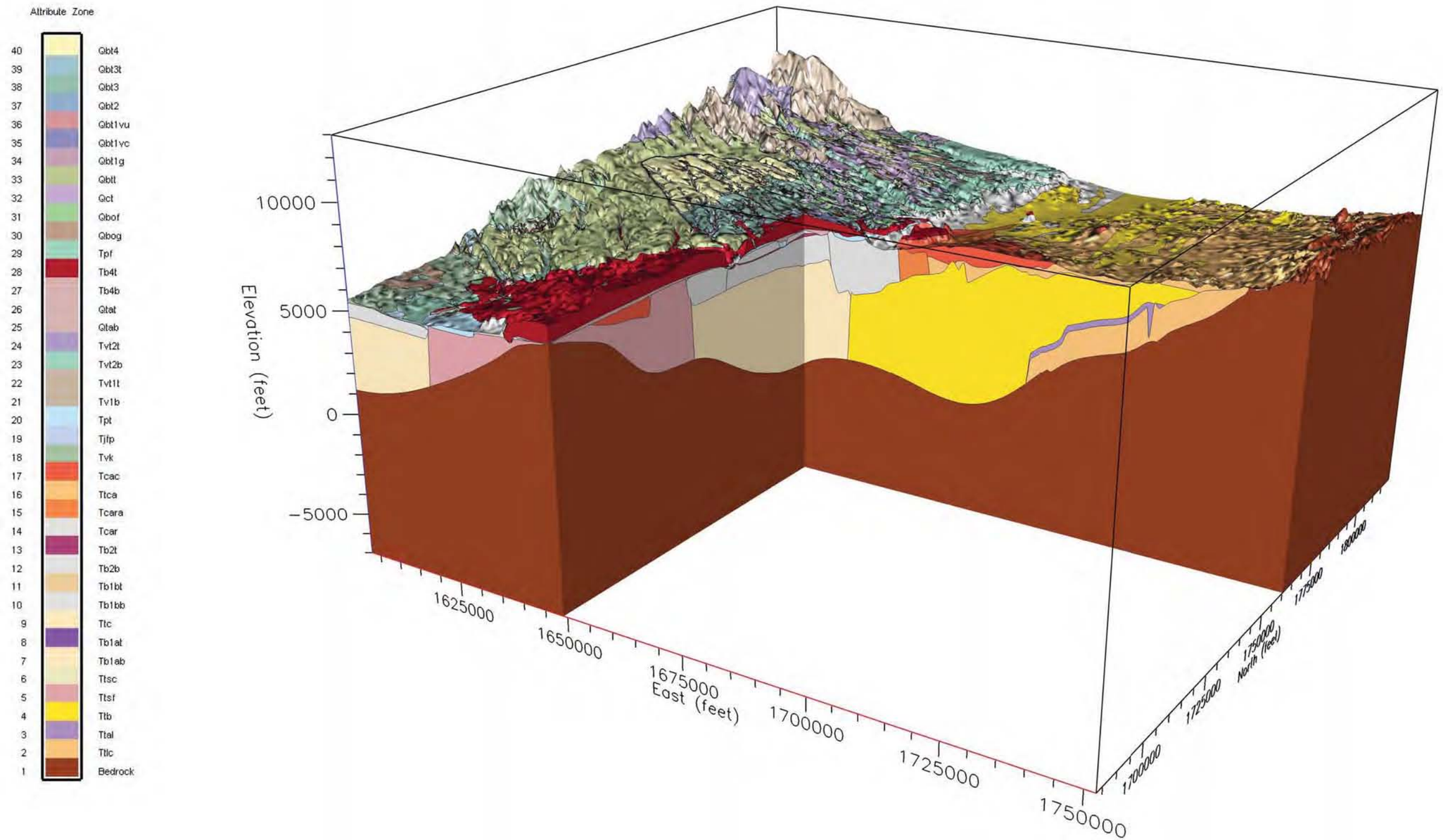
Constructed from the 2009 LANL Geologic Framework Model (Cole et al. 2009, 106101) Date: May 2009

Plate 2-92. Eastern north-south cross-section (E_1690000)



Constructed from the 2009 LANL Geologic Framework Model (Cole et al. 2009, 106101)
Date: May 2009

Plate 2-93. The atlas portion of the southern Española Basin model—view from the southeast



Constructed from the 2009 LANL Geologic Framework Model (Cole et al. 2009, 106101)
Date: May 2009

Plate 2-94. The southern Española Basin model—view from the southeast

1 0.5 0 1 2 Miles

State Plane Coordinate System, New Mexico Central Zone
1983 North American Datum
SCALE 1:80,000

N W E S

1,610,000 1,620,000 1,630,000 1,640,000 1,650,000 1,660,000 1,670,000 1,680,000 1,690,000

1,790,000 1,780,000 1,770,000 1,760,000 1,750,000 1,740,000

TW-4 6072 R-2 5871 R-24 5830 TW-2 5846 R-4 5831 H-19 6228 R-6 5838 R-7 5838 TW-3 5840 R-5 5767 TW-1 5856 R-8 5853 R-9 5692 R-43 5840 R-35a 5837 R-14 5880 R-42 5839 R-1 6228 R-46 5885 R-33 5871 R-28 5838 R-36 5839 R-15 5851 R-13 5836 R-18 6117 R-17 5885 R-26 6538 R-34 5834 R-10 5740 CdV-16-3i 6137 CdV-R-15-3 6020 R-40 5864 R-19 5887 R-20 5865 R-38 5859 R-21 5855 CdV-R-37-2 6137 R-41 5690 R-32 5853 R-39 5754 R-16 5693 R-27 5898 R-23 5697 DT-5 5958 DT-10 5919 DT-5A 5958 DT-9 5915 R-31 5827

Water table contours created by V. Vesselinov

Date: May 2009

- Spring location
- Well - water table elevation

Drainages

Strahler order

- 6
- 7
- 8
- Topography
- Roads
- Los Alamos National Laboratory

Plate 3-1. Regional water table elevations

1 0.5 0 1 2 Miles

State Plane Coordinate System, New Mexico Central Zone
1983 North American Datum
SCALE 1:80,000

N W E S

1,610,000 1,620,000 1,630,000 1,640,000 1,650,000 1,660,000 1,670,000 1,680,000 1,690,000

1,790,000 1,780,000 1,770,000 1,760,000 1,750,000 1,740,000

Tvk Tvt1 Tvt2 Tjfp Tpf Tb2 Tb4 Tcar Tcac Ttb Tpt

6500 6400 6300 6200 6100 6000 5900 5800 5700 5600 5500

Constructed from the 2009 LANL Geologic Framework Model (Cole et al. 2009, 106101)

Water table developed by V. Vesselinov, 2009

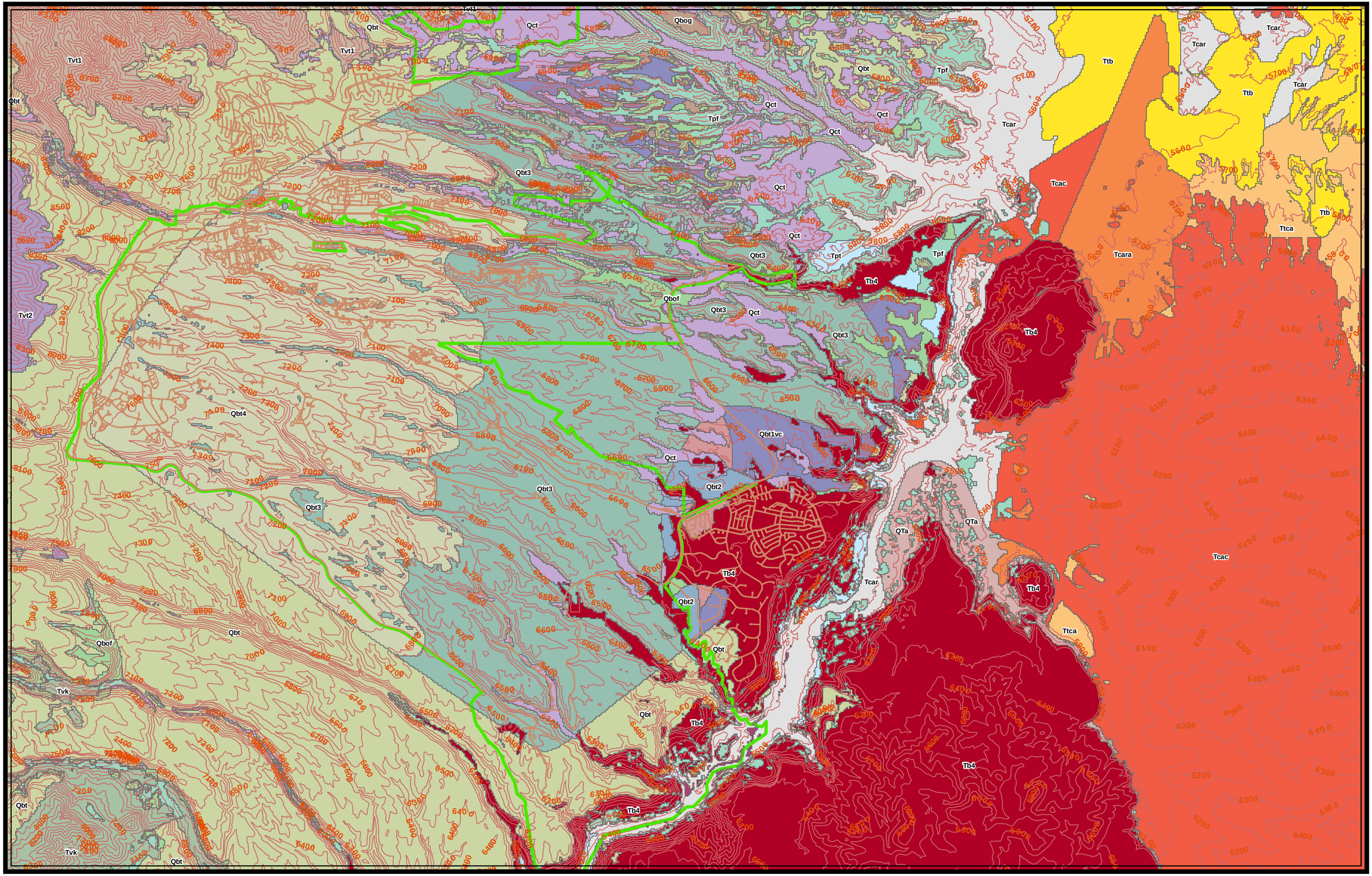
Date: May 2009

Roads
Los Alamos National Laboratory
Water table contours
Data limits

UNIT CODE - UNIT NAME

Tb4	Cerros del Rio Basalts
Tvt2	Younger Tschicoma dacite flows
Tvt1	Older Tschicoma dacite flows
Tpf	Puye Formation
Tpt	Totavi Lentil
Tjfp	Bearhead Rhyolite and Fanglomerates
Tvk	Keres Volcanics
Tcac	Chamita Fm - lithosome A
Tb2	8.4–9.3 Ma Basalts
Tcar	Chamita Fm - axial river deposits
Tb1	11.6–13.1 Ma Basalts
Ttb	Tesuque Fm - lithosome B

Plate 3-2. Geology at the water table


Tvt1
Qbt
Qct
Qbog
Tpf
Tcar
Ttb
Tcac
Ttca
Tcara
Qbt3
Tpt
Tb4
Qbof
Tvt2
Qbt4
Qbt1vc
Qbt2
QTa
Tvk